Can non-contact SIAscopy be used in the diagnosis and quantification of pigmentary skin changes associated with photodamage?

Joseph Alan Walls

A thesis submitted to the Institute of Health
of the University of East Anglia
for the degree of Doctor of Medicine

June 2012

Acknowledgments

Projects of this kind do not happen without a great deal of support and help from many people and I have been lucky enough to have been met with great kindness and support from all I have come across.

I must thank Mr Per Hall and Mr Marc Moncrieff who have not only supported me throughout this project, but have been truly inspiring in their continued interest and willingness to help. I am lucky that I can now include them as friends as well as supervisors.

Dr Symon Cotton and Mr Mark Chellingworth were utterly invaluable for their patience, time and skill. Mark's great help with the computer analysis and Symon's brilliance in keeping things focused and relevant were immeasurable.

I am grateful to Aris Perperoglou for his support in reviewing the statistics and in their presentation.

Throughout the time encompassed by this project I have lost and gained many things. The patience and understanding shown by my wife had been incredible and I owe her more than I could repay.

This work, in its entirety, is dedicated to my mother, who never saw it completed, but whose memory will always be associated with it.

Abstract

Can non-contact SIAscopy be used in the diagnosis and quantification of pigmentary skin changes associated with photodamage?

Introduction

Non-contact SIAscopy is a new imaging technique where a standard polarised photographic image of the skin is decomposed to produce independent colour, blood and melanin images using SIAscopy (a form of reflectance spectroscopy). Photodamage is a product of the physiological changes caused by chronic sun exposure on the skin. Measuring the extent of photodamage has always been difficult, with most analysis requiring subjective user interpretation of results. No one available method appears better at clearly identifying and quantifying photodamage within the skin and no truly objective method exists which enables automatic measurement of these characteristics without expert evaluation.

Methods and results

1140 images of skin of various ages and levels of damage were acquired using standard digital colour photography obtained through crossed polarising filters. The sample was split into a model and test set and analysis algorithms were employed to quantify features including dyspigmentation, sallowness, erythema and vessel dilation. Relevant features were isolated and the relationship with age was determined using linear regression. From this a predictive skin photodamage age was generated and tested with a sample set of images.

Conclusions

Specific pigmentary characteristic of photodamage can be identified and quantified using non-contact SIAscopy. It is an independent, repeatable, robust and inexpensive method of assessing the level of photodamage from a standard digital photograph and the results can be used to identify individuals most at risk of developing skin cancers.

Table of Contents

Chapter 1

Chapter 2

Chapter 3

Chapter 4

Chapter 7

List of figures

Chapter 1

Chapter 2

Chapter 3

Chapter 4

Chapter 5

Chapter 7

Appendix C

Appendix D

Appendix E

List of tables

Chapter 6

Appendix A

Appendix D

Chapter 1

Introduction

The aim of this thesis is to see if the multispectral imaging technique - non-contact SIAscopy - can be used in the identification and measurement of photodamage in the skin. Physiological changes occur within the skin which cause the characteristic features of photodamage and it has wider links with skin cancer formation. I will discuss why photodamage is difficult to measure and why SIAscopy may offer a unique approach to the question. To begin with I will discuss the affected organ, the skin, and some of its common features.

1.1 The skin

The skin is a fabulously complex and interesting structure. It is the largest organ of the body, covering its exterior and being continuous with the mucous membranes lining the orifices of the body. It weighs approximately one sixth of the mass of the body and shows marked variation in thickness across different areas, from less than 1mm on the eyelid to greater than 4mm on the back.

There is considerable regional variation in the structure of the skin across the body and also in the presence of various adnexal structures within it. A good knowledge of this is important in the accurate diagnosis of biopsies.

The skin has a wide range of functions, including:

- Waterproofs the surface of body
- Provides protection from external trauma and microbial invasion
- Detection of sensory information - temperature, pressure, touch, etc
- Absorbs ultraviolet (UV) light
- Metabolises vitamin D
- Regulates temperature
- Absorbs and excretes fluids
- Functions associated with immunity

It can be divided into 2 main parts - the epidermis (outer layer) and the dermis (inner layer).

1.2 The epidermis

The epidermis is a keratinising stratified squamous epithelium derived from ectoderm. It contains the cutaneous adnexal structures of pilosebaceous follicles, nails, sweat glands and sensory receptors. It consists of keratinocytes, melanocytes, Langerhans' cell and Merkel cells.

1.2.1 Keratinocytes

The epidermis continually renews itself and has a terrific potential towards regeneration, being renewed every 2 weeks throughout life. The source of this continual regeneration are the epidermal stem cells. These cells are thought to proliferate in the follicular bulge of hair bearing (thin) skin, though the site and source is a matter of controversy. In non-hair bearing (glabrous) skin it is suggested a sub-population of epidermis based stem cells exists.[11,12]

Cell kinetic studies have shown that the basal cells consist of 3 distinct populations:

1. Stem cells - relatively undifferentiated with an unlimited capacity for cell division, but do so relatively slowly.
2. Transit-amplifying cells - only have a limited capacity for mitotic division before being committed to cellular differentiation.
3. Committed cells - have lost the ability to divide and so progress along the keratinization pathway.

Histologically the epidermis can be seen to be arranged into 4 distinct layers as the cells change and migrate to the surface if the skin:

- basal cell layer (stratum germinativum)
- prickle cell layer (stratum spinosum)
- granular cell layer (stratum granulosum)
- keratin layer (stratum corneum)

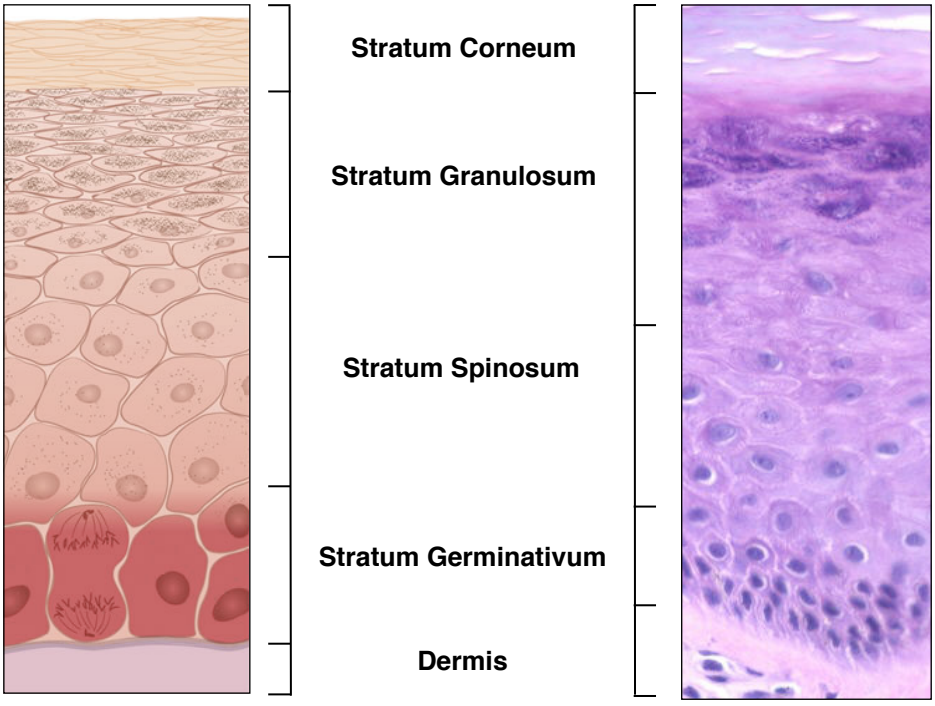

Fig 1.1 Cross-section of the epidermis at 40x magnification

Basal cells (stratum germinativum) reside on the basement membrane, which separates the epidermis from the dermis. They are typically cuboidal or columnar in shape and have a large, prominent nucleus.
Prickle cells (stratum spinosum) are adjacent to these and are histologically polygonal in shape with abundant eosinophilic cytoplasm and oval nuclei. Further maturation shows prominent keratohyaline granules (stratum granulosum) and progressive loss of the nucleus with flattening of the keratinocytes to form the plates (stratum corneum) of the keratin layer.
A fifth layer, the stratum lucidum, is present on the palms of the hands and soles of the feet. It is composed of Leidin, an intermediate form of keratin, and lies between the granular and keratin layers. It prevents shearing of the stratum corneum from the the stratum granulosum.

The epidermis contains two types of dendritic cells - melanocytes and Langerhans' cells.

1.2.2 Melanocytes

Melanocytes are usually located along the basal layer of the epidermis and within the hair bulbs, but are also present in the inner ear, eyes and meninges. They originate in the neural crest and migrate to the epidermis from about the fiftieth day of intrauterine development.[14] The ratio of melanocytes to basal cells is dependent on the site of the body, ranging from 1:4 on the face to 1:10 on the limbs.
Melanocytes produce the pigment melanin, a complex molecule and a derivative of tyrosine, which differs in colour from yellow to brown/black depending on racial variation.[1] Melanin is thought to protect the mitotically active basal epidermal cells from potential damage by ultraviolet light through photo-absorption and scavenging of free-radicals. Melanocytes are stimulated to produce more melanin by exposure to UV-light and this is seen as tanning of the skin, the overall response being dependent on the length of exposure, the spectral characteristics of the light and the genetic predisposition of the individual. Short term exposure to UV-light does not lead to an increase in the number of melanocytes, indicating a limited capacity to proliferate, though there is an increase

in the size and functional activity of the existing melanocytes, as well as the number of dendrites.[10] An increase in the population only occurs after repeated UV exposure and also produces very efficient movement of melanin from the melanocytes to the keratinocytes.*

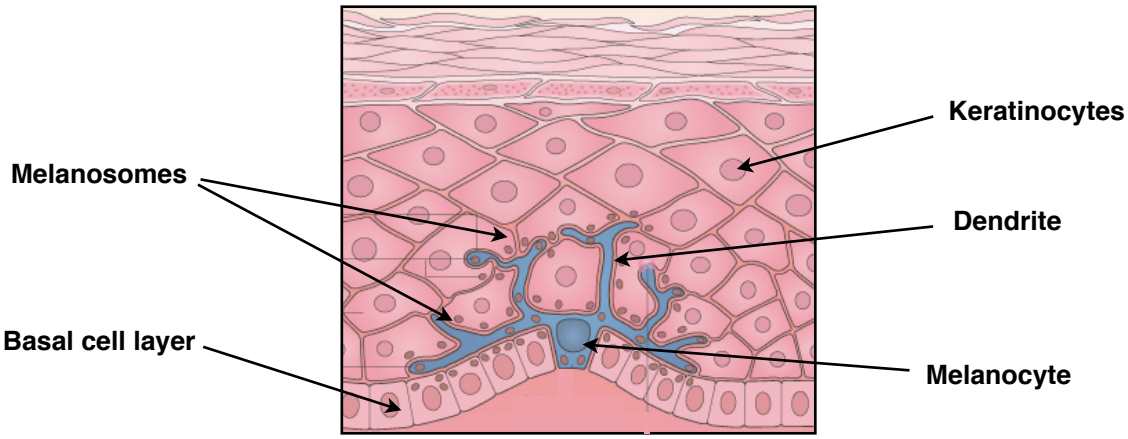

Fig 1.2 Position of a melanocyte within the epidermis

There are 2 subtypes of melanin in human skin, which differ in both their bio-chemical make up and their photo-protective ability:

- Eumelanin is a tyrosine derived brown/black pigment found in the darker coloured races.
- Phaeomelanin is derived from tyrosine and cysteine and is a yellow/red colour, predominant in Caucasian skin.

Melanin moves from the melanocytes in the form of melanosomes which are lysosome-like vesicles that are transported along the dendritic arms of the melanocyte. The melanosomes are engulfed by the (predominantly) basally located keratinocytes and come to lie within the cell, in an umbrella-like distribution over the nucleus.

Mature eumelanin melanosomes are ellipsoidal and very structured in shape, whereas phaeomelanin melanosomes are more spherical and less structured.[2] Melanosomes in darker skinned races predominantly contain eumelanin and

* Image modified from Bolognia JL, et al. Dermatology. Philadelphia: Elsevier; 2003

are typically more abundant and larger than in the paler skinned. Eumelanin is thought to be more UV-protective than phaeomelanin. It is relatively insoluble and stays within the epidermis for longer, often being seen in the stratum corneum.

In contrast, phaeomelanin is itself photo-labile, breaking down by the time it reaches the granular layer and has a tendency to produce free radicals on UV exposure.[15] The different levels of phaeomelanin and eumelanin production are moderated by Melanocyte Stimulating Hormone (MSH) and it is postulated that it may be genetic variation to the sensitivity to MSH which makes some skin types more susceptible to UV damage.[9]

The number of melanocytes is incredibly consistent within varying racial skin colouring, the amount and type of melanin produced, and the size of the melanosomes being the differing factors.

The ability to categorise skin type by looking at an individuals ability to burn or tan, to consistent levels of UV-light, was measured by Fitzpatrick in 1988[8] .

Fitzpatrick Skin Type	Description
1	Extremely fair skinned - Always burns, never tans
2	Fair skin - Always burns, sometimes tans
3	Medium skin - Sometimes burns, always tans
4	Olive skin - Rarely burns, always tans
5	Moderately pigmented brown skin - Never burns, always tans
6	Markedly pigmented black skin - Never burns, always tans

Table 1.1 Fitzpatrick skin types

1.2.3 Langerhans' cells

Langerhans' cells are intra-epidermal antigen-presenting cells found in the supra-basal areas of the epidermis and also in the dermis. They are derived from bone marrow and are responsible for the instigation of contact allergic hypersensitivity reactions and delayed T-cell related immunosensitivity.[16] They are the main intra-epidermal cellular response to tumour antigens and microorganisms and are also involved in skin graft rejection. Their dendritic processes extend upwards between the keratinocytes to the granular layer and down to the dermal-epidermal junction. After stimulation, they migrate to lymph nodes where they stimulate T-lymphocytes. The resultant antigen-specific T-cell then moves to the epidermis to effect the immune reaction.

Langerhans' cells may also be important in the development of cutaneous tumours due to a reduction in number and function which has seen to be induced by UV-light and chemical carcinogens. It is also typical with increasing age and may be an important early step in in the development of epidermal tumours.[3]

1.2.4 Merkel cells

Merkel cells are another group of cells that exist in the epidermis. They are associated with mechanoreceptors and are therefore particularly active in touch sensation.[4] They are widely distributed in the epidermis, hair follicles and mucous membranes, showing maximum concentrations on the lips, hard palate, palms, finger pads, proximal nail folds and the dorsum of the feet.[5] Elsewhere they are more abundant in sun-exposed than non-sun-exposed skin, increasing in areas of sun-damage such as actinic keratoses.[6] They are found supra-basally, where they synapse with sensory neurones and are common in areas with a rich vascular and nerve supply. It has been supposed that Merkel cells are also involved in the structure of sub-epidermal and perifollicular nerve plexuses.[7]

Joining the epidermis and the dermis is the basement membrane. The epidermis is anchored to the basement membrane via anchoring filaments in the hemidesmosomes and to the adjacent dermis by anchoring fibrils.

1.3 The dermis

The dermis supports the epidermis and is composed of collagen, elastic fibres and ground substance. Within it is found epidermal elements, blood vessels, nerves, smooth muscle (in the erector pili muscles) and various cellular elements, including mast cells, macrophages, fibroblasts and myofibroblasts. There is a marked regional variation in the thickness of the dermis, particularly on the palms and soles, and it tends to be thicker on the back of the body than the front.

The dermis can be divided into two layers:

1. Papillary dermis which is highly irregular and accounts for the complex arrangements of loops and whorls that make up fingerprints. It is bound by the epidermis superiorly, inferiorly by the superficial vascular plexus and reticular dermis, and laterally by the epidermal ridges.

2. Reticular dermis - this lies between the papillary dermis and subcutaneous fat. Collagen fibres within the reticular dermis are more organized and lie in a parallel arrangement, accounting for the lines of cleavage in the skin.

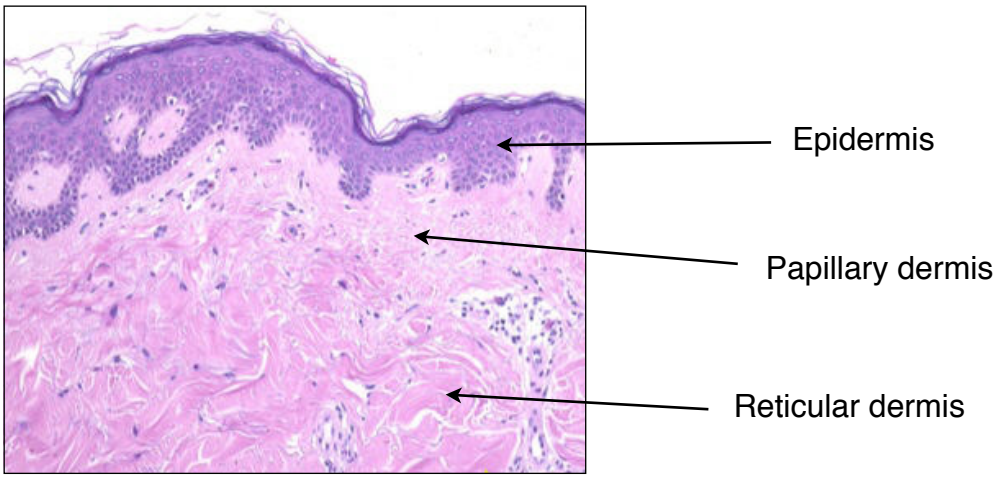

Fig 1.3 Cross-section of skin at 20x magnification

Collagen is an extremely complex protein synthesized in a number of different cell types and there are over 20 different antigenic subtypes recognized, depending on morphology, amino acid composition and physical properties.[20] Collagen molecules intertwine to form microfibrils, which form a tight network of collagen fibrils. These then interweave to form a mature collagen fibre. The dermis contains predominantly type I collagen (85-90%), type III (8-11%) and type V collagen (2-4%).[13]

Elastic fibres are intimately associated with collagen and make up a relatively small component of the dermis. They are primarily responsible for skin elasticity and are made by fibroblasts. In the papillary dermis they are thin and arranged at right angles to the skin surface, while in the reticular dermis they are parallel to it and are thicker.[21]

Ground substance is present in all tissues of the body and is not only an embedding matrix for cellular and fibrous components. It is involved in the transport of water and electrolytes, and the osmolarity of interstitial fluids.[22]

1.4 Skin appendages

There are various adnexal structures within the skin, all with specialised functions and anatomy.

1.4.1 Sebaceous glands

Sebaceous glands usually develop as protrusions from the root sheath of hair follicles, but can arise independently in areas such as the eyelid, lips, areolae and labia minora, draining directly onto the surface of the skin. They are found everywhere on the body except the palms and soles and are abundant on the face, scalp, mid-line of the back and perineum. They are concentrated around the orifices of the body. They consist of several lipid containing lobules which drain secretions into a sebaceous duct and then join the hair follicle. The duct is lined with squamous epithelium, continuous with the root sheath. Sebaceous

glands are generally inactive until puberty, appearing to be largely under the control of the androgen testosterone and inhibited by oestrogens. As a consequence the sebaceous glands of males are larger and more active than those of females. The glands secrete a fluid called sebum which is a complicated lipid mixture consisting mainly of triglycerides, wax esters and squalene. Its exact function in man is uncertain, but may include waterproofing, control of epidermal water loss and in preventing colonisation by bacteria and fungi.[17]

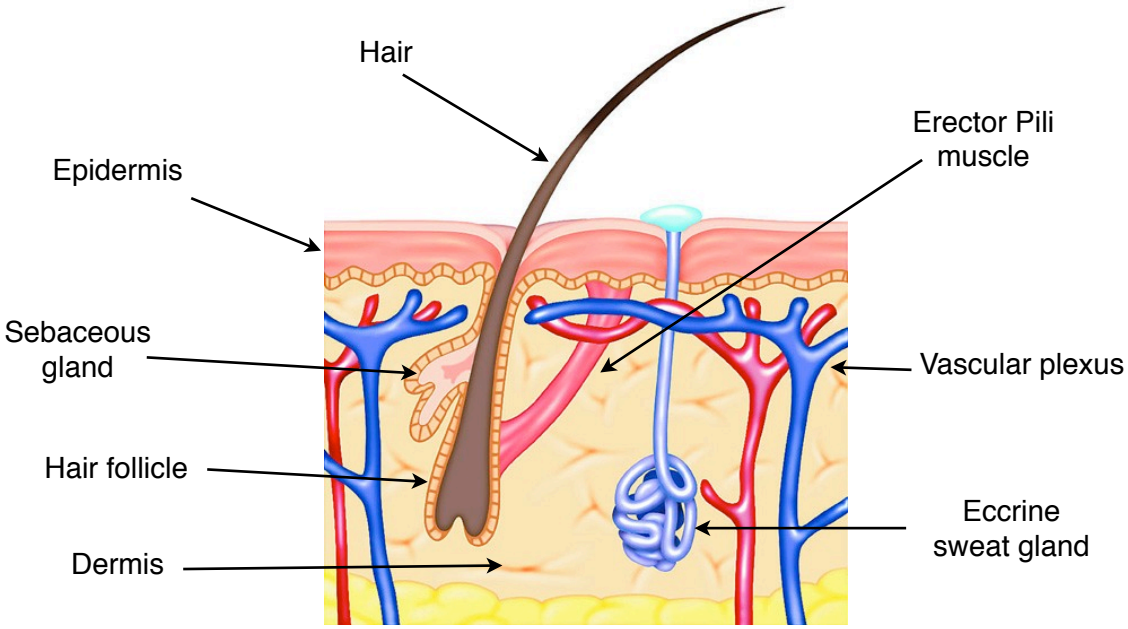

Fig 1.4 Cross-section of skin and related appendages

1.4.2 Eccrine sweat glands

Eccrine sweat glands are involved in the control of body heat in hot conditions or during exercise and are present all over the skin except mucous membranes. They concentrate on the palms and soles, forehead and axillae and are larger in size on the palms and soles. They are formed from a specialised down-growth of the epithelium and protrude through the full thickness of the skin, with the secretory component lying in the deep reticular dermis, close to the interface with the subcutaneous fat. There is an outer layer of myoepithelial cells, which respond to cholinergic stimulation, surrounding the inner secretory cells. The secretory element is highly vascularised and coiled while the remaining duct has both straight and coiled elements. The secretory component is is

stimulated by thermal, emotional and gustatory functions. Thermoregulatory sweating occurs mainly on face and upper trunk, while emotional sweating induces particular palmer sweating. Eccrine sweat is secreted slightly hypertonic, containing water, sodium chloride, lactate, urea and potassium, though there is some resorption of sodium chloride in the ductal system.[18]

1.4.3 Apocrine glands

Apocrine glands are generally found around the anogenital and axillary regions but are also found in the external auditory meatus, eyelids and within the areola. They develop as outgrowths of follicular epidermis and as with sebaceous glands, they are mostly active after puberty. In the external ear they are thought to lubricate and protect it from fungal and bacterial growth and although their exact function in man is unclear, in other mammals they are responsible for scent production. The mechanism of secretion remains uncertain, but they do receive adrenergic sympathetic innervation and secretion is stimulated by stimuli such as excitement or fear. The unpleasant odour of apocrine secretion is due to its breakdown by bacteria on the surface of the skin and not the secretion itself, which is odourless.[19]

1.4.4 Hair

Hair follicles are found on all surfaces of the body except for palms and soles of feet. Although the main evolutionary function of hair is for protection, these days it is more important in social interaction. They contain both dermal and epidermal components and have associated sebaceous glands and erector pili muscles. During development, epidermal germ cells invaginate into the dermis forming hair follicles.

The hair follicle is divided into two sections, separated at the insertion of the erector pili muscle. The upper section is very stable and not affected by maturation and shedding of the hair, whereas the lower section is active and involved in the various growth cycles of the hair.
The hair itself is composed of three layers. The medulla is the central region, but is not always consistently present in human populations. The cortex is the

outer part of the shaft and is the thickest layer, providing the strength of the shaft. The cuticle is the an external layer consistent with the internal lining of the root sheath. It undergoes basket-weave keratinisation at the level between upper and lower segments.[23]

1.4.5 The nail

The nail unit is a specialised structure providing the terminal portion of the digits with protection, rigidity for grasp and support for sensory structures. Nails grow from 0.1 to 1mm a day, faster in the summer than in the winter, fingernails faster than toenails. Like hair, nails are also formed of keratin and also from invaginations of the epidermis into the dermis. The nail unit is composed of many specialised sub-units, including the nail folds, nail plate, nail matrix (which produces the nail plate), cuticle, nail bed and supporting ligaments.

The dermis underneath the matrix is well vascularised and contains many collagen fibres which form the ligaments that attach the nail matrix and bed directly with the periosteum of the underlying phalanx. The nail is composed of 3 layers of keratin. A hard inner core produced by the matrix, a semi-hard dorsal layer produced by the dorsal nail fold and a semi-hard ventral layer produced by the nail-bed epithelium, which firmly adheres the nail plate to the nail bed.[24]

Fig 1.5 A fingernail

1.5 Blood and nerve supply of the skin

The skin receives a very rich blood supply, far greater than its metabolic requirements would suggest, due to its thermoregulatory capacity. The blood is supplied via perforating vessels within the skeletal muscle and subcutaneous fat and is concentrated around the more metabolically active components of the skin, namely the epidermis, hair papillae and other adnexal structures. Although the dermis is richly vascularised, no blood vessels enter the epidermis, which gets it nutritional requirements via diffusion.

There are two distinct vascular plexus within the skin, connected by numerous branches:

1. the superficial vascular plexus lies at the superficial aspect of the reticular dermis and supplies the papillary dermis and epidermis via a rich, looped capillary network.
2. the deep vascular plexus lies near the interface of the dermis with the subcutaneous layer and supplies the deeper reticular dermis and adnexal structures.[25]

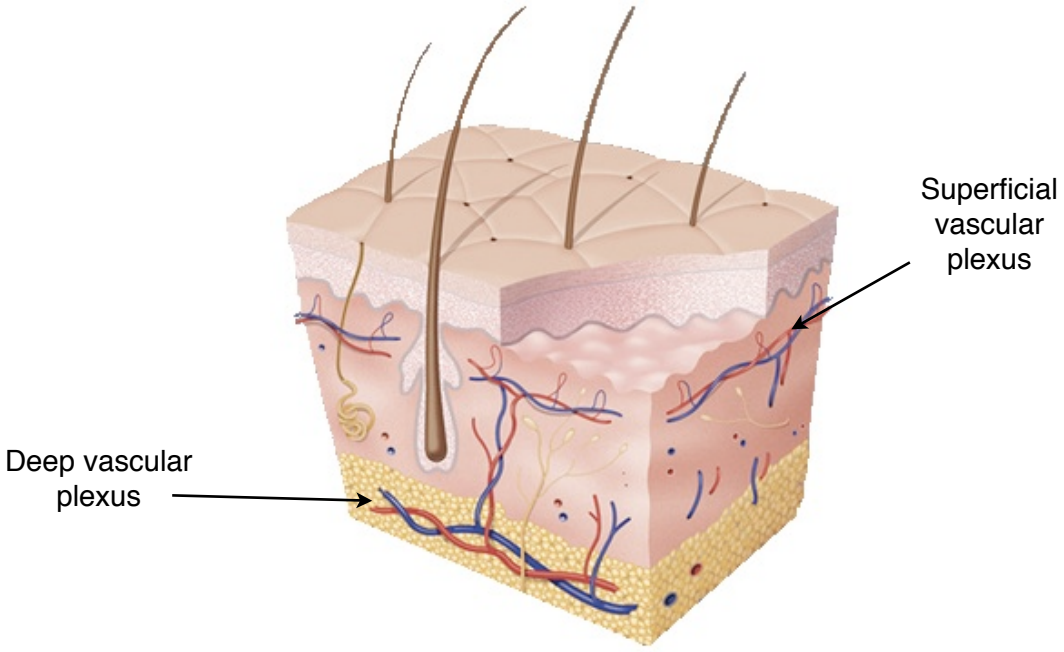

Fig 1.6 Cross-section of skin showing the arrangement of the superficial and deep blood supply

There are abundant arterio-venous anastamoses which are associated with specialised shunts called Glomus bodies (modified smooth muscle cells with a rich nerve supply). These surround an arterial segment connected directly to the venous limb and function as sphincters which allow the superficial dermal capillaries to be bypassed and so increase venous return from the skin. This control of cutaneous blood flow is extremely important in thermoregulation. In hot environmental situations, peripheral blood flow can be increased and along with eccrine sweating and evaporation, will maintain a stable body core temperature.[26]

An extensive lymphatic system also exists within the dermis and is closely associated with the vascular system. This allows for the removal of fluid, cells and macromolecules involved in the daily turnover of cellular activity. It also provides the pathway by which stimulated epidermal Langerhans' cells reach regional lymph nodes. Like the dermal vascular system, the lymphatic vessels are loosely arranged into superficial and deep plexuses which in turn drain into larger lymphatic trunks.[27]

The skin has a very rich nerve supply responsible for the control of many of its functions and the appreciation of sensation.[28] The efferent limb is non-myelinated and controls the vasculature and appendages, whereas the afferent limb is myelinated and transmits sensory information. There are prominent plexuses around hair bulbs and within the dermis.

Both afferent and efferent limbs have encapsulated and free nerve endings depending on the function of the nerve. Free nerve endings have relatively low conduction speeds and are associated with the appreciation of temperature, itch and pain. There are various encapsulated nerve endings including including the more specialised Pacinian and Meissner corpuscles.

Pacinian corpuscles are larger, myelinated nerve endings composed of laminated terminal elements. They are responsible for the appreciation of deep pressure and vibration and are mainly distributed around the subcutaneous fat of the palms of the hands and soles of the feet, as well as the dorsum of the digits, the genitalia and in ligaments and joint capsules.

Meissner corpuscles are relatively smaller, laminated nerve endings, supplied by both myelinated and non-myelinated fibres. They are involved in touch sensation and are intimately associated with basal keratinocytes, mainly distributed on the hands, feet, lips and front of the forearm. Each nerve may supply multiple corpuscles.

1.6 Common benign skin lesions

The following section describes some of the more commonly found and acquired, benign skin lesions. This is not an exhaustive list and the interested reader may want to refer to a more specialised text. A comprehensive review can be found in the excellent Pathology of the Skin, by McKee, Calonje and Granter.[29] Malignant and pre-malignant skin lesions are discussed further in chapter 2.

1.6.1 Congenital melanocytic skin lesions

Fig 1.7 Congenital melanocytic naevus

Congenital melanocytic naevi (CMN) are present from birth and can be substantial in size (Giant naevi measure 20cm, or more than 5% of body surface area), affecting up to 6% of the population. They are an important group which, as well as being associated with cosmetic and psychological trauma, have an increased risk of developing melanoma, particularly in the larger CMN. The estimated lifetime risk is in the range of 4-10%, with 70% occurring below the age of 10 years.[43]

1.6.2 Acquired melanocytic skin lesions

Fig 1.8 Ephilides

Ephilides, or freckles, are directly associated with sun exposure and so are commonly seen on the forearms, shoulders, cheeks, nose and forehead. Histologically they are areas of increased keratinocyte pigmentation and a normal number of melanocytes. Along with fair and red hair, blue eyes and pale skin, they are phenotypic markers of skin which is easily damaged by ultraviolet radiation (Fitzpatrick type 1).[30]

Fig 1.9 Lentigo simplex

A Lentigo simplex is a small, uniformly pigmented, well circumscribed macule that can occur anywhere on the skin, conjunctiva or mucosal surfaces. They become more common in childhood, may increase during pregnancy and can be associated with a variety of inherited systemic conditions. Histologically, there is an increase in the number of basally located melanocytes.[31]

Fig 1.10 Actinic lentigo

Actinic lentigines are also known as solar lentigo, senile lentigo or liver spots. They commonly occur in sun-damaged skin from middle age onwards and can vary in colour size, even coalescing over time. Histologically they occur in a background of solar elastosis and with a normal or slightly increased number of melanocytes which appear functionally hyperactive.[31]

Melanocytic naevi occur equally in men and women and the average caucasian can expect to develop 15-40 by the 3rd decade of life, before they start to regress. They can appear as flat, raised or even pedunculated lesions and arise as a focus of melanocytic proliferation at the lower levels of the epithelium. This dermal-epidermal junctional activity gives rise to a junctional naevus and with time will develop melanocytes in both the dermis and epidermis as a compound naevus. Further development gives rise to a completely dermal lesion, the intradermal naevus.[33]

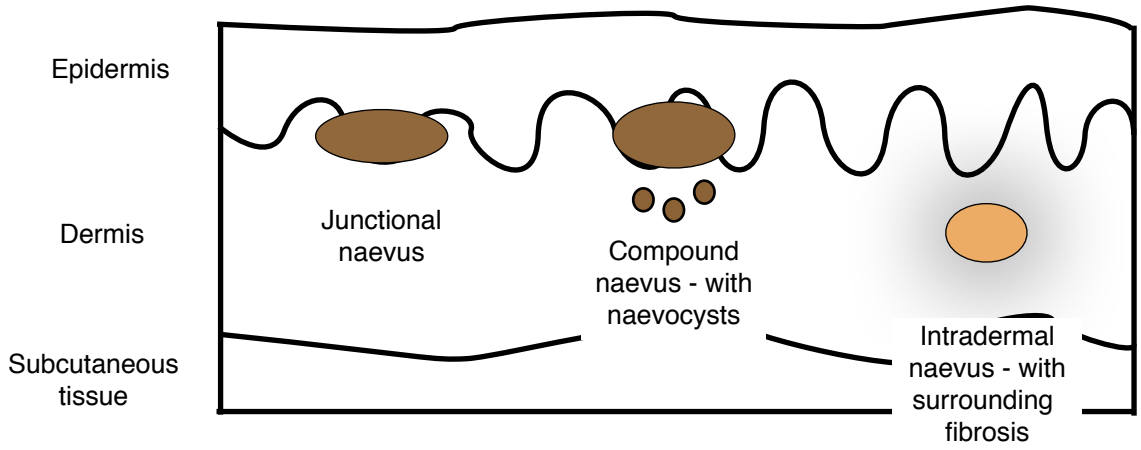

Fig 1.11 The evolution of melanocytic naevi

In children and adolescents, pigmentary increase is to be expected as the lesions are in an earlier stage of development, however evidence of increasing pigmentation and junctional activity in adults, including naevi arising de novo, should be evaluated histologically. The development of melanocytic naevi is related to the amount of sun exposure during the younger years of life, being particularly associated with episodes of intense sunshine rather than chronic exposure. Hence increasing numbers can correlate with an increased risk of subsequent melanoma development.[32]

Melanocytic naevi present in a variety of ways depending on their stage of evolution.[34]

Fig 1.12 Junctional naevus

Junctional naevi are usually macular or slightly raised, well circumscribed and pigmented. By definition, junctional naevi are an epidermal occurrence, but in heavily pigmented examples, melanin can be scavenged by macrophages (called melanophages when loaded with melanin) and can be found in the papillary dermis (called pigmentary incontinence).

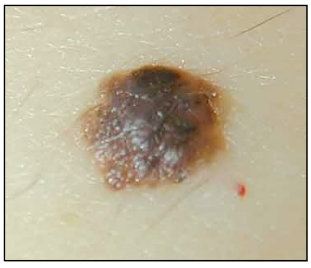

Fig 1.13 Compound naevus

Compound naevi are typically raised and may be deeply pigmented, with some coarse hairs growing from them. As well as junctional activity, melanocytes multiply to form naevocytes and are found in nests of naevus cells in the papillary and upper reticular dermis

Fig 1.14 Intradermal naevus

Intradermal naevi are often non-pigmented, appearing as a dome-like nodule. They are the 'end-stage' of melanocytic naevus maturation and are associated with decreasing pigmentation and atrophy. They are associated with loose fibrous tissue and occasionally dense fibrosis can occur.

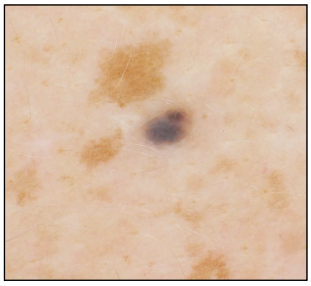

Fig 1.15 Blue naevus

The common blue naevus is a frequently occurring lesion found anywhere on the body. They represent the arrested migration of melanocytes en-route to the epidermis during embryological development and typically lie within the deeper reticular dermis, but can present in the superficial reticular and papillary dermis.[37]

Fig 1.16 Acral naevus

Acral naevi can appear as well circumscribed, symmetrical lesions or as irregular, poorly lesions and can be a diagnostic problem both clinically and histopathologically. There are two categories, acral palmar/plantar naevi and atypical acral naevi (generally termed acral naevi), with the latter found on the dorsal surfaces of the hands, feet, digit and beneath the nails.[35]

Fig 1.17 Halo naevus

Halo naevi are characterised by a small pigmented macule surrounded by a narrow border of hypopigmentation and are usually associated with regression of the naevus. They occur in the second decade of life, on the back and trunk and can have a familial link. They are caused by antibodies to the cytoplasmic antigens in melanoma cells.[36]

Fig 1.18 Spitz naevus

Spitz naevi are generally seen in childhood and young adults are a solitary, rapidly growing, pinkish, dome-shaped papule. They typically occur on the head and neck and, although biologically benign, can be misdiagnosed as a melanoma as malignant variants have been described.[38,39] There are many different varieties of Spitz naevi, which promote a great deal of discussion, further explanation of which is beyond the scope of this thesis.

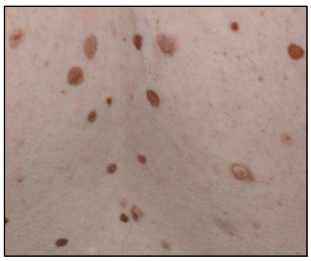

Fig 1.19 Dysplastic naevus

Dysplastic naevi are an important and controversial group of naevi which are technically benign. Much of the debate in the literature particularly revolves around defining their histological characteristics and the reproducibility of diagnosis.[40] The diagnosis of a dysplastic naevus identifies an individual as having a higher risk for developing melanoma, that risk being somewhere in the region of a 2-12 fold increase.[41] A large number of typically normal naevi develop in sun exposed areas in early childhood and acquire atypical features during puberty, with new lesions continuing to develop throughout life.[42] They show marked variability in size, shape, colour and symmetry, making the monitoring of changes difficult in moles which, by definition, always look suspicious.

It has been shown that dysplastic naevi have a higher phaeomelanin to eumelanin content, which may partly explain the increased malignant transformation ratio.[46] More recently, the term 'dysplastic' naevus has been abandoned in clinical use as there is a lack of correlation between clinical and histological features. The term 'atypical naevus' is now generally used, although it should be noted that not all clinically atypical naevi are histologically dysplastic.

1.6.3 Acquired non-melanocytic skin lesions

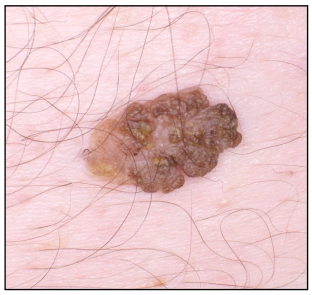

Fig 1.20 Seborrhoeic keratosis

Seborrhoeic Keratoses are extremely common lesions. They develop from middle age onwards and tend to be numerous and of varying presentation. Typically they are sharply defined, oval shaped, wart-like plaques that can vary in colour from flesh-like to brown/black. They can occur anywhere on the body but are commonly seen on the face, upper body and back and often have a genetic component to their aetiology. They are composed of proliferating keratinocytes giving rise to massive hyperkeratosis and are not melanocytic in origin, despite their colouration.[44]

Dermatofibromas are common skin lesions, frequently seen from middle age onwards as small, raised, hyperkeratotic nodules of a red-brown colour. They are most often seen on the limbs and are generally associated with minor trauma and insect bites.[45]

Keratoacanthoma is a controversial, uncommon skin lesion, which in the past have been classified as benign or pseudomalignant, but are now probably best regarded as having a small degree of malignant potential. They have a very characteristic ‘volcano-like’ appearance and can spontaneously regress with time. They are described in more detail in Chapter 2.

Actinic Keratoses are a very common solar induced skin problem characterised by rough, thickened lesions in sun exposed areas. They have a pre-malignant potential and are looked at in greater detail in Chapter 2.

Chapter 2

Skin ageing and photodamage

Characteristic and visible changes occur within the skin during the normal ageing process. Changes due to photodamage occur simultaneously with normal ageing and it can be difficult to differentiate between the two. In this chapter I will look at what those changes are, what causes them and how continued photodamage can result in characteristic transformations and malignancies.

2.1 Chronological skin ageing

Chronological, or intrinsic, skin ageing is the effect of the accumulation of changes within the skin that occur solely due to the passage of time. These changes are governed by the genetic 'potential' of that skin to resist the accumulation of endogenous damage from reactive products of oxidative metabolism within cells over time. These reactive oxygen species (ROS) interfere with intracellular activity and can damage cellular membranes, enzymes, DNA and DNA/protein interactions.[50]

The cellular debilitation that occurs with ageing is a consequence of several alterations within cellular components (DNA and proteins) which result in altered cellular responses to environmental effects, which in turn lead to poor viability and ultimately cell death.

One specific phenomenon linked to cellular ageing is telomere shortening.[55] Telomeres are the terminal endings of chromosomes and with each cell division, the telomere length shortens as the final bit of genetic code is not able to be replicated. Telomeres do not contain any functional genetic code and seem only necessary to prevent the loss of any functional code during cell replication. Once at a critically short length (thought to be after 50 cell divisions) they signal the arrest of further cell replication and the cell will age and die (cell senescence). The enzyme telomerase is responsible for the reconstruction of telomeres, thereby prolonging the cells ability to replicate. This explains the seemingly immortal tumour cell lines which rapidly divide, but are not governed by the '50 division' rule. Some very interesting research has been done in this field and the Nobel prize for medicine in 2009 was awarded to researchers who identified telomerase.*

Skin ageing is also influenced by the decrease in circulating hormones, cytokines and chemokines commonly seen with increasing age. Hormones such as oestrogen, testosterone, DHEA, melatonin, cortisol, growth hormone and vitamin D3 all have effects on the skin and all decrease with increasing age.[56,57] As well as a decrease in the amounts of circulating effecter molecules, there is also a decrease in the levels of receptors for these, thereby adding to the effect.[58]

2.1.1 Features of age associated skin changes

With time, the epidermis becomes thinner, indicated by a decrease in the number of keratinocytes and also by the decrease in size of these individual cells.[51] Paradoxically the skin squames become larger and flatter, resulting in less trans-dermal water loss and a drier looking surface.[52] Keratinocytes lose their proliferative capacity and the metabolic means to promote healing, resulting in delayed healing times. There is well demonstrated evidence that the ability to repair damaged DNA deteriorates with time and consequently a higher frequency of mutation occurs.[77]

---

* An excellent summary of this work can be found at http://nobelprize.org/nobel_prizes/medicine/laureates/2009/press.html

Age induced changes to the dendritic cells are also evident with a decease in the numbers and function of both the melanocytes and Langerhan's cells, with a less-extensive system of dendrites.[53] Loss of Langerhan's cells and a global reduction in humoral and cell based immunity has an impact in a diminished inflammatory response and an increased susceptibility to infections. Melanocytes become smaller and produce less melanin in response to UV-stimulation, so skin appears paler. Melanocyte depletion also leads to the 'greying' of the hair.[54]

Significant changes are seen at the dermal-epidermal junction, with a flattening of the rete ridges and a consequential reduction in the area of surface contact between the dermis and epidermis. This means there is a reduction in nutrient/metabolite exchange which is compounded by a reduction in the number of dermal blood vessels and capillary loops, with an associated decrease in dermal blood flow. A reduction in the number of sensory nerve endings leads to an reduced appreciation of light touch, vibration sensation, two-point discrimination and an increase in pain threshold.[54]

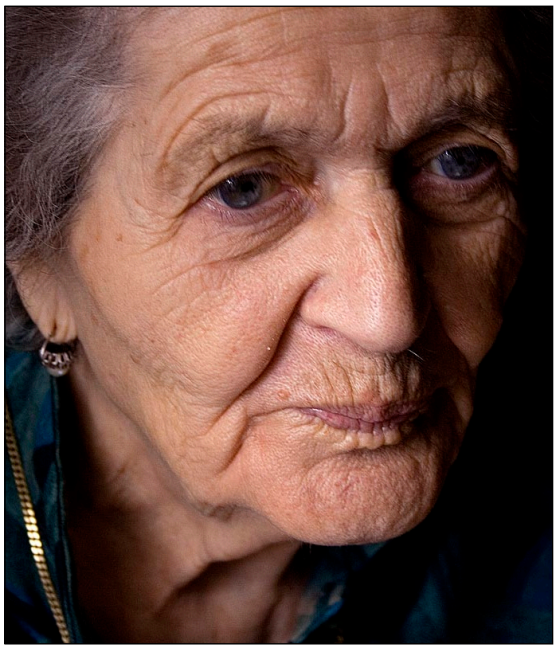

Fig 2.1 Age associated skin changes

The dermis also undergoes changes with time and there is a good deal of evidence to show that there is a loss of dermal volume associated with fewer fibroblasts and mast cells, with a reduction in the amount of ground substance and, as a consequence, water.[54] The number and replication function of fibroblasts decreases, as does the overall amount of collagen, with resultant skin easily traumatised.[59] There are also age related changes to the normally regular elastic network in the skin, with thickened, disorganized and irregular fibres becoming evident.[60,61]

Clinically the skin appears paler, drier and less radiant. Benign skin lesions also start to appear, such as seborrheoic keratoses and cherry angiomas (small benign venous malformations).

Beyond the skin there are other visible age-related changes. Loss of subcutaneous fat, bone mass and cartilage, associated with the prolonged effect of gravity and muscle action, create wrinkles and expression lines. Hair loss also occurs, characterised by the conversion of terminal hair to vellus hair.

2.2 Photoageing and photodamage

Photoageing comprises the changes in the skin that are the results of chronic sun exposure superimposed on chronological skin ageing. The term is somewhat misleading in that it implies that light has somehow aged the skin, even though nothing can cause something to age any faster than the time it has existed. However, the term has come to mean how much older excessively sun exposed skin *appears* to be in comparison to skin of a similar chronological age, which has not had excessive solar exposure.

Simply put, photoageing is how much older skin appears to be beyond its chronological age, as a result of photodamage.

This introduces the idea of photodamage as both a clinically visible result of chronic solar exposure. This is generally visible from the middle of the fourth decade onwards, but is dependent on the intensity and extent of the exposure, as well as the genetic potential of the skin to avoid accumulated damage. This can be seen with good effect in areas of high intensity solar exposure, such as Australia and New Zealand, where people with type 1 and 2 skin will show the effects of photodamage at younger ages.

2.2.1 What are the signs of photodamage?

Chronic solar exposure results in the formation of solar elastotic degenerative changes (solar elastosis) and in mechanical and pigmentary changes to the exposed skin.

Fine wrinkles are evident, particularly around the mouth and the cheeks. Wrinkles around the mouth are also associated with smoking and, in general, wrinkles are also associated with muscular spasm, habit and with normal age related changes in skin thickness and elastin content.

Pigmentary changes typically appear on chronically sun exposed surfaces of the skin. They can be patchy and uneven, with mottling of the skin which may darken on relatively minor exposure to sunlight. They may also manifest as flat brown macules, termed solar, or senile, lentigo and are common on areas such as the back of hands and forearms, the chest and the sides of the face. They can easily be mistaken for their similarity to seborrhoeic keratoses, solar keratoses and even lentigo maligna.

The skin can take on a yellow-brown sallow discolouration associated with areas of marked solar elastosis, sometimes referred to as 'citine skin', and may also appear thickened and waxy looking.

Fig 2.2 The clinical appearances of photodamage

Another familiar colour change associated with solar elastosis is an variable redness of the photodamaged skin - the so called 'ruddy complexion'. This is a background erythema, caused by tortuous dilated blood vessels (telangectasia)

and tends to be patchy, being more common in fair skinned individuals and on the cheeks of the face and the neck.

Some authors have suggested that the response to uv-induced damage can be dependent upon the skin type of the individual. Those with skin types 1- 3 display a more atrophic and dyplastic response with fewer wrinkles and smoother skin, but more actinic lesions and malignancies. Skin types 4 - 6 show a more hyperplastic response, with thickened skin, more course wrinkles, a permanently bronzed/yellow or hyperpigmented appearance with more pigmented lentigines.[93]

Histologically the epidermis shows irregular thickening and only after extensive solar exposure will it become thinner and atrophic. There is a loss of the usual structured organisation of the dermis, with changes generally occurring within the dermis at a fixed depth from the surface of the skin, at about 20-50 micrometers from the basal membrane, leaving an area of dermis just beneath the epidermis that shows signs of healing attempts and collagen synthesis. This area is called the Grenz zone. Beyond this there is a loss of the usual dermal fibrous connective tissue pattern and it is replaced by an amorphous material that forms large blobs, which stains positively for elastin. This material is, at least biologically, elastin, but lacks any of its usual structure, being disorganised and abnormal in its constituent parts.[86,87] The enzyme lysosyme is found extensively throughout sun damaged skin and, given that it inhibits elastase and collaginase activity, it may be responsible for the build up of this elastotic material.[88] Similarly, there is a decrease in collagen precursors (procollagen 1 and 3) seen in photodamage,[89] which may have an effect on the accumulative disorder of the dermis.

A widespread, but mixed and variable, inflammatory cellular infiltration of lymphocytes, macrophages and mast cells is seen in sun damaged skin. UVB realistically only penetrates to the basal layer of the epidermis and therefore can not have a direct effect on dermal changes seen in photodamage. However, its effect on the epidermis causes a release of cytokines, particularly Tumour Ne-

crosis Factor Alpha (TNF-α), which has an influence on the synthetic activities of fibroblasts and can also stimulate an inflammatory cellular response.[90] It is not unreasonable to suppose that this epidermal damage and inflammatory response may be fundamental to the solar elastotic changes.

Pigmentary changes are also seen, with the mottled and irregular pigmentation associated with uneven distribution of melanocytes and an irregular melanasome distribution. Some melanocytes appear hypertrophied through excessive stimulation, while others show no signs of active melanogensis, with a decrease in cytoplasm and a reduction in the number of dendrites.[53]

Vascular changes evolve with prolonged photodamage. Initially there is vessel wall thickening, but in severely damaged skin the vessel walls become thinned and the surrounding supportive cells decease in number leading to local dilatations, seen as telangectasia.[91] UVB has also been found to directly stimulate angiogenesis within the skin by increasing vascular endothelial growth factor (VEGF) expression.[92]

There is an increase in the number of hyperplastic dermal fibroblasts, mast cells, mononuclear cells and histiocytes, suggesting a a chronic inflammatory process occurs in photodamaged skin. It is not completely understood if this is an important part of the pathogenesis of photodamage, or simply a side-effect of UVR on the skin.[94]

Table 2.1 summarises the features of intrinsically aged and photodamaged skin.

Feature	Intrinsically aged (covered skin)	Photodamaged (exposed skin)
Clinically	Pale, smooth, looks & feels thin. Hair is grey, thin and sparse. Nails are brittle.	Irregularly pigmented, course and wrinkled. Sallow, leathery appearance with solar keratoses, lentigo and purpuric spots.
Epidermis	Thinner and flatter. Keratinocytes become smaller. Corneocytes become larger and flatter. Cell production rate decreased slightly or remains unchanged. Dendritic cells decease in number, size and activity	Initially becomes thickened and irregular, eventually becoming atrophic and thinner. Focal irregularities and dysplasia occurs. Increased cell proliferation. Irregular increase in melanocytes and melanin production. Decrease in number, size and activity of Langerhans' cells.
Dermis	Becomes thinner with increasing age, stiffer and less elastic. Fibroblasts decrease.	Can become irregularly thickened from proteoglycan deposition. Elastotic material deposited. Change in mechanical properties.
Inflammatory response	Decreased response to all forms trauma and decreased rate of healing.	Deceased vasculature with diminished inflammatory cell function.

Table 2.1 Intrinsic ageing and photodamage contrasted†

† Reproduced from Ortonne JP, Marks R. (1999) Intrinsic ageing of skin. In Ortonne JP, Marks R. (eds) Photodamaged Skin : Clinical Signs, Causes and Management. Martin Dunitz Ltd, London p93

2.3 Causes of photodamage

Photodamage is predominantly caused by solar UV radiation, though other sources of UV light can be implicated. Topical light treatments such as PUVA and sunbeds are examples, as are some some less common sources of UVR such as arc welding.

Of all these, UV radiation from sunshine is by far the most significant. Although the exact mechanisms are still a focus of much research, these factors influence the function, repair and replication of DNA, overall cellular activity and immunity.

2.3.1 Ultraviolet Radiation

Visible light, ultraviolet and infrared radiation are not energetic enough to cause ionisation of a molecule and are therefore known as non-ionising radiation. In order to have an effect on a biological systems, non-ionising radiation must be absorbed by it. Although these types of radiation are electromagnetic waves, they act as discrete packets of energy, or photons, which can interact with matter. The amount of energy each photon has is inversely related to its wavelength and the effect this has on human cells is complex, but essentially the molecule is raised to a higher, excited energy state. In returning to a more steady state that extra energy can be converted to chemical energy which in turn can result in biological alteration.[69]

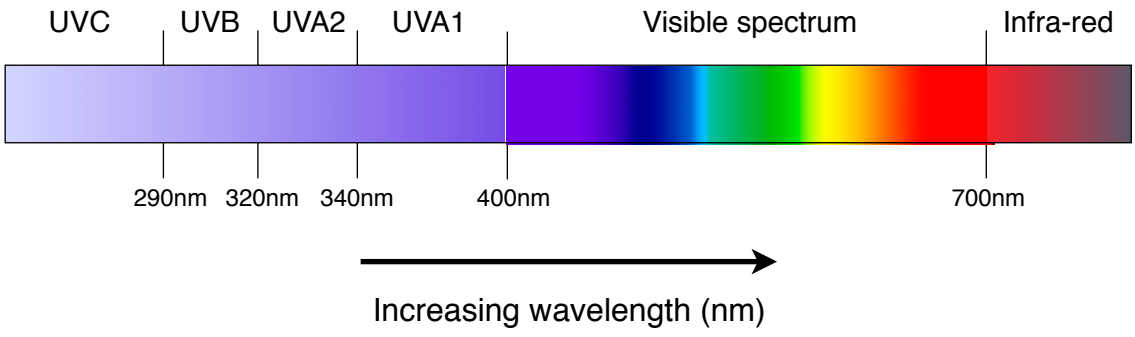

Fig 2.3 The ultraviolet, visible and infrared spectrum

UVC does not reach the surface of the Earth in any measurable amount as it is almost entirely absorbed by the ozone layer and upper atmosphere. Naturally occurring UVC is unlikely to have any effect on the skin. Artificially produced UV in the same wavelength as UVC (germocidal UV) is known to have an affect on micro-organism DNA and is commonly used for disinfection.[78] UVB is significantly attenuated by the ozone layer and upper atmosphere, such that at ground level only 4-5% of the measurable UV light is UVB and the remaining 95-96% UVA.
The effects of UVB are essentially limited to the epidermis and cause damage by the disruption of cellular DNA, resulting in a very specific and often identifiable mutation.

UVB has both immunosuppressive and DNA mutatory effects, leading to modifications in oncogene and tumour suppressor gene expression, both important factors in the initiation of skin cancers. UVB incident on the skin is absorbed by pyrimidine bases in DNA resulting in the formation of DNA photo-products. Certain areas of DNA where sequential pyrimidine bases (thymidine dimers) occur are specifically sensitive to this type of mutation.[64] This is the primary event in the initiation phase of carcinogenesis and is common in the genesis of SCC and most likely BCC also, though its effect in MM is uncertain. Unrepaired or incorrectly repaired pyrimidine bases lead to specific and consistent DNA base transition mutations, where cytosine is replaced for thymine when adjacent to one another or when in pairs (CC). This signature transition is specific for UVB induced DNA damage.

As well as direct damage to DNA, UVB induces the production of reactive oxygen species (ROS) within the cell, which consequently have the ability to induce single-stranded breaks in the DNA.[64]

UVB also induces immunosuppressive effects by influencing various cellular and tissue functions including the induction of apoptosis and decreasing the number of Langerhans' cells in the epidermis, as well as modifying their antigen-presenting capacity.

Although the majority of studies conclude that UVB is the primary UV-R protagonist in the formation of skin cancers, UVA is also carcinogenic, though not as efficient an effector as UVB, probably by quite significant levels. UVA remains important, however, as it makes up the vast majority of the incident UV-light on human skin. Whereas the effect of UVB is almost entirely limited to the epidermis, the longer wavelength of UVA also penetrates into the dermis, thereby having effect on both dermal and epidermal elements.

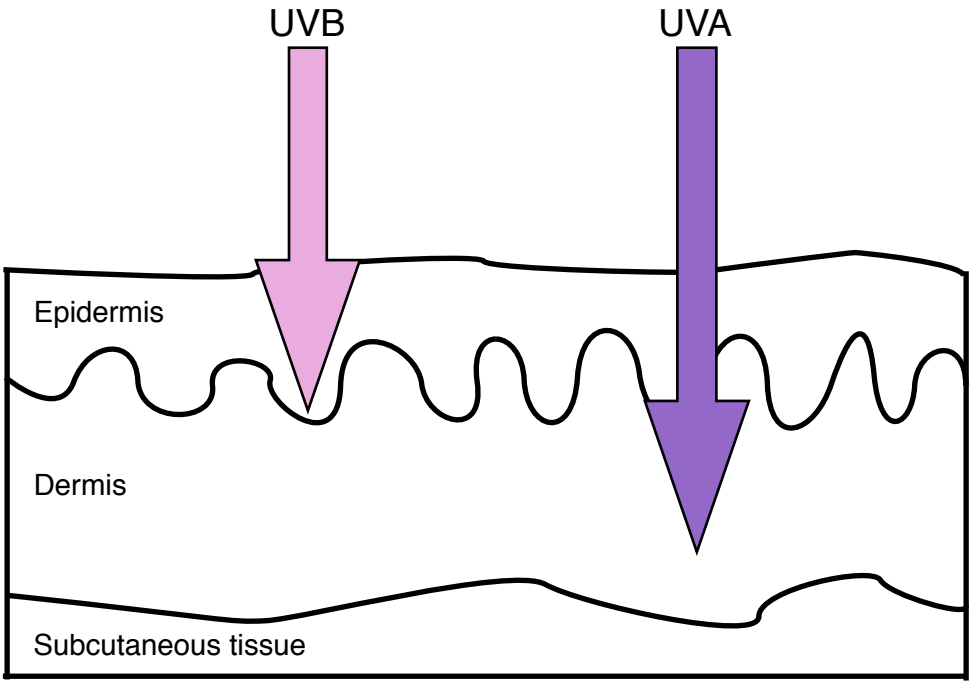

Fig 2.4 Ultraviolet light penetration of the skin

The mutatory effect of UVA is not limited to its direct damage to DNA as it can produce a persistent genomic and cellular stress through the formation of reactive oxygen species (ROS) from non-DNA elements which become sensitised. ROS such as hydrogen peroxide (H_2O_2) and singlet oxygen (O^-) can lead to DNA damage, breaks and eventual mutation. The major UVA induced ROS is 8-hydroxyguanine, which is highly mutagenic. These ROS can be produced within 15 minutes of UV exposure.[62] They also causes increased activity of the activator protein AP-1, leading to up-regulation of matrixmetalloproteinases (MMP's), both of which cause collagen breakdown and remain elevated for up to 24 hrs after UV exposure.[63] UVA also induces immunomodulatory effects, though through different mechanisms than from UVB.[65]

The effect of UVA and UVB in the transition of photodamaged skin to the carcinogenesis of skin is mainly related to their effect on the p53 tumour suppressor gene, which is the most commonly mutated tumour suppressor gene and shows characteristic mutations associated with UVR. Its mutated form is found in more than 50% of breast, colon and lung cancers and in more than 90% of squamous cell carcinomas (SCC) and the majority of basal cell carcinomas (BCC). p53 normally functions as a regulator of cell cycle progression and apoptosis (programmed cell death). Expression of p53 is induced by DNA damage resulting from UVR and through further gene activation it halts the cell cycle to allow DNA repair prior to replication. If the DNA is significantly damaged, it will institute apoptosis. If the p53 gene becomes damaged, the cell cycle would not be arrested and apoptosis would not occur, allowing DNA mutations to be retained, duplicated and potentially lead to carcinogenesis.[65]

PTCH tumour suppression gene mutations are also common in hereditary and sporadic BCC genesis. The PTCH gene appears to be responsible for cellular proliferation and differentiation such that the loss of its function can lead to unregulated cellular proliferation and ultimately carcinogenesis.

The effect of UV light on melanocytes is more complex and the effect on p53 in melanocytes is less dramatic than in keratinocytes. Malignant melanoma (MM) risk appears to be related to more intense, but intermittent exposure to sunlight, specifically during childhood, rather than the more chronic exposure seen to induce photodamage. It has been suggested that UVR may only be an initiator for cellular damage which leads to MM and is not required in a prolonged fashion for carcinogenesis as for other skin cancers. This would explain why a significant number of MM occur in areas of relatively low solar exposure. MM is also clearly a tumour which has complex genetic background. Familial MM has known defects in the CDKN2A tumour suppressor gene, but the same defect has also been found in sporadic MM. Other tumour suppressor genes and proto-oncogenes have been identified in MM, highlighting the complex nature of this condition.[71]

2.3.2 Genetics

There are many genetic conditions which affect the skin and of those relevant to this thesis are some which predispose to excessive photodamage by failure of the normal mechanisms of cellular protection and repair.

Albinism is a genetically recessive condition characterised by a partial or total absence of melanin pigment in the eyes, skin and hair. Melanocytes are present, but are unable to produce melanin to varying degrees due to decreased or absent Tyrosinase activity, the enzyme required for melanin production.

There are 2 main categories of albinism in humans:

1. Oculocutaneous - where pigment is lacking in eyes, skin and hair, ranging from total absence to the presence of near normal levels
2. Ocular - where only the eyes lack pigment, but again may be anywhere from total absence to almost normal levels.

Fig 2.5 Oculocutaneous albinism

The condition significantly predisposes the individual to non-melanoma skin cancer formation, predominantly from ultra-violet radiation.[161]

Xeroderma pigmentosum is a rare, autosomal recessive condition affecting men and women of all races equally. It is characterised by photosensitivity, premature skin ageing, pigmentary changes and skin neoplasia. There is an abnormality in DNA cross-link repair mechanisms, so solar induced damage to these elements are unable to be repaired and accumulated damage leads to the development of malignancy at an early age.[160]

Basal cell naevus syndrome (Gorlin's syndrome) is a rare autosomal dominant disorder which is present in all races and ethnicities. Defects to the PTCH tumour suppressor gene, involved in cell growth control and the regulation of development, lead to the early and regular development of BCC, more often seen in paler skinned individuals and those exposed to significant UVR.[163]

2.3.3 Other causes of photodamage

There is increasing evidence that other factors like infrared radiation, tobacco smoke and ozone may contribute to extrinsic skin ageing.

Infrared radiation easily penetrates all layers of the skin and makes up the abundance of energy radiated from the sun. It induces ROS formation and has also been linked with the production of solar elastosis.[79]

Tobacco smoke has long been associated with premature skin ageing, particularly wrinkling.[80] It has been shown that the synthesis of new collagen fibres is significantly decreased by smoking, along with procollagen types 1 and 3.[81] There is also an increase in protolysis of collagen fibres associated with abnormal MMP activity,[82] a decrease in elastin and an enhancement in elastotic activity.[83] Studies looking at the relationship between skin cancer and smoking suggest that there may be a link, showing up to a 50% increased risk of SCC compared with non-smokers and increased with both duration and amount smoked. It is specifically linked with intra-oral SCC and SCC of the lip. There appears to be no clear link with smoking and BCC.[69]

Although ozone protects our planet from from excess UV exposure when present in the stratosphere, it is a highly reactive oxygen species and has a damaging effect to biological systems at ground level. It is readily created from nitrous oxides and volatile organic chemicals from industry and car exhausts in a reaction with sunlight and studies have shown ozone can create oxidative stress in superficial and deep skin layers and also depletes vitamin E and C, [84,85] both natural anti-oxidants.

Some drugs can also have side effects as skin photosensitizers. Antiarrythmic drugs like amiodarone, thiazide diuretics and the antibiotic doxacyclin are just a few that can make the skin more sensitive to UVR, causing erythema, itching and scaling.

At this point it can be seen that the same mechanisms which lead to photodamage are also those that lead to potential malignant skin change. In fact, photodamage can be seen as the accumulation of solar induced damage within the skin that can potentially lead to the development of premalignant and malignant skin lesions.

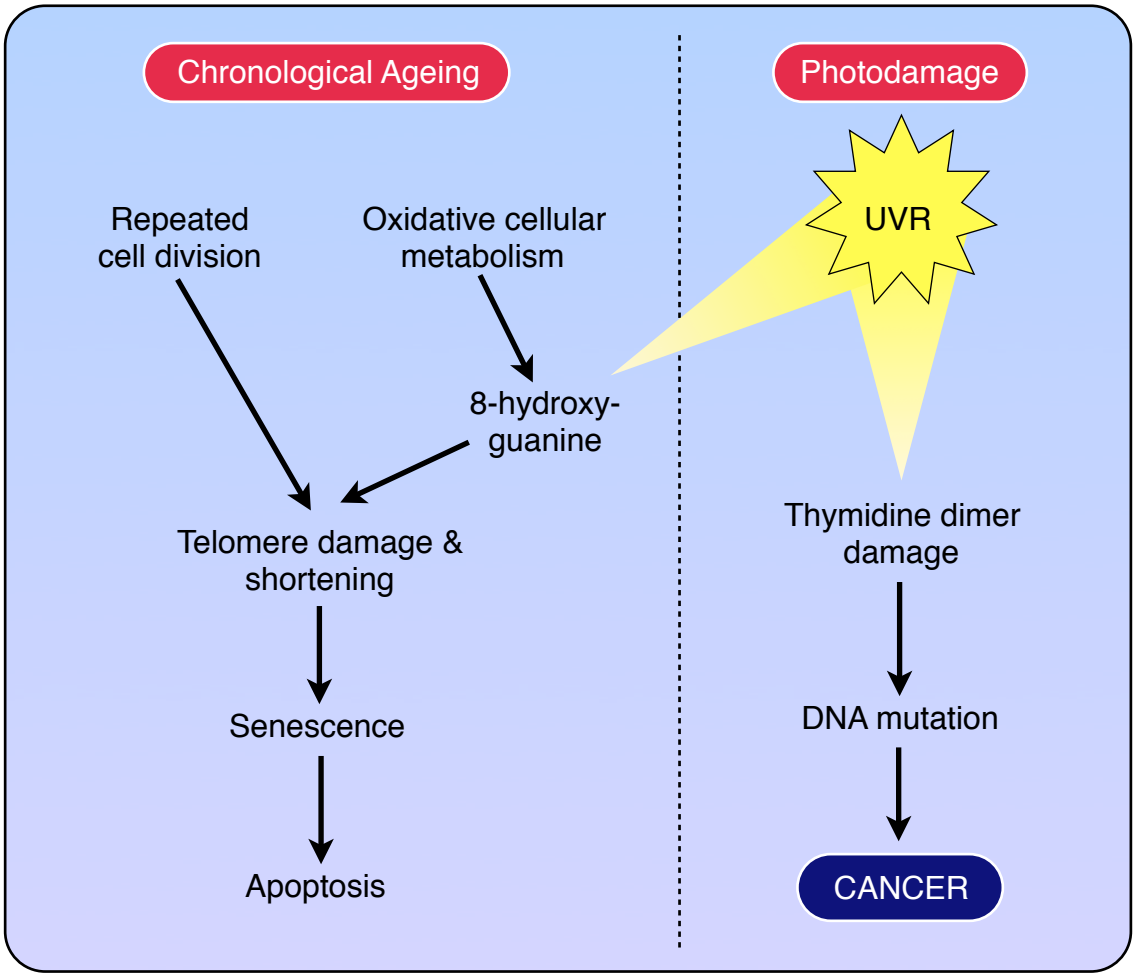

Fig 2.6 Hypothetical common pathway of photodamage and chronological ageing ‡

‡ modified from Krutmann J, Gilchrest BA. (2006) Photoageing of skin. In Gilchrest BA, Krutmann J (eds) Skin Ageing. Springer, Berlin, p35

2.4 Photodamage and skin cancers

In this section we return to look at the effects of UV light exposure on the skin as the predominant initiator of photodamage, with specific attention to how the changes in the appearance of the skin can be related to its potential for malignant transformation.

When an entire area of the skin has been exposed to the same stimulant, the whole area undergoes similar changes due to that stimulant. The term 'field change' can therefore be applied to the overall effect on the whole area. We know that within this area of damage, continued cellular stresses can occur such that a skin cancer may originate. However, within a field exposed to the same cellular stresses, it is down to chance that a cell, once damaged, may remain that way or goes down the route of malignant transformation. In relation to this thesis, the concept of field change as a measurable entity is important, as it underpins the quantification of photodamage.

The aetiological factors that underpin the development of skin damage and cancer formation are multiple and interrelated, a combination of genetic propensity to skin damage (endogenous) and exposure to external factors (exogenous). Involvement can be multi-factorial and changes are spectral.
There are classically 4 stages of oncogenesis:

1. Initiation is where the stimulant causes genetic damage resulting in mutation that alters control of cellular differentiation or proliferation.
2. Promotion is the expansion of the cell population, thought to be epigenetic in nature (inherited changes in gene function, without changes in DNA sequencing).
3. Progression and;
4. Conversion are categorised by cells with large amounts of genetic instability, chromosomal abnormalities, surface substance expression and oncogenetic activity.

If a cell goes down the route to malignant transformation, the resulting lesion will depend on the cell-lines affected, the majority of which will fall into two main categories - keratinocytic or melanocytic lesions. What follows is a description of the more commonly accepted sun induced skin lesions, which may spontaneously occur if photodamage is allowed to progress unchecked.

2.4.1 Actinic Keratosis

The term actinic keratosis (AK) is a fairly recent description of lesions previously described as solar and senile keratosis. Since UV of any source can cause them (solar radiation, tanning beds, UV phototherapy), the term 'actinic' is used to describe all forms of UV induced keratosis and at any age. Most people will develop AK given enough UV exposure and enough time, but there is a genetic predisposition to those with easily UV damaged skin (fair skinned, blonde haired, blue eyed). They are becoming increasing common due to lifestyle and social changes leading to greater and more intense UV exposure. Improvements in medical science through the use of immunosuppressive drugs in the control of auto-immune and inflammatory conditions, in the transplant and cancer populations, and the associated longevity of these improved techniques, mean that the prevalence is increasing.

AK tend to occur on sun (or UV) exposed areas of skin and appear as rough, macular, epidermal lesions, ranging in size from pinpoint lesions to large plaques. They may appear well circumscribed or blend into the skin and can be pigmented, erythematous, skin-coloured or any colour in between. They tend to be thicker on the hands and arms and may form horns on any area of the body. They mainly appear hyperkeratotic, but atrophic, lichenoid and Bowenoid variants are also seen.

AK are epidermal neoplasms, consisting of altered epidermal keratinocytes, and there is continued debate as to whether they should be classified as premalignant disease or an early form of in-situ carcinoma. The risk of an individual lesion becoming an invasive carcinoma is estimated as anything from 0.1% to 20%, though the exact number is a consequence of time.[111,112] Therefore,

given enough time and if left untreated, it is possible that any AK could become SCC and an alternative name of keratinocyte intraepidermal neoplasia (KIN) has been suggested to reflect this potential malignant progression to SCC.[133]

Fig 2.7 AK appearing as multiple lesions in an area of field change on a scalp, as a keratin horn and as an individual lesion

UV irradiation is the predominant causative factor, but the exact mechanism of damage, and whether it involves only the epidermis or dermis also, is not completely understood. However, AK's do contain similar changes to those found with invasive SCC, namely damage to DNA thymidine dimers and the p53 tumour suppressor gene. There can be a delay of several years in the development of an AK following UV damage and it is unclear if the progressive immunosuppression due to sunlight exposure and ageing are involved along with the formation of an abnormal clonal collection of damaged cells.
Differential diagnosis can be difficult and often biopsy is required for diagnosis. Keratotic AK can closely resemble early or well differentiated SCC and although spontaneous regression has been seen in some traumatised lesions, they tend to persist and if left untreated, the concern is that they can progress to invasive SCC. Importantly, their presence also indicates significant photodamage and serves as a risk indicator for other cutaneous malignancies.

Reports have suggested that up to 25% of AK may regress with simple sun protective measures,[134] but in general treatment is necessary. Given that the lesions are confined to the epidermis (by definition they do not penetrate the basement membrane), methods are usually conservative and cosmetically acceptable. They are adequately treated with curettage, electrodessication (cau-

tery), cryotherapy with liquid nitrogen, topical chemotherapy agents, photodynamic therapy (PDT), ablative laser therapy or surgical excision.

2.4.2 Radiation-induced keratosis

Pre-malignant keratoses can be induced by therapeutic or diagnostic ionising radiation and has been seen in the treatment of internal or cutaneous neoplasms, benign skin tumours or inflammatory conditions. The potential to malignant change is related to the dose of radiation given and the latent period can be up to 30 years. Keratosis formation is preceded by a radio-dermatitis, similar to chronic sun exposure. The clinical and pathological presentation of the keratoses are identical to those seen in AK, though malignant lesions arising from them may be more aggressive.[113] Agreed guidelines for management and follow-up exist and treatment is as for AK.

2.4.3 Bowen's disease

Bowen's disease is characterised by atypical epithelial cell proliferation, recognised as an intra-epidermal neoplasia occurring on sun-exposed or non-sun-exposed skin (lesions analogous to Bowen's are seen on mucosal surfaces such as erythroplasia of Queyrat on the glans penis). It is clinically and histopathologically distinct from in-situ SCC, though the processes are related. When seen on sun-exposed areas, it is associated with surrounding actinic damage and sometimes BCC and SCC. It appears as a slowly enlarging, discrete, slightly scaly, erythematous plaque with a well defined but irregular border. Surface characteristics can vary from hyperkeratotic to variable pigmentation and even ulceration.

Fig 2.8 Bowen's disease

Some controversy exists between the separation of Bowen's from non-Bowen's squamous intra-epidermal neoplasia (SIN), with the latter possibly a transitional phase between AK and SCC.

Studies have suggested that the risk of invasive carcinoma in Bowens disease is 3-5%.[98,99] Other studies have looked at links between Bowen's and non-Bowen's SIN with internal malignancy and although there does appear to be an varied frequency of internal malignancy in these patients, no relationship to the subsequent development of internal malignancy has been shown.[97]

Bowen's disease has been linked to various causative agents including actinic damage, viruses, radiation therapy and arsenical ingestion, while non-Bowen's SIN has been linked to actinic damage. Diagnosis is confirmed by skin biopsy, showing full-thickness epidermal dysplasia and marked atypia, well demarcated from from adjacent, normal epithelium and an intact basement membrane. Non-Bowen's SIN has less nuclear changes and atypia, with no demarcation and normal epithelium. Management is as for AK and revolves around accurate diagnosis, relevant treatment and review.

2.4.4 Basal Cell Carcinoma

Basal cell carcinoma (BCC) is the most common cancer occurring in man, accounting for 75-80% of new skin cancers.[114] The true incidence is difficult to put an exact figure on, mainly due to the underreporting of cases in cancer registries. Current UK guidelines means that an individual is only registered once as having a BCC, regardless of the number of BCC's they may develop over a lifetime. Many BCC's are also managed without histological diagnosis and so would never be presented to the cancer registry. This under-reporting is recognised for all non-melanoma skin cancers and is reflected in the cancer registry statistics produced by the Office of National Statistics (ONS), where they disclose that this is a problem across Europe, Australasia and the USA. 2006 statistics showed that there were 67,042 reported cases of non-melanoma skin cancer in the UK. Accurate incidences are difficult to produce, but a UK rate of about 100 cases per 100,000 population has been quoted,[100] although it is significantly higher in other parts of the world.

Death is rare from BCC, but they can be locally destructive if ignored and morbidity can be significant if diagnosis is delayed. Metastasis is very rare, esti-

mated at between 0.0028% and 0.1%.[115,116] A high incidence and necessary intervention mean that they are a significant health problem, not only at the level of patient well-being, but also in terms of the cost implications across the whole population. In the past decade, significant increases in incidence have been noted in Australia, Europe and USA. Although BCC is more common in men, this sex differentiation is reducing, perhaps as a consequence of the changing opinion in society towards clothing and sun exposure. Indeed, societies attitude towards sun-exposure and the 'healthy tan' are undoubtedly one reason behind the increase in incidence of BCC in young adults.

BCC was first described by Krompecher in 1903, suggesting that they arise from epidermal basal cells, although subsequent theories have suggested the site of origin as adnexal structures such as hair follicles, pilosebaceous cells and the pluripotent epithelial basal cells.[117,118,119] Histopathologically, most BCC appear to arise from the epidermis and hair follicles and whether BCC arise from pluripotent cells or adult basal cells may be academic, as epidermal basal cells and the germinative cells of adnexal structures all share a common progenitor.[120,121] This would imply a common genetic code which, although repressed, could undergo de-repression by some stimulus into a pluripotent state. This way a relatively well differentiated basal cell could become more 'primitive', or show differentiation towards related, adnexal-type structures. Even the carcinoma suffix has been debated as the incidence of metastasis is so rare, with many preferring to describe BCC as epitheliomas, naevoid tumours or hamartomas.

The most common factor involved in the development of BCC is ultraviolet light. Predominantly at risk are those fair skinned people who burn easily, tan poorly and those who live closer to the equator. The protective role of skin pigmentation is well demonstrated in coloured individuals with albinism, who develop BCC and other non-melanoma skin cancers from a young age, in contrast to those with normal dark pigmentation who rarely develop them. Cumulative exposure to UV appears to be influential in the development of BCC, though recent work has also suggested that intermittent, intense exposure early in life

(like with melanoma), may be a risk factor.[122,123] Areas affected are predominantly the head, neck and forearms, but up to 20% of BCC occur on areas of skin not exposed to the sun, with a third on areas of relative less exposure.[123] The quality and thickness of clothing must be considered when interpreting these figures.

When BCC are examined microscopically, the number of mitotically active cells would suggest a highly active and rapid growth phase, and this is supported statistically. However, clinical observation shows a relatively slow growth rate and this may be explained by the fact that BCC go through growth and regressive phases. Whichever phase predominates determines the rate of tumour growth.[124] In addition, cell death rates via apoptosis can control the rate of tumour growth.[125] BCC produce angiogenic elements to supplement a necessary growth rate and also produce prostaglandins and collagenases to suppress immune responses and promote infiltrative tumour growth.[126,127]

There are various clinical variants of BCC and classifications can vary among texts. The tumours may exhibit characteristics of multiple varieties making a single clinical and histological classification difficult. Recognised forms are:

1. Nodular
2. Superficial
3. Morphoeaform
4. Cystic
5. Infiltrative
6. Basosquamous
7. Pinkus Variant

Nodular is the most common variant, accounting for 60% of primary BCC. The lesions are typically a small, well defined, pink or red nodule with a 'pearly' appearance and overlying telangectasia. Although slow growing they can reach significant size and are locally very destructive, coining the historically descriptive phrase 'rodent-ulcer' by virtue of appearing like tissue 'gnawed by a rat'. As the lesion enlarges ulceration may develop in the centre, but the raised, telangectatic border typically persists. Melanin pigment may also be present to vary-

ing degrees, as random flecks of colour or an even, deep, blue/black pigmentation of the entire lesion.[164]

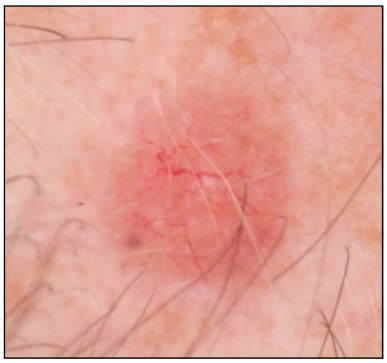

Fig 2.9 Nodular BCC showing telangectasia

Superficial variant BCC are most often found on the trunk and extremities. They are generally flat and pink/red and there may be a slight scaliness to some of them, with areas of spontaneous regression seen as atrophy and hypopigmentation. They can vary in size from a few millimeters to several centimeters and can occur multiply. This size can be explained by the fact that the primary growth pattern is in a lateral direction, but with time they can invade deeply, ulcerate and form nodules. Recurrence rates can be high, explained by extensive sub-clinical spread and by involvement of hair follicles and subsequent 'budding' from them after topical treatment.[164]

Morphoeaform BCC is derived from its clinical similarity to a plaque of morphea (localised scleroderma). They appear to be ivory coloured and indurated, sometimes with overlying telangectasia. Morphoeaform BCC is noted for its sub-clinical spread and high recurrence rates.[164]

Fig 2.10 Cystic BCC

Cystic changes within a BCC are not always obvious and many cystic BCC appear as a typical nodular BCC. If changes become significant then these lesions may appear truly cyst-like and exude a clear fluid if damaged.[164]

Infiltrative BCC account for up to 20% of primary BCC and are notorious for their destructive and aggressive behaviour, with sub-clinical spread and high recurrence rates. Early diagnosis is important for good control. Clinically they appear as flat or slightly raised plaque-like lesions and may be firm and morphoeaform-like. Importantly,

they are relatively ill-defined in comparison to other BCC variants, meaning great care must be used in considering their management.[164]

Basosquamous BCC is primarily a histological variant with no obvious clinical features to differentiate it. It deserves mention here, however, as it behaves more like an SCC than BCC, being much more aggressive, recurrent and likely to metastasize, estimated at up to 9.7%.[128] The more squamoid a tumour appears microscopically, the more likely they are to metastasize.[164]

Pinkus is a rare variant of BCC that tends to appear as a bland, smooth, slightly red, firm nodule, that can sometimes be pedunculated and clinically looks like a fibroma.[164]

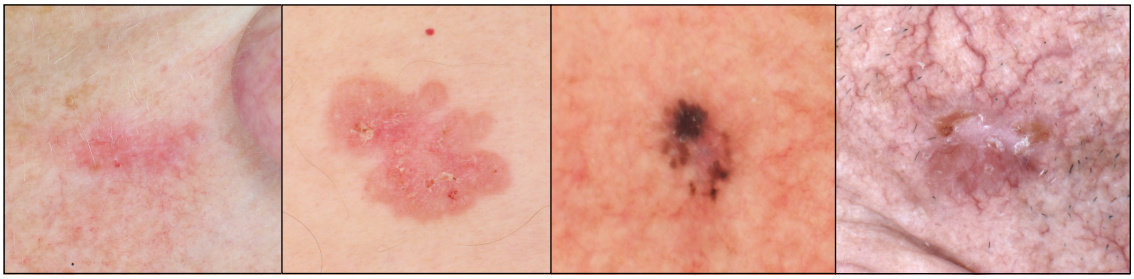

Morphoeic BCC | **Infiltrative BCC** | **Pigmented nodular BCC** | **Superficial BCC**

Fig 2.11 Other examples of BCC subtypes

BCC rarely metastasize, in-vitro studies have shown them to be highly dependent on a fibrous stroma for survival. This surrounds the islands of dependent epithelioma cells and it is this very dependence which may limit their metastatic ability.[129] How some BCC acquire the ability to metastasize is not fully understood, but the development of clonal cells with metastatic ability, or immunomodulation has been suggested.[115] The primary lesion of metastatic BCC is generally a long-standing, treatment resistant lesion on the head and neck which tend to be extremely locally invasive with areas of neural and vascular invasion. Spread most commonly occurs via lymphatics to local lymph nodes, but also via bloodstream to lung and long bones.

Although metastasis is rare, BCC can be locally very destructive. Growth tends to follow the 'path of least resistance', with invasion of bone, muscle or cartilage at a late stage. The tumour tends to spread around them on perichondral, periostial or fascial planes. Dermis also acts as a barrier to invasion, so on the back where dermis is thick, lateral tumour growth is more common in the looser superficial layers. Invasion of sub-cutaneous fat is rare due to its poor blood supply and perineural or perivascular spread is usually only seen with highly aggressive, infiltrative tumours.[130]

Fig 2.12 Nodular ulcerating BCC

Management of BCC revolves around the principle of making the patient tumour free. A positive diagnosis can be achieved from adequate lesion biopsy if clinical diagnosis is uncertain and surgical resection with margin control provides the most reliable method of ensuring total tumour removal. Mohs micrographic surgery§ is an effective method for poorly defined, infiltrative or morphoeaform lesions, disease in high risk areas, recurrence or when tissue preservation is important. Further destructive methods that offer no margin control are easy and popular, but are best used for low grade tumours in areas of low sensitivity. Curettage, electrodessication, cryotherapy, laser ablation, photodynamic therapy (PDT), radiotherapy, topical chemotherapy or immune response modifiers are all recognised and effective methods. The skill of the clinician is in choosing the right management for the patient at the correct time.

2.4.5 Squamous Cell Carcinoma

Cutaneous squamous cell carcinoma (SCC) accounts for 10-20% of skin cancers and is the second most common form of skin cancer type behind BCC. Epidermal keratinocytes undergo malignant transformation and there is a strong association with cumulative UV-exposure, predominantly affecting eld-

§ Mohs surgery is a technique pioneered in 1936 by Frederic E Mohs that was modified by in the 1970's by Perry Robins. It is a method of excision where all of the excision margin is histologically analysed to ensure total tumour removal. 5-year cure rates vary from 96-99.8% [101]

erly, white, male populations. If left untreated, tumours can become aggressive and local tissue destruction can be extensive. Due to a high rate of recurrence and metastasis, SCC accounts for the majority of deaths attributed to non-melanoma skin cancers. As with BCC, incidence is difficult to predict due to under-reporting seen on a global scale. In the UK the ONS records that 67,042 non-melanoma skin cancers were recorded in 2006, but more importantly, there appears to be a continued rise in the incidence of SCC reported across the globe.[102] After having one SCC, the 3-year incidence for developing another has been estimated at 18%.[131]

Another population particularly at risk are the immunocompromised. This immunosuppression may be either acquired (disease related - CLL, HIV, renal failure) or iatrogenic (drug induced - rheumatoid, transplant). Transplant patients are at significant risk of developing skin cancers, specifically SCC. Indeed, the usual incidence of SCC:BCC seen in the general population, which is in the range of 1:2-4,[103,104] is reversed in this population.[105]

The development of SCC is influenced by both genetic and environmental sources described earlier in this chapter, but as with BCC the most significant factor is UV light exposure. Over 80% of SCC are found on sun-exposed areas (head, neck and upper extremities), with incidences higher in paler skinned groups with little melanocytic protection to UV, as is evident in African albino cases. Statistics from around the globe suggest that as with BCC, populations with poor genetic protection living closer to areas of high UV-intensity over long periods of time, will develop more SCC. Other oncogenetic factors associated with SCC are discussed earlier in this chapter.

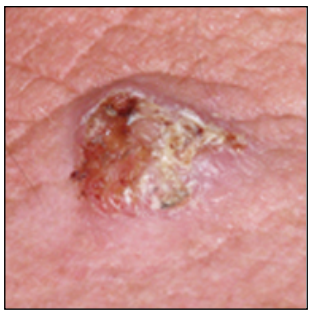

Fig 2.13 A well differentiated SCC

Presentation is dependent on site and clinical setting. As mentioned, they are found mainly on sun exposed areas, with 70% alone on the head and neck and 10-15% on the upper limbs.[132] A smaller group is found in sun-protected areas,

such as the genitalia and buttocks, indicating a multi-factorial influence in the genesis of this type of tumour. In the majority of cases SCC will develop within a background of solar damage and are strongly associated with the presence of AK. Early SCC are easily mistaken for keratotic AK and rapid growth, erosion and pain are often early signs of malignant transformation. As tumour growth progresses, there is an increase in size and thickness resulting in a more palpable, firm appearance. More advanced tumours will be nodular and can ulcerate and become painful. The rate of growth is very much dependent on the grade of tumour, with more aggressive features being seen in the more poorly differentiated tumours. SCC in darker skin individuals is rare and essentially isolated to the elderly, occurring more frequently in sun-protected areas. Unfortunately due to late presentation and diagnosis, mortality has been reported as high as 18.4%.[135]

Fig 2.14 Squamous cell carcinoma on the hand

Within the head and neck group, SCC of the lip is generally more aggressive than other areas, with lymph node metastasis in up to 20% at presentation.[136] Anogenital SCC also tend to be aggressive, again possibly due to a later presentation and delayed symptoms.

SCC metastasizes primarily via lymphatic spread and recurrent disease is often present at this time, with distant spread rare without regional nodal involvement. 5 year survival with regional metastasis is poor at only 25%. The overall risk of metastasis is 2-6%, but may be as high as 47.3% depending on various clinical and histological characteristics such as size, differentiation, immune status and depth of invasion.[137]

SCC may be histologically categorised as either well, moderately or poorly differentiated depending on how closely it resembles the cells it originates from. The prognosis for poorly differentiated tumours is significantly worse than for well differentiated. Other factors like vascular, lymphatic and perineural in-

volvement are associated with high recurrence and metastatic rates and so are important considerations for management and prognosis. Most metastatic tumours are well differentiated, due to greater numbers, but a greater percentage of the poorly differentiated variety will metastasize (17%) compared with well differentiated (0.6%).[138]

Fig 2.15 A poorly differentiated SCC

As with BCC, treatment modalities must respond to the primary concern of making the patient disease free. Recurrent lesions are harder to cure due to the high metastatic rate (42%),[132] so the first chance is the best chance at cure. Methods of treatment are as for BCC, with surgical resection with margin control being widely accepted as the best method, but radiotherapy can be a valuable treatment for certain patients. Multiprofessional guidelines on management have been are published and the interested reader may find them at the British Association of Dermatologists website.**

2.4.6 Variants of SCC

There are various histological variants of SCC, though clinical diagnosis of these variants is impossible. They include spindle cell SCC, adenosquamous SCC, acantholytic SCC and verrucous carcinoma.

Keratoacanthoma (KA) is widely considered a variant of SCC, but deserves special mention here as it can often be clinically distinguished from SCC, while sometimes histological differentiation can be difficult. Clinically it is a dome, or volcano, shaped exophytic nodule of 1-3 cm in diameter, with a central keratin 'plug'. It tends to occur on sun-exposed areas in white males, or in areas of trauma and inflammation. KA rapidly develops over several weeks then stabilises in size before

Fig 2.16 Keratoacanthoma

** http://www.bad.org.uk

spontaneous involution occurs over several months or even years. Persistent tumours can be locally destructive and disfiguring. Histological diagnosis can sometimes be difficult and there is controversy over whether they are best classified as a 'self-healing benign tumour' or as a true malignancy. Current thinking suggests KA should be regarded as a variant of SCC and excised rather than managed by prolonged monitoring.[139] Many pathologists prefer to classify them as well differentiated SCC of a keratoacanthotic-type.

2.4.7 Less common keratinocytic tumours

Pre-malignant keratoses due to exposure to arsenicals (arsenic based compounds) occur mainly on the volar surfaces of acral skin, due to topical exposure from compounds such as insecticides, fungicides and herbicides, or by chronic exposure to tar, pitch, coal, soot and mineral oils. They present as multiple (sometimes in the hundreds), hyperkeratotic, punctate lesions, growing to reach a stable size and must be distinguished from common warts. Rapid change and growth can indicate SCC change, which occurs in up to 5% of patients.[113] Lesions occur within skin which also shows other related changes and are generally becoming less frequent with improving industrial worker protection. Treatment is for symptomatic lesions, or those growing rapidly and is similar to that of AK.

2.4.8 Predisposing conditions

Many cutaneous diseases and inherited conditions are associated with photosensitivity and the potential to develop epithelial neoplasia.
Albinism, xeroderma pigmentosum and epidermodysplasia verruciformis have previously been mentioned.

Transplant patients are iatrogenically immunocompromised and have long been known to develop multiple warts that can be associated with malignant change. Skin cancer is the fourth most common cause of death in these patients, though absolute numbers remain low.[76]
Scars resulting from chronic irritation to the skin or multiple injuries are known to develop malignant epithelial tumours, specifically SCC. Burns, chronic

wounds and infections have all been known to develop SCC falling into two variant groups, described by Headington and Callen. One shows very aggressive growth with early metastases and a high morbidity and mortality, while the other with rare metastatic potential and easily cured with excision.

2.4.9 Malignant Melanoma

Malignant melanoma (MM) is perhaps the most well know and dangerous of the skin cancers. It accounts for 3-4% of the incidence of all skin cancers, but approximately 80% of deaths caused by skin diseases.[106] The incidence of MM continues to rise in all areas of the world, with estimates in USA of a 5% annual increase. Worldwide the average incidence has tripled in caucasian communities in the past 20 years and in the UK the incidence of MM has doubled in the last 10 years (Cancer Research UK 2007). In 2004 the estimated lifetime risk of developing an invasive MM in USA was 1 in 65, by 2010 this is expected to be 1 in 50. If in-situ disease is included, the risk is about 1 in 37.[106] It is clear that MM represents a significant and growing public health issue worldwide.

MM is predominantly seen in adults but can occasionally presents in children, although these are usually associated with risk factors such as xeroderma pigmentosum, congenital naevi, familial dysplastic naevus syndrome, familial melanoma and immunosuppression. Approximately 35% of MM arise within pre-existing melanocytic naevi,[108,109] with the remaining majority arising de novo. Other conditions with an increased risk are giant congenital naevi (3-18% undergo malignant transformation),[110] dysplastic naevi (2-12 fold increase in malignant change)[140] and, rarely, blue nevus.

Patients who have a melanoma have an increased risk in developing a second, independent, primary melanoma. This is estimated at some 10-25x the risk for an individual with no previous melanoma history,[141] but is contentious within scientific literature and when all factors are taken into account, it may tend towards the lower end of these numbers.

Familial melanoma accounts for some 5-10% of cases and patients are often younger than those developing sporadic MM. Studies of susceptible families have shown links with specific genetic mutations on chromosome 9p21 in the p16, CDKN2A and CDK4 gene locus.[142] Patients with these gene mutations have a 30-70x increased risk of developing melanoma than the general population.[143]

As with other skin cancers, aeitiology is multi-factorial with both genetic and extrinsic influences, but UV light is the predominant initiating agent.[107] As discussed previously, melanoma pigment protects against the effects of solar radiation and so MM is rare in dark skinned races and more common in UV susceptible people (skin types 1 and 2). Epidemiological studies have also shown that melanoma does not correlate with outdoor occupations, but rather with higher income and indoor occupations.[144]

It is suggested that melanoma is more associated with sporadic, intense episodes of sunlight and particularly with episodic severe sunburn in childhood, than with chronic life-long sun exposure, which is more associated with a related condition, lentigo maligna (melanoma).[145] This would imply that solar naive individuals are most likely to experience sunburn while on holiday and put themselves at higher risk of developing a future melanoma. Some corroboration may be implied when we consider that the most common site for melanoma in men is on the back, an area not usually exposed unless on holiday.

There is some disagreement about how melanoma develops and evolves, although a suggested pathway was proposed by Ackerman and has been widely accepted as the best current model.[146,147] He postulated that an oncogenetic stimulus, typically UV-radiation, occurs within one or more melanocytes at the dermo-epidermal junction. These melanocytes start to proliferate, appearing as a macule and with time coalesce into small nests. Proliferation progresses and these clonal melanocytes fill all levels of the epidermis, visible as irregular pigmentation. Adnexal structures become involved and with further progression the melanocyte nests start to invade the papillary dermis, propagating through-

out it. This propagation throughout the epidermis and papillary dermis is described as the ‘radial growth phase’ of the tumour and at this level, it is thought that melanomas do not have the biological ability to metastasize.[148] Typically lesions are 6mm in diameter at this stage and display all the recognisable features of a MM. If left untreated, invasion of the reticular dermis will occur, followed by sub-cutaneous fat. This more extensive growth pattern is termed the vertical growth phase, where tumour cells become much more biologically active and can metastasize.[149] Nodules will be obvious now as well as features like ulceration and variegation of colours, caused by differing degrees of regression. True ulceration (defined as a neoplasm that outgrows its blood supply leading to necrosis) is a relatively late sign related to thick tumours with high mitotic rates and a high risk of metastasis. Metastasis occurs via lymphatics and blood and can effect all areas of the body.

Four major sub-types of melanoma are recognised:

- Lentigo Maligna
- Superficial spreading melanoma
- Acral lentiginous melanoma
- Nodular melanoma

Lentigo Maligna (LM), also known as a Hutchinson's melanotic freckle, is typically seen on the chronically sun-exposed areas of skin of the elderly, the face being the most common site. It is a relatively uncommon variant accounting for approximately 4% of cases in the USA and there is strong correlation with increasing age, typically presenting in the sixth and seventh decades of life.[150] Atypical melanocytes are seen singularly and in nests dispersed irregularly throughout the epidermis.[151] Macroscopically they appear as an irregularly shaped and pigmented, slowly growing macule with areas of hypopigmentation indicating regression. In-situ lesions can be present for 10-15 years before invasive nodular melanoma transformation can occur (lentigo maligna melanoma - LMM).[150]

Superficial spreading melanoma (SSMM) is the most common variant and most frequently arise on the back in men and the lower leg in women. The lesion will appear as a flat, scaly, often irregular macule which may show irregular pigmentation over a variable period of time, with a protracted radial growth phase. If left untreated, it may continue to develop nodules of invasive melanoma. Hypopigmented areas of regression can occur and 'scalloping' of the border is characteristic. Amelanotic variants are particularly difficult to diagnose, both clinically and histologically and may look erythematous or flesh coloured.[150]
Acral lentiginous melanoma account for up to 10% of melanoma in caucasian groups, but is the most common variant seen in Afro-Caribbean and Asian groups due to the lower incidence elsewhere on the body. They frequently occur on the digits, particularly beneath the nails, and on the weight-bearing plantar areas. As with SSMM, they present as irregular, slowly growing, irregularly pigmented macules, most often in the seventh decade. Prognosis is generally poor due to delayed presentation.

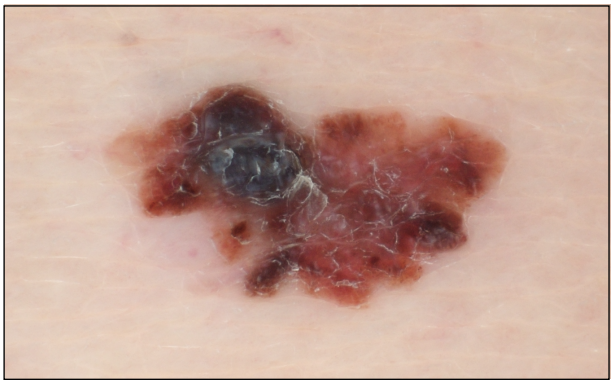

Fig 2.17 A malignant melanoma displaying the characteristic signs of asymmetry, irregularity of outline and variegation in colour.

Nodular melanoma make up 3-4% of cutaneous MM and may arise de-novo or within areas of macular melanoma. By definition they have no, or a very short, radial growth phase which distinguishes them from other melanoma nodules. They most commonly occur on the trunk and limbs in the fifth and sixth decades of life and are twice as common in men than women. As with other melanomas, an amelanotic variant is often clinically misdiagnosed due to similarities with vascular tumours like pyogenic granuloma.[150]
It has been suggested that as melanoma thickness is such a significant feature, the development of a nodule in a melanoma should be seen more as a sign of metastatic potential than as a distinct form of MM.[146,152]

Other sub-types of melanoma exist, including desmoplastic, verrucous, animal, nevoid, clear cell, spitzoid and spindle cell melanomas, however they are rare variants and further explanation of them is beyond the scope of this thesis.

In terms of the management of MM, it has long been known that early diagnosis imparts significant advantages in terms of morbidity and mortality. Many studies have shown that the thinner the melanoma and the earlier the intervention, the better the survival rate.[158] A high clinical suspicion and an early diagnosis are therefore essential.

It is worth noting that with melanoma the volume of the tumour is related to its potential to metastasize and is inversely related to survival. It was initially noted by Clark in 1969 [153] that the extent of anatomical tumour invasion predicted 10-year survival probability.

This was superseded by the actual thickness of the tumour as a measure of vertical depth by Breslow in 1970,[154] and this still remains the most significant prognostic indicator for MM. The Breslow thickness is a histological measurement, given in millimeters, from the top of the granular cell layer in the epidermis (or the base of an ulcer if present) to the deepest extension of the tumour and is a major prognostic indicator of survival in primary cutaneous melanomas.

The Clark level is a histological measure of depth of the anatomical layers of involvement in the skin and is measured in levels 1 to 5. It is a significant modifier of prognosis for those patients whose MM is less than 1mm in thickness, given that a thin (<1mm) tumour with Clark level 3 invasion has a significantly poorer prognosis than either the Breslow thickness or Clark level alone would have predicted.[155]

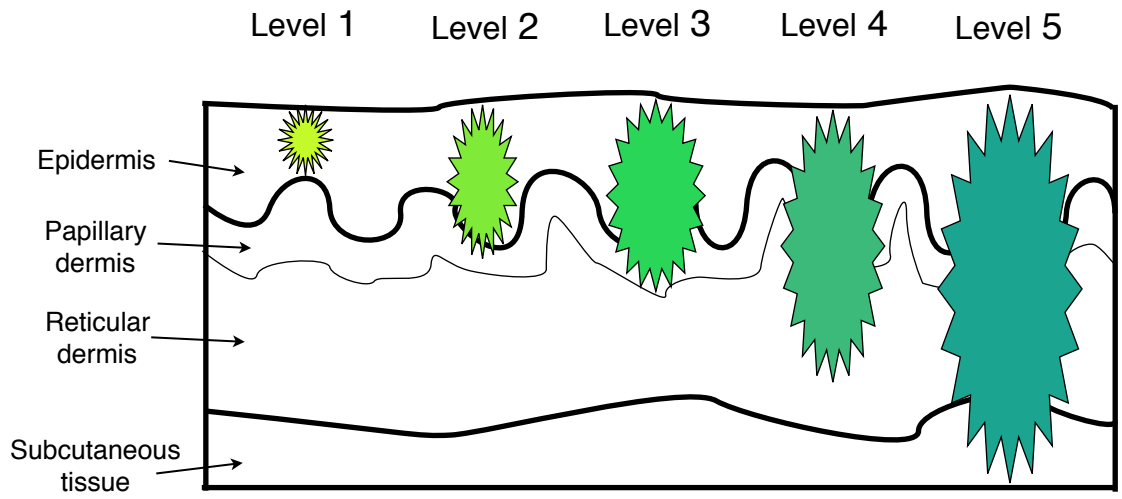

Fig 2.18 Clark Levels for melanoma - showing the gradual progression of tumour from the epidermis, down into and then through the papillary dermis, into the reticular dermis and finally the subcutaneous tissue.

Other prognostic indicators are also used to give a comprehensive picture of the potential of the MM to metastasize. These include the presence of metastases, anatomical site, mitotic rate, ulceration, tumour infiltrating lymphocytes, associated vascular or neural invasion and regression. The American Joint Committee on Cancer (AJCC) have agreed upon a melanoma staging system which links all of these different factors and is a well accepted algorithm for assessing melanoma prognosis [159] (see appendix A).

Sentinel lymph node biopsy is a technique which has been advocated in staging melanoma by sampling the draining lymph node basin and analysing the primary (sentinel) node for the presence of metastases.[156] The sentinel node is the first lymph node, or nodes, which drain the lymph from the area of skin which contains the melanoma. Lymphatic mapping, using colloid radiolabeled with Technetium-99 (Tc-99m) and a Patent Blue vascular dye injected into the dermis adjacent to the tumour, is used to identify the sentinel node and sampling usually occurs at the same time as wider excision of the primary tumour site. A considerable amount of debate surrounds its universal acceptance and at present there are no specific recommendations for its commonplace use, other than as an accurate method of staging.

Management of MM is very much dependent on accurate diagnosis and staging of the tumour, with treatment tailored to the needs of individual patients. Surgical excision remains the cornerstone and sentinel lymph node biopsy may also have a place in identifying patients for therapeutic lymph node basin excision. Adjuvant therapy is considered in cases with a higher risk of recurrence, particularly thick tumours or metastatic spread.[157]

UK multiprofessional guidelines on management and relevant follow-up have been agreed and the interested reader may find them at the British Association of Dermatologists website.

2.4.10 Other tumours of the skin

Merkel cell carcinoma is also known as primary neuroendocrine carcinoma of the skin and is a rare, but highly aggressive cutaneous neoplasm. They probably account for less than 1% of all skin malignancies, but have a 5-year survival rate reported to be between 30% and 64%.[169] Typically they present as a rather non-specific, solitary, smooth, red nodule on the head and neck and are most often miss diagnosed clinically as BCC. Diagnosis is confirmed pathologically and treatment primarily revolves around wide excision or using Moh's surgery. Sentinel lymph node sampling may also be offered due to the aggressive metastatic potential of the tumour. Radiotherapy and chemotherapy are frequently employed as adjunctive therapies. Prognostic outcome s are generally quite poor, with very high rates of regional and distant metastases.[170]

Adnexal cancers of the skin are rare tumours that arise in the subtypes of skin appendages (hair, eccrine, neural, apocrine and sebaceous units). As they occur so infrequently, they are often misdiagnosed as more common skin cancers. Wide excision and careful follow-up are advocated due to a recurrent tendency.[165]

Sarcomas of the skin are non-epithelial primary skin tumours which are locally aggressive and have the capacity to metastasize. They can effect patients at any age and are a complex category of rare skin tumours.[166]

Dermatological manifestations of internal malignancies are defined as tumours metastatic to the skin. They include mammary Paget's disease (adenocarcinoma of the breast)[167] and Kaposi's sarcoma (now most commonly associated now with immunodefficiency in HIV patients).[168]

Further discussion of these tumours is beyond the scope of this thesis.

Chapter 3

Making a Diagnosis

In the previous chapter we looked at the specific changes which occur in skin exposed to excessive UV light. Particularly we saw how the changes associated with photodamage will progress to malignant transformation if given the necessary time and exposure. In this chapter we will look at the current methods of measuring photodamage and how they have variable success. I will then consider why the application of SIAscopy may be an effective method in identifying cutaneous photodamage.

3.1 How can photodamage be measured?

Being able to measure a disease process or condition is important as it allows a quantitative assessment of the process involved and of any treatment that may be available. It is clinically quite easy to see the manifestations of photodamage - fine wrinkles, erythema, dyspigmentation, skin roughness and the sallow complexion associated with solar elastosis, however measuring photodamage provides specific challenges in being able to produce accurate, reproducible, repeatable and simple results with good inter-user agreement. Many of the clinical methods currently available are highly subjective.

3.1.1 History and examination

The majority of the literature regarding the analysis of photodamage has commented that for any method of analysis, sensitivity is increased when adjusted for specific criteria known to be associated with photodamage (age, sex, location, skin type, etc). Therefore, as with most things in medicine, a good history and examination remains invaluable.

This can be divided into a general and a specific history. The general history would encompass all relevant information relating to general health, skin disease, sun history, skin type, environmental exposures, family history and drug history.

As we have seen that photodamage and cutaneous carcinogenesis are part of the same spectrum of physiological response, a specific lesion history can be included and may give additional information as to the extent of the photodamage.

A lesion history would include information on the length of time a lesion has been present, how it has changed over that period of time and if there has been any attempt at healing. Changes in size, shape, colour and the presence of ulceration are important for pigmented lesions. The seven point check list (table 3.1) is used specifically as an aid to identify the most commonly occurring features of a lesion that are associated with melanoma.[171,172]

For non-pigmented lesions, changes in size, pain and bleeding are common presentations. BCC tend to have a rather slow and benign sounding genesis, with incomplete or non-healing highlighted by many patients. They often go unrecognised or ignored for considerable periods as they may be put down to minor trauma. Conversely, SCC can be painful and grow rapidly in a field of damaged looking skin.

Specific questions	
How long has it been there	
How was it noticed	
How has it changed	
7-POINT CHECKLIST	Change in size
	Change in shape
	Change in colour
	Inflammation
	Crusting/bleeding
	Sensory change (e.g. itch)
	Diameter >7mm

General Questions
Age
Family history of skin cancer or skin diseases
History of sun exposure and burning (esp. in childhood)
Job history (esp. welding, radiation, chemical exposure)
Drug history
Other medical problems and treatments
Smoking history
Hobbies and pastimes

Table 3.1 Lesion specific and general questions

The history not only gives the clinician vital information with which to make a diagnosis, but also allows an understanding of the patients perception of the problem and their ability to manage any potential treatment regimens.

The skin type is an important indicator in identifying skin at risk of photodamage. The tendency of the skin to be susceptible to solar damage seen as 'sunburn' or 'tanning' was classified by Fitzpatrick in 1988 and roughly equates to the amount of melanin production naturally occurring in the skin.[8] The classification describes type 1 skin burning easily and never tanning (as seen in Celtic populations) through to type 6 skin always tanning and never burning (Afro-Carribean populations) (table 1.1). While this is a useful marker in identifying those at higher risk of developing photodamage, it does not attempt to categorise features of photodamage itself.

Clinical examination is also both generalised and specific, looking for the characteristic features associated with photodamage (table 2.2) and also specific lesion characteristic which can be attributed to excess solar exposure.

Specific signs associated with MM have been subject to a significant amount of debate and there are many guidelines to help with the early diagnosis of suspicious lesions (e.g. 7-point checklist, ABCDE),[173] but the variable presentation of MM makes these no more than guidelines and they should not be seen as a set of specific diagnostic criteria. A good history along with clinical evaluation by an experienced clinician remains essential.

Some studies have shown that a good history with the collection of intrinsic, demographic and specific information alone can be highly effective at identifying those with high accumulated doses of UV radiation.[202]

3.1.2 Clinical diagnostic accuracy

Clinical diagnostic accuracy is dependent on the skill and ability of the person doing the examination and most authors agree that this can be quite difficult. In the diagnosis of melanoma, diagnostic accuracy with the naked eye is reported at about 60% on average.[179] Statistically a GP is likely to see very few melanomas in a career, whereas a consultant dermatologist will likely see many more, so it can be anticipated that the specialist's ability to diagnosis a skin cancer would be higher due to both a specific interest and a higher exposure to atypical lesions. The diagnostic differences also extend to the grades of doctor, where a consultant dermatologist of 10 years experience may have a diagnostic accuracy of 80%, while senior and junior registrars have an accuracy of 62% and 56% respectively.[174] Reproducibility of a diagnosis and the ability to recognise subjective features (such as variegation and irregularity) is also an important facet of diagnostic accuracy over time and different studies have measured this at approximately 80%.[175,176] It is likely that some of the more subtle pigmentary changes associated with photodamage have similar clinical diagnostic accuracies.

The problem with examination alone as a method of measuring photodamage is that both photodamage and normal skin ageing produce signs that can not always be easily separated using simple clinical methods. For this reason various different techniques have been employed to try to standardise results.

3.2 Diagnostic techniques

The most simple methods employed to categorise photodamage involve users being asked to judge visual signs of skin damage. The severity can be recorded on a numerical scale and while this may be easy to use, inter-user interpretation of the differences between say 2 and 3 on a score can lack reproducibility and sensitivity. Visual analogue scales (a straight line on which an 'X' can be marked) have better reproducibility and graded photographs have also been used in comparison studies with patients, with good inter-user agreement.[95]

3.2.1 Histopathological analysis

The microscopic examination of a specimen and the identification of solar elastosis and dermal degradation products by a trained pathologist is held by many as the current standard for the diagnosis of photodamage.

Keratinocytes can show photodysplastic effects with minor structural changes in cellular and nucleus size, shape and uptake of stain. Increased epidermal cell proliferation can be assessed histochemically as can the abnormal cellular infiltrates, angiogenesis and elastosis within the dermis. Epidermal thickening is a particularly inconsistent measure in extreme solar exposure as skin may also become atrophic after prolonged exposure.

While studies support the histological identification of solar elastosis as a robust method of diagnosis of photodamage,[221,222] it does not follow that it is a good method of measuring photodamage. It is invasive, uncomfortable and the effects of wound healing may distort visual and histological features if further biopsy is performed close to the initial site. Histological analysis of small samples is also not a consistently good measure as most samples vary from one area of skin to another, thereby relying on consistently accurate biopsy each time. It is estimated that around about 3% of the actual specimen is examined microscopically and that level may be closer to 1% in certain circumstances. There are also no standardised criteria for quantifying the amount of photo-

damage in a specimen, so diagnosis is as much to do with the opinion and experience of the pathologist as it is for any other clinician.

The acquisition of a tissue specimen requires the surgical removal of all, or part, of a lesion followed by various methods of preservation, sectioning and staining of the sample. There are many factors that can influence the accuracy of histopathological analysis and it is widely accepted that diagnostic accuracy is related to the size of the specimen being examined and whether the sample is from the most diagnostically significant part of the lesion. An amount of shrinkage and artifact is introduced to a specimen during the histological preservation and fixation process, which would clearly have more of an impact on smaller specimens, so where possible the complete excision of the lesion is advocated. This also enables not only a more accurate lesion diagnosis, but also evaluation of overall architecture, surgical excision margins, grading and staging of any tumours present. A wide range of techniques are available to acquire a skin sample for analysis.

Incisional biopsy samples only a representative area of the lesion or skin and requires less surgical skill, is often quicker and more easily tolerated. Punch biopsy is a commonly used method of incisional biopsy where a variably sized, round 'punch' of skin can be removed for evaluation.

Excision biopsy allows for complete removal of the lesion, but may require more surgical skill, particularly in areas of cosmetic consideration or areas where poor healing is anticipated.

Fig 3.1 Biopsy Punch

Curettage and shave biopsy are simple techniques that require little surgical skill and involve shaving or scraping a lesion from the skin either en-bloc or with multiple passes. The method is doubly effective in that it can also act as a treatment for the condition, but can only give the pathologist enough sample to make a diagnosis of the condition and no detail on the extent can be offered. It is useful as a method of lesion man-

agement in individuals with numerous lesions within an area of field change or if multiple excisions are not practical.

Fine Needle Aspiration (FNA) is a technique used to sample cells for pathological evaluation. A fine bore hollow needle is passed through a target lesion while a negative pressure is applied to it, usually generated by a standard syringe. The contents of the needle are then expressed onto a slide and fixed before staining and evaluation. This cellular sampling technique is mainly used for subcutaneous mass sampling and is not used for skin lesion diagnosis as it is relatively painful and less effective than a diagnostic punch biopsy. It is more useful in the diagnosis and prognosis of patients with metastatic skin cancers, particularly melanoma.[183]

3.2.2 Immunohistochemistry

Immunohistochemistry is a technique which uses antibodies to specific antigens in a specimen to identify biomarkers of a protein from a cellular process. The antibodies are tagged with an easily identifiable substance to make these proteins visible under microscopy.[214] The process requires very specific tissue collection, processing and sectioning to maintain relevant architecture and antigens. Solar elastosis has been shown to be composed of elastin material, as well as other matrix components, which are notably increased in photodamaged skin. Some studies have looked at identifying and quantifying these products[215, 216] and it is often used in conjunction with histopathology.

3.2.3 Photography

Basic photography is a simple and cost effective practice, but has always been let down by difficulties in reproducibility. Lighting inconsistencies, curvature of the target, variability in film, camera settings and production techniques mean that this is not a particularly reliable procedure when recording sometimes subtle skin appearances over time. More recently the use of digital photography and controlled photographic studios, with consistent lighting and trained photographers can limit these problems significantly, making it a more attractive option.

3.2.4 Skin surface microscopy

Skin surface microscopy is also known as epiluminescence microscopy, dermatoscopy or dermoscopy. With this technique an illuminated hand-held device, typically with a ten-times magnification lens, allows microscopic architectural detail to be seen with the naked eye. Oil is applied to the skin to eliminate any light scatter at the lens-surface interface, rendering the stratum corneum essentially transparent, though newer devices use polarised light to produce the same effect. This allows architectural detail of the epidermal-dermal junction to be seen. It has been used extensively in the identification of features in the diagnosis of pigmented lesions and, to a lesser extent, non-pigmented skin lesions. Publications have concluded that for equivocal lesions, where diagnosis is difficult, it can increase the sensitivity of diagnosis of melanoma by 10-27% when used regularly in expert hands.[177,178] However, in untrained hands, it can actually make diagnostic ability worse than a diagnosis on clinical grounds alone.[178]

Fig 3.2 Heine® DL3 Dermatoscope

3.2.5 Skin surface topography

This is a cutaneous contour measurement method which uses fine silicone moulds of the skin that are then evaluated under a microscope and graded according to a scale. One system of grading is that described by Beagley and Gibson and relates to changes in the skin surface texture. This looks at the change in skin texture from normal skin with multiple fine lines with multiple intersecting transverse and parallel lines, through six stages to that of more course lines with flatter looking skin associated with actinic damage. It is relatively easy to perform and has good inter-user agreement and reproducibility, but studies have relied on biopsy for correlation. [202] More recently digital photographic techniques and image analysis have been used to measure the depth and length of wrinkles.

This method is limited in that variations in skin hydration and resting muscle tone, particularly of the face, can alter the appearance of fine wrinkles making consistency a problem.

3.2.6 Skin surface stripping

Skin surface stripping is a non-invasive technique allowing collection of cells from the stratum corneum for microscopic analysis. It simply involves pressing some vinyl adhesive tape onto the skin and pulling it off to lift some stratum corneum cells with it. One study looked at use of a cyanoacrylate skin glue as a stripping agent to differentiate dysplastic (atypical) naevi from malignant melanoma and found that atypical melanocytes were found in the stratum corneum in 95% of malignant melanoma and always absent from the atypical naevi.[181] While this may be of some use in the identification of the epidermal malignant transformation associated with photodamage, it does not offer any direct measurement of the intradermal changes previously described as so is of little use in the quantification of photodamage.

3.2.7 High-frequency ultrasound

Another non-invasive skin imaging technique is high resolution B-scan ultrasound, which has been employed to look at solar elastosis.[75] The principle relies on the different acoustic properties of dermis, with the globular elastin deposits of solar elastosis appearing echolucent due to the loss of fibrillar architecture (sub-epidermal non-echogenic band - SENEB), compared to the normally echoreflective, fibrous dermis. This has been described in the literature as the ultrsonographic marker of photodamage.[203,204,205] It has also been used in the examination of melanoma and other solid tumours of the skin. Due to its limitations in resolving power, its main strength has been recognised in the determination of tumour margins, both laterally and in depth, where there is some good correlation with Breslow thickness.[185]

3.2.8 Laser-doppler perfusion

This technique has been used to show a reduced flow of blood in a photodamaged area of skin and can potentially be used to show such changes over time.[218] It is, however, particularly sensitive to external temperature variations and so has little use in the generalised photodamage screening of a large population. It has also been used in cutaneous burn assessments prior to surgery and in examining the increase in total blood flow to and through a malig-

nant lesion when compared to surrounding skin. It has been suggested that the boundary of this increased flow indicates the true margin of the tumour.[184]

3.2.9 Confocal scanning laser microscopy

This is a powerful imaging technique that can see in-vivo detail of the epidermis and papillary dermis down to the cellular and, occasionally, sub-cellular level. A low powered laser is focused onto a specific area of skin and the light reflected back is scanned over a 2D grid to give a section akin to a histopathological section. The focal length of the laser can be adjusted to give slices at varying planes and longer wavelength lasers will allow deeper imaging. While it is claimed that real-time visualisation of circulating erythrocytes is possible, it has a very narrow field of view making useful identification of lesion structure difficult. It is also limited to viewing very small areas of skin and remains a rather bulky and costly device.[184] Early studies have looked at photoageing features with variable results,[206,207] though it would seem that in its current form that it is relatively unsuitable for measuring photodamage over large areas or in larger populations.

3.2.10 Optical coherence tomography

This is a method akin to ultrasound, but using light waves instead of acoustic waves. It has a resolution of approximately10 microns to a depth of roughly 1mm, although excessive photon scattering past a depth of 500 microns means that, realistically, structures down to the papillary dermis may only be visualised.[180] It has been tried in the characterisation of photodamage with varying results, the best of which showed the ability to distinguish features of AK and normal skin.[208]

3.2.11 Multiphoton tomography

Multiphoton tomography is an in-vivo technique which uses rapid firing near-infrared lasers (in the femtosecond range) and second generation harmonics to produce very high resolution images of cellular and intracellular features. This causes auto-fluorescence from naturally occurring fluorophores and protein structures such as porphyrins, elastin, collagen and melanin. It has been used

in conjunction with other techniques, such as OCT or high-frequency ultrasound, to capture 3-dimensional information used in a wide variety of medical research.[209, 210] Some studies have used it to look at photoageing and in the diagnosis of skin tumours.[211, 212] One study has suggested that increased autofluorescence and decreased second generation harmonics in the superficial dermis correlated with ageing changes.[213]

3.2.12 Magnetic resonance imaging (MRI)

MRI has also been used in research techniques to look at contrasts in tissue density to try to identify tumours, but the current image resolution is not good enough and it is realistically too large, immobile and expensive to consider for photodamage at present.[182]

3.2.13 Mechanical methods

The altered mechanical properties of photodamaged skin can be assessed by simply pinching the skin and looking at degradation of the elastic properties. Clinical devices have been invented to analyse these changes. A Cutometer® (Courage + Khazaka electronic GmbH) is a device that sucks small areas of skin into ports of varying size and the resistance of the skin to deformity can be measured optically. Pierrard proposed a scale of measure with this device showing a decrease in elasticity, extensibility and maximal deformation.[74]

Fig 3.3 Cutometer

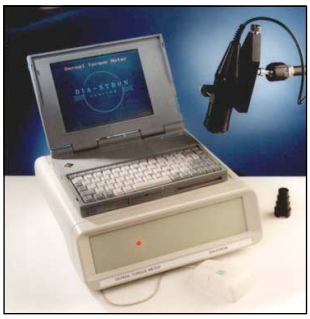

Fig 3.4 Dermal Torque Meter

Other devices including the Dermal Torque Meter® (Dia-stron Ltd, UK), which measures the skins resistance to torsion and the Extensometer® (Instron, USA) which measures the amount of force required to stretch the skin by 30%.

These devices have been used to measure skin suppleness and elasticity, but results can be difficult to interpret depending on environmental conditions and the 'stress history' of the measured area of skin.

3.2.14 Colourimetry

Skin colour changes in photodamaged are particularly evident and various techniques have been employed to try and measure these. A chromometer® (KonicaMinolta) is a device that uses LAB colour space* and assigns a 3D value to the colour of the skin. A mexameter® (Courage + Khazaka electronic GmbH) uses reflectance spectrophotometric principles outlined by Diffey and Farr in 1984 and can be used to measure melanin and erythema.[96] The measurement of erythema is complicated by the other pigments in the skin, particularly melanin, which can mask the red colour of erythema. The thickness of the skin down to the blood vessels (i.e. the epidermis and upper dermis) can also impact results, as can pooling of blood in dilated, damaged blood vessels. The flow of blood in the skin is usually decreased in normal skin ageing and a much more accurate measure of blood flow can be achieved using a scanning laser doppler technique.

Fig 3.5 Mexameter

* LAB is a method of describing colour, where L stands for luminosity, or the black and white tones of an image, and a and b are channels that specify colour as either a green or magenta hue, or a blue and yellow hue, respectively. Colour space is further described in Ch3.

3.3 Is there a true gold standard?

To answer this I think we have to think about what would be the ideal test for cutaneous photodamage. Photodamage is a prevalent condition, so any test would need to be easily distributable over a wide population. It would need to be reproducible, easily tolerated, reliable and not interfere with the process being measured.

For some people, histological analysis has long been thought of as the gold standard through the identification of solar elastosis, but it is limited in that analysis can only tell you there are markers of photodamage in the examined specimen and can not identify it over a wider field than that processed. Also there is currently no standardised method of quantifying the amount of solar degenerative material which indicates photodamage using histopathology.[201] Its widespread use as a method of quantification has some fundamental limitations making it unsuitable and relatively impractical for application to a wider population as a test for photodamage.

Certainly, histological analysis and immunohistochemistry are widely accepted as the best current method of diagnosis for many conditions we seek to identify in medicine, but in the case of cutaneous photodamage, it appears a limited technique when used alone. True *measurement* of a condition goes beyond just identification.

Within published literature, all of the aforementioned techniques have been assessed as viable methods of identification of photodamage and all have merits to varying extents. Some of the studies have used relatively small sample groups, and some have not performed any specific statistical analysis of the results. All show good potential at identifying some of the features associated with photodamage and clearly many of the techniques are relatively new. With further modification and implementation they may produce a great tool for cutaneous analysis.

A paper by Marks and Edwards reviewed many techniques employed in measuring photodamage and concluded that there was no singular method which excelled at quantifying photodamage.[218] A recent study by Baillie et al made a review of all available published literature on the various methods used for assessing photodamage and examined the robustness of published evidence.[201] They summarised that histological analysis alone should not be viewed as the gold standard and was inappropriate in widespread application in the assessment of photodamage. They concluded that no one method of analysis was currently available which accurately quantifies the degenerative changes associated with photodamage and that there was a need to explore further non-invasive methods of measurement.

Interestingly, despite the desire to find a specific technique to quantify photodamage, intrinsic, demographic and constitutional data appear to be strong predictors for cutaneous photodamage. In fact, age alone has been shown to be a good marker as an estimation of the total accumulated UV exposure and the presence of photodamage. This has been identified in several studies, with one showing a statistical significance in the prevalence of severe photodamage associated with increasing age.[202, 217, 219, 220]

It would appear there is currently no convincing evidence for any method of assessing photodamage as being better than any other, but that moving forward, non-invasive methods should be identified as holding the most hope for the future. For this reason SIAscopy may be a useful method of quantifying photodamage.

SIAscopy is a non-invasive technique which uses spectral and infra-red light to measure pigmentation in the epidermis and upper dermis. It is a proven, portable, quick and cheap method of looking at intracutaneous pigmentation and would seem a good potential method for quantifying the pigmentary features of photodamage.

3.4 Spectrophotometric Intracutaneous Analysis (SIA)

This is the technique which underpins this thesis and I will explain it in more detail so we can see why it would be useful in identifying photodamage.
I will start with basic principles regarding light and how it interacts with skin.

3.4.1 Light and colour theory

Visible light is part of the electromagnetic spectrum and as such has a frequency and wavelength, extending from approximately 400nm (blue/voilet) to 750nm (red).

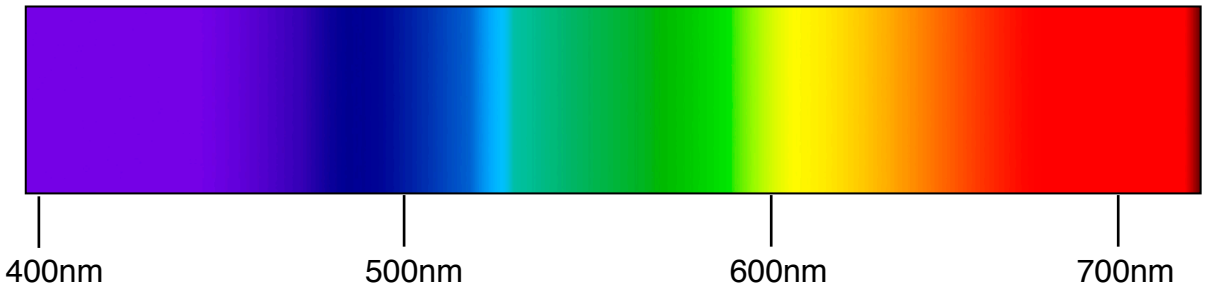

Fig 3.6 Wavelengths of the visible light spectrum

When light is incident on a surface there are two possible outcomes - the light may be *reflected* at the surface or it may pass through it, where a change in the refractive index at the air/material interface will cause the light to slow and deviate, called *refraction*. If the material is non-homogenous, light will be *scattered* by particles, some of which may be returned to the air, called *remittance*. Light passing through a material is *transmitted* and light neither scattered or transmitted is *absorbed*.

A *chromophore* is a term loosely used to describe a molecule which absorbs light. The absorption properties of a material are usually wavelength dependent, with molecules transforming the light into heat or electrical energy, or even re-emitting it at a different wavelength, as with fluorescence. The way light is scattered is dependent on the size of the particles it comes into contact with.

Larger particles cause scattering in a forward manner and this is described as *Mie scattering.* When the particles are smaller in relation to the light (typically <1000nm) the scattering is wavelength specific and varies inversely to the fourth power of the wavelength of the incident light and is called *Rayleigh scattering.* This would suggest that blue light, with a shorter wavelength, is scattered far more than red light.

A concept of colour science was proposed in 1801 by Thomas Young (later extended by Helmholtz) in the theory of trichromacy in vision. This suggested that any colour can be formed by the combining of three properly chosen primary colours, with a primary colour being a colour which can not be formed by a combination of the other two. Using this theory, a 3-dimensional colour model can be constructed, called the *Tristimulus space*. This contains all possible colours and any specific colour can be defined by a specific vector within this space, called the *Tristimulus value*.

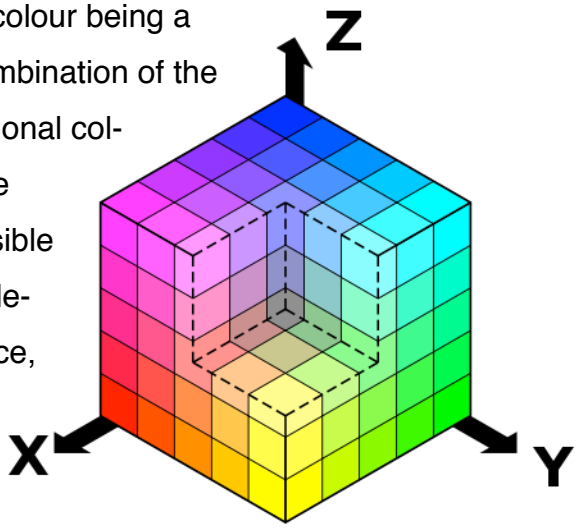

Fig 3.7 Tristimulus or colour space

The *colour space* describes the range of colours, also called the gamut, that a device can register (in the case of a camera) or reproduce (in the case of a printer or monitor). Each gamut is constructed from certain primary colours. The specific choice of primary colours and how they are mixed (to produce all possible colours) will allow each colour space to have specific attributes that make it useful for the application it has been chosen for. This way, each colour space has slightly unique variables. A simple example might use red, green and blue as the primary colours. If these were arranged in a 2D triangle with the purest colour intensity (called saturation) at each point of the triangle, white in the centre and all possible colours between, this would represent the colour *model* and enclose every possible colour. The colour *space* would reside within this triangular model as a bubble and would encompass all the potential colours that could be created by that specific colour

space. The surface of the bubble would represent all the most saturated colours and any colour outside the bubble would not be reproducible by that colour space.

Colour spaces can be specific to certain tasks, so high end design and image manipulation may use a colour space that contains a bigger bubble, so not only could more colours be rendered, but also colours of a higher saturation. A more simple colour space would limit the available number and saturation of colours, but may be suitable for applications of lower specification where such detail is not required.

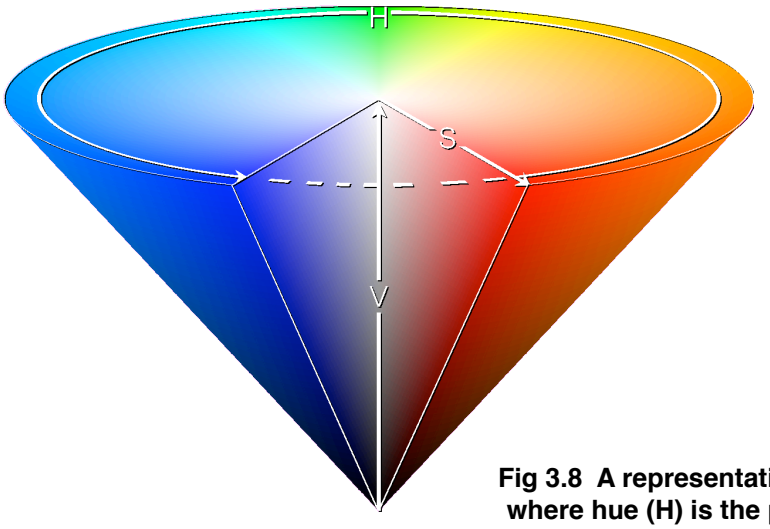

Fig 3.8 A representation of the HSV colour space where hue (H) is the peripheral co-ordinate and relates to the colour, saturation (S) is the intensity of that colour and value (V) is the brightness.

Examples of colour spaces include RGB (red, green and blue), sRGB, CMYK (cyan, magenta, yellow and black) and HSV (hue, saturation and value or brightness). The CIE 1931 xyz colour space is described as the master colour space and was designed in 1931 from experiments looking at the range of colours potentially discernible by the human eye. There are other colour spaces, each with specific attributes that make them suitable for specific tasks, from printing, image manipulation or compression, image recognition and display.

3.4.2 The optics of human skin

Once the basic principles of light physics and the non-uniform structure of the skin is understood, it becomes clear that the passage of light through skin can be complex. Light is subject to absorption, reflection, scatter, remission, transmission or any of these in combination, which in turn may be influenced by the wavelength of the light itself. A good review of this complex relationship was published by Anderson and Parrish in 1981.[186] In broad terms the path of light can be divided into the the effects caused by the different properties of the epidermis and those of the dermis.

The epidermis is composed of keratinocytes, melanocytes and epidermal appendages and the surface of the skin is neither flat nor smooth. Anderson and Parrish showed that typically 5% of incident light is reflected at the surface of the (Caucasian) skin, uniformly across the entire spectrum (infrared to ultraviolet). Given that the surface of the skin is uneven, incident light on the epidermis is refracted and made diffuse, with absorption being the predominant activity due to essentially weak epidermal scattering.

Proteins, nucleic and urocanic acids within the epidermis strongly absorb in the ultraviolet band, between 200 - 280nm (urocanic acid is a cellular breakdown product found only in the skin and secreted in sweat), however in the visible band, melanin is essentially the only pigment affecting light in the epidermis. Melanin does more than just filter light and studies have shown that light absorption is not uniform across the spectrum, showing an increase at the shorter wavelengths (UV/blue) and negligible interference at the near IR end of the spectrum.

The dermis is divided into two distinct architectural layers, the papillary and reticular dermis, and differences between the two have a significant effect on light. In-vitro studies of the dermis show it to have negligible absorption of light if the skin is bloodless, but it does have significant scattering effects which are not consistent across all wavelengths, with greater scattering at the shorter wavelengths. Anderson and Parrish stated that dermal scattering therefore

plays a major role in the depth to which radiation of specific wavelengths penetrates the dermis, with longer wavelengths penetrating deeper than shorter ones. As previously mentioned, particulate size is the determinant to the degree of scatter, so the smaller and more loosely associated collagen fibres in the papillary dermis produce Rayleigh scattering which is wavelength specific. Collagen fibres in the reticular dermis are organised into larger bundles and cause Mie scattering in a forward direction. This means that radiation entering the dermis is remitted by the papillary dermis for most of the visible spectrum whereas near infrared is transmitted to, and through, the reticular dermis with little or no remittance.

In very broad terms, the papillary dermis can therefore be considered a reflective layer of the skin. The absorption effects of the dermis therefore depend upon its in-vivo characteristics, essentially derived from the pigments found in blood, namely oxy- and deoxyhaemoglobin, bilirubin and beta-carotene.

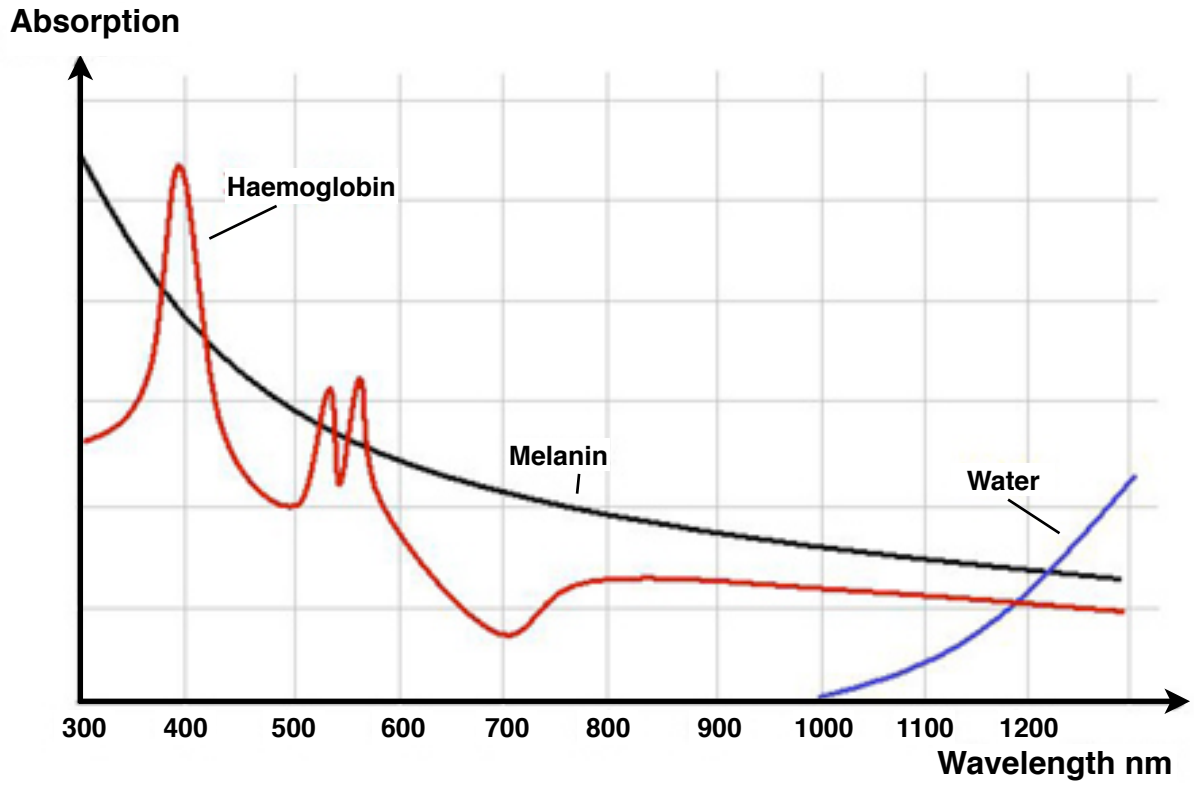

Fig 3.9 The absorption spectra of blood, melanin and water

The absorption spectra of bilirubin and beta-carotene are mostly in the blue/ green area (400-500nm), with oxyhaemoglobin (543nm and 576nm) and de-oxyhaemoglobin (554nm) absorbing mostly green light.

To summarize, the interaction of light within the skin is a complex function of absorption, remission and scattering. Absorption of light by a chromophore is not only dependent on its unique absorption properties, but also on the specific depth of that chromophore within the dermis, since this determines the range of wavelengths that each chromophore is exposed to.

SIAscopy is a multispectral scanning technique which utilises the distinct achitectural differences in the epidermis and dermis in conjunction with the absorption and remission characteristics of the skin pigment chromophores to produce colour images detailing blood, melanin and collagen characteristics of the skin.

I have written a more detailed account of the theory and mathematical model building of SIAcopy in Appendix E. This is based on the work by Dr Symon Cotton in 1998[187] and includes an explanation of how the different SIAscopic images are generated.

3.4.3 The SIAscope

The SIAscope is an evolution of the the theory work described in appendix E, manifest as a skin imaging tool. Light of wavelengths in the range of 400-1000nm is emitted from a handset in contact with the area of interest on the skin, the window of the handset being 12mm in diameter. Remitted light is collected in the same handset by a charged coupled device (CCD), is digitised and then passed to a computer for analysis by software performing the spectrophotometric analysis. Two infra-red and one set of RGB measurements are analysed for every pixel of the image, comparing them to all the potential possibilities of the skin models and converting them into four separate SIAscans -

papillary collagen thickness, papillary (dermal) blood content, total melanin content and papillary (dermal) melanin content.

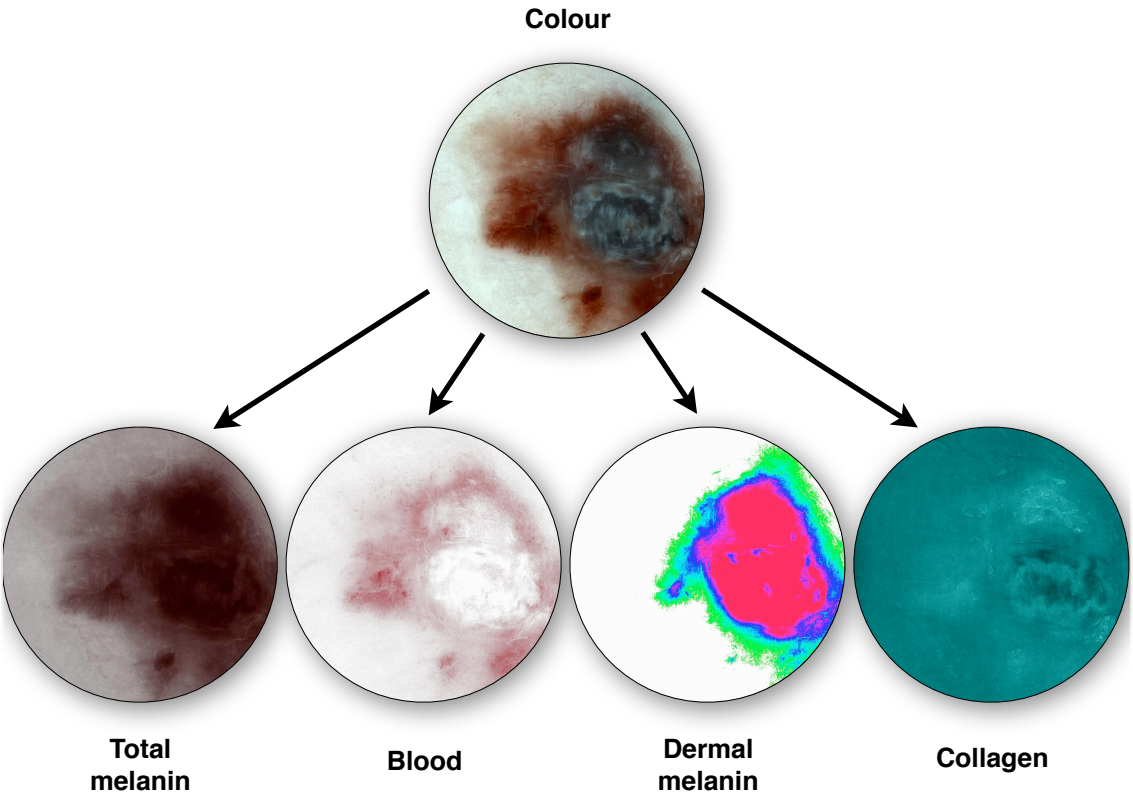

Fig 3.10 SIAscans

The SIAscope has undergone various modifications and refinements over time. The original device was heavy and slow and has evolved into a more rapid and portable laptop based system.

3.5 Non-Contact SIAscopy

The described method of producing the spectrographic image of skin components requires certain variables to be known for all colours, one in particular is surface geometry. The geometry of the surface of the skin has significant effects on the level of light reflection and is dependent on distance and angle. The SIAscope, and other spectrographic techniques, avoid this problem by being in contact with the skin, so the optical path is constant and can be calibrated. This eliminates any geometrical effect but also limits the size of the area being imaged.

Non-contact SIAscopy uses a method of eliminating these surface geometrical properties without being in contact with the skin and therefore enabling imaging over a wider area.

3.5.1 Eliminating the effect of skin geometry

The basic principle behind spectrometry of the skin can be described in the following equation:

$$P_n = I_n S_n G_n$$

Here the remitted light from the skin, P, for a particular wavelength range, n, is a function of 3 main variables, the illumination, I, (dependent on the light source), the scene geometry, G, (clearly an object further away and at an angle will remit less light than one close to the light source and orthogonal to it) and the effect of the skin components on the incident light, S.

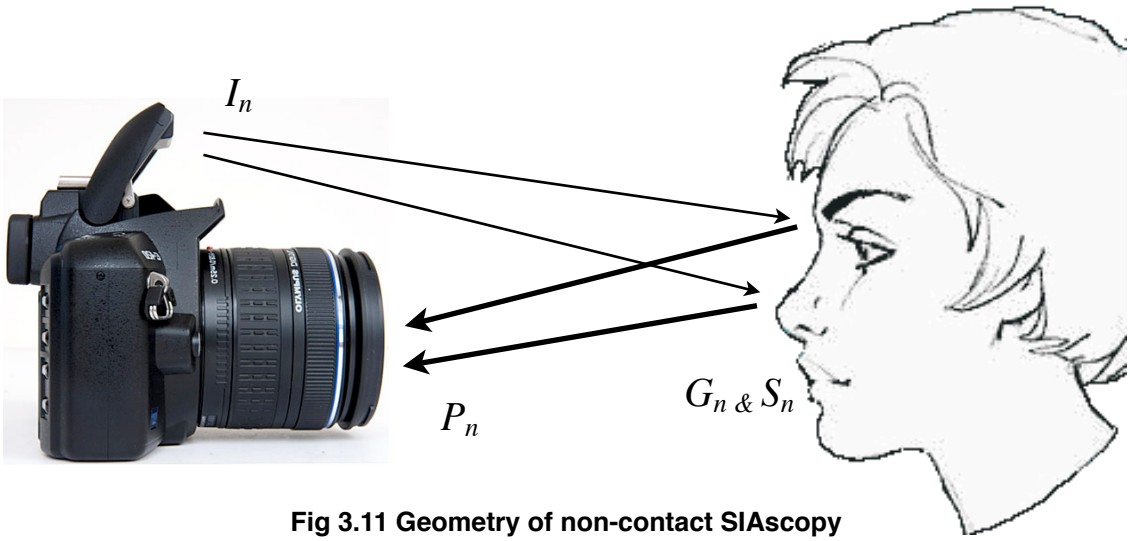

Fig 3.11 Geometry of non-contact SIAscopy

For each pixel in an image, all spectral ranges travel the same path (from light source to subject to light collector) and are therefore exposed to the same geometric effects. There are some minimal differences in the reflection of different wavelengths, but at the first order (ie. the main measurable influence) these differences are minimal and are significantly less than the effect of the skin components, S. As the spectrum of the illumination can be known and the amount of remitted light is measurable, the skin property can be deduced if the scene influence and illumination influence can be eliminated.
The principle behind non-contact SIAscopy is not to look at specific measurements of individual wavelengths but to consider ratios, R, of two of them, specifically green and red (gr), and blue and red (br).

Therefore using gr as an example we have:

$$R_{gr} = \frac{P_g}{P_r} = \frac{I_g S_g G_g}{I_r S_r G_r}$$

I, is known (or measurable) and if first order assumptions are applied then, G, can be eliminated, as the geometric effect of the scene is the same for green and red wavelengths.

It can therefore be seen that the ratio of the effect of the skin component is proportional to the function of the effect of the components of the skin which influence light, namely blood, melanin and collagen.

$$S_{gr} \propto f(blood, melanin, collagen)$$

We know from previous discussion that the presence of blood and melanin has different absorption effects over different wavelengths, with different chromophore concentrations having different effects. However the same is not true for collagen. The measured effect of different concentrations of collagen changes in a similar and proportional way for all wavelengths of light that we measure.

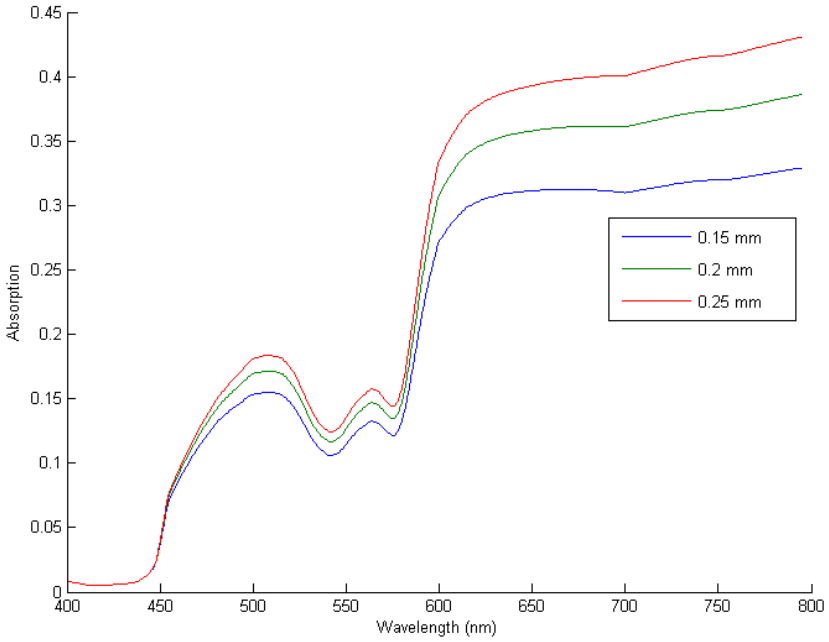

Fig 3.12 Graph showing the curve generated for a sample concentration of blood and melanin at three different collagen levels

From this graph, it can be seen that, to an approximation, that the collagen concentration simply acts as a multiplier to the response. As we are taking ratios of the two spectral measurements, the underlying effect of the collagen on the wavelength is eliminated as it acts as a constant multiplier to both readings.

3.5.2 Generating the skin model

As before with the contact SIAscopy method, a skin model can now be constructed for the non-contact system to predict the reflectance spectrum of the skin for varying amounts of blood and melanin. Given the assumption that the collagen effect is essentially eliminated in the ratio method, a fixed value of collagen is used. Every possible combination of blood and melanin can be linked to the ratios of different wavelength measurements, invariant to changes in illumination and viewing angle and with a unique concentration combination for g/r and b/r value.

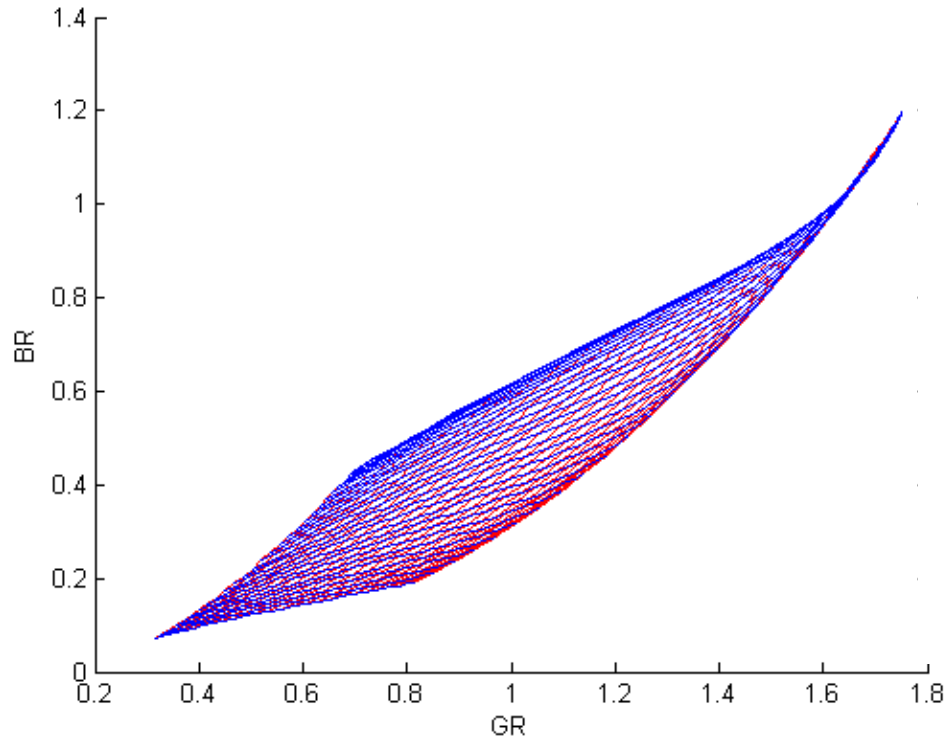

Fig 3.13 Graph of a feature space showing all the possible combinations of skin colour

Each vector point in the graph has a blood and melanin concentration associated with it.

From this, individual plots of the blood and melanin within the varying ratio space can be constructed.

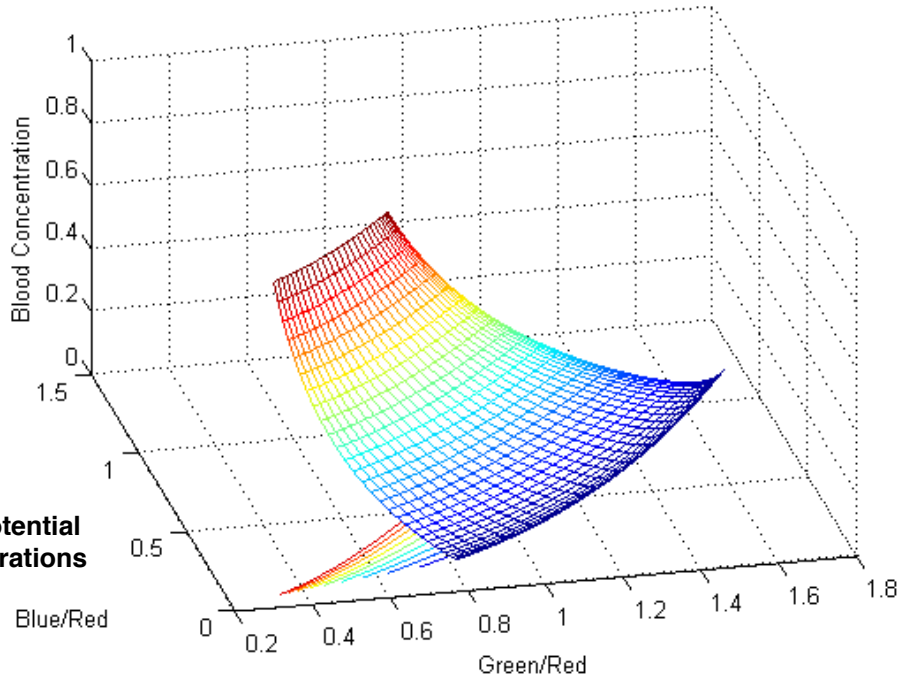

Fig 3.14 All potential blood concentrations

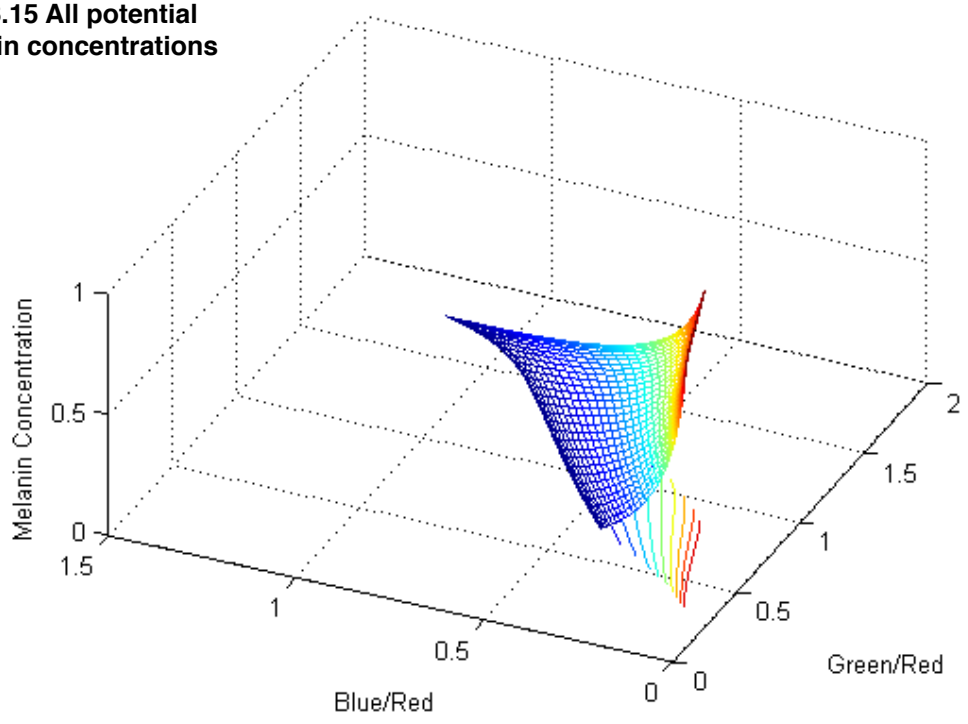

Fig 3.15 All potential melanin concentrations

3.5.3 The non-contact SIAscope

For the application of non-contact SIAscopy, a standard digital camera and powerful spectral flash is used. Linear polarised filters are applied to the flash and camera lens at 90 degrees to each other, to eliminates specular reflection from the skin surface. The flash and camera are set up such that the image is independent of external lighting when using the flash.

Fig 3.16 A non-contact SIAscope

The CCD of a digital camera registers the light incident on it but the colour of light it registers is dependent on the Bayer filter. This is a colour filter array which resembles a coloured mosaic that sits above the photosensors and allows either red, green or blue light to be registered. The combination of colours being 50% green, 25% red and 25% blue. It is named after its inventor - Bryce E. Bayer of the Eastman Kodak Company and contains twice as many green elements than blue or red to resemble the greater resolving power of the human eye to green light. Each of the colour elements transmitted by the Bayer filter and registered by the photosensor represents a single pixel† and is generally thought of as the smallest single component of a digital image. The more pixels used to represent an image, the more closely that image can resemble the original, though other aspects such as lens quality and processing algorithms are also important for the final image quality.

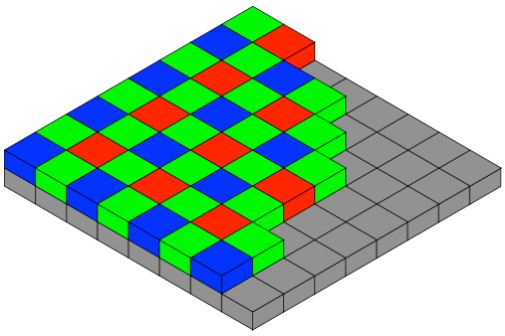

Fig 3.17 A Bayer filter

The flash gun output and the response of the cameras Bayer Filter are measured in order for it to be calibrated for use as a broadband spectrometer.

† The word pix-el is derived from *pic*-ture *el*-ement

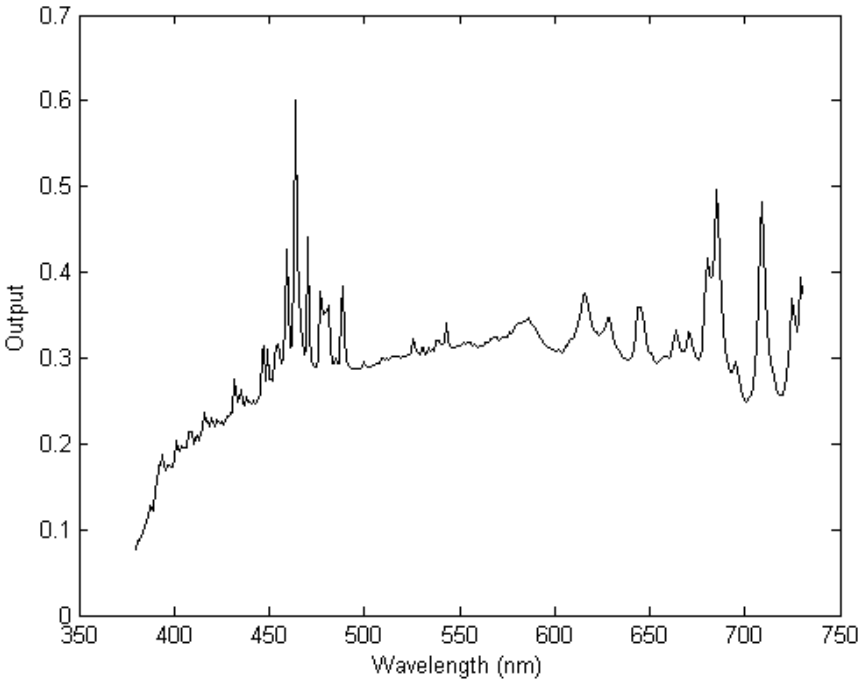

Fig 3.18 Flash output spectrograph

The output of the camera gives three spectral range images in standard R,G,B format. This image is decomposed and the data processed through the skin model to construct blood and melanin data for each pixel within the image

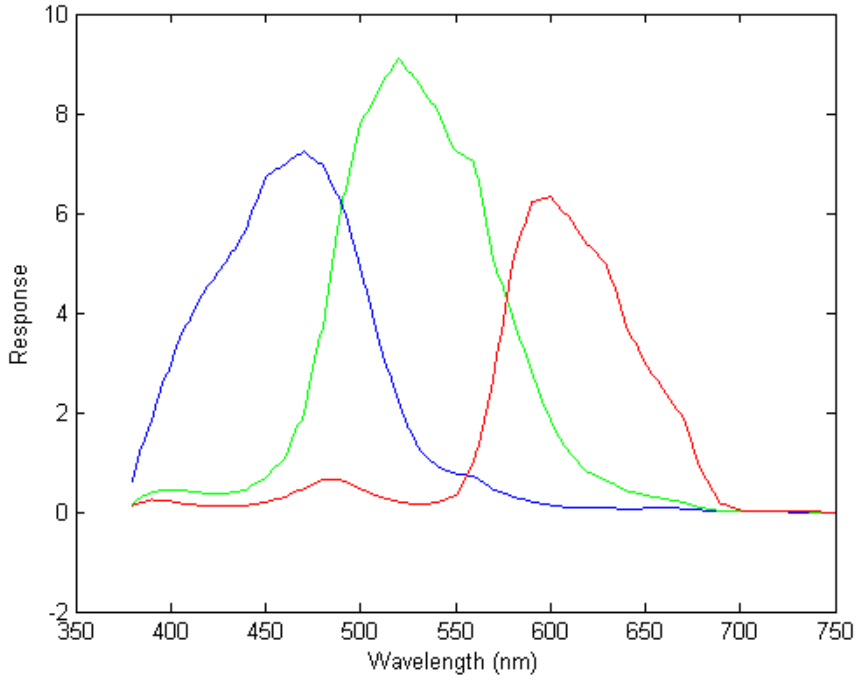

Fig 3.19 Spectral response curves of Bayer filter/CCD

Using the SIAscopy principles described in appendix E, the colour image can then be reconstructed as separate blood and melanin non-contact SIAscans.

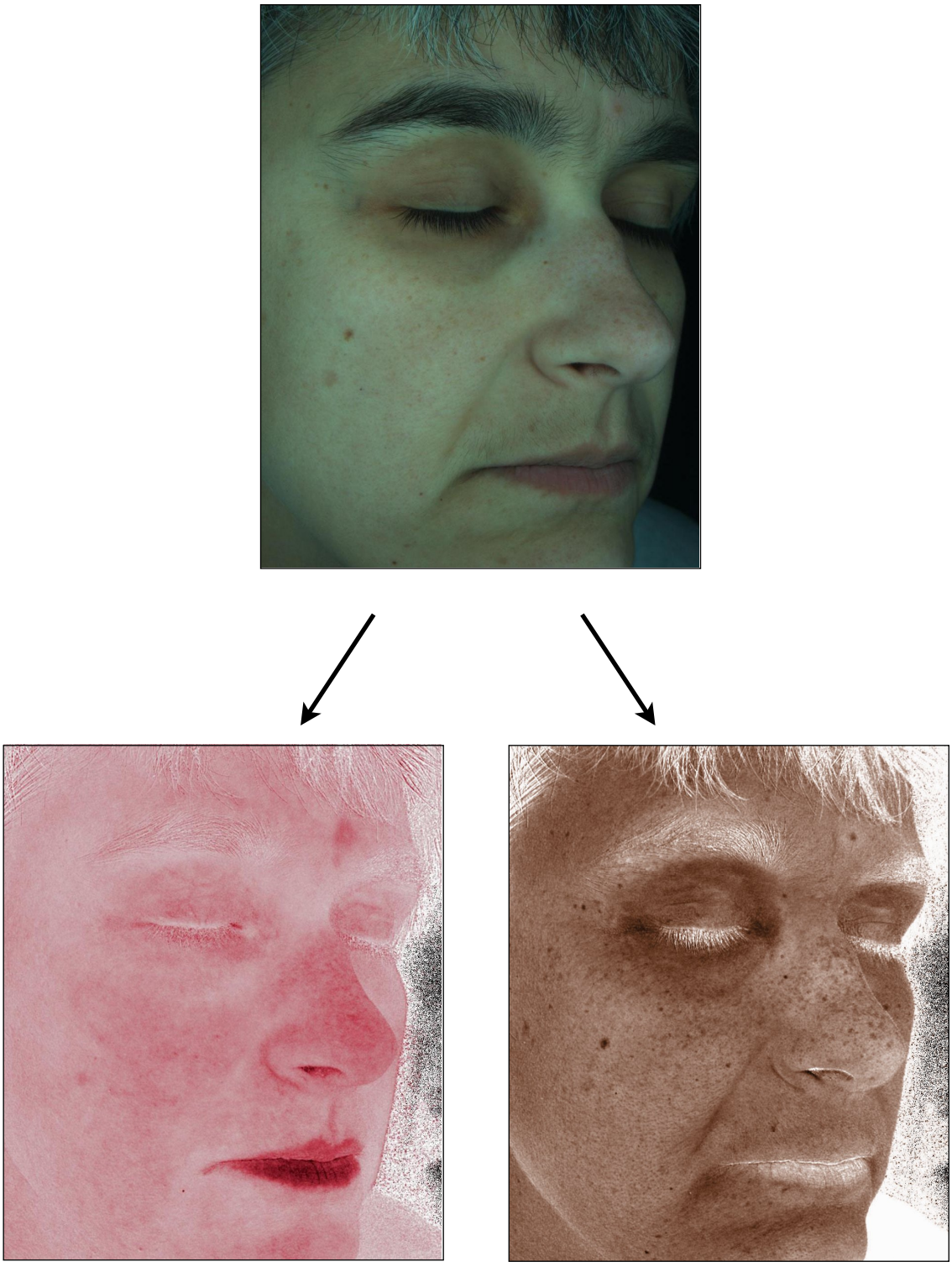

Blood Image **Melanin Image**

Fig 3.20 Non-contact SIAscans

Chapter 4

Methods

4.1 Defining the question

The hypothesis of this thesis is to see if the non-contact SIAscope is an effective device at identifying and quantifying pigmentary signs of photodamage.

In some, the accumulation of enough photodamage to cause potential malignant changes may take several decades, so diagnosis alone is of little value. The process is dependent on many variables and will occur at different rates and at different times in everyone. However identification is the first step in quantification.

In order to identify photodamage we will look for pigmentary characteristics associated with field changes known to be associated with photodamage. In order to quantify this photodamage we need to have a variable scale to identify the point when someone is most likely to develop malignant changes within a photodamaged field. This means using a variable predictor rather than a dichotomous predictor, like diagnosis alone.

To do this I am going to make 2 main assumptions.

The first is that certain skin malignancies and pre-malignancies are accepted as being associated with photodamage. There is abundant evidence for this and I have explained it in some detail in chapter 2. It would seem logical that we can use the presence of these malignancies to identify an associated 'field of photodamaged skin' adjacent to the lesions. I will also use the clinical diagnosis (of photodamage or not) by an experienced clinician where histological confirmation is not available. While histological diagnosis would be the consistent method to apply to all individuals, this is neither practical nor ethically acceptable on every patient who has a clinically benign lesion in a photodamaged field or who has non-photodamaged skin. It is also unrealistic in large population studies. In current clinical practice, an expert opinion supported by dermatoscopic (or magnified digital imaging) and 7-point clinical history is considered sufficient. We have already discussed the lack of a gold standard in this matter (section 3.3) and I feel this is a justified move, especially as it is an accepted practice in this country.

The second assumption is in using age as a proxy for photodamage to create a variable scale. Diagnosis of photodamage is a dichotomous function (it is either present or not) and does not tell us the extent or severity to which photodamage may be present. It may be present to varying degrees without it causing any visible sign, but once it accumulates to a unique level in an individual, that person is then at a higher risk of developing a spontaneous malignant lesion. This means that analysing just the presence of photodamage would be of little value as it does not quantify the level of the damage present. We therefore need to predict a variable rather than a dichotomous outcome.

We know from published research that age is as good a predictor for the severity of photodamage as other available diagnostic methods at present (section 3.3), so it is therefore reasonable to use increasing age as a variable for increasing photodamage.

At a fundamental level, both of these assumptions are linked. Research shows that the older we are the more photodamage we accrue and the more photodamaged we have, the higher the risk of malignant transformation.

At this point we could ask what is the need to diagnose photodamage in the skin if we then use age as a proxy for photodamage? We will use age as it has been shown to be as effective a marker for photodamage as any other method and at present there is no current gold standard in photodamage diagnosis. Age is also a variable so we will be able to quantify an 'age score' where photodamage is likely to become malignant. There is little benefit in just being able to diagnose that photodamage is present if you can not say to what extent.

If we can predict age using SIAscopy it will be with the suspected pigmentary features we are analysing, so what we are really measuring is 'photodamage age'. We will be able to ultimately test this by superimposing the actual photodamaged and non-photodamaged data onto the model. If photodamage and increasing age correlate then we will have a model which can use increasing age as a marker for photodamage.

We should then be able to identify a measure of the 'photodamage age of the skin' and so identify individuals who have 'biologically' older skin (from a photodamage point of view) and who are at a higher risk of malignant transformation. This would be a much more useful measurement than the presence of photodamage alone.

4.2 What features could we identify?

Analysis consists of looking for and measuring any photographic and SIAscopic features which may be associated with photodamage. However, not all features of photodamage are measurable using photography or SIAscopy.

Feature of photodamage	Measurable from photo/SIAscopy
Fine lines	✗
Fine wrinkles	✗
Sallowness	✔
Dyspigmentation	✔
Erythema	✔
Telangectasia	✔
Laxity	✗

Table 4.1 The measurable features of photodamage

SIAscopy is a proven and effective method of imaging blood and melanin and would seem to be ideal for identifying the pigmentary changes occurring in the skin associated with photodamage, either visible or invisible to the naked eye, which we would then be able to analyse. We will also use the standard photographic images and colour spaces to look for patterns in the colour spectrum. All these findings can then be compared to diagnosis for correlation.

Fine lines, wrinkles and laxity are all features of the mechanical properties of photodamaged skin which SIAscopy would not be helpful with. Quantification of these properties would rely on other investigations that are not part of this particular study, although it is recognised that they may play an important role in the subconscious formation of a diagnosis in the clinical judgement of photodamage.

4.2.1 Sallowness

In Chapter 2 I mentioned that photodamaged skin may look ‘sallow’. The word sallow has Old English and Old Norse origins, meaning dusky, yellow or dirty. Its use in the description of complexion tends to define a rather unhealthy appearance of the skin and is particularly accurate in describing photodamaged skin. The dirty yellow appearance has been attributed in some texts to the presence of solar elastosis,[190] probably with some associated dyspigmentation.

As solar elastosis is a well recognised component of photodamage and would seem to have a colour associated with it, we would aim to identify that specific colour and quantify its value.

4.2.2 Dyspigmentation

Dyspigmentation generally refers to melanin disorder in the skin and is a characteristic feature of sun damaged skin. It manifests as variegated patches of hyper- and hypo-pigmentation and may be much more subtle than can be appreciated with the naked eye. SIAscopy would appear to be a good tool to extract the melanin information to allow measurements of relative disorder across the image field.

4.2.3 Erythema and telangectasia

Erythema is a superficial reddening of the skin, usually in patches, as a result of injury or irritation which causes dilatation of the blood capillaries. Visibly dilated blood vessels that branch and course in the surface of the skin are called telangectasia. Both of these features should show up well in the SIA blood field and the relative irregularity of the the blood across the image could be analysed as a measure of disorder.

4.3 Image Capture

The Non-Contact SIAscope consisted of a standard 5 megapixel digital camera (Canon G5, Canon Inc.) with a Macro ring-flash (Canon MR-14EX, Canon Inc.) fitted with crossed linear polarised filters (Edmundoptics Inc.).

Given that this was the first time the camera had been used to collect SIAscopic data, much consideration was put into how to get the most consistent results, specifically regarding the many variables that are encountered when taking a photographic image.

Fig 4.1 Non-contact SIAscope

By using the manual settings of the camera, any combination of aperture size, shutter speed and flash intensity could be configured and the optimum combination found. A series of images were taken of a skin lesion under identical, and then varying, environmental conditions to deduce the optimum set-up of the camera. In order to obtain good, accurate, consistent images, a number of problems had to be resolved.

4.3.1 Differences in environmental light

For the SIAscopic calculations, it is necessary for the incident light wavelengths to be known, however the quality of the light depends on the source. All light is composed of a spectra of wavelengths which differ depending on the source being used to generate the light, thus the spectrum of light from an incandescent light source differs from that of fluorescent light, which in turn differs from sunlight. This spectral quality is called the *colour temperature* and is defined on a measurable colour scale. This scale equates spectral quality of a light source with the heating of a blackbody radiator (a theoretical black body which can equally absorb and radiate energy at all EM wavelengths) until it glows. The specific temperature that a particular colour is seen at is the colour temperature, measured in kelvin. These colours can be correlated with all light sources and photographers use this scale to qualify the differences in colour tone that varying light sources have. They account for these changes by using the white balance of the image to adjust for the different temperature of the light. Even using the sun as a light source can mean a different quantity of spectral frequencies make up the light depending on the time of day. This can be seen at dusk, when the reddening of the sky is explained by the increased amount of sunlight scattering as it passes through more atmosphere, and hence more atmospheric pollutants and water vapour, as the incident light is at more of a tangent to that point on the earth.

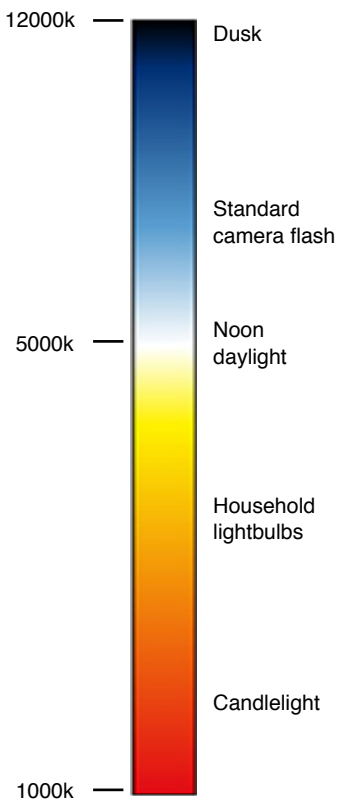

Fig 4.2 Colour temperature scale

The camera was set up so that only light produced by the flash (which can be measured and is consistent) is captured by the camera and any polluting, environmental light (which can be variable in quality) is eliminated. This was done by using polarising filters (one on the flash and one on the lens) arranged perpendicular to each other, which has the effect of blocking any scattered light which is not emitted from the flash and is not directly incident to the lens. In order to get an image a powerful flash was required to swamp the field with a consistent light. A very fast shutter speed is also necessary so that only the light generated by the flash is recorded. However, a fast shutter speed means that to register an image, the aperture of the camera must be sufficiently large to allow enough light in for the short period of time the shutter is open. Thus, in consistent lighting conditions, the aperture size must increase as the shutter speed increases. A series of images were taken to get the correct combination of flash strength, shutter speed and aperture size which would eliminate any environmental light and ensure that only measured light from the flash illuminated the image. This was found to be 50% flash strength, a shutter speed of 1/125 of a second and an aperture value of f/8.0*. This was confirmed by taking a picture under normal, ambient illumination without the flash and seeing that no image was recorded by the camera.

Fig 4.3 Picture showing depth of field - note that images in the immediate foreground and in the background are out of focus

The consequence of the fast shutter speed and larger aperture is that the depth of field of the image is reduced. The depth of field is the range of distance within the subject where the image remains sharp. This does not appear as an abrupt change, from sharp to ‘un-sharp’, but rather as a gradual transition. However, the more narrow the depth of field is, the more abruptly the image becomes out

* The amount of light reaching the cameras sensor is not just dependent on the size of the aperture, but also on the focal length. Photographers refer to the F-stop number or f/value; a number calculated by dividing the diameter of the aperture by the focal length. The smaller the number, the larger the aperture.

of focus. The ‘in-focus’ range of the depth of field could be improved by altering the characteristics of the polarising filters and using a brighter flash, which would allow changes in the shutter speed and aperture, however these would limit the quality of the image. The useful output of the flash is also limited by issues such as portability, power requirements and patient comfort.

4.3.2 Curvature of the surface

It can be deduced that areas of the body with more extreme degrees of curvature may only have a small area which can be in focus when the depth of field is limited. The direction of imaging must be such that the flattest possible surface is imaged to isolate the largest possible field. The camera also needed to be perpendicular to the surface being imaged, to avoid exacerbating the curvature error and limiting shadow effect.

4.3.3 Differences in temperature

As we use our skin to regulate our body temperature, environmental temperature variations have the potential to effect cutaneous blood flow, which would have an impact on the dermal haemoglobin concentration seen by SIAscopy. The temperature in hospitals is kept relatively constant throughout the year at approximately 21-23 degrees centigrade and varies only when there is localised influence from heating or ventilation. The images were taken in one clinical area of the hospital which was thermostatically heated and all the subjects had been in that area for more than 30 minutes. This reduced significant temperature variations as much as possible and limited any effect on dermal blood flow. Within photodamaged skin, the significant factors that could be assessed using the SIAscopic blood image would be the increase in blood flow seen as erythema and the relative disorder of that blood flow within the damaged area. Although the average blood flow in the area may vary with environmental temperature, the relative disorder in a skin field should be consistent in any temperature range.

4.3.4 Consistent image size

Various methods can be employed to ensure a consistent image size from one subject to the next. One well tried method is to use a stick or piece of string of known length, attached to the camera, to keep a fixed focal distance and thereby ensure similar dimensions in each image. This sort of equipment can be inaccurate, bulky and prone to damage.

Fig 4.4 Camera with fixed distance device

The Canon G5 allowed us a more flexible approach to this problem. Due to the use of linear polarisers, the auto-focus function of the camera was disabled, so manual functions were used to fix the aperture and shutter speed. One of the manual functions available on this camera was the ability to select and fix the focal distance. This was fixed as close to the subject as possible (15cm) and although this reduced the size of the field being imaged, most skin lesions are small enough that a usable field could be captured. The camera has a 1.8 inch LCD screen on the back which displays the image seen through the lens and under the macro setting a magnified image is shown in the centre of the screen to allow for accurate focus control. With the focal distance fixed manually, physically moving the camera towards or away from the subject allowed the image on the LCD to move in and out of focus, thereby allowing sharp images to be taken even with a limited depth of field. By fixing the focal length this way, a consistent image size was achieved if the picture was in focus, thereby eliminating the need for cumbersome camera attachments and ensuring good quality images each time.

Each field image measured 43mm by 54mm and with the 5-megapixel CCD this meant a digital image size of 2600 by 1944 pixels. Using a short focal distance also reduced the problem of image shake from manually holding the camera at greater distances from the target, a problem that would be exacerbated by the reduced depth of field.

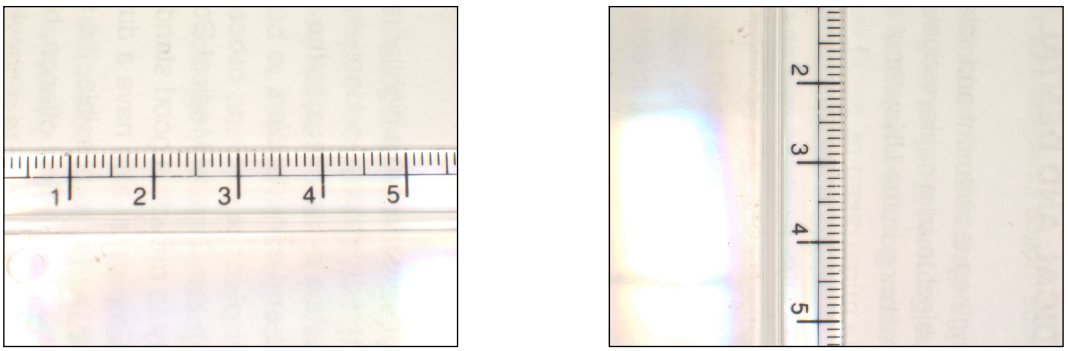

Fig 4.5 Field image sizing pictures

4.3.5 Image format

The format of the image is the method in which the data received from the CCD is recorded by the camera. The most common format used in most cameras today is the JPEG format (Joint Photographic Experts Group)[189]. This is a standardised image compression algorithm designed to compress 'real world' images into a smaller file size ready for sharing or printing. It can achieve significant compression (up to 90%) by exploiting the resolving limitations of the human eye, particularly the fact that small colour details are not as well perceived as small details of light and dark. This means there is an increase in the contrast and sharpness of the image at the expense of some of the colour and resolution. JPEG is described as a 'lossy' image format as some of the image data is lost in the compression, but as this is limited to that which the eye cannot perceive, it is ideal for most basic photographic needs. However, this 'lost' information may be the very data we want to analyse.

The RAW format stores the entire data from the camera CCD, with no image processing or compression applied by the camera. It is not a true image file per se, as it requires specific software to read the data, but it allows much more flexibility in subsequent image manipulation without the loss of any data. It maintains all of the colour and dynamic characteristics of the image and as a result file sizes can be 5-10 times larger than for JPEG images from a similar CCD. It is not as popular in lower-end photography as the images need further software manipulation or 'post-processing', but this very flexibility to manipulate the image is why it is referred to as the 'digital negative' and why it is popular

with professional photographers. This was thought to be the ideal format choice.

4.3.6 Camera calibration

All the individual components of the non-contact camera were calibrated to ensure that the captured images were consistent with one another and that any small inaccuracies in the images, caused by the inherent individual features of the equipment, could be compensated for. For each of the components (camera CCD, lens, flash unit and polarising filters) the exact emission/absorption spectra were measured. To assess the response of the CCD (or more accurately the Bayer filter) and the camera lens to light, the absorption spectra of each was measured using a monochromator. This device acts as a very accurate light source and emits a specific, selected wavelength of light. The response of the component in question, in this case the camera lens and the CCD/Bayer filter combination, can then be evaluated for each of the chosen wavelengths and thus the response to multispectral light can be built up.

The output spectrum of the flash was measured using a spectrometer so the relevant amount of each wavelength of light could be known. A spectrometer works in the opposite way to a monochromator, essentially measuring a multispectral emission and defining the amounts of each wavelength of light making it up. The transmission spectrum of the polarising filter (a measure of just how much light travels through) was also measured with a monochromator.

Fig 4.6 A Monochromater

The ideal camera set-up and lesion position was found to be :

Format - RAW image capture
Focal length - 15 cm
Aperture - f/8.0
Shutter speed - $\frac{1}{125}$ of a second
As flat an image surface as possible

Table 4.2 Ideal non-contact camera settings

It takes approximately 10 seconds to acquire the image i.e. turning the camera on, positioning the camera so that the image is in focus, ensuring it is parallel to the surface of the skin and taking the image.

4.4 Data Collection

Patients were recruited from the departments of Plastic Surgery and Dermatology at Addenbrooke's Hospital, Cambridge, UK. Ethics committee approval was sought and granted at this site (Ref. 05/Q0106/90). Patients were referred to these departments by their general practitioners for assessment of a suspicious skin lesion and were assessed by either a consultant dermatologist or consultant plastic surgeon. From here they were either reassured that the lesion was completely benign and discharged back to the GP, or they were placed on a surgical list for either a diagnostic or excision biopsy of the lesion. Histological analysis was performed on all of the excised lesions and the diagnosis by the consultants of the benign skin was also recorded.
Eligible patients were asked if they would have the lesion photographed and were given an information sheet. An outline of the study was explained prior to

them signing a consent form (see appendix B). The entire process did not significantly lengthen the time taken in either the clinic or the operating theatre. Exclusion criteria were those patients who could not understand English sufficiently well to give informed consent to imaging, or patients who were unable to consent for any other reason.

4.4.1 Which data was recorded

The recorded details consisted of image specific and demographic data:

- Date the image was taken
- Image number (an arbitrary identification number used during the analysis process to identify the image for automatic analysis)
- Age
- Sex
- Location on the body (one of 24 specific areas)
- Binary location (either head & neck or body)
- Clinical diagnosis of lesion (as per suspicion of medical specialist)
- Clinical diagnosis of the field damage (as per suspicion of medical specialist)
- Histology result (from hospital database)
- Binary diagnosis of lesion (benign or malignant - relating to evidence of the presence of photodamaged or not)
- N/C SIA Image Number (unique number digitally attached to each image)
- Picture rating (quality rating 1-4)

Collection of this data is required so that statistical analysis can be employed to measure the effect each has on the final photodamage score and so control for it. This means certain characteristics can be removed from a final analysis to exclude an arbitrary function, such as location, being interpreted as a measure of photodamage. It is accepted at this point that more photodamage may be present in certain areas of the body (like the head and neck, exposed areas of the hands and lower legs, etc.), or may be more abundant in older men than

younger women, but the purpose of this thesis is to ascertain if the non-contact SIAscope can identify pigmentary features within the skin which would be attributable markers of photodamage age.

4.4.2 Location

Modified locations	
Dorsum of nose	Shoulder
Alar of nose	Chest
Ear	Abdomen
Scalp	Upper back
Malar	Lower back
Forehead	
Temple	Upper arm
Lower lip	Lower arm
Upper lip	Hand
Cheek	Thigh
Chin	Lower leg
Front of neck	Foot
Back of neck	

Head & neck Trunk Limb

Table 4.3 Modified locations

93 locations were recorded in the original data table (including laterality), but this was found to be far too detailed for efficient data analysis. This was reduced to 24 specific locations depending on the relative frequency that lesions were found in those areas and also on an anatomical basis. As expected, this meant that there was a greater number of areas in the head and neck as the majority of photodamage is found in that region.

4.4.3 Diagnosis

There were 55 different histological diagnoses identified and for the purposes of analysis, sub-classification of lesions was not thought to be useful. This meant all sub-types of BCC were classified as BCC and not by the specific variant. Similarly all naevi were classified as naevus and not by specific sub-types. Although this information was present on many histology reports, it was not consistent throughout the reporting and added no further information with which to identify photodamaged skin. Within the histology report there was not only the primary (lesion) diagnosis, but occasionally other information relating to the skin surrounding the lesion (e.g. solar elastosis or actinic changes). Although this was also not consistent throughout the histology reporting, it did give valuable additional information to isolate images with photodamaged field change. Where no histological analysis was available, the decision of the clinical expert was used to identify those images with evidence of photodamage. Each of the different diagnoses were grouped into 14 categories with accepted links to skin photodamage.

Diagnoses associated with photodamage	
BCC	Elastosis
SCC	Solar elastosis
Bowens disease	Actinic lentigo
LM	Actinic granuloma
LMM	Actinic keratosis
Adnexal tumours	Solar keratosis
KA	Keratosis

Table 4.4 Diagnoses associated with skin photodamage

4.4.5 Why melanoma was excluded from the photodamaged group

In order to use the principle of field damage and carcinogenesis through accumulated photogenesis, we could only use lesions which were recognised as a *consistant* marker of photodamage. MM is described in section 2.4.9 and although UV radiation is recognized as a stimulus to the carcinogenesis of melanocytes, current evidence suggests there is no specific requirement for continued UV exposure as a promoter of malignant transformation. This can be seen by the significant number of MM that arise in non-chronically solar exposed skin (such as the trunk) and by the increasing number of MM found in younger age groups. It is becoming increasingly clear that short, intense bursts of sunlight in solar naive areas of the skin, particularly in childhood, are a significant risk factor.

MM is clearly a complex disease and most likely has strong genetic and multifactorial facets to its progression and conversion. It would be incorrect to imply that the formation of melanoma is simply a function of the cumulative role of UV light.[191] Within the melanoma family, Lentigo maligna melanoma (LMM) is the only variant which consistently occurs in photodamaged skin and the link to excessive UV irradiation is more widely accepted. Evidence would suggest that a direct relationship between photodamage and melanoma, other than LMM, is unlikely[192,145] and in the absence of a general acceptance of its association with photodamage, MM and in-situ MM were excluded from the photodamaged group.

In this thesis, the diagnosis of the skin lesion is only used as a marker of the potential field damage present in that image. This meant that some of the MM images were included in the study, where other elements within the histology, diagnostic of solar damage (such as the presence of solar elastosis) supported their inclusion. Of the 22 MM/LM(M) in the data group, 8 had other evidence of photodamage and were retained within the study and 14 were excluded.

4.5 Preparation of the data set

Before data analysis can begin the data set must first be prepared. All of the images were checked for their suitability for further analysis and the basic image data was extracted from the images.

4.5.1 Image selection and preparation

All images needed to be of good quality and sharply in focus. Once the initial data set was collected, all the images were visually examined to identify any that were not of a sufficient quality to undergo further analysis. This included images which were out of focus or where the flash, aperture or shutter speed settings were not accurate. This information is associated with all digital images as metadata† and is easily accessed. I applied a visual picture rating of 1-4 to all the images, representing out of focus, poor, good and excellent images respectively.

It is reliably noted that most skin solar damage occurs on the head, neck and dorsum of the hands, areas which are exposed to daylight throughout our lives on an almost daily basis. Our bodies, particularly our heads, are inherently curved, meaning that the area of skin in focus varied depending on the amount of curvature of that area of the body being imaged. To isolate the field of interest, areas of the image that were out of focus or in shadow due to the narrow depth of field, needed to be excluded. Hair and clothing were also excluded, as were any excessive areas of pigmentation which were unrelated to the measure of photodamage within the field, such as tattoos, simple naevi or seborrhoeic keratoses. The central skin lesion in each image was also excluded so what remained was a usable area of well focused 'field skin' for further analysis.

† Metadata is a term for the descriptive information embedded inside an image or other type of data file. The metadata captured by a camera is called EXIF data (Exchangeable Image File Format) and is easy to display, but is not usually editable.

A software script was written for the mathematical software package MATLAB® (MathWorks, Inc), which allowed me to manually 'crop out' any undesirable artifact from the image.

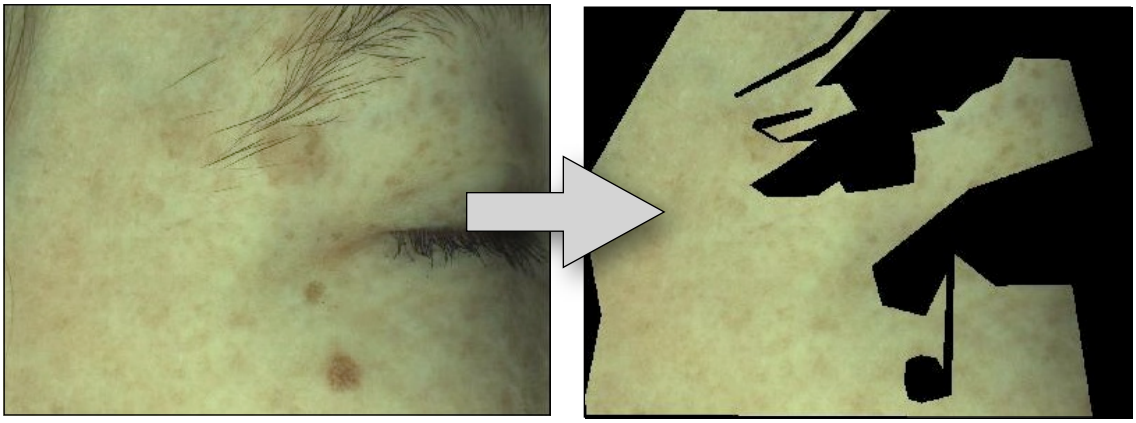

Fig 4.7 Exclusion of hair and areas of shadow

In flat areas, like on the back, removing artifact from the image was very straight forward. However, on particularly curved or hairy areas, this became a little more challenging.‡

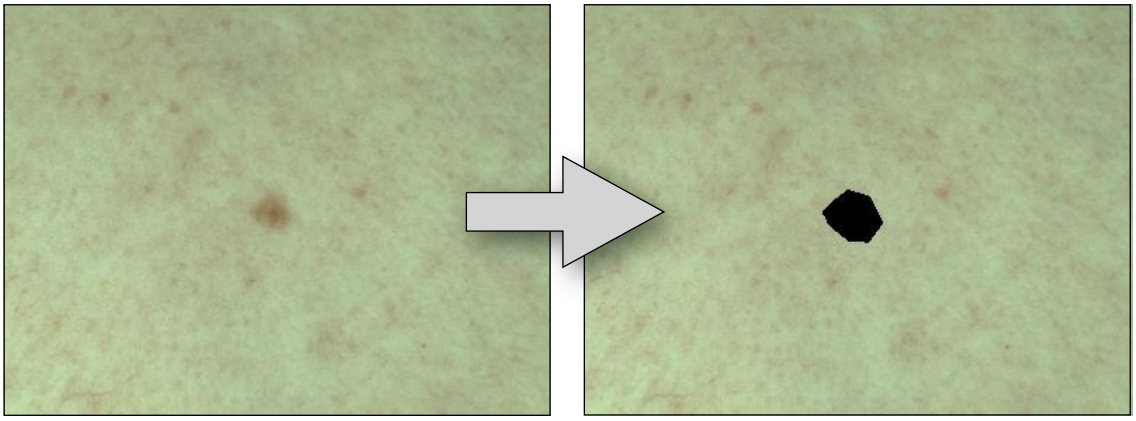

Fig 4.8 Exclusion of a naevus unrelated to the skin field analysis

‡ Note how washed out these RAW format images look. This is due to the lack of image optimisation usually done by the camera firmware and from the effect of the polarising filters on the camera.

4.5.2 Images that were excluded

Images in groups 1 and 2 were excluded, as were those with inaccurate camera and flash settings, confirmed from the image metadata.

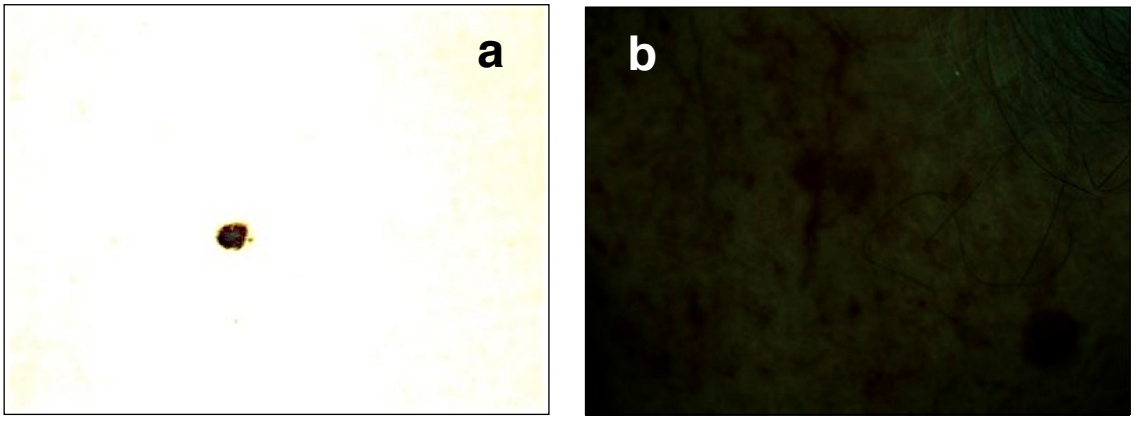

Fig 4.9 Images with inaccurate camera settings a) aperture too wide resulting in too much light exposure b) shutter speed too fast resulting in under exposure

A field area of specific size was required to perform certain aspects of the analysis and in some images the cropping process left insufficient area to analyse. This occurred particularly where the surface was highly convoluted (such as the ear) or where there was large amounts of artifact pigment (like hair), so any images which did not meet these requirements were also excluded.

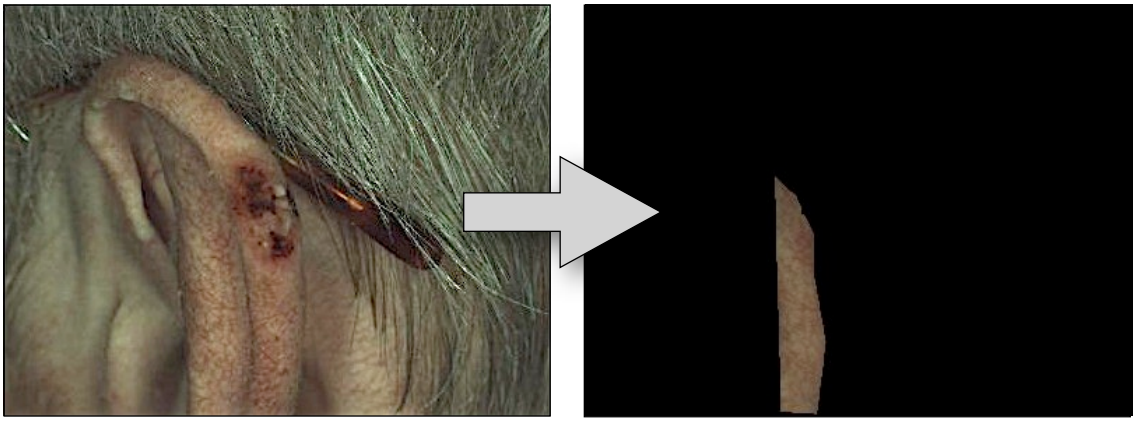

Fig 4.10 Images with insufficient area for analysis after cropping

In total, 1340 images were taken of which 1141 were used for analysis, all of which were good quality, well focused images with no excessive curvature and a good sized, flat area to analyse. These were split into a standard ⅔ model set and ⅓ test set, of 761 and 380 images respectively.

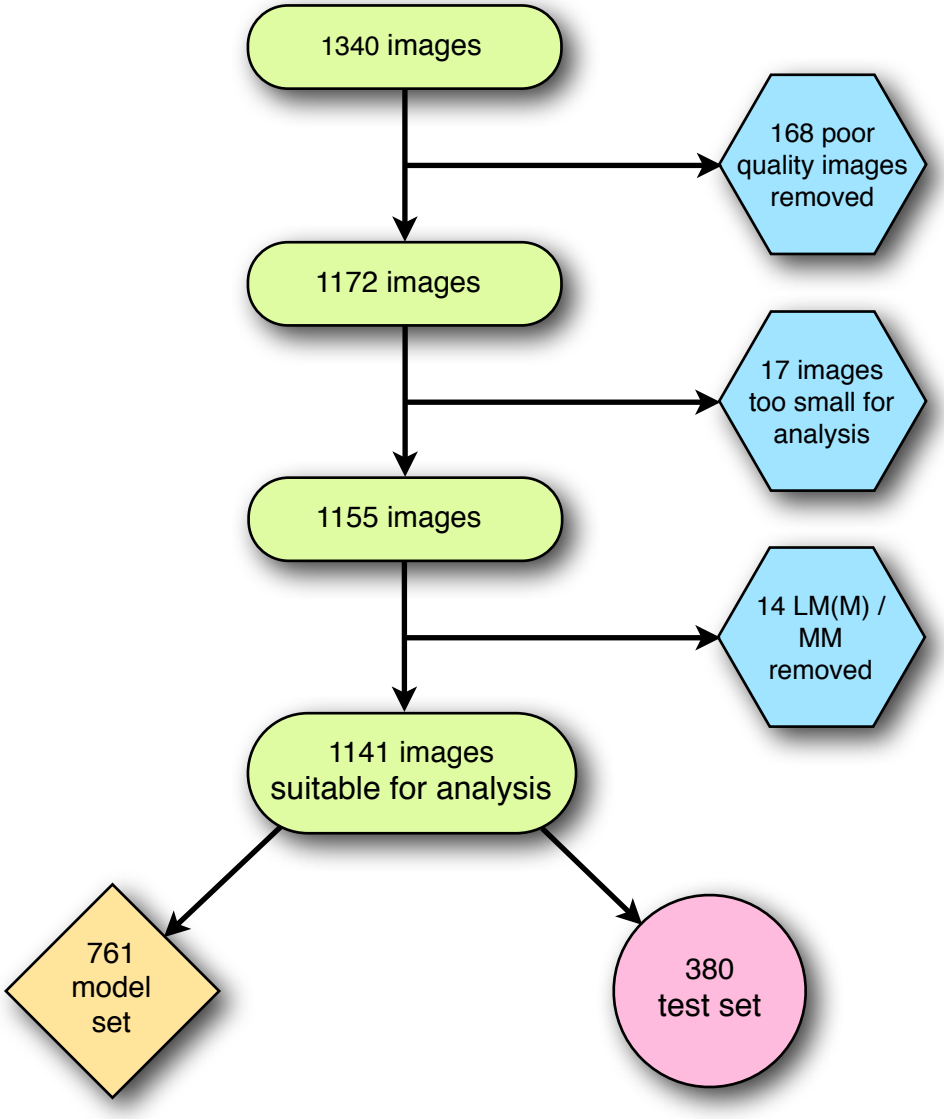

Fig 4.11 Flowchart showing the separation of images into model and test sets

4.6 Data Analysis

From each of the 1141 images within this data set, the following individual elements were produced or measured -

1. Image red
2. Image green
3. Image blue
4. Image blood
5. Image melanin
6. Skin area of interest
7. Lesion area of interest
8. Fourier analysis area of interest

The RAW image data was decomposed into individual red, green and blue colour data. As described in the previous chapter, it is the transmission properties of the Bayer filter which allows either red, green or blue wavelength data to be registered by each pixel. This means the CCD naturally produces RGB data.

Blood and melanin image data was generated using the non-contact SIAscopy algorithms from the RGB data.

The skin area of interest relates to the uncropped area of the image, i.e. the area of the image excluding the central lesion and other artifact, in which we were interested in doing the analysis for photodamage. This had to be sharply in focus and free from shadow, hair or unrelated areas of pigmentation.

The lesion area of interest is the cropped area of the field taken up by the central lesion in the image originally identified as potentially suspicious and prompting consultation.

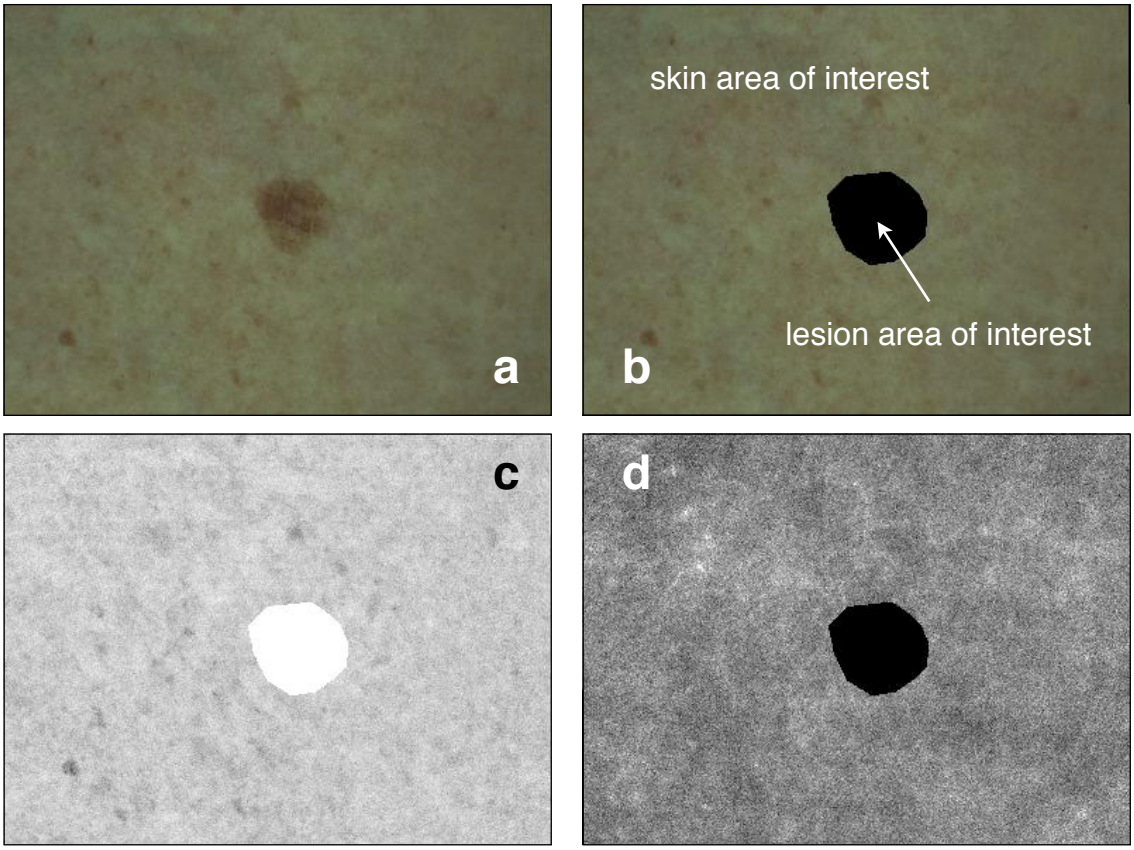

Fig 4.12 Series of pictures showing the basic analysis images. a) RAW colour image, b) Cropped image showing the lesion area of interest and the skin area of interest, c) SIA generated melanin image, and d) SIA generated blood image

4.6.1 Fourier analysis

Fourier analysis is a branch of advanced mathematics that can decompose a complex element (a sound, picture or any data stream) into the most basic sin and cosine waveforms. It has diverse applications in all manner of data analysis and is widely used in image analysis and manipulation.

One well known application was in the analysis of sun spot activity, which has been recorded since the time of Galileo, but began in ernest in the 19th century. A plot of the data shows no clearly discernible pattern, but when Fourier analysis is applied to the square root of the data, a frequency peak can be seen at approximately 11 years. This is the time frame of the Schwabe cycle, the time between two subsequent maxima or minima of solar activity.

In this study, Fourier analysis was performed on the blood and melanin images within 256x256 pixel squares placed in the skin area of interest. A representative area of 256x256 pixels was chosen as it is a simple binary number and would make relevant computations more straight forward. Individual boxes were used rather than analysing the entire image as the cropped areas and straight lines from image preparation would have introduced error into the result. Each box was analysed to look for any common, recurrent or specific frequencies of colour, brightness and image that may relate to photodamage age. The frequencies were divided into 65 sections and the mean of each section was analysed.

I have written a more detailed description of Fourier analysis technique in image analysis, which can be found in Appendix C.

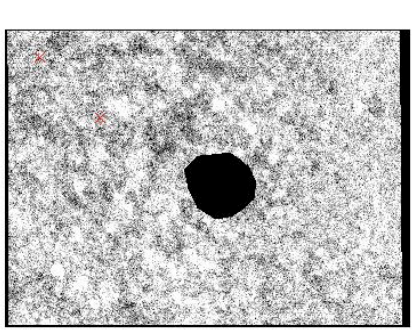

Melanin image

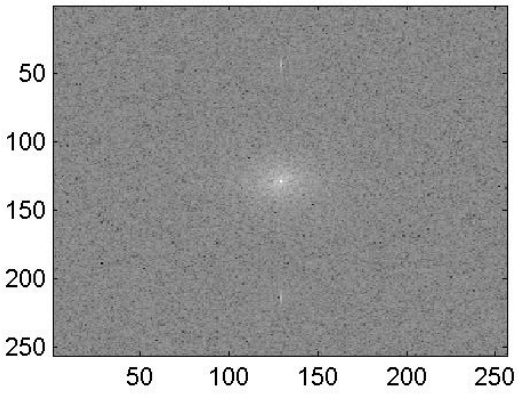

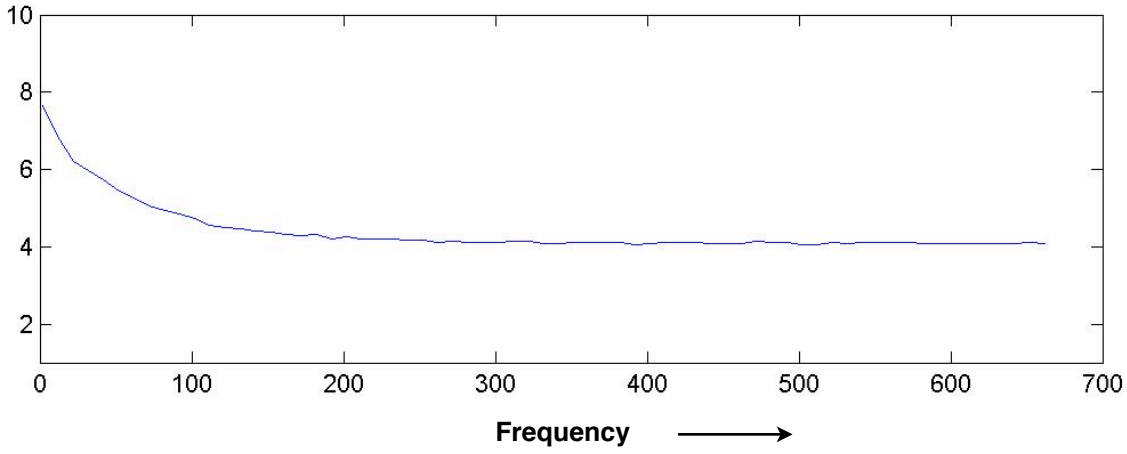

Fig 4.13 Melanin Fourier analysis

4.6.2 Red, green, blue, melanin and blood data

Basic analysis was done on the extracted red, green and blue (RGB) image data and the SIA generated images of blood and melanin. For each RGB, melanin and blood image, the following were measured within the skin area of interest:

- mean value
- standard deviation
- covariance
- maximum value
- minimum value
- range (max - min values)

4.6.3 Entropy

The entropy of the RGB, blood and melanin images was also calculated (entropy being the quantitative measure of disorder in a system, or in this case the image). From what we know about the visible pigmentary changes in photodamage (section 2.3.1), we would expect there to be a difference in entropy in photodamaged skin compared to non-photodamaged skin.

4.6.4 Freckles

One particular feature of dyspigmentation that can be easily seen are solar lentigines. These initially appear as freckling of the skin and it is anticipated that the number of freckles would increase with progressive photodamage, along with changes in their colour, size and shape, becoming more confluent and darker as damage progresses. Analysis of the SIA-generated melanin image to identify and measure the freckles was performed and as well as a simple count of the number of freckles in each image, various measurements associated with the size, shape and pigmentation of the freckles were made.

The mean, standard deviation, covariance and range were measured for each of the following freckle categories:

- area
- eccentricity
- solidity
- extent
- melanin in the freckle
- total melanin
- hue

The ‘area’ is a simple measurement of the size of each freckle and ‘eccentricity’ relates to how *not* round the freckle is. ‘Solidity’ is calculated by fitting the smallest possible box around the freckle and then measuring how much dead space there is around it. ‘Extent’ is the proportion of the image taken up by the freckle. The melanin level in each freckle was measured as the ‘melanin in the freckle’ and the ‘total melanin’ was the total amount of melanin in the image. The ‘hue’ identified any changes in colour of the freckles on the HSV colour scale.

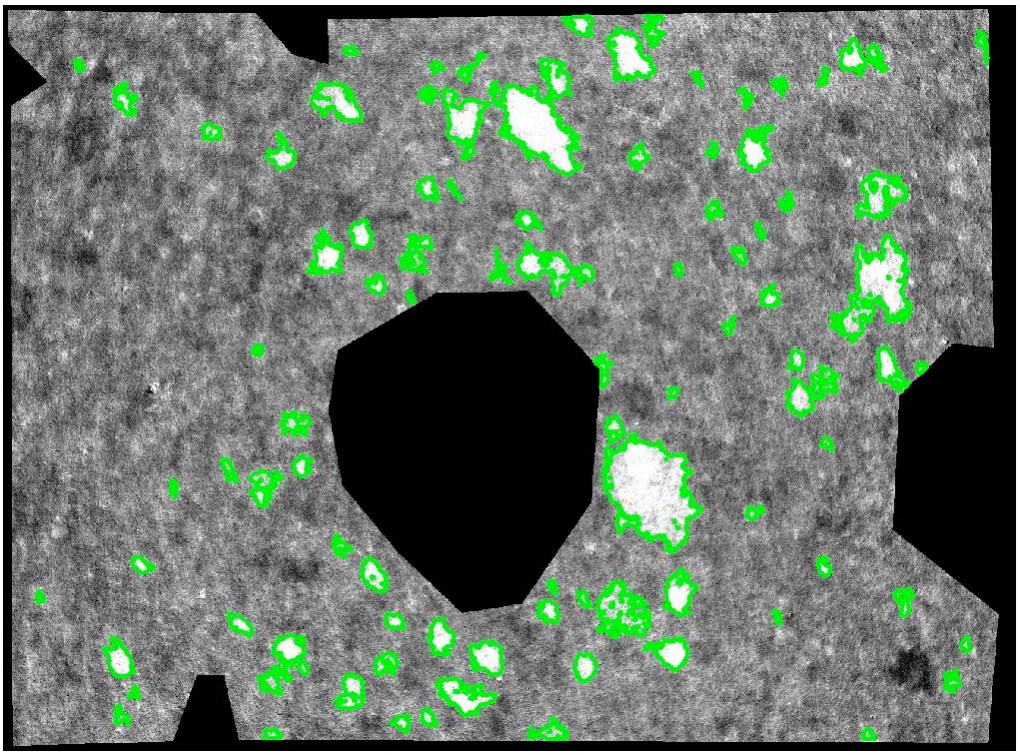

Fig 4.14 Inverted melanin image identifying the freckles within the skin field

The intensity of the pigmentation of the freckles was identified using a threshold intensity filter. This adjusts the image by looking at the mean melanin value for the image, applying a standard deviation to it and then applying that colour to the image as a filter. The result of this is to effectively change the contrast of the image and so exclude the paler freckles. The number and size of the remaining freckles above the filter intensity can then be measured. Increasing the filter by further standard deviations will sequentially exclude the paler freckles. As the starting point is the mean of the melanin for the entire image, you can effectively eliminate any skin colour bias and so isolate the freckles from the background pigmentation.

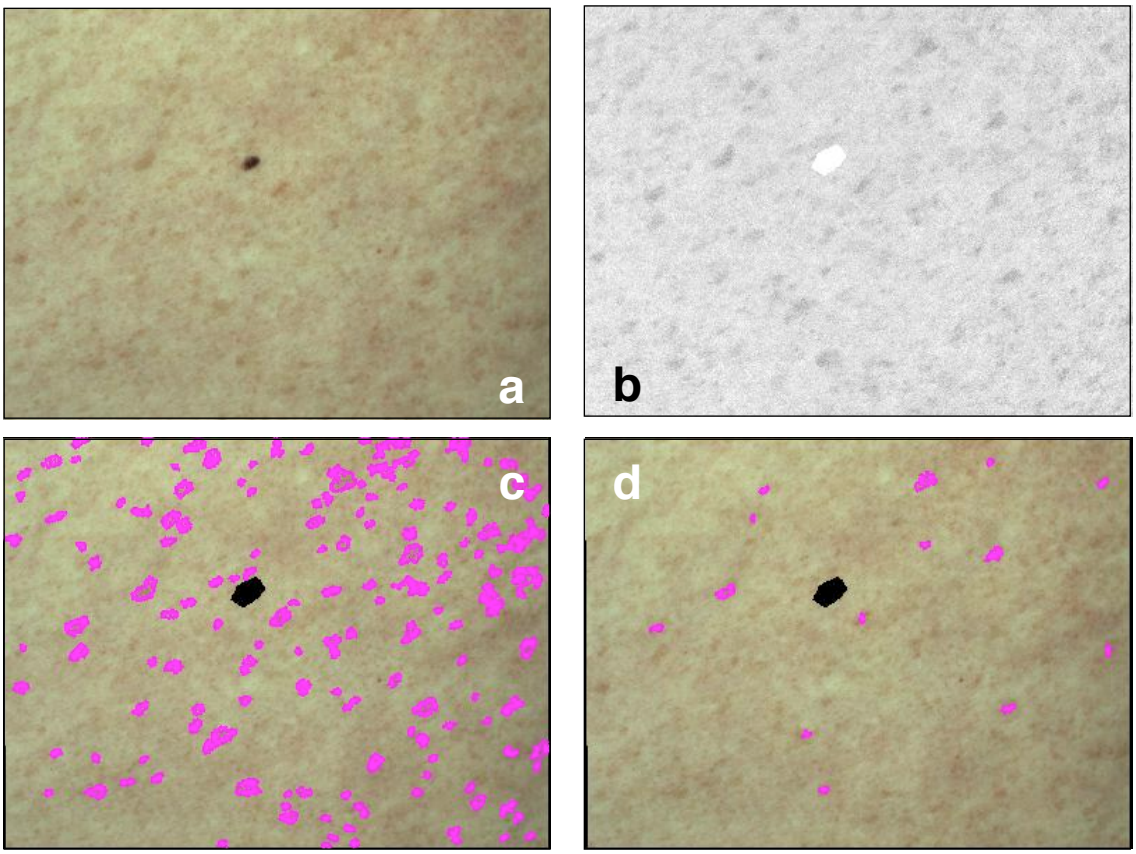

Fig 4.15 Examples of freckle threshold intensity filtering
a) the initial picture of the skin field, b) the cropped melanin image,
c) & d) identification of freckles with progressive standard deviation filters

The following measurements were made for 11 standard deviation filters in each image:

- mean freckle size
- standard deviation freckle size
- covariance freckle size
- number of freckles
- threshold fraction

The threshold fraction looked at how much of the image remained after each standard deviation filter was applied, so calculating the fraction of the melanin image that was above that threshold.

4.6.5 Blood threshold

As with the melanin image, a standard deviation filter was applied to the blood image to measure how much of the image is made up of blood above that specified threshold limit. The initial threshold was the mean blood for the image and each threshold increment was a further standard deviation, for a total of 13 further increments.

4.6.6 Colour

As well as analysing the RGB data for each image, an HSV colour space measurement was made, looking at the hue of the overall image. This was to see if there was any underlying colour in the image which may be associated with photodamage. Hue is a measure of the colour in the HSV colour space and can be seen as a colour wheel showing all the possible colours reproducible within that colour space in a continually variable space. For the purpose of calculations, we divided the colour wheel into 50 sections and analysis was then done to find out what fraction of the pixels in the image had a hue value within the range defined by each slice, as can be seen in Fig 4.17. Using the measurements of the of the transmission properties of the camera lens/filter and the CCD/Bayer filter, the colour analysis can compensate for any effect these may impart on the recorded image. This means that a true representation

of the colour of the skin is analysed, despite the rather bland looking colour palate seen in the decoded RAW images presented throughout this chapter.

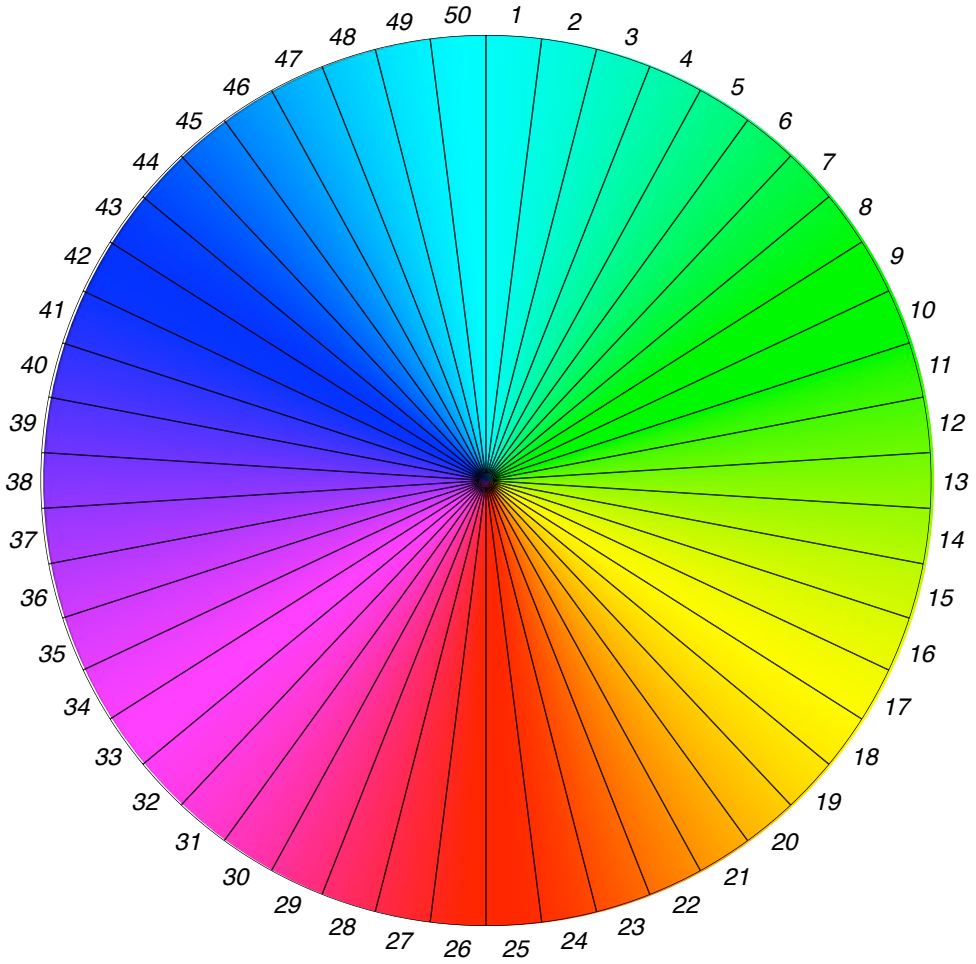

Fig 4.16 Fully saturated HSV colour space divided into 50 fractions

4.6.7 Populating the results table

An image analysis script was written for MATLAB® which detailed all the calculations to be made for each image. In total there were 347 different variables analysed on each of the 1141 pictures. These results then populated an Excel® (Microsoft Corporation) spreadsheet and was then run through SPSS® (IBM Corporation) for statistical analysis to identify characteristics which could reliably be associated with increasing age. Regression analysis was used to create predictive models for each of these features and to construct an equation incorporating the most useful functions with the lowest possible collinearity.

4.7 Regression analysis

Regression analysis is a statistical method by which it is possible to build a model from a data set that can be applied to predict a value of an unknown variable from one or more known variables.

Linear regression is a tool that can be used to show a relationship between two variables by fitting a linear equation to observed data. One variable is considered to be an explanatory, or known, variable (x), and the other is considered to be a dependent, or unknown, variable (y). This does not necessarily imply that one variable causes the other, but that a change in x is *associated* with a change in y. Simple linear regression uses a single predictor, whereas multiple regression uses many predictors.

4.7.1 Assumptions

There are 4 main assumptions of regression analysis:

1. Normality (the variables being measured lie in a normal distribution)
2. Linearity (the relationship between the known and unknown variable should be linear. If this is not the case we may get underestimation of the outcome)
3. Little or no collinearity (Multicollinearity occurs when the independent variables are not independent from each other)
4. Homoscedasticity (the error terms along the regression line should be equal)

4.7.2 Scatterplots

Before attempting to fit a linear model, it is first wise to see if there is a potential relationship between the two variables and that it is, in fact, a linear one. A scatterplot gives a good visual picture of the relationship between the two variables and is often employed to identify potential associations between two variables.

There may be a positive association, where an increase in y is seen with an increase in x, a negative association, where a decrease in y is seen with an increase in x, or no association.

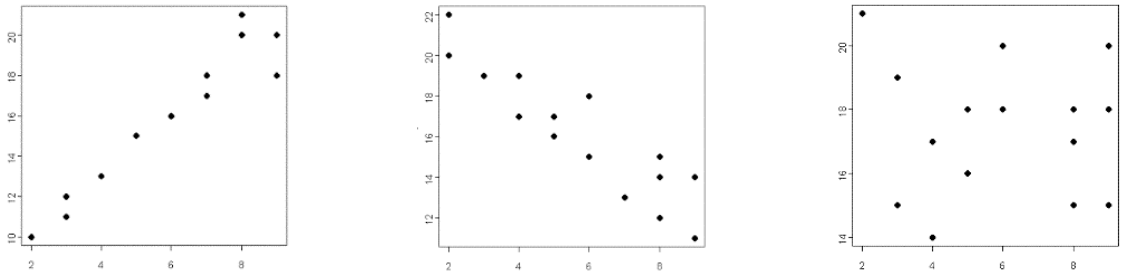

Fig 4.17 Examples of scatterplots showing the relationships between two variables

If there appears to be no association between the proposed explanatory and dependent variables (i.e. the scatterplot does not indicate any increasing or decreasing trends), then fitting a linear regression model to the data probably will not provide a useful model.

4.7.3 Least squares and the regression equation

Simple linear regression attempts to find a straight line that best 'fits' the data, where the variation of the real data above and below the line is minimised.

The most common method for fitting a regression line, or a line of best fit, is the method of least-squares. This method calculates the best-fitting line for the observed data by minimizing the sum of the squares of the vertical deviations from each data point to the line of best fit. If a point lies exactly on the fitted line, then its vertical deviation is 0. The deviation of a particular point from the regression line (its predicted value) is called the *residual value*. It indicates the difference between the predicted and the observed values.

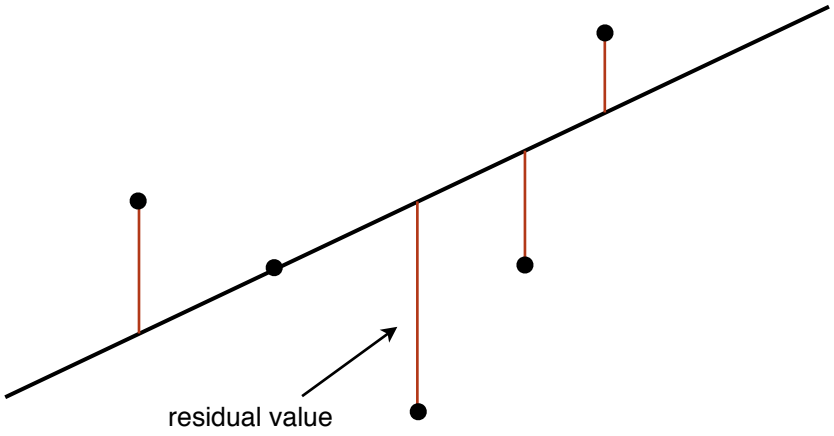

Fig 4.18 The line of best fit and residual values

If the deviations are simply added together, positive and negative deviations would cancel each other out, so the deviations are first squared before being summed. The line with the smallest sum of the squares is most representative of that data set.

This whole process would be a very time consuming if done manually and is now done by statistical computer programs.

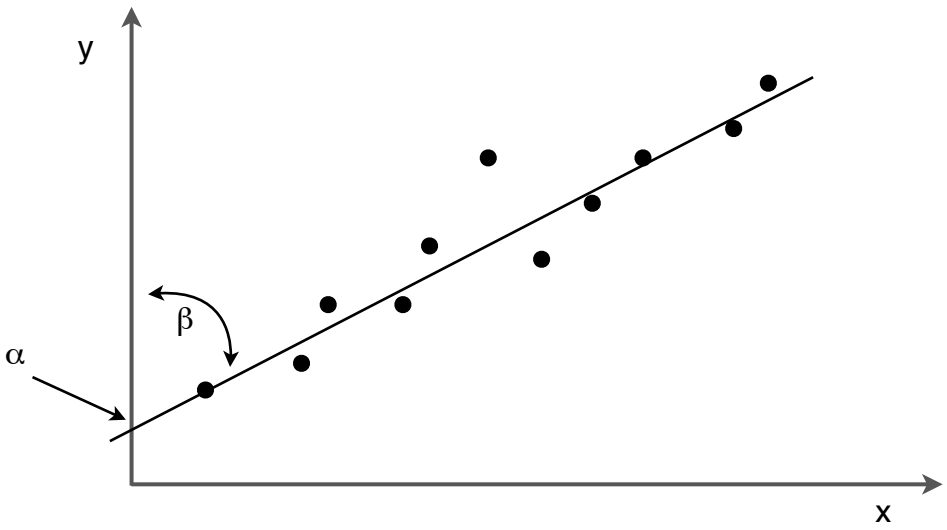

Fig 4.19 A regression line for a data set

If there does appear to be a relationship then the line may be described mathematically as:

$$y = \alpha+\beta x$$

- where x is the explanatory (or known) variable, y is the dependent (or unknown) variable, α is a constant (the intercept value of y when x = 0) and β is the slope of the line. β is also known as the regression coefficient or β-coefficient. This is the mathematical model describing the functional response of y to x.

In a multivariate scenario the regression line can not be visualised in a 2-dimensional space, but can still be computed as the equation can be extended to include the effects of multiple variables, such that:

$$y = \alpha+\beta_1 x_1+\beta_2 x_2+\ldots \ldots +\beta_n x_n$$

4.7.4 R-squared

R-squared (R^2) is a commonly used statistic to evaluate the model fit and is also called the *coefficient of determination*. It is a measure of the amount of variability in one variable that can be explained by the other and allows us to see how well the model fits the data. It is calculated as 1 minus the ratio of residual variability, where the residual variability is a measure of the variability of the residual values around the regression line. If this variability is small, then the predictions from the regression equation are good. The ratio of variability have values between 1 and 0, so if there is no relationship between the x and y variables, the ratio of variability to the original variance will be 1, so making R^2 equal to 0. If x and y were perfectly related there would be no residual variance, making the ratio of variability 0 and so R^2 would be equal to 1. In real terms R^2 falls somewhere between 0 and 1. If R^2 was 0.45, this would suggest that the variance of the y-value around the regression line is somewhere between 1 and 0.45 times the original variance. It therefore shows us that we have explained

45% of the original variability and are left with 55% of the variability unaccounted for.

Therefore, for any model, the closer its R^2 value is to one, the greater the ability of that model to predict a trend. A value of R^2 equal to one would imply that your model provides perfect predictions.

The strength of the linear association between two variables is given by the *correlation coefficient*, R, which is the square root of R^2. It has values ranging from -1 to 1, with -1 and 1 explaining perfect correlation i.e. all points lying on a perfect straight line. If the correlation is positive, then there is a positive association between the variables (one increases as the other increases). A negative correlation suggests a negative association (as one variable increases the other decreases) and a correlation of 0 indicated no association between the variables.

4.7.5 Limitations

The major conceptual limitation of all regression techniques is that you can only ascertain a relationship between variables, but not causation between them. This can be illustrated by thinking of the damage a fire has done and the number of firemen attending the fire. There may be a strong correlation between the two, but it does not follow that the firemen caused the damage. Other variables, such as the size of the fire, its site, wind direction, accelerants, etc, may have stronger correlation to the damage caused, but were not considered. This example illustrates how alternative causal relationships can be considered in correlation research.

4.7.6 Choosing the number of variables

By using as many predictor variables as possible to identify a variable of interest, you rely on chance to a degree to find a few which may be significant. This problem is made worse if the number of observations is relatively low i.e. it is difficult to draw accurate conclusions from an analysis of 100 pictures if only 10 are good enough to analyse. It is beneficial to have many more observations

than variables for robust modeling. However, simply adding as many variables as possible and seeing what happens can introduce error into the results and it is recommended that the number of variables is kept as relevant as possible and at least based on some robust theory or research.

4.7.7 Multicollinearity

Multicollinearity is a problem in correlation analysis and occurs when two or more predictors are strongly correlated. This makes it difficult to obtain unique estimates of the correlation coefficients as their values effectively become interchangeable. Collinearity at some level is unavoidable and low levels are not generally a threat to generated models, but higher levels of collinearity can lead to unstable results. This is because it becomes impossible to assess which predictor is important in generating the equation if they are interchangeable. Simply adding a variable into a model that is highly correlated with another will mean that the amount of unexplained information in the model is unlikely to change much. There are several methods of detecting and measuring multicollinearity including correlation matrices, variance inflation factor (VIF) and tolerance statistic analysis. Often it is not immediately clear that multicollinearity exists and may only become apparent after several variables have already been entered into the regression equation. Once detected there is very little that can be done to satisfactorily remedy the situation. If a predictor is removed then an equally important one should replace it that has weaker collinearity. It is suggested that the safest option is to acknowledge the unreliability of the model.[193]

4.7.8 The importance of residual analysis

Residual analysis is an important part of the model checking process so that any outlying points can be identified which exert a significant influence on the model. In some cases these can seriously bias the result by moving the regression line in a certain direction and leading to biased regression coefficients. Residuals can be standardised by dividing their value by an estimate of the standard deviation. It would be expected that 95% of residuals have values between ± 2 and 99% of values between ± 2.5. Any residuals with a value greater than 3 are cause for concern as they are extremely unlikely to have occurred

by chance and if 5% of residuals have a value greater than 2 then there is evidence that the model is a poor fit of the data. Once outliers have been identified they should be analysed to see why they have occurred. It may be that there was an error in the data inputting or a malfunction in equipment which can be easily corrected, but often no reason is found. In certain circumstances it may be justified to remove an outlier that is not representative of the data, but excluding a single extreme case can create a completely different set of results and should not be done just to make a model fit the data better.

4.7.9 Model testing

Once the model is constructed and diagnostics have been performed to ensure 'goodness-of-fit' and rule out outliers or influential points, it is necessary to see how well the model actually performs. The model could be tested on the data used to create it, but this can make the model look better than it actually is. One solution is to split the data into a model and a test set. This eliminates any error from using the modeling set of data and is the best method of producing an unbiased estimation of the real time function of the model.

The statistical element of this chapter has been written using Andy Fields excellent book Discovering Statistics[193] and from the Electronic Statistics Textbook by Statsoft, Inc.[194]

4.7.10 Constructing the model

Using age as a proxy for photodamage, regression analysis of the variables can be performed to create a model to predict age. Each variable has a coefficient which can be added up to give a predicted measure of age as the regression equation, though not all variables will be relevant to the model. The amount of variation in age explained by the model is expressed as R^2. The higher R^2, the better the model is at describing age. As we are using multiple variables, multiple regression analysis would be the most appropriate analysis to run. If we were using continuous *and* dichotomous variables then logistic re-

gression would have been better, but as we discussed, a dichotomous result is not beneficial in this study.

A suggested strategy for multiple regression analysis is to run an analysis in which all the predictors are entered into the model and then examine the output to see which predictors contribute the most to the models ability to predict the outcome. The predictors should not be random variables however, and should be based on some sound theoretical basis on which to believe they are significant.

An Excel sheet with all of the individual measurements was run through SPSS using a forced entry method. This was chosen as all of the predictors could be of equal benefit in describing the outcome, but there were too many of them to manually look at the effect of each and there has been no previous research in this matter to use a hierarchical method of data entry at first. Random scatterplots were assessed to judge if there was any likelihood of a relationship between the data prior to their further analysis.

Chapter 5

Results

In this chapter the results of the data set analysis and the statistical output of SPSS is presented. The most relevant statistical output is presented here and all of the SPSS output can be found in Appendix D. Essential explanation is provided here, while the relevance of the results is discussed in chapter 6.

5.1 Demographic data

What follows are graphical representations of the demographic data. From these we can look at the variation of the data sample and to see if it was representative of a general population. We can also see if any of our data agrees with published data trends.

The data set consisted of 416 men and 725 women, with an age range of 13 to 97 years.

Fig 5.1 shows the age distribution of the data set. There is a fairly symmetrical distribution of people, though it is slightly weighted towards the older end of the age spectrum.

This is expected as we would assume that people in these age groups have more accumulated UV skin damage requiring attention and so would be more likely to be referred for review.

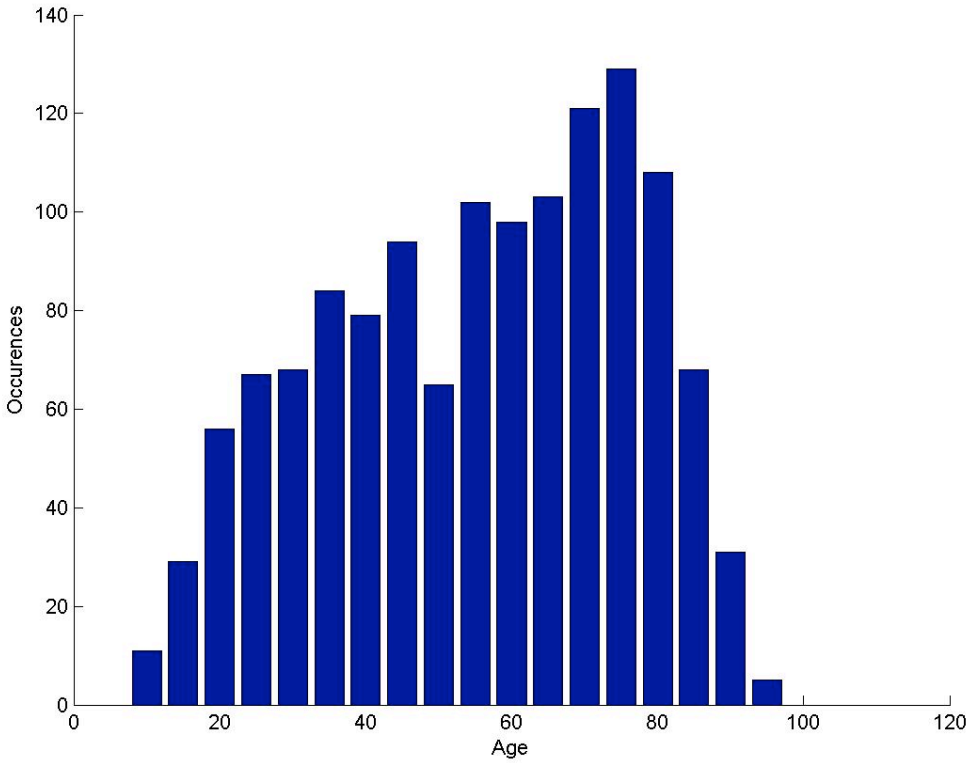

Fig 5.1 Age distribution

Fig 5.2 shows sex in relation to the age distribution. The clear distinction between the sexes is in the 20 to 65 age groups, where there was markedly more women (n=491) than men (n=176), by a ratio of nearly 3 to 1. From the age of 65 onwards there was a similar number of men and women in our group.

Fig 5.3 shows the distribution of photodamage and non-photodamage with age in our group. It quite clearly demonstrates a gradual increase in photodamage occurrences with increasing years in this group.

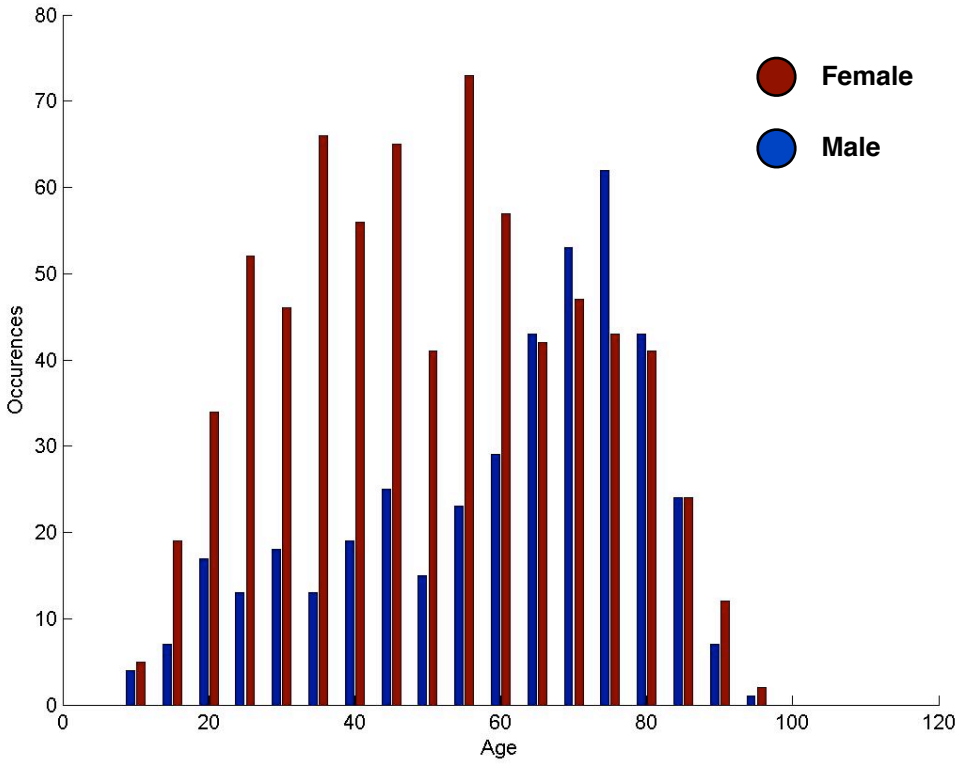

Fig 5.2 Sex to age distribution

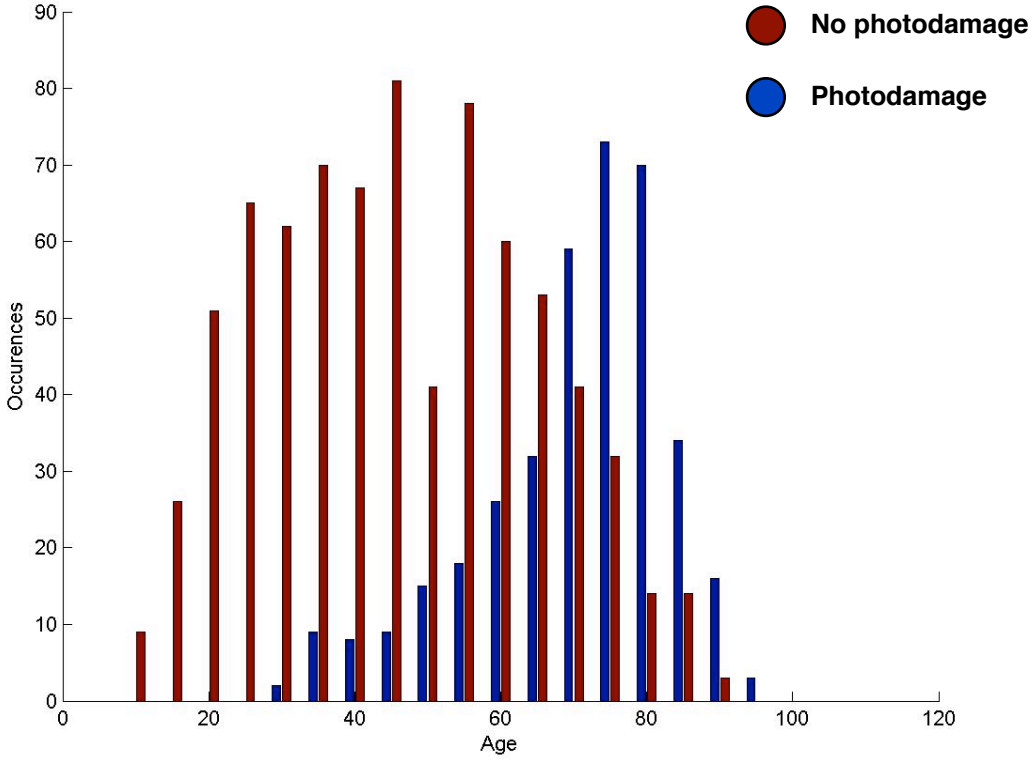

Fig 5.3 Photodamage occurrences with age

When we look at this photodamage group further, we can also plot the percentage chance of photodamage with age in our group.

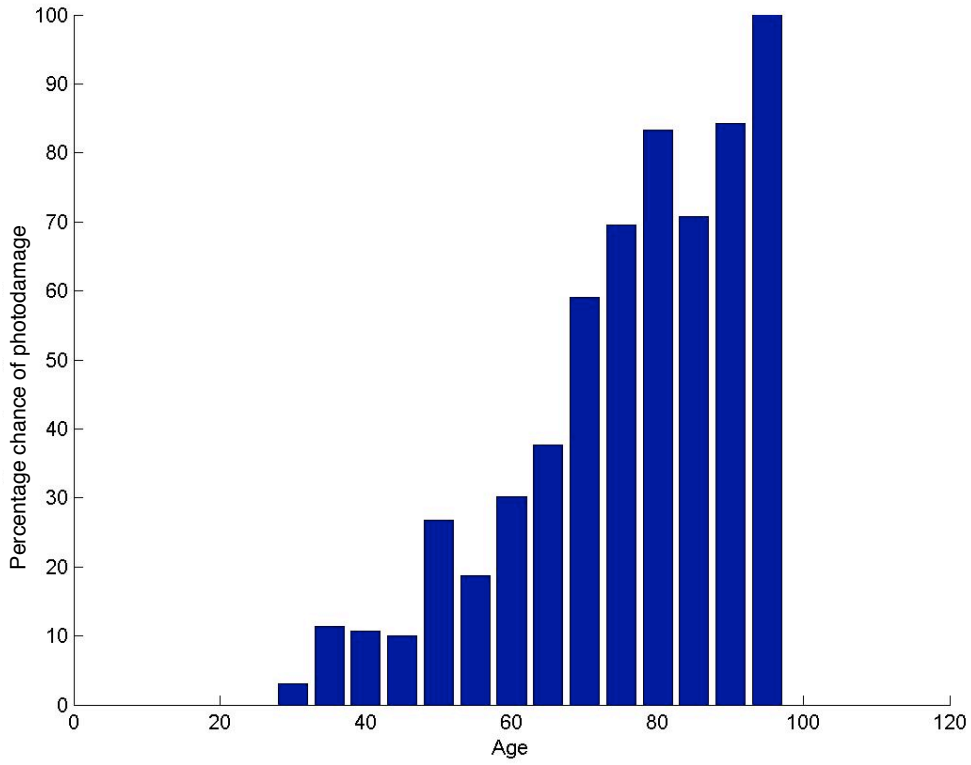

Fig 5.4 The relationship of photodamage with age within the data set

This shows a distinctive trend in the presence of photodamage with increasing age and is an important finding, corroborating the published evidence described in the previous chapter.

When we look at the photodamage figures and relate them to sex (table 5.1), we find that photodamage was less prevalent in the female group. Even accounting for the disparity in the size of the male and female groups, almost half of the data set was composed of females with no skin photodamage.

		number	% of sex set	% of data set n=1141
Male n=416	Photodamage	210	50.5	18.4
	No photodamage	206	49.5	18.1
Female n=725	Photodamage	164	22.6	14.4
	No photodamage	561	77.4	49.2

Table 5.1 Photodamage distribution with sex

Table 5.1 shows that the male data was fairly evenly divided between photodamage and no photodamage, but there were large differences in the female data. Almost half of the group were females with non-photodamaged skin.

Fig 5.5 shows which locations in the body were imaged at different ages. Rather than produce a confusing graph of each specific area of the body, the areas are grouped into head and neck and the rest of the body. Looking back to the 24 individual body areas which were defined in section 4.4.2, this grouping is relevant as 13 of the 24 areas were related to the head and neck. The trend here is that the head and neck becomes a more popular site to image in older individuals, while the rest of the body is much more common in age groups under 60 years.

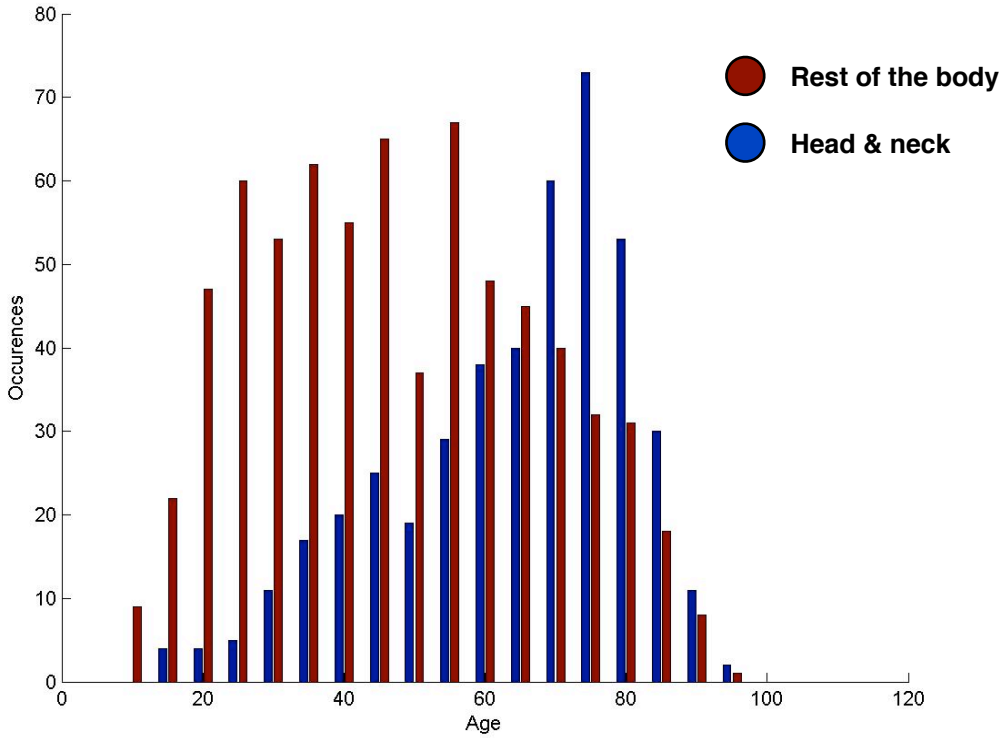

Fig 5.5 Site imaged with age

Table 5.2 gives a more detailed breakdown of which body areas were imaged and the prevalence of photodamage in each area. It also shows how many images were taken of each body site and shows just how many images had to be discarded for each site from the original set during the data preparation stage.

The locations are ranked according to the level of photodamage present and are also colour coded to identify the general areas of the body involved. This allows a clear visualisation of the damage to different body areas and shows that the head and neck is predominantly affected, followed by the peripheral limbs and then the trunk.

Location	No. of images taken	No. usable images	No. usable images with photodamage	% of site images with photodamage
Dorsum nose	77	45	39	86.7
Ear	64	19	16	84.2
Scalp	15	10	8	80.0
Forehead	91	77	59	76.6
Lower lip	5	4	3	75.0
Alar of nose	46	39	29	74.4
Temple	75	64	46	71.9
Malar	70	62	44	71.0
Hand	18	13	9	69.2
Front of neck	30	27	13	48.1
Back of neck	35	29	13	44.8
Upper lip	10	9	4	44.5
Shoulder	29	26	11	42.3
Cheek	86	78	32	41.0
Lower leg	109	91	31	34.1
Forearm	33	31	10	32.3
Chin	12	10	3	30.0
Foot	13	9	2	22.2
Chest	84	73	10	17.9
Thigh	10	9	1	11.1
Lower back	129	127	8	6.3
Upper back	175	169	9	5.3
Upper arm	72	70	2	2.9
Abdomen	52	50	1	1.9
Total	**1340**	**1141**	**403**	

Table 5.2 Body areas and skin damage figures ranked in order of prevalence

5.2 Descriptive statistics

SPSS compared each of the variables with age and 16 variables were identified as contributing substantially to the model. A forward stepwise analysis of these was then run to define the individual contribution of each and identify the most significant predictors to build the regression model.

Freckle eccentricity range
Standard deviation hue
Blood Fourier section mean 32
Blood Fourier section mean 652
Melanin standard deviation
Melanin Fourier section mean 2
Max hue
Blood mean

Table 5.3 The significant pigmentary features associated with increasing age

Table 5.3 shows the variables identified with the most significant coefficients and lowest collinearity which together produce the best model for predicting age. The final outcome of the regression analysis done by SPSS and the full correlation sequence can be found in Appendix D, along with a summary of the descriptive statistics.

5.2.1 The model parameters

This deals with the parameters which make up the regression equation. In multiple regression, the equation has several unknown variables and the coefficient statistics give us estimates of these values, which indicate the contribution of each predictor to the equation.

Model	Unstandardised coefficients		Standardised coefficients	t	Sig.	Correlations			Collinearity Statistics	
	B	Std.error	Beta			Zero-order	Partial	Part	Tolerance	VIF
(Constant)	-10.06	15.814		-.636	.525					
std Hue	363.2	146.595	.126	2.477	.013	.514	.090	.070	.305	3.277
freckle eccentricity range	8.697	2.847	.108	3.055	.002	.328	.111	.086	.629	1.590
Blood fourier section mean32	11.231	2.013	.203	5.579	.000	.445	.199	.157	.596	1.678
Blood fourier section mean652	-18.33	3.726	-.238	-4.921	.000	-.353	-.177	-.139	.338	2.956
mel Std	7215	1193.775	.266	6.043	.000	.382	.215	.170	.408	2.451
Mel fourier section mean2	6.517	1.264	.195	5.154	.000	.351	.185	.145	.555	1.803
max Hue	8.331	3.093	.084	2.693	.007	.288	.098	.076	.808	1.238
blood Mean	-.009	.004	-.158	-2.513	.012	.414	-.091	-.071	.201	4.973

Table 5.4 Coefficient statistics

I have reproduced and divided this larger output table into the three significant statistical sections for further explanation.

5.2.2 Coefficient and significance statistics

Model	Unstandardised coefficients		Standardised coefficients	t	Sig.
	B	Std.error	Beta		
(Constant)	-10.06	15.814		-.636	.525
std Hue	363.2	146.595	.126	2.477	.013
freckle eccentricity range	8.697	2.847	.108	3.055	.002
Blood fourier section mean32	11.231	2.013	.203	5.579	.000
Blood fourier section mean652	-18.33	3.726	-.238	-4.921	.000
mel Std	7215	1193.775	.266	6.043	.000
Mel fourier section mean2	6.517	1.264	.195	5.154	.000
max Hue	8.331	3.093	.084	2.693	.007
blood Mean	-.009	.004	-.158	-2.513	.012

Table 5.5 The coefficient and significance statistics

The first part of the table (unstandardised coefficients) gives an estimate of the β-values (shown as B in the SPSS output) and indicates the individual contribution of each predictor in the model. The sign of B indicates the direction of the relationship between the predictor and the outcome, with a positive value indicating a positive relationship and a negative value indicating a negative relationship. Each value has an associated standard error which is used to determine how much the beta value differs from zero.

The standardised B coefficient (Beta) values are not dependent on the units of measurement of the variables, but are measured in standard deviation units, so making them more directly comparable. They tell us the number of standard deviations that the outcome will change to each standard deviation change in the predictor.

In multiple regression the t-test (t) is a measure of the contribution a predictor has to the model. If the t-test associated with a beta value is significant (Sig) and is less than .05, then the predictor is making a significant contribution to the model. From the table we can see that all of our predictors have a significance of less than .05.

5.2.3 Correlation statistics

In the correlation statistics (Table 5.6), the zero-order represents the Pearson correlation coefficient (R), which is a standardised measure of an observed effect with a value between +1 and −1 (where ±1 indicates a perfect relationship and 0 indicates no relationship). In terms of the size of the effect, ±0.1 represents a small effect, ±0.3 represents a medium effect and ±0.5 represents a large effect.

If R > .9, there is suspicion of collinearity and further investigation would be needed. None of our predictors have an R > .9, so it would appear that there is no problem with multicollinearity.

Partial correlation is a measure of the correlation between two variables when the effects on these by the other variables are held constant. Therefore, it is a measure of the unique relationship between two variables, in this case each predictor and the outcome.

Model	Correlations		
	Zero-order	Partial	Part
(Constant)			
std Hue	.514	.090	.070
freckle eccentricity range	.328	.111	.086
Blood fourier section mean32	.445	.199	.157
Blood fourier section mean652	-.353	-.177	-.139
mel Std	.382	.215	.170
Mel fourier section mean2	.351	.185	.145
max Hue	.288	.098	.076
blood Mean	.414	-.091	-.071

Table 5.6 Correlation statistics

Part correlation controls for the effect of the other variables on only one of the two variables being measured. It represents the relationship between each predictor and the part of the outcome *not* explained by the other variables and is so the unique effect each predictor has on the outcome.

In these results, the reduction in the values of the partial and part correlations suggest there is quite a complex relationship between the predictors.

A correlation matrix is also produced by SPSS showing the Pearson correlation coefficient, the one-tailed significance of each correlation and the number of cases involved for each correlation. The correlation matrix is reproduced in appendix D.

5.2.4 Collinearity statistics

Model	Collinearity Statistics	
	Tolerance	VIF
(Constant)		
std Hue	0.305	3.277
freckle eccentricity range	0.629	1.590
Blood fourier section mean32	0.596	1.678
Blood fourier section mean652	0.338	2.956
mel Std	0.408	2.451
Mel fourier section mean2	0.555	1.803
max Hue	0.808	1.238
blood Mean	0.201	4.973

Table 5.7 Collinearity statistics

Collinearity data was measured as its effect on the predictors can undermine the entire regression equation. It is shown here as the VIF (variance inflation factor) and the tolerance (1 divided by VIF). The VIF indicates whether a predictor has a strong linear relationship with other predictors and to exclude collinearity the VIF should be less than 10 and the tolerance statistic above 0.2.

Collinearity diagnostics allow a further check for multicollinearity. A diagnostic chart is produced by SPSS and is included in Appendix D.

5.2.5 Summary of the model

The model summary shows us just how successful our model is at predicting our outcome (age) and gives us the values of R, R^2 and adjusted R^2.

R	R square	Adjusted R square	Std. error of the estimate	Change statistics				
				R square change	F change	df1	df2	Sig. F change
0.64	0.404	0.398	15.74980	0.005	6.316	1	752	0.012

Predictors; (Constant), stdHue, freckleEccentricityRange, bloodFourierSectionMean32, bloodFourierSectionMean652, melStd, melFourierSectionMean32, maxHue, bloodMean

Table 5.8 Model summary statistics

The adjusted R^2 gives us an idea of how well the model generalizes (i.e. how well it would approximate for a population rather than a sample) and should be as close to the R^2 value as possible. In our model, the difference between R^2 and the adjusted R^2 is .006, which equates to 0.6%, so if the model were constructed from a population it would account for only 0.6% less variance.

The value of adjusted R^2 can be verified by using Stein's equation to check cross validation of the model. In this case it was .392, which is very close to our observed R^2 from the model, which was .398, indicating good cross validity of the model.

Change statistics tell us if the change in R^2 is significant for each step in building the model. The significance of R^2 can be tested using the F-ratio, which is a measure of how much the model has improved the prediction of the outcome compared to the level of inaccuracy of the model.[193] The bigger F is, the better the change in the model. A full summary of the model for each predictor is reproduced in Appendix D.

5.2.6 Analysis of variance (ANOVA)

ANOVA tests to see if the model is better than the mean at predicting the outcome. It uses the F-ratio to represent a ratio of the improvement in prediction of the outcome from using the model, relative to inaccuracies that exist in the model.

	Sum of Squares	df	Mean square	F	Sig.
Regression	126510.9	8	15813.859	63.751	0.000
Residual	186538.2	752	248.056		
Total	313049.1	760			

Predictors; (Constant), stdHue, freckleEccentricityRange, bloodFourierSectionMean32, bloodFourierSectionMean652, melStd, melFourierSectionMean32, maxHue, bloodMean

Table 5.9 ANOVA statistics

The table shows us the sum of the squares of the regression line, which is the improvement in the prediction due to fitting a regression line as opposed to using the mean. There is also the sum of the squares of all the residuals, which indicates the difference between the predicted and the observed data. Degrees of freedom (df) are also included and relate differently to each of the regression and residual squares. The df for the sum of regression squares they are equal to the number of predictors in each model, in our case 8. For the sum of residual squares, the df represents the number of observations minus the number of coefficients in the regression model. If the improvement in fitting the model is greater than the inaccuracy in the model then F will be greater than 1 (the bigger the better).

The possibility of this happening by chance is calculated and seen in the significance score. In these results $p < .001$ indicating that it is very unlikely this happened by chance. The full ANOVA output can be found in Appendix D.

5.2.7 Residuals statistics, casewise diagnostics and model assumptions

The residuals statistics identified that there was only one residual outlier outside our parameters. A casewise diagnostic was performed of the data points in question.

Case Number	Std. Residual	Age	Predicted value	Residual
463	3.049	88	39.9234	48.07657

Dependent Variable: Age

Table 5.10 Casewise diagnostic of the residual

This showed the standardized deviation of the residual at 3.049 and though this was only marginally above 3, it is high enough that it should be investigated. Therefore a Cook's distance was performed on this variable to see what influence it would have on the model if it were deleted. The result of the Cook's distance test was <1, indicating it is not having an undue effect on the model.

The residuals statistics includes plots and histograms to check the normality of the residuals and also regression plots to check the various assumptions of the model. These can be found in Appendix D.

5.3 Testing the model

Once the model has been created, it can be verified using the test data set. Fig 5.6 shows a graph of actual age against predicted age with the model and the test set data plotted. This allows us to see how well they are distributed against each other and to visually assess the fit of the regression line for both data sets. The x-axis shows the chronological age and the y-axis gives our predicted age score.

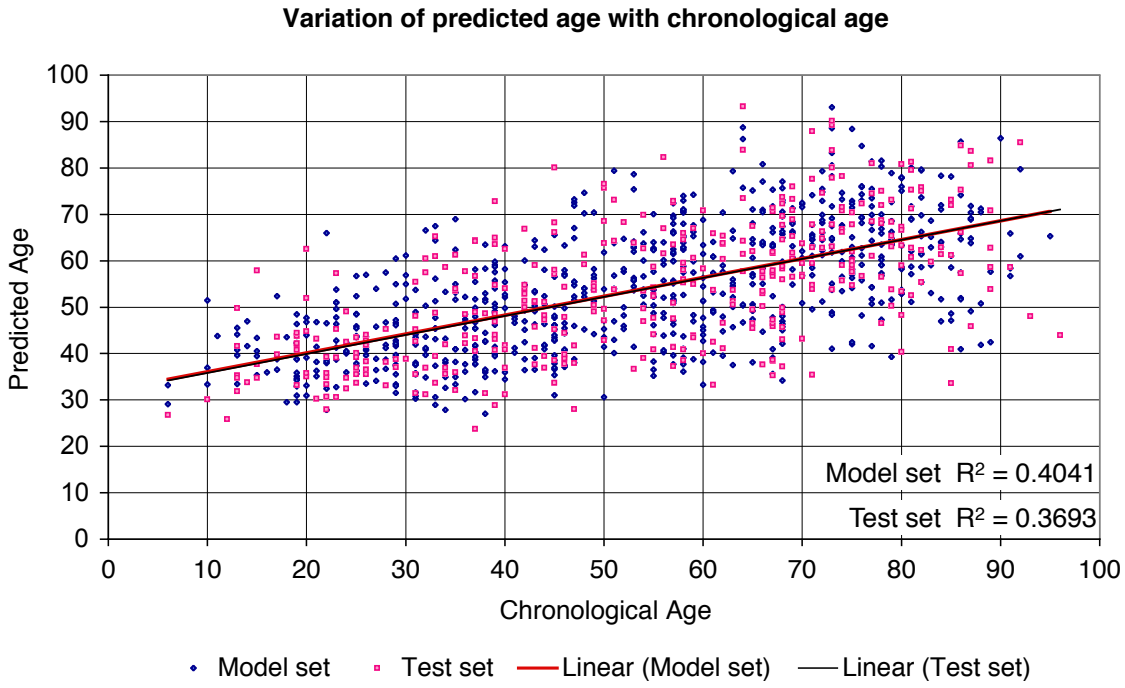

Fig 5.6 Plot of the model and test sets with line of best fit*

From the distribution of the two data sets we can see that there is good matching of the model and test sets. This means that the measured R^2 for each of the tests is also very similar. The differences could be put down to slight individual variations within the data sets and also the fact that the model set was twice the size of the test set.

The model can further be tested by looking at the distribution of photodamage in the test set data. As we saw in Figs 5.3 and 5.4, there is a good association between increasing age and photodamage, so if our model is accurate we should see a general cluster of photodamage towards the top right of the distribution.

* This figure is reproduced in Appendix D

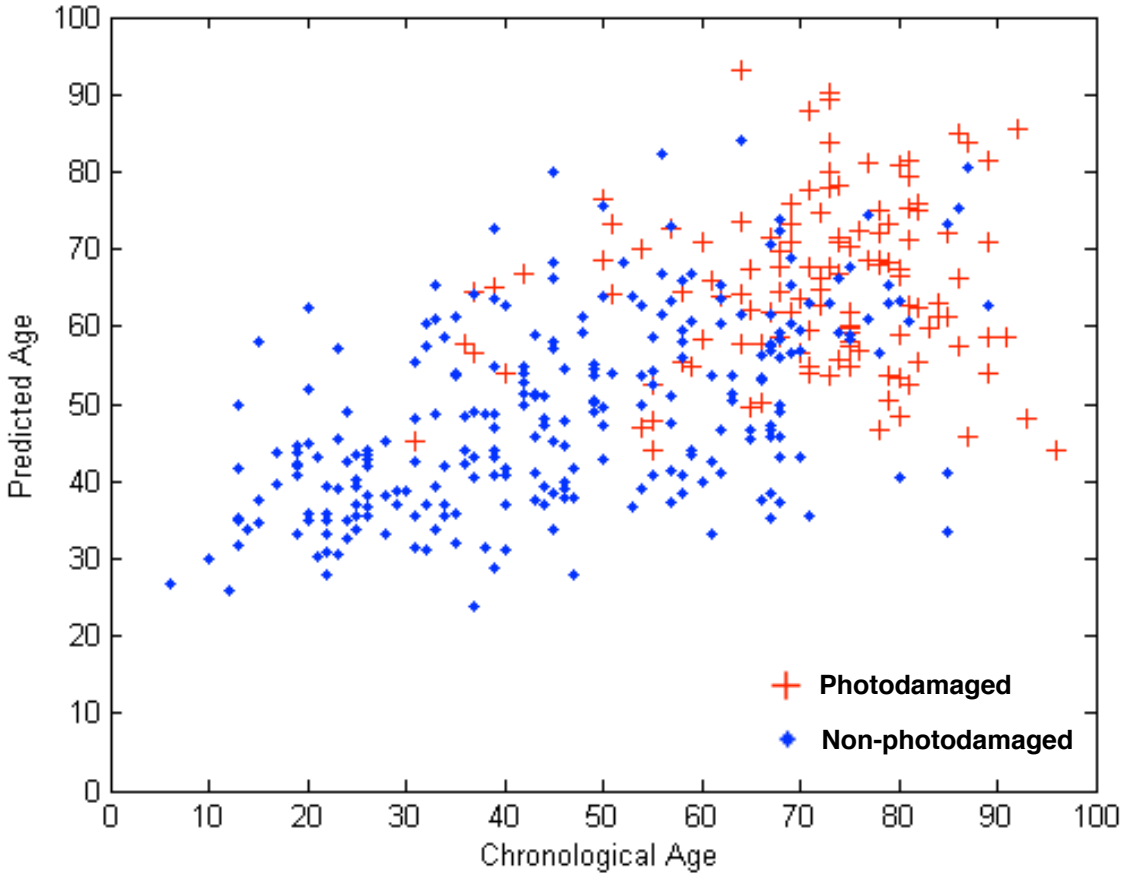

Fig 5.7 The test set with identified cases of benign and damaged skin

Fig 5.7 shows that there is a gradual increase in photodamage with increasing chronological and predicted age. The vast majority of damage is present after 60-70 years chronological and 50-60 years predicted and we can see the clustering of the photodamage in the top right of the graph.

Chapter 6

Discussion

In this chapter I will discuss the relevance of the results from this study and explore the limitations of the technique.

6.1 The demographic data

The demographic data which was collected gives us lots of information which is not only relevant to the validity of the subsequent analysis, but is useful in its own right.

I imaged 1340 people which was reduced to 1141 for analysis and Fig 5.1 shows that we had a large cross sectional group with a wide age range.

With regard to the age distribution of males and females in the group, Fig 5.2 shows that there were more women up to the age of 65 and from the age of 65 onwards there was a similar number of men and women analysed. Table 5.1 shows that the male data was fairly evenly divided between photodamage and no photodamage across the whole data set, but there were large differences in the female data. Even accounting for the differences in the size of the male and female groups, almost half of the entire data set was composed of females with no skin photodamage. By comparing both Fig 5.2 and Table 5.1, it would seem

the disparity is much more apparent in the ‘working age group’ i.e. 20-60 years of age, where over three quarters of women presented with no photodamage.

This raises the question as to why more women than men were presenting and why was it with mostly non-photodamaged skin?

To answer this we should consider such things as current public health concerns, the changing attitudes of people over the years towards their health and also their expectations of health provision.

Studies have identified delays in presentation by patents to be higher in the elderly, in male populations, lower-educational individuals, those living out of towns and those with poor skin awareness.[195,198] There are certainly different conventional attitudes between men and women when it comes to visiting their doctor and in attitudes towards appearance. Men tend to be less bothered about what they may consider to be minor health issues or trivial skin changes than women and are less likely to see doctors.[196] Indeed, one of the big pushes in public health campaigns for melanoma has been in getting people more aware of their skin and changes in it which may be significant, especially men who are recognised as being at high risk directly *because* of this attitude.

We must not underestimate fear, embarrassment (of presenting with an inconsequential lesion and being seen as time-wasting, as well as the physical embarrassment of an examination) and lack of understanding in the importance of changing features.[197] These non-disclosure of symptoms and negative attitudes towards doctors are also reasons for patient delay.[198]

We should also consider that older generations have not always had access to health care with the ease of today and many come from a more stoical time where you tended not to complain. Many older people actually put up with worrying lesions for long periods as they see their symptoms as trivial or unimportant.[198,199] Sun care and sun safety were also not as well understood as

they are today and access to good quality, rapid health care is now more expected in current generations than in previous ones.

Fig 5.4 shows some interesting results. Within this group it shows that the chance of having photodamage increases almost proportionately with age. This is quite reassuring as it validates the hypothesis of using age as a proxy for photodamage and agrees with the previously published evidence regarding using age as a measure of photodamage. [202, 217, 219, 220] However, we must remember that only about 15% of the group (n=169) are represented in the 80 years and over group and only about 1.5% (n=17) in the 90 years and over group. Non-the-less, this is a very distinctive trend and given that it is reflective of previous research, it suggests that the overall group may be representative of the general population.

On reviewing Fig 5.3 and Fig 5.4 we can see that the photodamage trend appears to start from the third decade. This was somewhat unexpected and is generally ten or even twenty years earlier than we would expect to see easily noticeable skin changes to the naked eye within a general population.

Figure 5.5 shows another interesting finding regarding the different areas of the body imaged in different age groups. As we would expect from previous discussion, there is an increase in the presentation of damaged skin in the head and neck with increasing age, which is consistent with the ‘weathering’ of those areas over time. The interesting outcome was the large number of skin lesions being presented by people in the 20-60 years age groups in non-head and neck areas. It is possible that the drop in the body presentations which coincides with the rise in head and neck presentations from the sixth decade onwards is in fact due to a decrease in the physical ability of the individual to inspect their body due to failing eyesight or infirmity. It is also possible that the increase in the onset of the more obvious, facial lesions, has an overriding importance to the individual compared to other areas of the body.

Table 5.2 takes a more detailed view of this location data and correlates it with the presence of photodamage. Each body area was colour coded for easy identification and as we would expect, the majority of the areas showing photodamage were in the head and neck. Looking at the table, the areas with the higher percentages of photodamage are also the areas which we would expect to see people get excessive sun exposure most often - the forehead, nose and ears. These are the more prominent areas of the face and combined with the overhead position of the sun, can explain why they are more susceptible to cumulative UV damage. Indeed, when we look at the relative frequency of the areas involved we can see that they seem to appear in an order we could anticipate if we imagine overhead solar exposure.
The one outlier to this pattern is the hands, but given that they are used and exposed every day of our lives, it is easy to understand their more prominent presence in this table.

Table 5.2 also shows how many images were not usable in the subsequent analysis for each of the body sites. From previous discussion we know that due to the set up of the camera and the narrow depth of field, the more highly curved areas of the body posed more of a problem in terms of being able to image enough in-focus skin field for the analysis to be valid. As was anticipated, most of the images that had to be eliminated were in the highly curved areas, such as the ear and the nose. The forehead was one notable area where we would have expected some good quality images, but 14 images (15%) had to be excluded. This was either due to excessive hair artifact, near the eyebrow or hairline (4 images), or because the imaged area was quite lateral on the forehead, where it curves (3 images). The remainder of the images were excluded due to errors in focus or camera settings, which was disappointing.

It is worth pointing out at this stage that the loss of images due to poor technique (incorrect camera setting or being out of focus) became less common throughout the study, indicating that there was some small element of learned skill involved in taking a good quality image first time.

Looking at all the figures in section 5.1, from this data alone it could be interpreted that more men present later in life with more photodamaged skin, particularly in the head and neck. Similarly, more young women present with less photodamage in non-head and neck areas. This is generally a reflection of what is seen clinically and could be interpreted as a confirmation that the data set is a representative sample of what is apparent in the general population.

From our data only 32.8% actually had any photodamage, not that photodamage is the only reason to see a specialist or GP regarding your skin. We should not forget that presenting with a benign skin lesion can sometimes be a way of starting a conversation with a doctor about more pressing matters and also that the mention of a skin lesion is sometimes added onto a consultation about something else, or even incidentally noticed by a GP.

However, this again strengthens the idea of finding some method of identifying the most relevantly photodamaged members of the population for review by a specialist, not only to make the system more efficient, but also to prevent the cost and trauma of dealing with established malignancy.

I was generally reassured that the demographic results I had were similar to those already published. Photodamage is more prevalent as you get older and more frequent in the head and neck and there was good data to show this.

6.2 The model

The results showed there were eight significant pigmentary features for predicting age in our model giving an R squared value of 0.404. The adjusted R squared was very close at 0.398 suggesting the model could be generalised to a population with marginal difference. The ANOVA statistics showed that the model was statistically significant and could not have occurred by chance.

Freckle eccentricity range
Standard deviation hue
Blood Fourier section mean 32
Blood Fourier section mean 652
Melanin standard deviation
Melanin Fourier section mean 2
Max hue
Blood mean

Table 6.1 The significant pigmentary features associated with increasing age

Each predictor was chosen as it made a significant contribution to the prediction of age, can be reliably measured (via SIAscopy), has low collinearity and have good cross validation of the adjusted R^2.

Freckle eccentricity relates to the shape of the freckle and this is not an unsurprisingly important finding. It is well accepted that our eyes are very sensitive to the perception of contrast. The identification of ageing skin as a change in chromophore contrast has already been established[223] and is the focus of much study in the cosmetics industry. Increasing sun exposure pushes spatial chromophore distribution in a way that causes visible coalescence of melanin in an irregular way, leading to eccentric freckling. The increased contrast associ-

ated with changing levels of melanin would make these more visible. This result could suggest that the change in spatial chromophore distribution is part of a measure of age, as well as the perception of age.

The number associated with the Fourier predictors relates to the measured frequency of the image which had the best correlation with age (section 4.6.1). As three of the predictors are Fourier based it confirms that Fourier analysis was a worthwhile method of deconstructing the images and allowing analysis of the disorder. This is expected in that the whole process of photodamage as physiological pigmentary change is random, both spatially and temporally. The technique is further described in Appendix C.

Importantly, six of the model features were SIAscopic images of either blood or melanin. Even the freckles were identified from a melanin SIA image using a melanin threshold fraction (section 4.6.4).

This was an interesting finding, validating the use of SIAscopy in identifying features of skin damage. As a method of analysis, the particular advantage with SIAscopy is that it is very easy to take an image. It is quick, reliable, reproducible and pain free. There is no subjectivity involved in assessing the images as they are analysed by computer. More difficult measures like the number and depth of wrinkles, or the extent of laxity are less reliable and open to significant user error.

Many individual measured characteristics appeared to have some good correlation with increasing age. For example, the analysis identified a specific hue colour (fraction 18 (R^2 = 33.3) which corresponds to a very bright yellow colour) which we thought may be associated with solar elastosis, but ultimately made no improvement to the regression model. Other features like melanin standard deviation (R^2 = 14.0) and hue standard deviation (R^2 = 26.4) seemed to have good correlation with age, but when combined had an R^2 =29.0, lower than expected and likely due to a degree of collinearity. Despite this they did remain in the model.

The collinearity data in table 5.7 was measured as the effect of collinearity can undermine the regression equation. As mentioned, the VIF indicates if a predictor has a strong linear relationship with other predictors and the absolute value which is of concern is open to a degree of interpretation. It is generally accepted that to exclude collinearity the VIF should be less than 10 and the tolerance statistic above 0.2. All of our results fulfilled these criteria, although the result for 'blood mean' showed a tolerance statistic of .201, only just above the suggested level of concern. All the individual VIF statistics were below 10, with an average of 2.496. It is unrealistic to think that there is no degree of collinearity, but the results would suggest that it is not worthy of any real concern for our regression model.

Further checks for collinearity between predictors using collinearity diagnostics were performed using Eigenvalues, condition indexes and variance proportions to identify any. The mathematics around Eigenvalues is complex and an interested reader may want to look into this further in a more specialised text. In essence, they show the evenness in the distribution of the variables and gives us an estimate to how accurate the regression model is. In terms of collinearity, we look for predictors with high variance proportions on the same small Eigenvalue, indicating the variance of the regression coefficients are dependent. The collinearity diagnostic chart is included in Appendix D and there does not seem to be any such dependency between variables, confirming the previous VIF collinearity statistics.

The model summary in table 5.8 shows that the R^2 value for our model is 0.404. meaning the features we have identified as specific to our model, account for about 40% of the actual measure of age.

It also shows that the difference between R^2 and the adjusted R^2 was very small at 0.006. This suggests that if the results were scaled to a general population, the results would differ by only 0.6%, confirming that we have a robust model from a representative population group. The full model summary is re-

produced in Appendix D and shows how the addition of each predictor to the equation improves the prediction of the outcome. Changes in the F-ratio with each addition to the model are presented, as is the significance in the change of F. This tells us the difference in benefit of adding new predictors to the model. Our results show significant changes in the first 6 steps of the model formation ($p<.001$), but less in steps 7 and 8, although the results remain significant with $p<.05$.

The ANOVA statistics showed how much better our regression line was than just using the mean of all the figures, with a $F_{8,752}= 63.751$. It also showed that the chance of the results happening by chance was very unlikely, with a significance of <.001.

Testing the model against the test set of data gave a good correlation with the model set. The R^2 was 0.37 for the test data set which is very close to the model R^2 of 0.40.

Figure is 5.7 is very interesting. It shows a plot of the test set and identifies the photodamaged and non-photodamaged points. The clustering of the photodamage in the top right of the graph is an important finding. It suggests that the individuals who we predicted would be older, and who are older, had an increased amount of photodamage.

We have already seen from figures 5.3 and 5.4, backed by published evidence, that increasing age can be used as a measure for the presence of photodamage. This would then suggest that our predictor of age was also a good predictor of photodamage.

6.3 Why was R^2 only 40%?

The limitations of SIAscopy in terms of what it can identify in the skin have been discussed throughout chapter 4 and it was hypothesised that we could assess the pigmentary and colour changes in the skin with this technique.

However the signs of photodamage are much more than just changes in skin pigmentation. Other features of photoageing like fine lines, wrinkles and laxity of the skin also occur and were not included in this study.

Another significant feature that should be considered is the area of the body being imaged, as this relates to the thickness of the skin and the type and quantity of extrinsic photo-exposure it will be subject to.

Constitutional factors like sex, skin type and socioeconomic groups could also be assessed as they undoubtedly have an influence on risk to the patient and their relevance has previously been described in the literature.[202,219,220] All these things can give skin its unique biological appearance and may all have an impact on age and photodamage assessment.

6.4 Limitations, bias and influential factors

In terms of the overall approach to the study, the individuals were identified from a population who had been sent by their GP for examination by a specialist. This was necessary in this study as we needed that specialist evaluation to identify photodamaged individuals for comparison with non-photodamaged individuals when histopathology was not available. This is a bit of a forced scenario but was ultimately effective as all I needed was a good cross section of the population, with as varied a distribution of normal and damaged skin in as many body sites as possible.

I have already outlined above the other features of age and risk which could be added to improve the assessment of skin age.

While the overall results from this thesis would appear to be encouraging, there are inherent limitations to all research which should be identified.

6.4.1 Population

The population were screened twice before being imaged, firstly by themselves and secondly by the GP who referred them for specialist assessment. While this is not inherently a limitation to this thesis, it does not give a real view of the general population. For this thesis I only needed a good cross section of the population to create have enough skin variation to analyse. This could have been improved by having more people in the under 20 year age groups and in the 50 year age group, where a low number was clear (Fig 5.1). There were also more women than men in our population and this may have influenced the overall numbers of benign or damaged skin.

The size of the sampled group could be improved to help refine the skin characteristics. There were too few people in the under 20 years age groups and more in the 20-40 year age groups would also have helped (Fig 5.1). An unusually small group in the 50 year age group introduced some artifact into subsequent use of the data, though statistical analysis did not highlight population distribution as a problem. More men in the study would be of benefit to help balance sex risk as male:female ratio was 1:1.75.

6.4.2 Imaging

The imaging technique was set up in such a way as to be relatively straight forward, but there was a short learning period where some images were unusable. It also became clear during the image processing stage that the images from the particularly curved areas of the face were less useful due to problems with focus.

While the volume of images taken helped to reduce any population distribution error, many of the errors were simple technical errors that could easily have been rectified, such as focus, aperture and flash settings. The imaged body sites could also be improved in term of the numbers and distribution, to improve the overall occurrence ‘map’. This would particularly help with areas of the body which were under presented, such as the thigh, foot and hand.

6.4.3 Diagnosis

For some, the use of a skin lesion associated with photodamage as a proxy for the presence of photodamage may be contentious, but I believe there is sound, accepted, physiological evidence why it is a novel approach to this use. I have included some rather detailed evidence within chapter two as to just how sunlight, photodamage and the genesis of certain skin lesions are linked with the passage of time. I have also presented evidence from published literature which suggests that the histological diagnosis of photodamage should not be seen as the gold standard (section 3.3). Ultimately I used age as a proxy for photodamage and the data associated with the presence of photodamage within the skin was combined in figure 5.7 to confirm that the model described in this work also shows photodamage as a function of increasing age.

6.4.4 Analysis

As much as possible, the analysis was done using computers, so bias and error would be limited and consistent. However, I did have to prepare the images prior to computer assessment and that relied on me deciding which parts of the image were to be excluded from analysis (Section 4.5.2). Error was limited here by having just one person doing the image preparation and images were also prepared in batches to avoid errors of judgement brought on by repetition or fatigue.

6.4.5 Exclusions

The exclusion of melanoma from the analysis group was, in my opinion, reasoned and justified, however I am willing to accept that the move may be a little contentious for some individuals. I have included a detailed description of melanoma in chapter two specifically as I chose to exclude melanoma from the study. Here I detailed that evidence is available which shows that consistent UV exposure is not required for melanoma to occur, but I am also aware that the majority of melanoma occur in the head and neck and in the elderly. As I was using the skin lesion as a proxy for the presence of photodamage and that the absolute number of images which could be excluded was small (14 images out

of 1155 potential images = 1.21%), I decided that it was reasonable to exclude melanoma in the face of conflicting published evidence.

6.4.6 Outliers

Only one outlier was identified in the residuals statistical analysis. This was examined and tested and was shown not to have any undue effect on the model.

6.5 What did we measure?

The principle idea behind this research was to see if SIAscopy was a technique which could identify and quantify the pigmentary characteristics of photodamage. In chapter 2 we discussed the fact that this 'damage' is actually a combination of intrinsic and extrinsic influences on the skin, which make it more or less likely for a spontaneous malignant transformation to occur over a period of time. The cumulative effect of this photoageing and intrinsic senescence is what we see as ageing.

The various features of photodamage are identified in Fig 4.2 and we hypothesised at the time that SIAscopy may be able to identify the pigmentary changes (sallowness, erythema, telangectasia and dyspigmentation) present.
We also used some mathematical models to quantify the random nature of some of these features, such as freckle eccentricity, dyspigmentation and telangectasia.

It would be almost impossible to identify features only associated with intrinsic ageing or only associated with photodamage, as the two exist simultaneously. We have seen that photodamage is more profound in the elderly, who by definition have more intrinsic skin ageing. Once we had proven the relationship between actual ageing and the presence of increasing numbers of skin lesions associated with skin damage, we defined the characteristic we were trying to measure as age.

Analysis then revolved around looking for relevant pigmentary and image analysis features which had some association with increasing age. This was proven by looking at the distribution of photodamage on the test set in Fig 5.7.

So should we call it predicted age? Our outcome is not truly a measure of age, but an approximation of it based on the pigmentary changes associated with increasing age, that happen to occur in damaged skin. So although it is a measure of age from a limited perspective, realistically it could be called any type of relative score. I would hesitate to use the term photodamage score as that implies that we have measured all the features of photodamage, rather than just some of them. Biological skin damage score or screening score may be more appropriate to others, but I like the term predicted skin age. Everyone is familiar with how skin looks as we get older and we spend billions on trying to keep the visible signs of age at bay, so using predicted age puts the relevance of the test into perspective immediately. It may just help people to understand that we all have genetically controlled rates of intrinsic ageing and responses to extrinsic damage. While we currently can not do anything about intrinsic ageing, we can protect ourselves as much as possible if we know we are at risk.

Suffice to say we have measured some pigmentary changes that were statistically associated with increasing age, of which photodamage will undoubtedly be a part.

Chapter 7

Conclusions and further considerations

This thesis set out to see if the non-contact SIAscope was a useful tool in identifying and quantifying the pigmentary features in skin associated with photodamage, a preceding feature of certain skin malignancies.

It became apparent during the process was that there is a complex relationship between intrinsic skin ageing and extrinsic influences, including photodamage. This relationship has a synergistic nature such that, at the level of change to potential malignant transformation in the skin, they cannot realistically be separated and the attempt to define one from the other becomes irrelevant to the purpose of identifying skin which is at risk of transformation.

There are many variables involved in understanding just what makes skin damaged enough that spontaneous malignant transformation is possible. It is the cumulative effect of that individuals genetically predetermined responses to extrinsic stimuli combined with the effect of intrinsic senescence. Clearly how much skin damage one can accumulate before malignant transformation is likely is extremely variable, even within different areas of the same person, never mind between individuals. What is consistent within a population is that everyone gets older, and the older we get, the more photodamage we accumulate.

Trying to specifically identify only photodamage would be very difficult as we would first have to eliminate all the effects of intrinsic skin changes and the two processes are both complementary and concurrent.

What we therefore set out to do was not to just identify photodamage, but use SIAscopy to identify pigmentary skin changes consistent with increasing age and thereby potentially identify people who are most at risk of potentially developing malignancy as a result of this photodamage. This is exactly the process that happens subconsciously when a clinician forms a diagnosis by looking at the overall quality of a patients skin.

This thesis has been successful in that the results have shown that non-contact SIAscopy can identify pigmentary characteristics present in ageing skin of which photodamage makes up a significant part. We have also shown that this can be used to identify just what this risk may be for that specific area of skin and so identify an individual for closer monitoring.

This technique is inexpensive, reliable, robust, repeatable and free from subjective user interpretation.

We have identified other modifiers of risk which may be useful in refining the skin damage identification process (wrinkles, fine lines, skin laxity, sex, site, socioeconomic status, etc), and extending the study to look at those extra features will help refine the predicted skin age score.

An interesting consideration would be to extend the analysis to look at defining the risk associated with intrinsic ageing alone as opposed to intrinsic and extrinsic combined, possibly by using genetic data, skin typing and risk defining data like socioeconomic status, job and social activity.

7.1 Clinical application - Doing something with the results

Looking back at Fig 5.7 we can see the graph shows that within this study, people with an increased chronological age and high predicted age, were more likely to have damaged skin that has, or is likely to have, an increased risk for spontaneous malignant transformation.

We know from the analysis of the statistics in chapter five and from agreed principles, that older people have more photodamage in general and that they develop more skin cancers, so being able to tell someone who *is* old that they have old skin which may develop skin cancer is not really anything significant. It may be useful in helping to predict the likelihood of an undiagnosed lesion being cancerous or benign in people unwilling to consider biopsy, but in current practice, most of these indistinct lesions are biopsied or removed.

What would be more effective would be to identify a group of people who are more susceptible to potential skin damage at an early stage, or before it becomes established. These people would be those who have an older predicted skin age with regard to their chronological skin age and could be identified at a primary care level for regular screening and education.

From the data plot (Fig 7.1) we could say that anyone with a predicted skin age over 45 years should be screened, but this would be a huge proportion of the group and there is a significant number of people with benign skin in that sample. This would make screening relatively inefficient. This graph alone does not tell us anything about how much more risk someone has if their predicted skin age is higher than their actual age. To do that we have to consider what the likelihood is that the skin will be damaged or undamaged in someone of that chronological age.

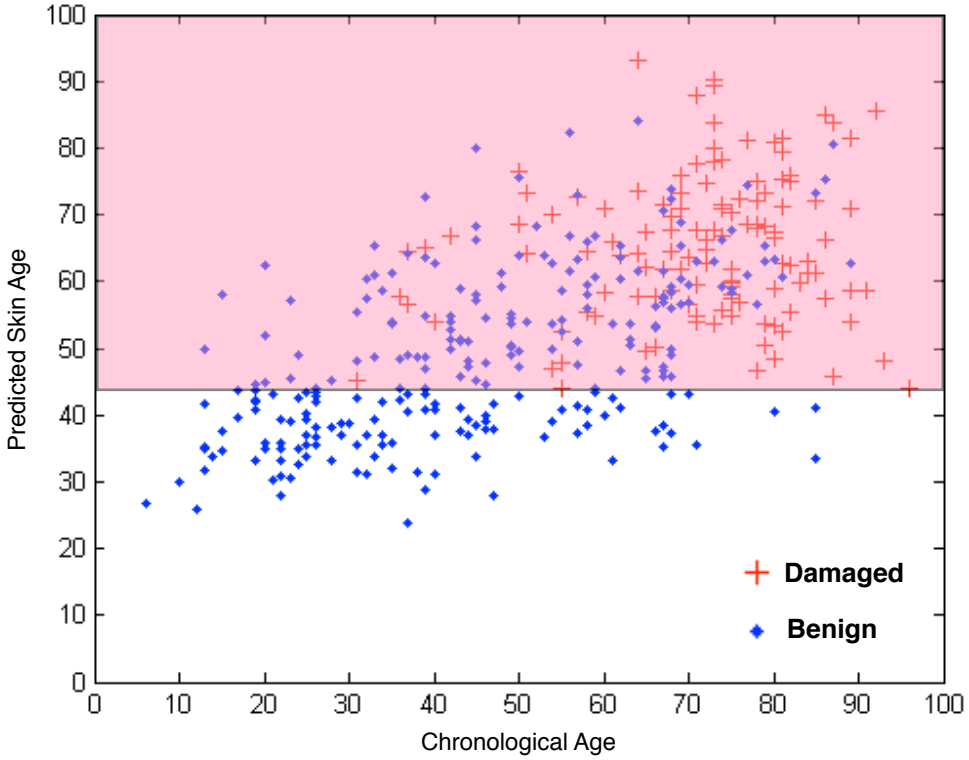

Fig 7.1 Identifying the population most at risk

To make this graph useful we need to construct a chart that will show a relative risk associated with each age and use this to identify the screening model, i.e. just how much more damaged is the skin, rather than is it just damaged.

To look at this further the output data was run back through MATLAB, but instead of a continually varying chronological age, a range of 10 year age groups were compiled together and a graph was produced for chronological age against the occurrence of photodamaged or non-photodamaged skin.

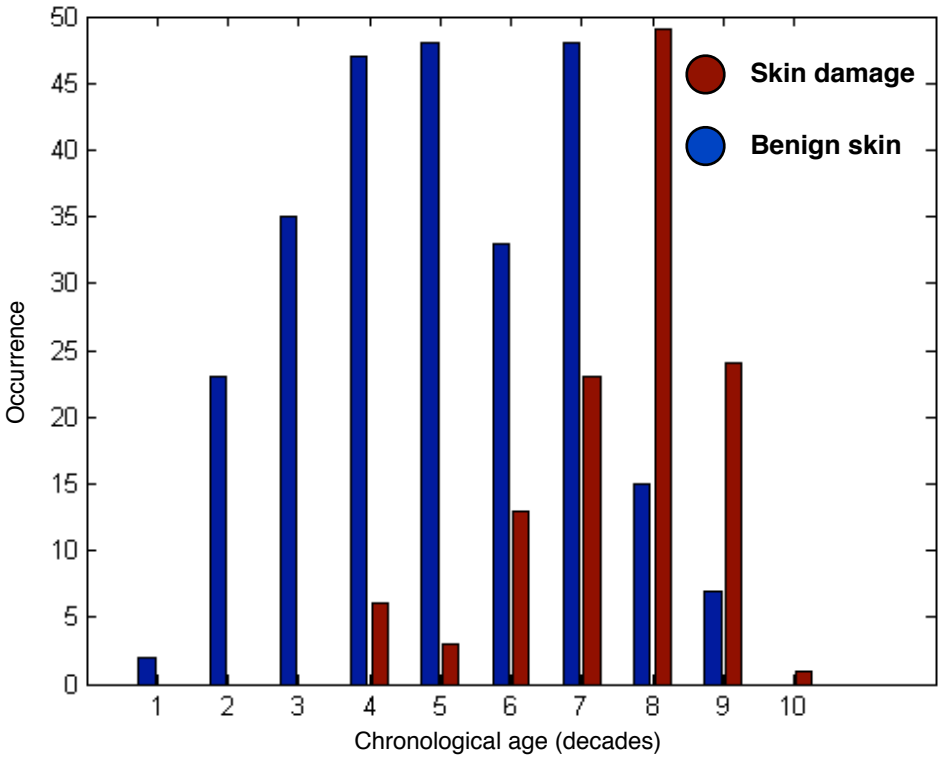

Fig 7.2 Occurrences of benign and damaged skin against age

We can see the effect of the limitation on the size of the data set in the chronological age graph, where it would seem that you are less likely to develop skin cancer in the 5th decade than the 4th. This outlier is most likely due to the lower numbers in that age category and does not follow conventional thinking, or the rest of the data, which assumes skin cancer risk to be higher with progressing age. A larger sample group would most likely correct this error.

Now we know what the relative occurrence of photodamage is in each 10 year age group, we can compare one against the other to look at the prevalence of skin damage in one age group to the next. This way we can create a ratio of prevalence from one age group to the next. This will give us a crude estimate of the relative risk of developing cancer at a certain age, within our sample groups.

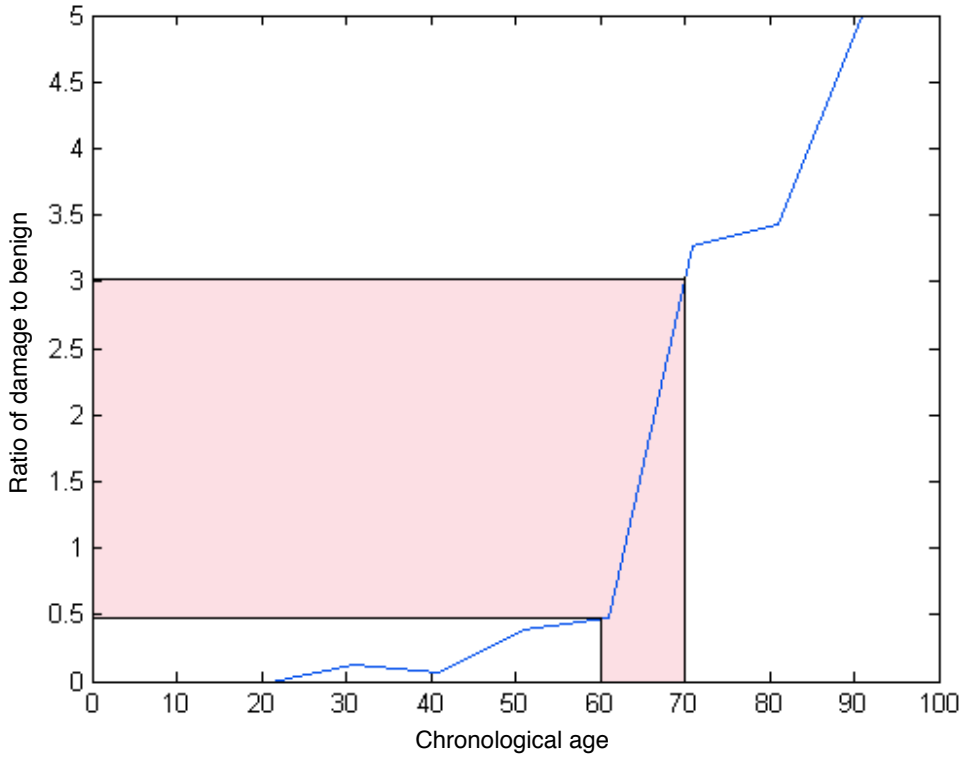

Fig 7.3 Ratio of damage to benign skin against age

Fig 7.3 illustrates the ratios in a graphical form. Again, this graph shows the artifact in the sample group, in that it appears there is a higher cancer risk in the 30's than the 40's. Further analysis and a more detailed data set would likely improve this line and the ratios.

The most striking aspect of this graph is that the change in the ratio of damage to benign skin over the age of 60 is quite significant. Even in this crude form, the likelihood of someone aged 70 having damaged skin can be seen to be almost 2½ times that of someone aged 60.

It could therefore be inferred from this alone that anyone with a predicted skin age of more than 60 may be worthwhile monitoring for potential malignant transformation.

From this we can extrapolate the potential risk of having a predicted skin age score higher or lower than your actual age.

Each vector point on the previous graph (Fig 7.3) can be converted into a number. We can then calculate the differences between the ratios for each point and assign a colour to that number. When we then plot predicted skin age against chronological age, we get a graphical representation of the change in the ratio of damaged skin to undamaged skin between ages.

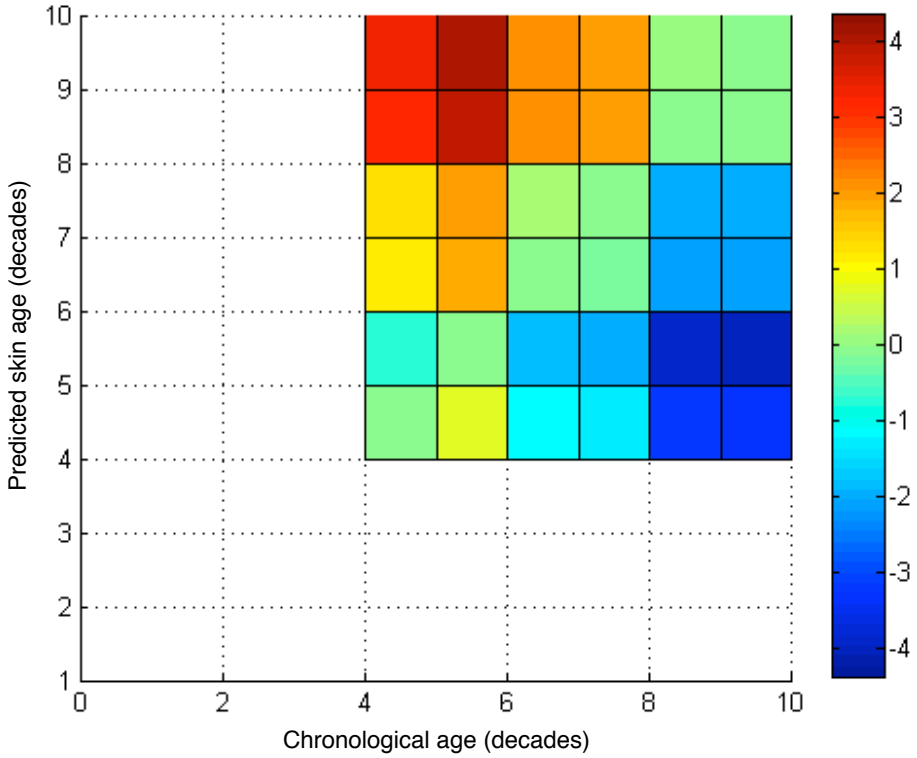

Fig 7.4 Plot showing the change in the ratio of skin damage for age

This image is rather crude as we previously grouped the chronological ages together into 10 year aliquots. As there is little skin damage in the younger decades, ratio data can not be calculated, resulting in too little data to fill the 10-40 year age groups.

We can compensate for this to some extent by plotting the log of the change in ratio vector and interpolating the colours on the graph to give a more visibly detailed chart.

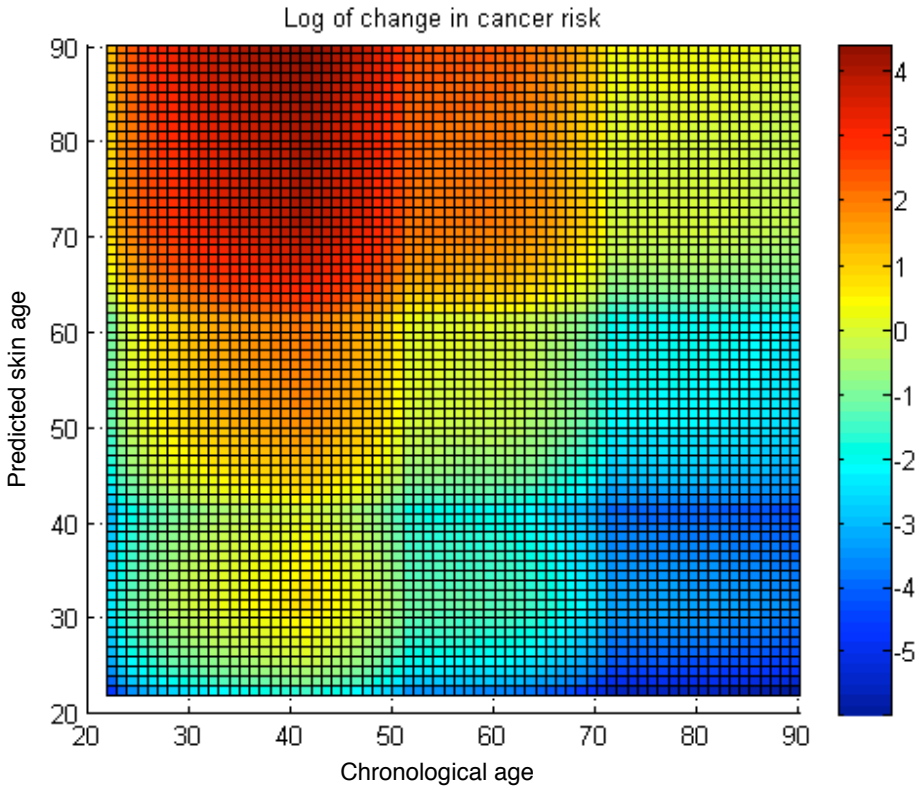

Fig 7.5 Interpolated log of change in the ratio of skin damage for age

The scale on this plot is the number of multiples of the likelihood ratio, but could equally be changed to make it more useable. Green/yellow could simply relate to no extra risk and orange through red and black could be allocated mild, moderate and severe respectively. This is similar to what is done for the body mass index charts, where colour coding makes the chart instantly understandable.

This graph now shows us something more useful. We have a plot of age showing how the change of ratios of damaged and benign skin varies as we get older. Now we can use the predicted skin age score (on y-axis) and the chronological age (x-axis). Measuring off predicted skin age on the y-axis is acceptable as we are looking for the ratio change for the actual to the proposed age of the skin - both are measures of age of the skin.

We can see that if you are 40 years old with a high predicted skin age of 80 years, then the likelihood of having severe photodamage is 4 times what it should be for your age, whereas if you are 70 years old with a predicted age of 80 years, your risk is not so dissimilar than you would expect for your chronological age.

Again, the artifact we saw earlier due to the low sample numbers in the 40-50 year age group is present here, which is why there appears to be a higher risk of skin damage if you are 40 years old with a predicted skin age of 30 years. A larger data set would likely smooth out the ratio line from Fig 6.3 and the result of that would be a more defined zero line on our coloured risk chart. A larger data set would also give a more even colour change from one ratio change to the other.

It is worthwhile remembering at this stage that the risk identified is for the specific SIAscan image taken and is not a risk for the patient as a whole, so it may just be for a forearm or chest. This means it will vary for each image from different areas of the body. It may be possible to take images at selected areas of the body and analyse them to create an overall risk map of the whole body. This could also be colour coded to identify the areas of the body at significant risk. This would help patients to visualize the areas they need to protect and help with areas for self monitoring.

From previous discussion, we know that solar induced skin damage can lead to a certain class of skin cancers, a group that make up >90% of all skin cancers. We know that skin cancer is a widespread problem and that the epidemiology statistics only show it is getting worse. Therefore some sort of a measure, or score, of underlying skin damage would certainly be a useful tool, particularly in a primary care scenario to identify a population for monitoring or to reinforce self examination or sun care.

Another application of the technique relates to iatrogenically induced skin damage from radiotherapy. We often see in our clinics, people who have had radiotherapy for some relatively minor ailments. It was the treatment of choice for scalp ringworm in the 1950's to 1960's and the result is delayed presentation of skin cancers. The effect is dose related and it is something that oncologists still worry about today in people with photodamaged skin, radio-recurrent or adjacent malignant disease. This technique may be useful in identifying skin which has signs of extrinsic damage or that maybe has fared better than anticipated from previous treatments. This will allow more accurate and effective dosing.

Appendix A

Table A1 2009 AJCC staging system for melanoma

Stage	Primary tumour (pT)	Lymph nodes (LN)	Metastases (M)
IA	< 1 mm, no ulceration, mitosis < 1/mm^2		
IB	< 1 mm, with ulceration or mitoses ≥ 1/mm^2*		
	1.01-2 mm, no ulceration		
IIA	1.01-2 mm with ulceration		
	2.01-4 mm, no ulceration		
IIB	2.01-4 mm, with ulceration		
	> 4 mm, no ulceration		
IIC	> 4 mm, with ulceration		
IIIA	Any Breslow thickness	Micro-metastases 1-3 nodes	
IIIB	Any Breslow thickness, with ulceration	Micro-metastases 1-3 nodes	
	Any Breslow thickness, no ulceration	1-3 palpable metastatic nodes	
	Any Breslow thickness, no ulceration	No nodes, but in-transit or satellite metastasis	
IIIC	Any Breslow thickness, with ulceration	Up to 3 palpable lymph nodes	
	Any Breslow thickness, with or without ulceration	4 or more nodes or matted nodes or in-transit disease + lymph nodes	
	Any Breslow thickness, with ulceration	No nodes, but in-transit or satellite metastasis	
IV, M1a			Skin, subcutaneous or distal nodal disease
IV, M1b			Lung metastases
IV, M1c			All other sites or any other sites of metastases with raised LDH

*In the rare circumstances where mitotic count cannot be accurately determined, a Clark's level of invasion of either IV or V can be used to define pT1b melanoma.

Appendix B

Patient information sheet and consent form

Mr JA Walls
Clinical Fellow
Dept. of Plastic & Reconstructive Surgery
Box 186

Tel: 01223 245151 ext 2170
Email: joseph.walls@addenbrookes.nhs.uk

Addenbrooke's NHS
NHS Trust
Hills Road
Cambridge CB2 2QQ
Tel: 01223 245151
www.addenbrookes.org.uk

Patient Information Sheet

CAN THE PROCESSING OF DIGITAL IMAGES HELP IN THE DIAGNOSIS OF SKIN DAMAGE?

You are being invited to take part in a research study. Before you decide it is important for you to understand why the research is being done and what it will involve. Please take time to read the following information carefully and discuss it with others if you wish. Ask us if there is anything that is not clear or if you would like more information. Take time to decide whether or not you wish to take part.

What is the purpose of the study?

This is a 1 year study organised with the help of Addenbrookes University Hospital. It uses a digital camera called a SIAscope to see if there are any features in the skin not visible to the human eye, which can help in the diagnosis of skin blemishes.

Why have I been chosen?

You have been seen by a hospital specialist regarding a skin blemish and you are now due to have it sampled or removed. This makes you suitable to take part in the study. We aim to enrol about 700 patients in total.

Do I have to take part?

It is up to you to decide whether or not to take part. If you do decide to take part you will be given this information sheet to keep and be asked to sign a consent form. Whether you decide to take part or not, your treatment will not be effected in any way.

What will happen to me if I take part? What do I have to do?

It will take less than a minute to take a digital picture of your skin and is exactly the same as taking any other sort of picture. It won't hurt and has no side effects. You won't be asked to take any other part in the study and it will have no effect on the treatment you will receive.

What is the procedure being tested?

A modified digital image is taken that looks at skin features invisible to the human eye. This has been tested in the past and is now used worldwide for the diagnosis of certain skin problems. The results of your biopsy or excision will be compared with the image taken to see if any features can be seen which will help in more accurate diagnosis in the future.

What are the possible benefits of taking part?

Aside from helping with the advancement of medical knowledge, there are no benefits to taking part and your treatment will not be effected in any way. No payment is being made to the researchers or hospital in doing this study and no fee is payable to anyone who wishes to participate in this study. This study is purely for the advancement of medical knowledge to help in the future diagnosis of skin problems.

What about confidentiality? What will happen to the results of the research study?

All information is strictly confidential. No identifying details will be recorded in any way. The picture taken and the laboratory results will be matched and studied and all stored on an encrypted, secure computer, accessible only by the investigator. It is standard NHS practice that all research data is securely stored for 15 years. The results of the study will help in the writing and presentation of scientific presentations and papers.

No pictures or data will be kept that may identify you.

Thank you for taking the time to consider this. Please ask if you have any questions.

Contact for Further Information: Mr Joe Walls (Research Fellow) 01223 245151

Mr JA Walls MRCS
Clinical Fellow
Dept. of Plastic & Reconstructive Surgery
Box 186

Tel: 01223 245151 ext 2170
Email: joseph.walls@addenbrookes.nhs.uk

Addenbrooke's NHS
NHS Trust
Hills Road
Cambridge CB2 2QQ
Tel: 01223 245151
www.addenbrookes.org.uk

CONSENT FORM

Patient Identification Number:

Title of Project: Using The Non-contact SIAscope to Diagnose Skin Damage

Name of Researcher: Mr Joseph Walls

Please initial box

1. I confirm that I have read and understood the information sheet for the above study and have had the opportunity to ask questions. ☐
2. I understand that my participation is voluntary and that I am free to withdraw at any time, without giving any reason and without my medical care or legal rights being affected. ☐
3. I understand that sections of any of my medical notes may be looked at by responsible individuals and I give permission for these individuals to have access to my records where it is relevant to my taking part in research. ☐
4. I consent to any image or recording to be used in educational presentations, publications, journals or textbooks and used in any form or medium including all forms of electronic publication, storage or distribution anywhere in the world. ☐
5. I understand that no fee is payable to me by the researchers or any other persons in respect of the material either now, or at any other time in the future. ☐
6. I agree to take part in the above study. ☐

_____	_____	_____
Name of Patient	Date	Signature
MR J WALLS		
_____	_____	_____
Researcher	Date	Signature

1 for patient; 1 for researcher; 1 to be kept with hospital notes

Appendix C

Fourier analysis

Fourier analysis is a technique of advanced mathematics that was realized by Baron Jean Baptiste Joseph Fourier (1768-1830). It was postulated while trying to answer the question of predicting the transference of heat along a metal rod of fixed length. Since its publication in 1826 the technique has been refined, but still bears close resemblance to the original proposed equation.
It has application in number theory, signal processing, imaging, acoustics, probability theory, cryptography, optics and numerous other outlets. It has even been applied to the stock market.
Fourier analysis is a complex form of advanced mathematics and I have come across numerous different definitions and explanations of it. In fact, to the non-mathematician, it seems there is a slightly different explanation depending on which application of it you are looking at and they are associated with some complex mathematical equations, well beyond the scope of the question asked in this thesis.

Basic Fourier theory

At its most basic element, Fourier Analysis is the ability to break a complex function down into simpler components. This calculation is called a Fourier Transform and results in a function which explains how many pieces makes up the original and how much of each are present. This is most easily described using acoustics as an example as we are more accustomed to considering sound in waveforms.
Consider a musical chord, made up of different individual notes. The sound produced is a function of all these individual notes and if we analysed the waveform of the chord we would see it was made up of the sum of all the different waveforms of each note. The unique composition of the chord is not just dependent on the frequency of the individual note, but also on how loud that note was played (its amplitude) and when the waveform started (its timing).

Fourier analysis gives us the ability to decompose that complex waveform into the basic waveforms which devise it, identifying not just presence, but also quantity and timing. The same process can be used in reverse to create a function from a series of individual components. Each wave may be either a sine or cosine wave and when combined, their presence, amplitude and timing can result in the formation of any complex waveform. The term Fourier Analysis tends to cover both the construction and deconstruction of a function.

During my literature search, I found many different explanations of Fourier theory and analysis, each differing slightly in the application for which it was being used. I came across an excellent explanation of basic Fourier theory by Steven Lehar* and it is with his kind permission that I base my explanation of Fourier analysis on his work, specifically with regard to the application it was used for in this thesis - that of digital picture analysis.

Fourier theory suggests that a signal can be represented by the sum of basic sinusoidal waves. In optical analysis, an image can be considered as the signal and the sinusoidal waves are essentially the variations in brightness and/or colour across that image i.e. spatial variance as opposed to temporal variance. The resulting transform will code for spacial frequency, magnitude (or amplitude) and phase. Frequency implies some function which changes with time, however it may relate to something which changes with space and in this example it is the change in brightness across x-axis the image.

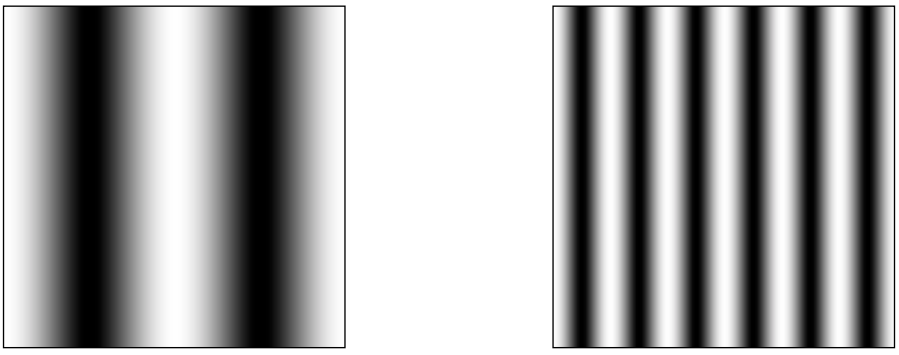

Fig C1 A visual example of different frequencies

* An intuitive explanation of Fourier theory by Steven Lehar (http://sharp.bu.edu/~slehar/fourier/fourier.html)

These examples show two different sinusoidal images of different spacial frequencies and we can see that the frequency is higher in the image on the right than that on the left. In the transform, the magnitude corresponds to the contrast of the image i.e. the variations in the darkest and lightest areas of the image, and may be positive or negative when an average contrast level for the image is considered. Phase represents how much the sinusoid has shifted in relation to its origin (left or right) and is effectively an element of timing

If an image contains only a single spatial frequency, f, this will be plotted as a single peak along the frequency (x-) axis, with the amplitude corresponding to the contrast plotted on the amplitude (y-) axis.

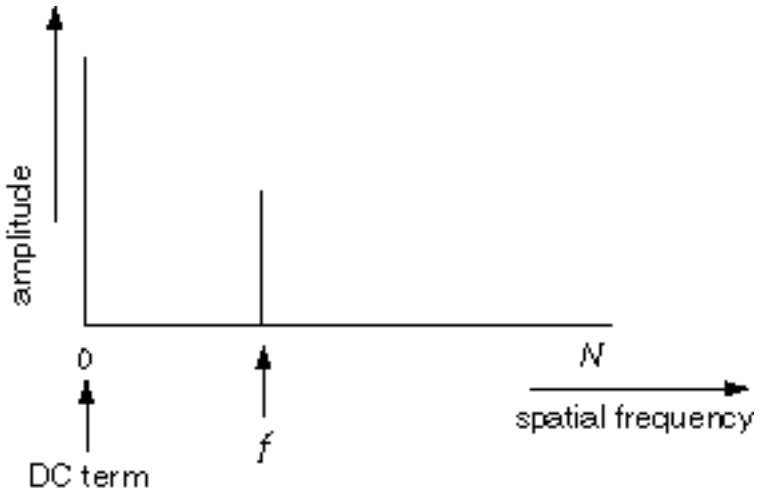

Fig C2 Plot of a specific spacial frequency

The DC term represents the average brightness across the whole image. An average of 0 would represent an image that alternates between positive and negative values, but as there can never really be such a thing as negative brightness, all real images will have a positive DC term.

The transform will encode for a whole series of sinusoids through the entire range of available spacial frequencies, from zero through to the 'Nyquist', or cut-off, frequency. The 'Nyquist frequency' is the highest possible spacial frequency that can be encoded for and is dependent upon the resolution of the image or the pixel size.

For mathematical reasons beyond the simple explanation here, the transform also plots a mirror image of the spatial frequency at -*f*.

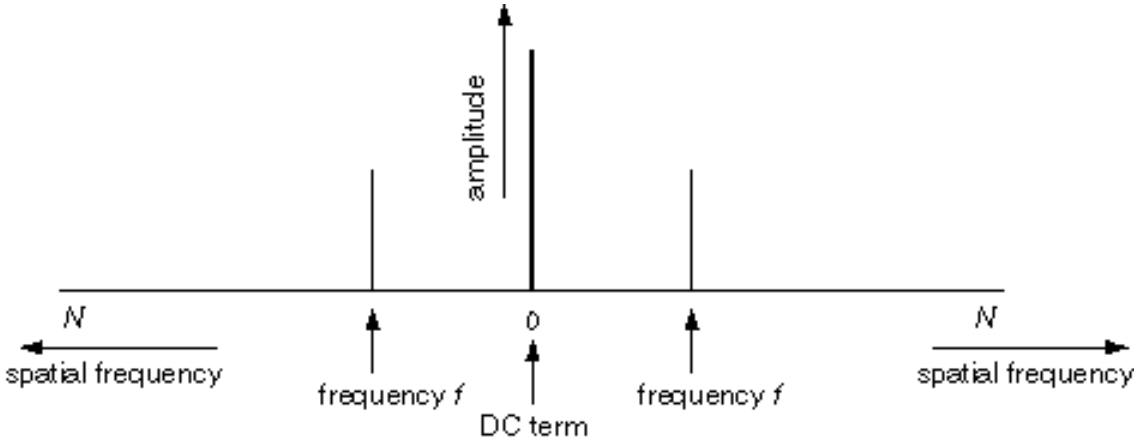

Fig C3 Plot of a specific spacial frequency at f and -f

This plot will represent the transform of a single scan line of the sinusoidal image i.e. a one-dimensional signal. The Fourier transform will produce repeated 1-D transforms on every line of the image to give a cumulative 2-D transform the same size as the original image.

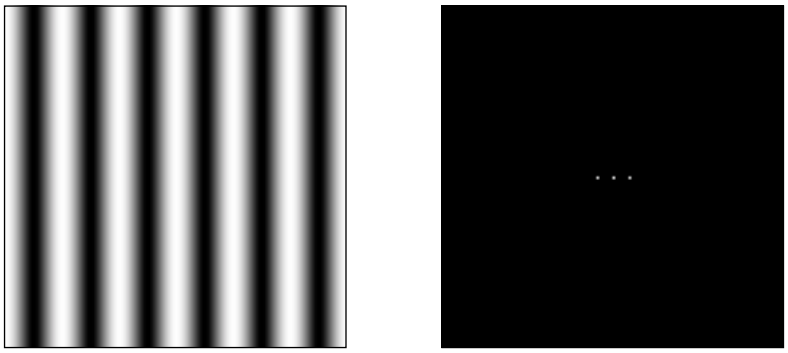

Fig C4 Simple sinusoid and corresponding Fourier transform

The above example shows a simple sinusoidal brightness image and its corresponding 2-D Fourier transform, also presented as a brightness image. The position of each pixel in the Fourier image denotes the spatial frequency, with the central pixel denoting the DC term and the flanking pixels indicating the frequency of the sinusoid. The amplitude of the sinusoid is encoded as the

brightness of the pixel, so the brighter the frequency peak, the higher the contrast in the image brightness. As this is a single frequency component image, all the other frequencies are zero and a depicted as black.

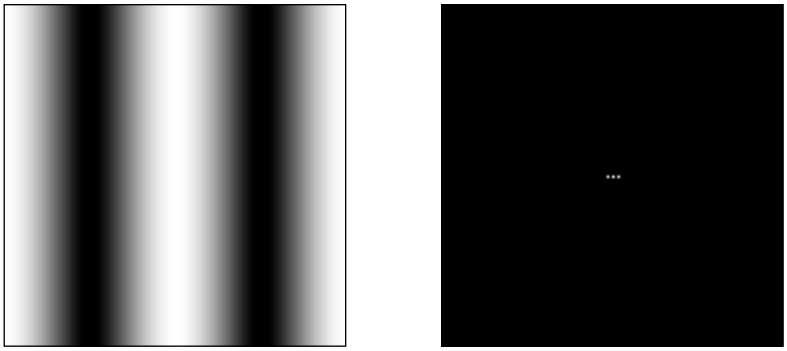

Fig C5 A lower frequency image and corresponding Fourier transform

This example shows a lower frequency sinusoidal brightness image with the corresponding frequency peaks in the Fourier transform being closer to the DC term, indicating the lower spatial frequency.

The Fourier image codes exactly the same information as the brightness image, merely expressed in terms of amplitude as a function of spacial frequency, rather than brightness as a function of spacial displacement. An inverse transform of the Fourier image will produce an exact replica of the original brightness image.

SInusoids from different directions correlate with the orientation of the peaks on the Fourier image relative to the DC term.

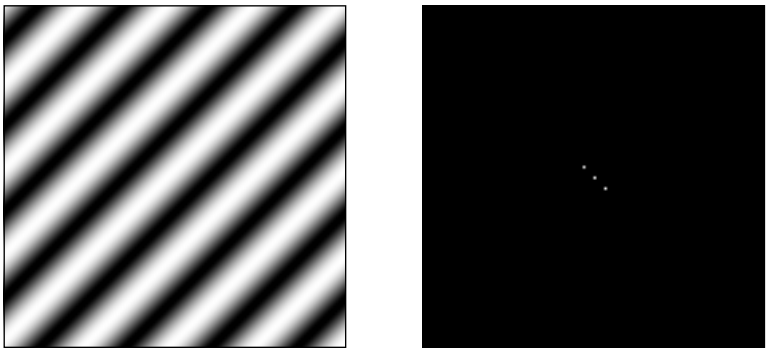

Fig C6 An oblique sinusoid and corresponding Fourier transform

It therefore goes without saying that different sinusoids from different orientations will combine to produce specific patterns and this will be coded in both orientations in the Fourier analysis.

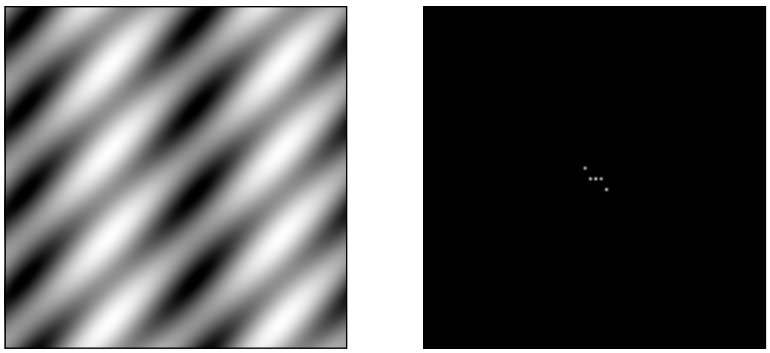

Fig C7 A complex frequency pattern and corresponding Fourier transform

These example have focused on smooth alternating shapes, but real life images have sharp edges and delineated boundaries. These can also be transformed to a Fourier image as even a straight line waveform can be constructed from multiple sinusoids by means of *harmonics*.

The following images show a series of sinusoidal brightness images of different spacial frequencies. The first image is the fundamental frequency and the others are higher harmonics, being integer multiples of the fundamental frequency.

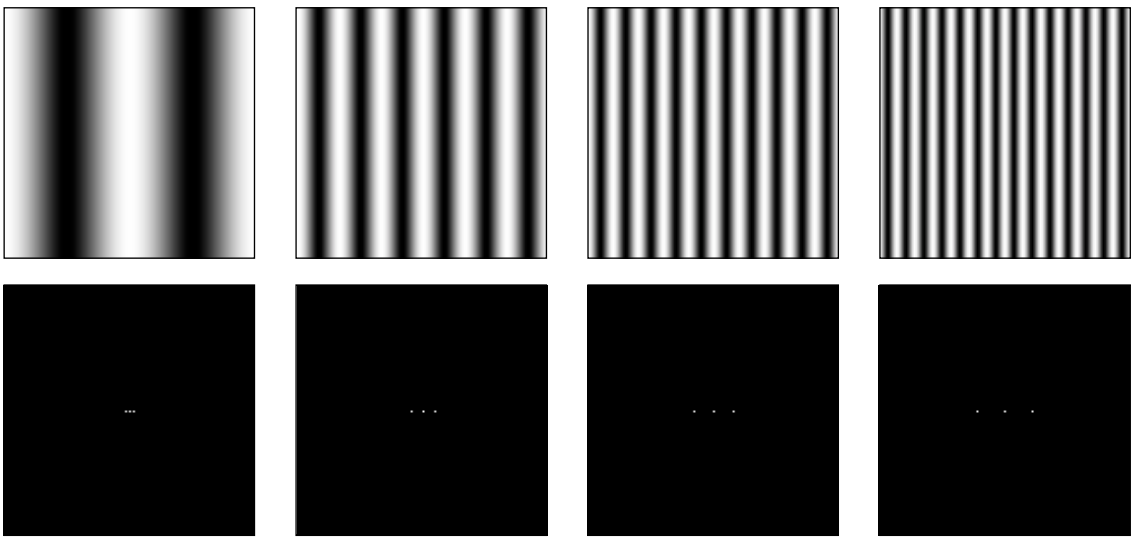

Fig C8 A range of harmonic frequencies and corresponding Fourier transforms

The following images show the result of progressively adding the higher harmonics to the fundamental frequency.

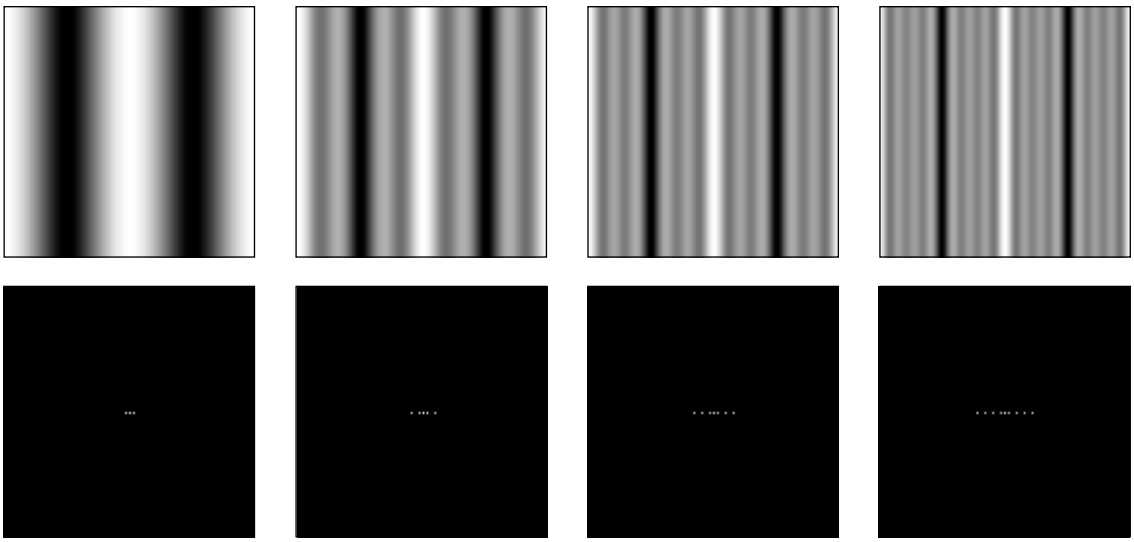

Fig C9 Adding a range of harmonic frequencies and corresponding Fourier transforms

Note how the addition of successive higher level harmonics creates a central band which gets successively stronger and sharper, while the background drops back to a more uniform shade.

If this were continued out to the Nyquist frequency, it would produce a thin stripe with sharp boundaries in the brightness image, i.e. a square wave. The corresponding Fourier image shows an infinite series of harmonics within the boundaries of the original image.

Fig C10 The Fourier transforms from adding an infinite range of harmonic frequencies

The ability of the Fourier image to code exactly for an image and then reversing the transform resulting in recreation of the image, means that any alteration of the spatial frequency in the Fourier image would result in the recreated image being altered.

In this example, the image is transformed into the Fourier image and a low frequency filter is then applied. This only allows low spatial frequency components to pass and blocks all higher frequency signals. The filter is seen as a circle as we know that all the low frequency components are located close to the DC term point, so a circle with a specific radius will block all frequencies beyond that radius in the Fourier image.

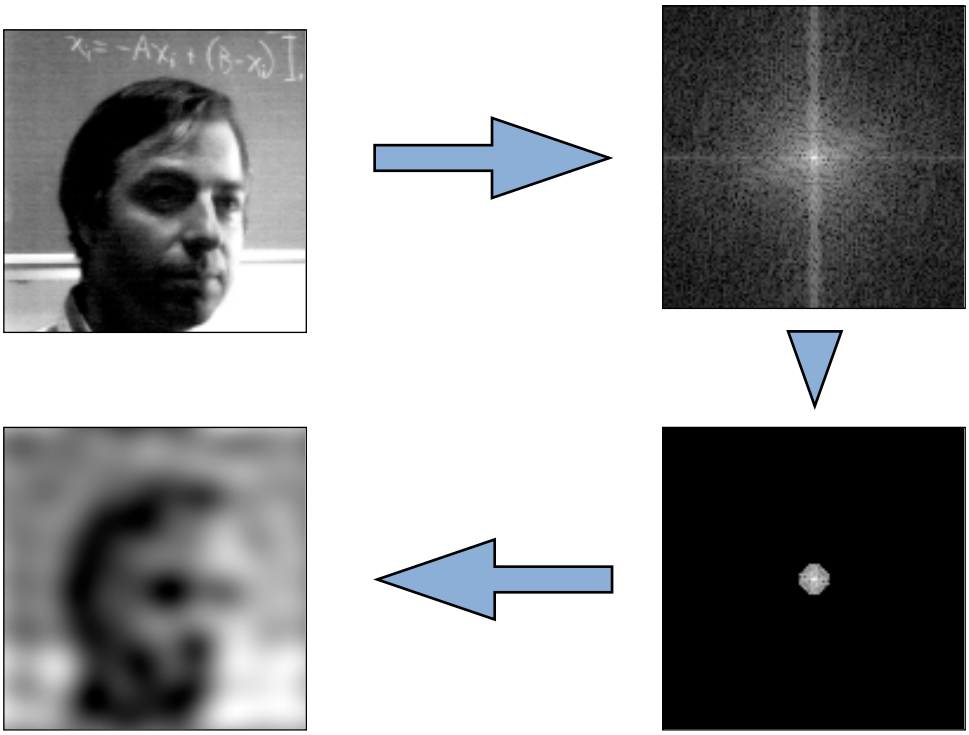

Fig C11 Using a low-pass Fourier filter to manipulate an image

We can see that the result of a low-pass filter is an image that looks blurred. From the previous example of using higher harmonics to create sharp edges in a image, we would expect the loss of the sharp contours of the original image due to blocking of the higher spatial frequencies.

If we applied a high-pass filter we would block these lower spatial frequencies and keep all of the higher frequencies.

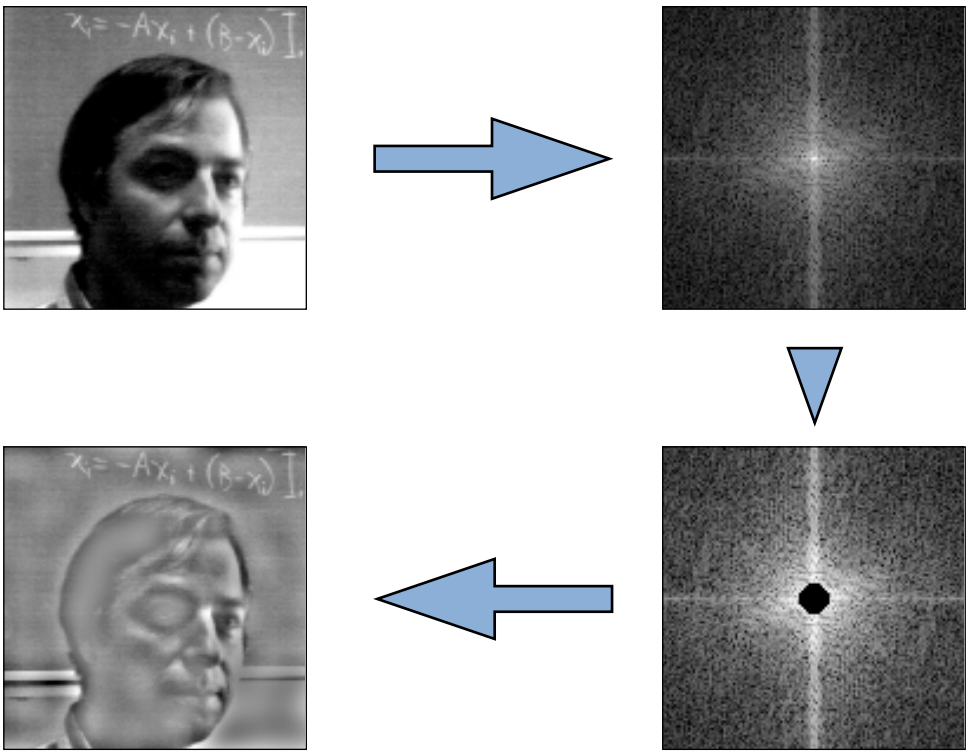

Fig C12 Using a high-pass Fourier filter to manipulate an image

This maintains the sharp contours of the original image, but loses the larger area of dark and light.

By constructing a filter to specifically manipulate or limit the spatial frequencies in the Fourier transform, images can be reconstructed with varying results. This is the principle behind image filtering performed by picture manipulation software such as Photoshop (Adobe, USA). Think of applying a digital effect to an image. First the Fourier transform creates a Fourier image of the original and then the appropriate spatial frequency and amplitude adjustments are made by the filter to the entire image before reverse transformation to create the modified image. Proprietary filters can be constructed to apply all sorts of image manipulation, such as paintbrush effects, frosted glass effects, etc.

Appendix D - SPSS output tables

Table D1 Coefficient statistics

Model		Unstandardised coefficients		Standardised coefficients	t	Sig.	Correlations			Collinearity Statistics	
		B	Std.error	Beta			Zero-order	Partial	Part	Tolerance	VIF
1	(Constant)	21.266	2.045		10.398	.000					
	std Hue	1479	89.569	.514	16.514	.000	.514	.514	.514	1.000	1.000
2	(Constant)	19.333	1.992		9.707	.000					
	std Hue	1341	88.433	.466	15.162	.000	.514	.482	.456	.956	1.046
	freckle eccentricity range	18.462	2.465	.230	7.49	.000	.328	.263	.225	.956	1.046
3	(Constant)	-30.9	8.326		-3.711	.000					
	std Hue	1006	101.797	.35	9.883	.000	.514	.338	.290	.688	1.454
	freckle eccentricity range	17.481	2.411	.218	7.249	.000	.328	.255	.213	.952	1.05
	Blood fourier section mean32	12.026	1.938	.218	6.205	.000	.445	.220	.182	.699	1.431
4	(Constant)	7.168	12.364		.58	.562					

	std Hue	727.8	121.208	.253	6.004	.000	0.514	0.213	0.174	0.475	2.105
	freckle eccentricity range	17.501	2.386	.218	7.334	.000	0.328	0.258	0.213	0.952	1.05
	Blood fourier section mean32	13.535	1.953	.245	6.932	.000	0.445	0.244	0.201	0.674	1.483
	Blood fourier section mean652	-11.31	2.739	-.147	-4.129	.000	-0.353	0.149	0.12	0.666	1.502
5	(Constant)	17.259	12.585		1.371	.171					
	std Hue	560.6	128.956	.195	4.437	.000	.514	.156	.125	.413	2.42
	freckle eccentricity range	15.503	2.432	.193	6.374	.000	.328	.226	.184	.902	1.108
	Blood fourier section mean32	12.158	1.975	.220	6.156	.000	.445	.219	.177	.649	1.541
	Blood fourier section mean652	-13.75	2.801	-.179	-4.907	.000	-.353	-.176	-.141	.627	1.595

	mel Std	3452	961.054	.127	3.592	.000	.382	.130	.103	.659	1.517
6	(Constant)	-20.83	14.505		-1.436	.151					
	std Hue	278.2	138.709	.097	2.005	.045	.514	.073	.057	.346	2.891
	freckle eccentricity range	11.356	2.531	.142	4.487	.000	.328	.161	.127	.807	1.239
	Blood fourier section mean32	10.269	1.979	.186	5.188	.000	.445	.186	.147	.626	1.598
	Blood fourier section mean652	-13.62	2.757	-.177	-4.939	.000	-.353	-.177	-.140	.627	1.595
	mel Std	6134	1084.930	.226	5.654	.000	.382	.202	.160	.501	1.995
	Mel fourier section mean2	6.286	1.246	.188	5.046	.000	.351	.181	.143	.580	1.724
7	(Constant)	-25.79	14.575		-1.769	.077					
	std Hue	241.7	138.892	.084	1.740	.082	.514	.063	.049	.342	2.921
	freckle eccentricity range	12.003	2.533	.150	4.738	.000	.328	.170	.134	.800	1.251

	Blood fourier section mean32	10.137	1.973	.184	5.139	.000	.445	.184	.145	.625	1.599
	Blood fourier section mean652	-12.14	2.805	-.158	-4.329	.000	-.353	-.156	-.122	.601	1.664
	mel Std	5935	1083.517	.219	5.477	.000	.382	.196	.155	.499	2.005
	Mel fourier section mean2	5.952	1.248	.178	4.762	.000	.351	.171	.135	.573	1.744
	max Hue	8.064	3.102	.082	2.600	.100	.288	.094	.073	.809	1.237
8	(Constant)	-10.06	15.814		-.636	.525					
	std Hue	363.2	146.595	.126	2.477	.013	.514	.090	.070	.305	3.277
	freckle eccentricity range	8.697	2.847	.108	3.055	.002	.328	.111	.086	.629	1.590
	Blood fourier section mean32	11.231	2.013	.203	5.579	.000	.445	.199	.157	.596	1.678

	Blood fourier section mean652	-18.33	3.726	-.238	-4.921	.000	-.353	-.177	-.139	.338	2.956
	mel Std	7215	1193.775	.266	6.043	.000	.382	.215	.170	.408	2.451
	Mel fourier section mean2	6.517	1.264	.195	5.154	.000	.351	.185	.145	.555	1.803
	max Hue	8.331	3.093	.084	2.693	0.007	.288	.098	.076	.808	1.238
	blood Mean	-.009	.004	-.158	-2.513	0.012	.414	-.091	-.071	.201	4.973

Dependent variable: age

Table D2 Collinearity diagnostics

Collinearity Diagnostics[a]

Model	Dimension	Eigenvalue	Condition Index	Variance Proportions							
				(Constant)	stdHue	freckle Eccentricity Range	bloodFourier Section Mean32	bloodFourier Section Mean652	melStd	melFourier SectionMean2	maxHue	bloodMean
1	1	1.951	1.000	.02	.02							
	2	.049	6.320	.98	.98							
2	1	2.613	1.000	.01	.01	.05						
	2	.338	2.781	.04	.04	.95						
	3	.049	7.321	.94	.95	.00						
3	1	3.566	1.000	.00	.00	.02	.00					
	2	.375	3.085	.00	.01	.96	.00					
	3	.057	7.876	.02	.77	.01	.01					
	4	.002	39.560	.98	.21	.00	.99					
4	1	4.521	1.000	.00	.00	.01	.00	.00				
	2	.399	3.367	.00	.00	.96	.00	.00				
	3	.076	7.731	.00	.44	.02	.00	.01				
	4	.003	37.614	.00	.49	.00	.80	.36				
	5	.002	54.353	.99	.06	.00	.20	.63				
5	1	5.474	1.000	.00	.00	.01	.00	.00	.00			
	2	.402	3.691	.00	.00	.93	.00	.00	.00			
	3	.079	8.344	.00	.29	.03	.00	.01	.04			
	4	.041	11.501	.00	.18	.03	.00	.00	.88			
	5	.003	41.395	.00	.42	.00	.77	.35	.00			
	6	.001	62.038	.99	.10	.00	.23	.64	.07			
6	1	6.454	1.000	.00	.00	.01	.00	.00	.00	.00		
	2	.411	3.964	.00	.00	.83	.00	.00	.00	.00		
	3	.082	8.860	.00	.23	.04	.00	.01	.06	.00		
	4	.046	11.850	.00	.16	.02	.00	.00	.56	.01		
	5	.003	43.000	.00	.58	.07	.04	.46	.24	.47		
	6	.003	45.962	.00	.03	.02	.89	.04	.14	.24		
	7	.001	74.565	.99	.00	.02	.07	.48	.01	.28		

7	1	7.336	1.000	.00	.00	.00	.00	.00	.00	.00	.00	
	2	.422	4.170	.00	.00	.81	.00	.00	.00	.00	.01	
	3	.117	7.906	.00	.02	.00	.00	.00	.00	.00	.63	
	4	.075	9.909	.00	.19	.06	.00	.00	.13	.00	.20	
	5	.043	13.067	.00	.24	.01	.00	.00	.47	.01	.11	
	6	.003	46.704	.00	.53	.08	.04	.45	.24	.49	.04	
	7	.003	49.003	.00	.03	.02	.88	.04	.14	.25	.00	
	8	.001	80.125	.99	.00	.02	.07	.50	.00	.25	.02	
8	1	8.259	1.000	.00	.00	.00	.00	.00	.00	.00	.00	.00
	2	.434	4.361	.00	.00	.62	.00	.00	.00	.00	.01	.00
	3	.136	7.797	.00	.03	.01	.00	.00	.00	.00	.15	.04
	4	.097	9.240	.00	.03	.01	.00	.00	.03	.00	.73	.03
	5	.046	13.413	.00	.04	.03	.00	.00	.49	.01	.08	.02
	6	.022	19.389	.00	.75	.08	.00	.00	.00	.00	.00	.43
	7	.003	51.781	.00	.00	.05	.62	.00	.24	.50	.00	.00
	8	.002	58.913	.06	.14	.16	.38	.24	.20	.43	.01	.20
	9	.001	96.982	.94	.00	.03	.00	.75	.05	.06	.01	.28

a. Dependent Variable: Age

Excluded Variables[i]

Model		Beta In	t	Sig.	Partial Correlation	Collinearity Statistics		
						Tolerance	VIF	Minimum Tolerance
1	blueCov	.056[a]	1.618	.106	.059	.821	1.217	.821
	melStd	.182[a]	5.270	.000	.188	.783	1.277	.783
	bloodMean	.055[a]	1.155	.249	.042	.424	2.358	.424
	covFreckleSize	.115[a]	3.577	.000	.129	.918	1.089	.918
	maxHue	.109[a]	3.259	.001	.118	.857	1.167	.857
	minHue	-.164[a]	-4.257	.000	-.153	.638	1.568	.638
	fraction16	.089[a]	2.456	.014	.089	.735	1.361	.735
	covFreckleArea	.166[a]	5.194	.000	.185	.920	1.086	.920
	freckleEccentricityRange	.230[a]	7.490	.000	.263	.956	1.046	.956
	bloodRangeNormalSkin	.047[a]	1.200	.231	.044	.626	1.597	.626
	bloodMinNormalSkin	.056[a]	1.581	.114	.057	.780	1.282	.780
	bloodThreshFraction1000	.081[a]	1.670	.095	.061	.408	2.452	.408
	bloodFourierSection Mean32	.234[a]	6.478	.000	.229	.702	1.425	.702
	bloodFourierSection Mean652	-.097[a]	-2.594	.010	-.094	.690	1.449	.690
	melFourierSectionMean2	.155[a]	4.523	.000	.162	.807	1.239	.807
2	blueCov	.017[b]	.494	.622	.018	.801	1.249	.801
	melStd	.130[b]	3.763	.000	.136	.741	1.349	.741
	bloodMean	.160[b]	3.364	.001	.121	.393	2.543	.376
	covFreckleSize	.040[b]	1.191	.234	.043	.811	1.233	.811
	maxHue	.125[b]	3.864	.000	.139	.854	1.172	.817
	minHue	-.138[b]	-3.669	.000	-.132	.632	1.583	.630
	fraction16	.099[b]	2.821	.005	.102	.734	1.363	.706
	covFreckleArea	.027[b]	.663	.507	.024	.546	1.832	.546
	bloodRangeNormalSkin	.119[b]	3.069	.002	.111	.593	1.687	.568

Table D3 Excluded variables

	bloodMinNormalSkin	.071[b]	2.076	.038	.075	.777	1.286	.745
	bloodThreshFraction1000	.169[b]	3.529	.000	.127	.387	2.583	.370
	bloodFourierSection Mean32	.218[b]	6.205	.000	.220	.699	1.431	.688
	bloodFourierSection Mean652	-.101[b]	-2.796	.005	-.101	.690	1.449	.667
	melFourierSectionMean2	.111[b]	3.280	.001	.118	.778	1.285	.778
3	blueCov	.002[c]	.050	.960	.002	.797	1.255	.622
	melStd	.085[c]	2.441	.015	.088	.700	1.428	.634
	bloodMean	.120[c]	2.556	.011	.093	.385	2.598	.348
	covFreckleSize	.057[c]	1.736	.083	.063	.806	1.241	.649
	maxHue	.122[c]	3.881	.000	.140	.853	1.172	.615
	minHue	-.106[c]	-2.849	.004	-.103	.618	1.619	.534
	fraction16	.080[c]	2.347	.019	.085	.728	1.374	.567
	covFreckleArea	.052[c]	1.313	.190	.048	.540	1.851	.540
	bloodRangeNormalSkin	.083[c]	2.145	.032	.078	.577	1.734	.496
	bloodMinNormalSkin	.080[c]	2.410	.016	.087	.776	1.289	.561
	bloodThreshFraction1000	.154[c]	3.272	.001	.118	.386	2.590	.331
	bloodFourierSection Mean652	-.147[c]	-4.129	.000	-.149	.666	1.502	.475
	melFourierSectionMean2	.101[c]	3.048	.002	.110	.776	1.289	.612
4	blueCov	.009[d]	.290	.772	.011	.794	1.260	.435
	melStd	.127[d]	3.592	.000	.130	.659	1.517	.413
	bloodMean	.008[d]	.131	.896	.005	.247	4.044	.247
	covFreckleSize	.043[d]	1.314	.189	.048	.796	1.256	.465
	maxHue	.100[d]	3.129	.002	.113	.818	1.222	.461
	minHue	-.085[d]	-2.289	.022	-.083	.604	1.655	.418
	fraction16	.062[d]	1.792	.073	.065	.713	1.403	.434
	covFreckleArea	.048[d]	1.213	.226	.044	.540	1.852	.462
	bloodRangeNormalSkin	.058[d]	1.500	.134	.055	.561	1.782	.401
	bloodMinNormalSkin	.021[d]	.556	.578	.020	.605	1.653	.464

	bloodThreshFraction1000	.062[d]	1.084	.279	.039	.255	3.918	.255
	melFourierSectionMean2	.085[d]	2.559	.011	.093	.763	1.311	.453
5	blueCov	-.003[e]	-.103	.918	-.004	.784	1.275	.390
	bloodMean	-.089[e]	-1.407	.160	-.051	.208	4.797	.208
	covFreckleSize	.041[e]	1.262	.207	.046	.796	1.256	.407
	maxHue	.097[e]	3.077	.002	.111	.818	1.223	.403
	minHue	-.049[e]	-1.246	.213	-.045	.546	1.832	.390
	fraction16	-.007[e]	-.166	.868	-.006	.504	1.984	.408
	covFreckleArea	.035[e]	.880	.379	.032	.535	1.870	.407
	bloodRangeNormalSkin	.021[e]	.524	.600	.019	.517	1.935	.376
	bloodMinNormalSkin	.011[e]	.309	.757	.011	.602	1.661	.408
	bloodThreshFraction1000	-.016[e]	-.262	.793	-.010	.220	4.547	.220
	melFourierSectionMean2	.188[e]	5.046	.000	.181	.580	1.724	.346
6	blueCov	-.019[f]	-.594	.552	-.022	.777	1.287	.334
	bloodMean	-.152[f]	-2.412	.016	-.088	.201	4.967	.201
	covFreckleSize	.023[f]	.712	.477	.026	.786	1.273	.344
	maxHue	.082[f]	2.600	.010	.094	.809	1.237	.342
	minHue	-.057[f]	-1.488	.137	-.054	.545	1.835	.327
	fraction16	.004[f]	.091	.928	.003	.503	1.989	.341
	covFreckleArea	.011[f]	.294	.769	.011	.527	1.897	.344
	bloodRangeNormalSkin	-.018[f]	-.444	.657	-.016	.498	2.009	.331
	bloodMinNormalSkin	-.011[f]	-.303	.762	-.011	.593	1.686	.345
	bloodThreshFraction1000	-.074[f]	-1.200	.230	-.044	.213	4.702	.213
7	blueCov	-.022[g]	-.676	.499	-.025	.776	1.288	.331
	bloodMean	-.158[g]	-2.513	.012	-.091	.201	4.973	.201
	covFreckleSize	.017[g]	.537	.591	.020	.782	1.279	.341
	minHue	-.010[g]	-.234	.815	-.009	.411	2.433	.327
	fraction16	.005[g]	.121	.904	.004	.503	1.989	.338
	covFreckleArea	.016[g]	.407	.684	.015	.526	1.900	.341
	bloodRangeNormalSkin	-.039[g]	-.953	.341	-.035	.480	2.083	.330
	bloodMinNormalSkin	-.005[g]	-.140	.889	-.005	.591	1.693	.341

	bloodThreshFraction1000	-.075[g]	-1.227	.220	-.045	.213	4.702	.213
8	blueCov	-.030[h]	-.943	.346	-.034	.768	1.302	.199
	covFreckleSize	.009[h]	.276	.783	.010	.773	1.293	.199
	minHue	-.022[h]	-.507	.613	-.018	.406	2.461	.199
	fraction16	.021[h]	.533	.594	.019	.490	2.042	.196
	covFreckleArea	-.004[h]	-.105	.917	-.004	.504	1.982	.193
	bloodRangeNormalSkin	.002[h]	.050	.960	.002	.404	2.476	.169
	bloodMinNormalSkin	.046[h]	1.122	.262	.041	.469	2.131	.160
	bloodThreshFraction1000	.068[h]	.781	.435	.028	.106	9.450	.100

a Predictors in the Model: (Constant), stdHue
b Predictors in the Model: (Constant), stdHue, freckleEccentricityRange
c Predictors in the Model: (Constant), stdHue, freckleEccentricityRange, bloodFourierSectionMean32
d Predictors in the Model: (Constant), stdHue, freckleEccentricityRange, bloodFourierSectionMean32, bloodFourierSectionMean652
e Predictors in the Model: (Constant), stdHue, freckleEccentricityRange, bloodFourierSectionMean32, bloodFourierSectionMean652, melStd
f Predictors in the Model: (Constant), stdHue, freckleEccentricityRange, bloodFourierSectionMean32, bloodFourierSectionMean652, melStd, melFourierSectionMean2
g Predictors in the Model: (Constant), stdHue, freckleEccentricityRange, bloodFourierSectionMean32, bloodFourierSectionMean652, melStd, melFourierSectionMean2, maxHue
h Predictors in the Model: (Constant), stdHue, freckleEccentricityRange, bloodFourierSectionMean32, bloodFourierSectionMean652, melStd, melFourierSectionMean2, maxHue, bloodMean
i Dependent Variable: Age

Partial regression plots for the model predictors

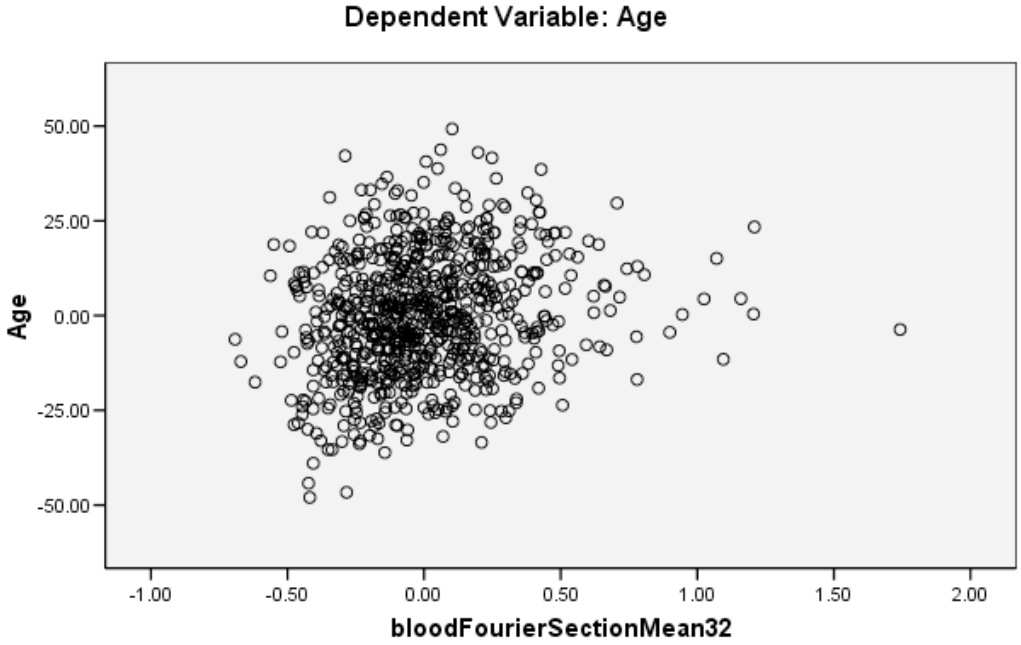

Fig D1 Partial regression plot Blood Fourier Section Mean32

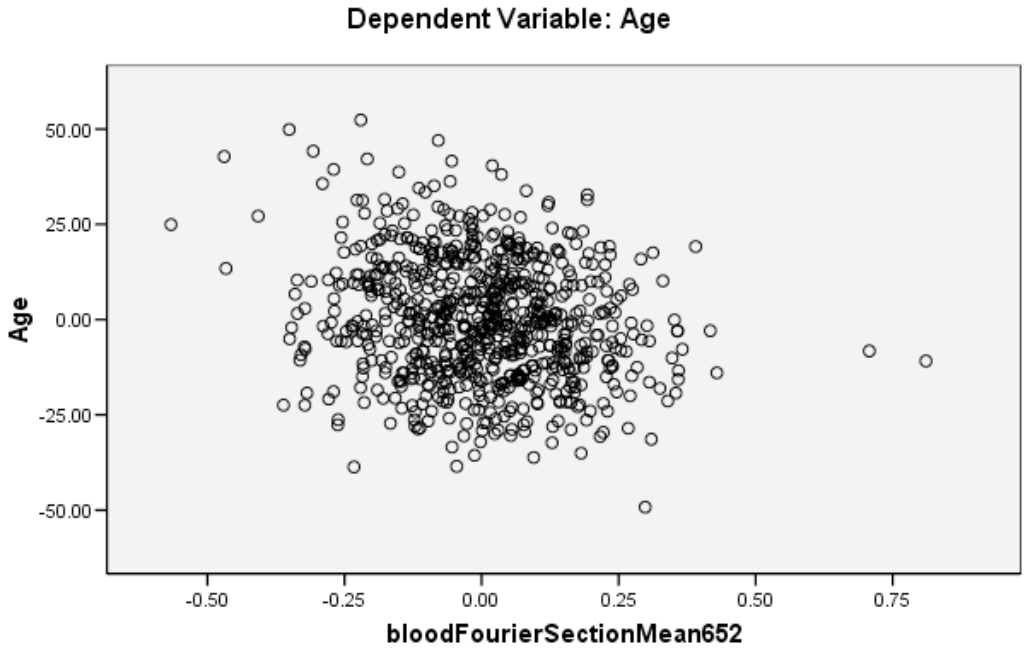

Fig D2 Partial regression plot Blood Fourier Section Mean652

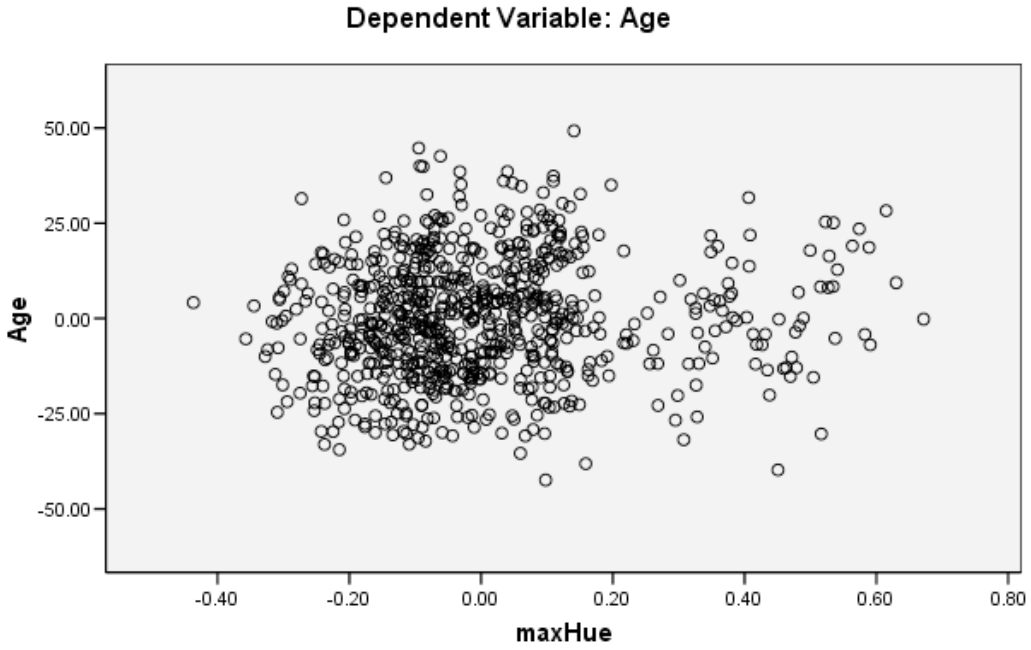

Fig D3 Partial regression plot max Hue

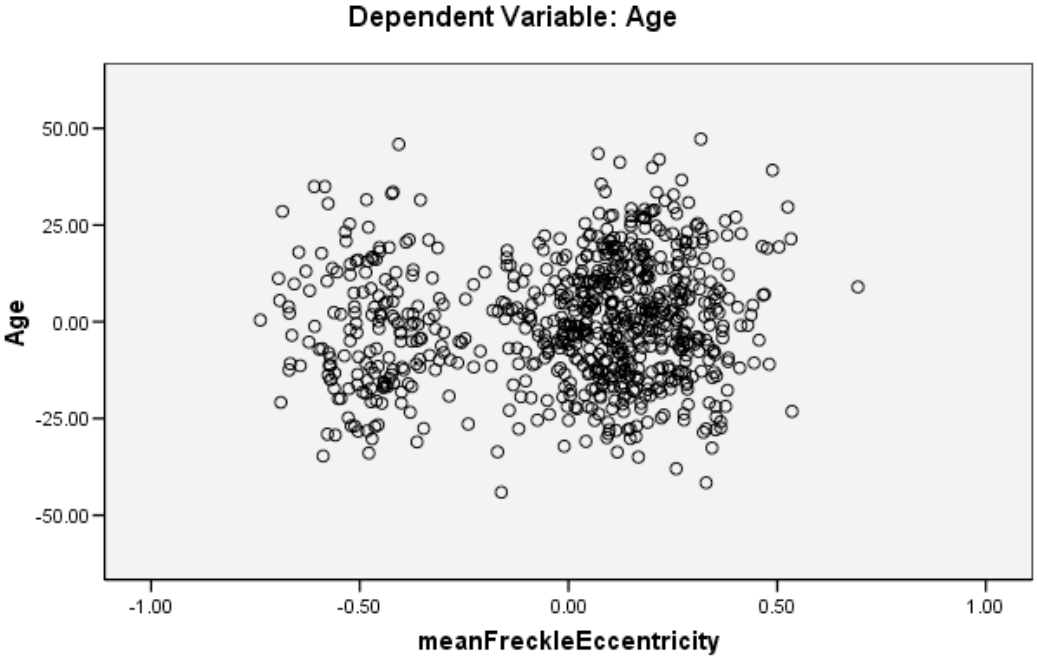

Fig D4 Partial regression plot mean freckle eccentricity

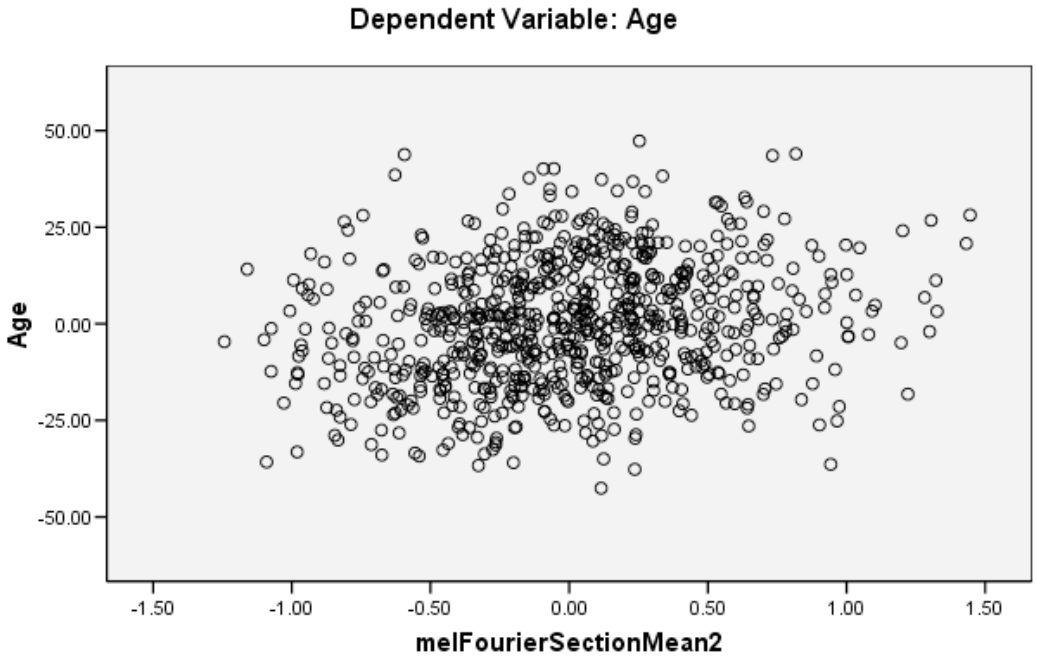

Fig D5 Partial regression plot mel fourier section mean2

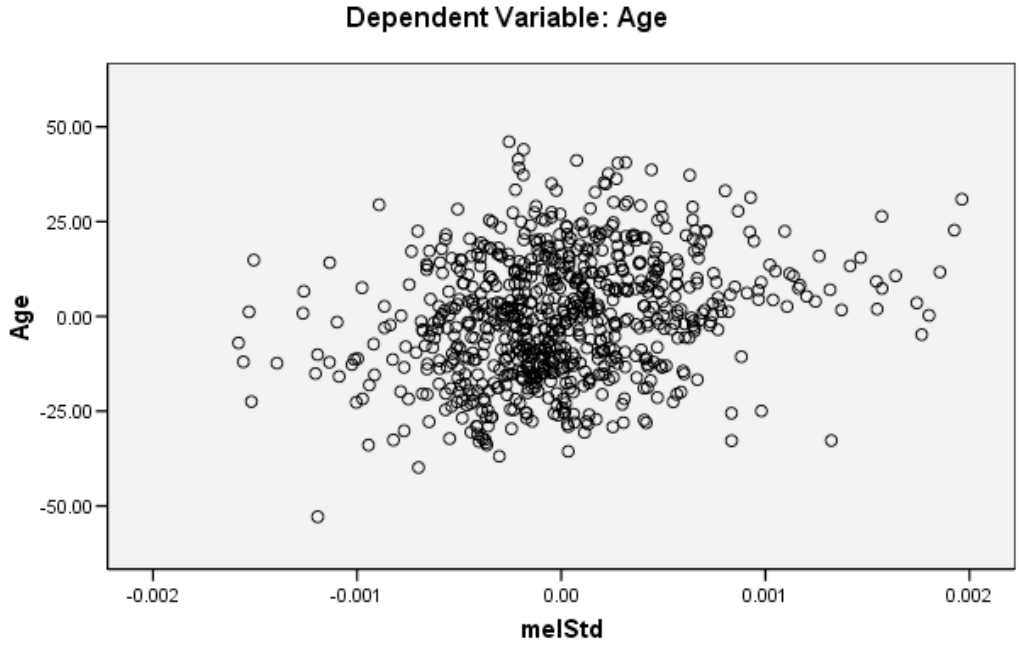

Fig D6 Partial regression plot mel std

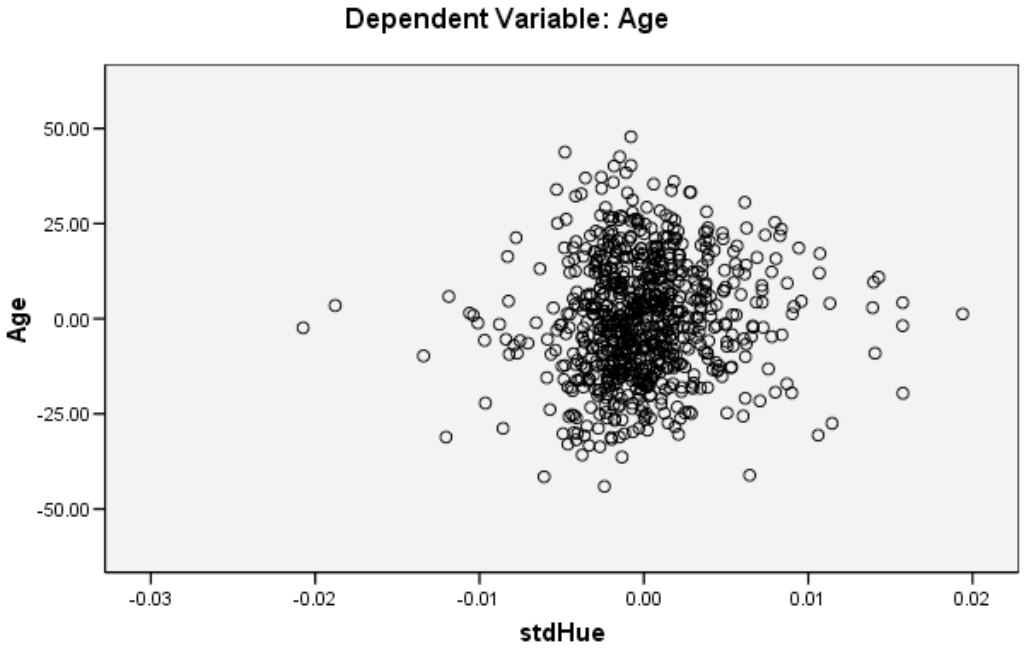

Fig D7 Partial regression plot std Hue

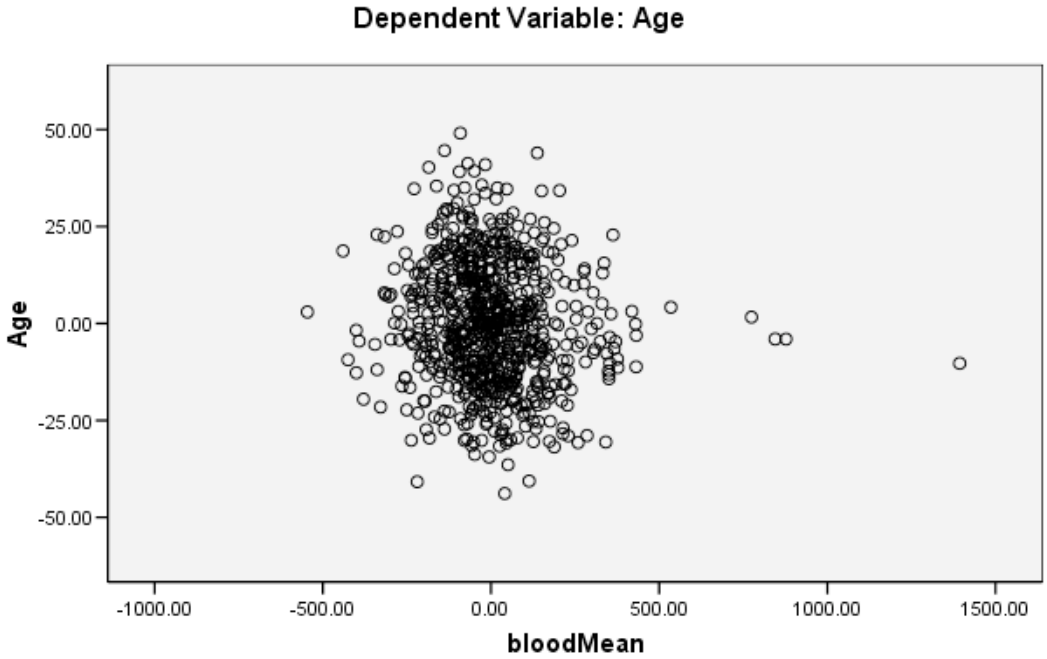

Fig D8 Partial regression plot blood mean

ANOVA[i]

Model		Sum of Squares	df	Mean Square	F	Sig.
1	Regression	82747.056	1	82747.056	272.707	.000[a]
	Residual	230302.0	759	303.428		
	Total	313049.1	760			
2	Regression	98616.454	2	49308.227	174.300	.000[b]
	Residual	214432.6	758	282.893		
	Total	313049.1	760			
3	Regression	108993.8	3	36331.276	134.781	.000[c]
	Residual	204055.3	757	269.558		
	Total	313049.1	760			
4	Regression	113494.0	4	28373.509	107.491	.000[d]
	Residual	199555.1	756	263.962		
	Total	313049.1	760			
5	Regression	116846.8	5	23369.355	89.927	.000[e]
	Residual	196202.3	755	259.871		
	Total	313049.1	760			
6	Regression	123256.0	6	20542.668	81.611	.000[f]
	Residual	189793.1	754	251.715		
	Total	313049.1	760			
7	Regression	124944.2	7	17849.165	71.452	.000[g]
	Residual	188104.9	753	249.807		
	Total	313049.1	760			
8	Regression	126510.9	8	15813.859	63.751	.000[h]
	Residual	186538.2	752	248.056		
	Total	313049.1	760			

a. Predictors: (Constant), stdHue

b. Predictors: (Constant), stdHue, freckleEccentricityRange

c. Predictors: (Constant), stdHue, freckleEccentricityRange, bloodFourierSectionMean32

d. Predictors: (Constant), stdHue, freckleEccentricityRange, bloodFourierSectionMean32, bloodFourierSectionMean652

e. Predictors: (Constant), stdHue, freckleEccentricityRange, bloodFourierSectionMean32, bloodFourierSectionMean652, melStd

f. Predictors: (Constant), stdHue, freckleEccentricityRange, bloodFourierSectionMean32, bloodFourierSectionMean652, melStd, melFourierSectionMean2

g. Predictors: (Constant), stdHue, freckleEccentricityRange, bloodFourierSectionMean32, bloodFourierSectionMean652, melStd, melFourierSectionMean2, maxHue

h. Predictors: (Constant), stdHue, freckleEccentricityRange, bloodFourierSectionMean32, bloodFourierSectionMean652, melStd, melFourierSectionMean2, maxHue, bloodMean

i. Dependent Variable: Age

Table D4 ANOVA statistics

Table D5 Correlation matrix

Correlations

		Age	melStd	stdHue	bloodMean	mean Freckle Eccentricity	bloodFourier Section Mean32	bloodFourier Section Mean652	melFourier SectionMean2	maxHue
Pearson Correlation	Age	1.000	.382	.514	.414	.266	.445	-.353	.351	.288
	melStd	.382	1.000	.465	.420	.222	.434	-.060	-.122	.144
	stdHue	.514	.465	1.000	.759	.179	.546	-.557	.439	.378
	bloodMean	.414	.420	.759	1.000	-.014	.481	-.713	.330	.394
	meanFreckleEccentricity	.266	.222	.179	-.014	1.000	.107	-.108	.170	.020
	bloodFourierSection Mean32	.445	.434	.546	.481	.107	1.000	-.173	.286	.213
	bloodFourierSection Mean652	-.353	-.060	-.557	-.713	-.108	-.173	1.000	-.328	-.363
	melFourierSectionMean2	.351	-.122	.439	.330	.170	.286	-.328	1.000	.243
	maxHue	.288	.144	.378	.394	.020	.213	-.363	.243	1.000
Sig. (1-tailed)	Age	.	.000	.000	.000	.000	.000	.000	.000	.000
	melStd	.000	.	.000	.000	.000	.000	.050	.000	.000
	stdHue	.000	.000	.	.000	.000	.000	.000	.000	.000
	bloodMean	.000	.000	.000	.	.352	.000	.000	.000	.000
	meanFreckleEccentricity	.000	.000	.000	.352	.	.002	.001	.000	.290
	bloodFourierSection Mean32	.000	.000	.000	.000	.002	.	.000	.000	.000
	bloodFourierSection Mean652	.000	.050	.000	.000	.001	.000	.	.000	.000
	melFourierSectionMean2	.000	.000	.000	.000	.000	.000	.000	.	.000
	maxHue	.000	.000	.000	.000	.290	.000	.000	.000	.
N	Age	761	761	761	761	761	761	761	761	761
	melStd	761	761	761	761	761	761	761	761	761
	stdHue	761	761	761	761	761	761	761	761	761
	bloodMean	761	761	761	761	761	761	761	761	761
	meanFreckleEccentricity	761	761	761	761	761	761	761	761	761
	bloodFourierSection Mean32	761	761	761	761	761	761	761	761	761
	bloodFourierSection Mean652	761	761	761	761	761	761	761	761	761
	melFourierSectionMean2	761	761	761	761	761	761	761	761	761
	maxHue	761	761	761	761	761	761	761	761	761

Descriptive Statistics

	Mean	Std. Deviation	N
Age	53.3903	20.29548	761
melStd	.0027	.00075	761
stdHue	.0217	.00705	761
bloodMean	968.9013	342.92865	761
meanFreckleEccentricity	.5788	.33153	761
bloodFourierSection Mean32	4.8030	.36755	761
bloodFourierSection Mean652	3.4724	.26364	761
melFourierSectionMean2	7.4536	.60666	761
maxHue	.5165	.20552	761

Table D6 Descriptive statistics

Casewise Diagnostics[a]

Case Number	Std. Residual	Age	Predicted Value	Residual
463	3.049	88.00	39.9234	48.07657

a. Dependent Variable: Age

Table D7 Casewise diagnostic of the residual

Residuals Statistics[a]

	Minimum	Maximum	Mean	Std. Deviation	N
Predicted Value	24.9117	91.7758	53.3903	12.88156	761
Residual	-43.39899	48.07657	.00000	15.68350	761
Std. Predicted Value	-2.211	2.980	.000	1.000	761
Std. Residual	-2.753	3.049	.000	.995	761

a. Dependent Variable: Age

Table D8 Temporary variables used in SPSS calculation of residual statistics

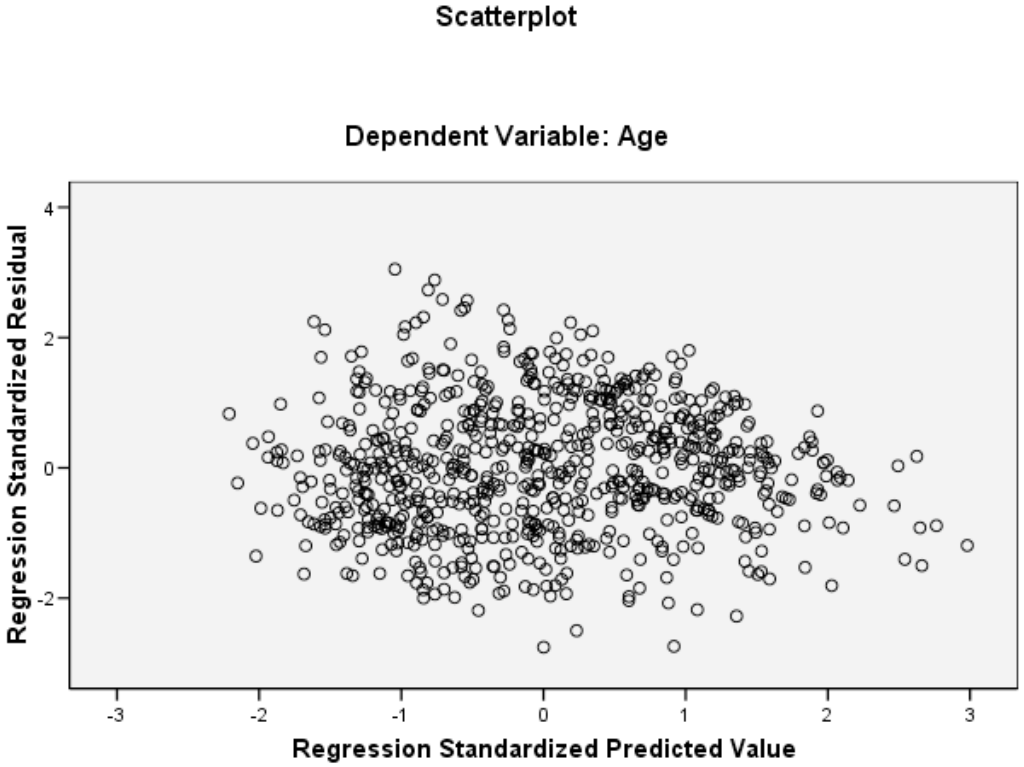

Fig D9 Scatterplot of the variability of the residuals

Model Summary

Model	R	R Square	Adjusted R Square	Std. Error of the Estimate	Change Statistics				
					R Square Change	F Change	df1	df2	Sig. F Change
1	.514[a]	.264	.263	17.41919	.264	272.707	1	759	.000
2	.561[b]	.315	.313	16.81941	.051	56.097	1	758	.000
3	.590[c]	.348	.346	16.41822	.033	38.498	1	757	.000
4	.602[d]	.363	.359	16.24690	.014	17.049	1	756	.000
5	.611[e]	.373	.369	16.12050	.011	12.902	1	755	.000
6	.627[f]	.394	.389	15.86553	.020	25.462	1	754	.000
7	.632[g]	.399	.394	15.80529	.005	6.758	1	753	.010
8	.636[h]	.404	.398	15.74980	.005	6.316	1	752	.012

a. Predictors: (Constant), stdHue

b. Predictors: (Constant), stdHue, freckleEccentricityRange

c. Predictors: (Constant), stdHue, freckleEccentricityRange, bloodFourierSectionMean32

d. Predictors: (Constant), stdHue, freckleEccentricityRange, bloodFourierSectionMean32, bloodFourierSectionMean652

e. Predictors: (Constant), stdHue, freckleEccentricityRange, bloodFourierSectionMean32, bloodFourierSectionMean652, melStd

f. Predictors: (Constant), stdHue, freckleEccentricityRange, bloodFourierSectionMean32, bloodFourierSectionMean652, melStd, melFourierSectionMean2

g. Predictors: (Constant), stdHue, freckleEccentricityRange, bloodFourierSectionMean32, bloodFourierSectionMean652, melStd, melFourierSectionMean2, maxHue

h. Predictors: (Constant), stdHue, freckleEccentricityRange, bloodFourierSectionMean32, bloodFourierSectionMean652, melStd, melFourierSectionMean2, maxHue, bloodMean

Table D9 Model summary statistics

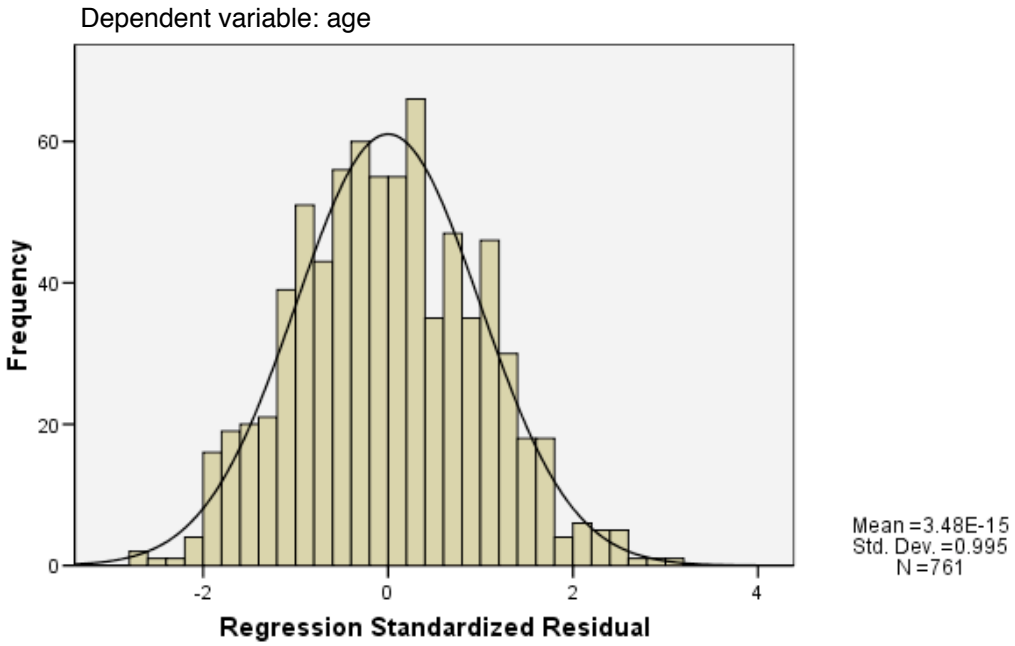

Fig D10 Histogram of distribution of the residuals

Fig D11 Normal P-P plot of regression standardized residuals

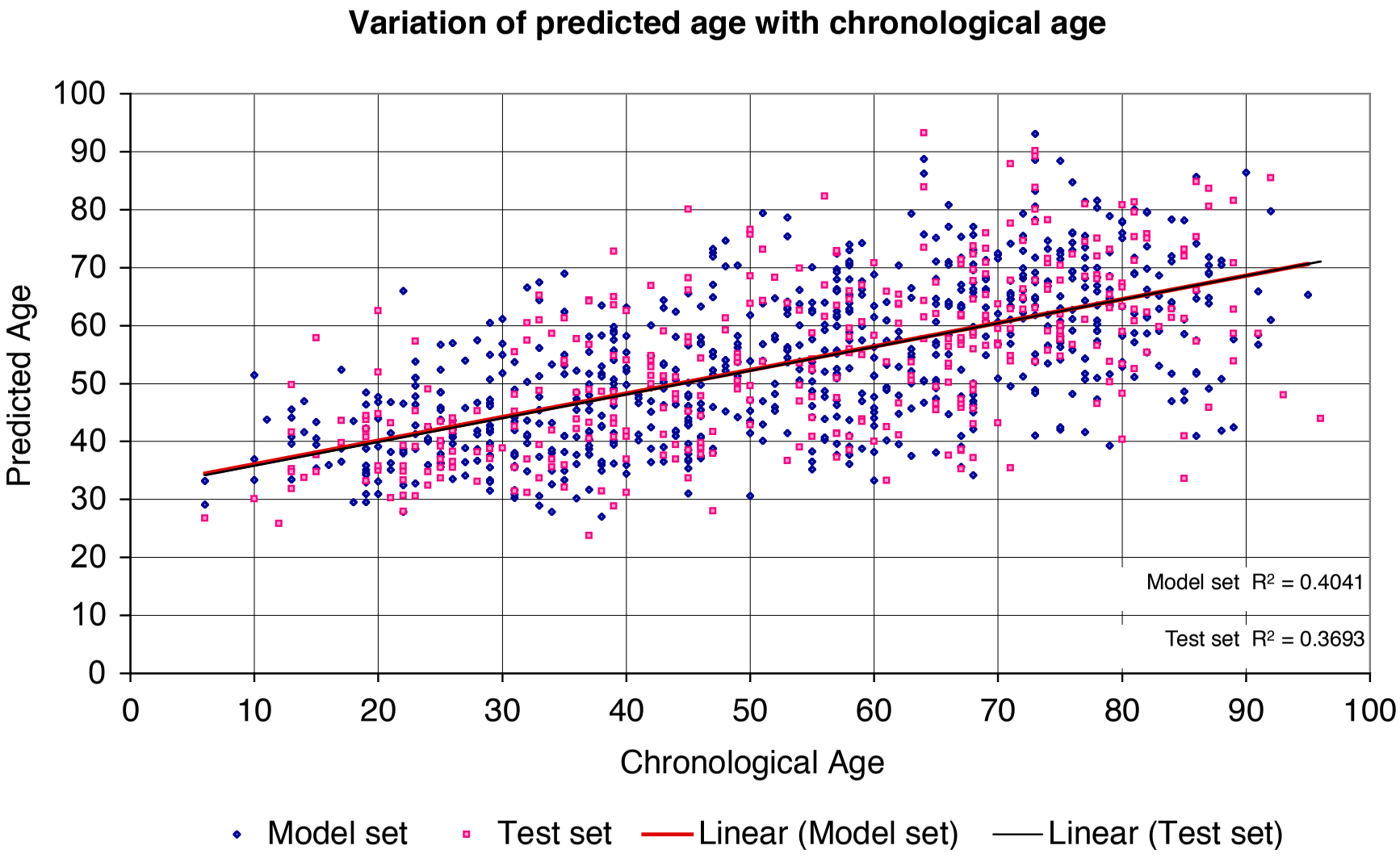

Fig D12 Plot of the model and test sets with line of best fit

Appendix E

The theory of Spectrophotometric Intracutaneous Analysis

The formation of a predictive model of human skin is a complex interaction between the architectural and chromophore effects of the skin on light in both the epidermis and dermis.

The epidermal model

Light moving through the epidermis is either reflected or absorbed by melanin. Any scattering occurring in this layer is forward scattering and is so small as to be best described as negligible.
Therefore, Bouger's law can be used to describe the attenuation of light by melanin in this situation:

$$\theta(\lambda,d_m) = e^{-dm(\lambda)}$$

- where $\theta(\lambda,d_m)$ is the ratio of transmitted radiation to incident radiation at a given wavelength and path length, d is the path length and $m(\lambda)$ is the spectral absorptivity of the material.

The intensity of light remitted from the epidermis because of epidermal melanin, S_e, can be shown as:

$$S_e = \theta(\lambda,d_m)s(\lambda)$$

- where $s(\lambda)$ is the intensity of the incident light against wavelength.[187]

The dermal model

The distinct architectural difference in the papillary and reticular dermis means that any predictive model of the dermis must account for both the scattering of light produced by the collagen of the papillary dermis and absorption by the

chromophores, as previously discussed. The Kubelka-Munk theory has often been used to describe the passage of light through the skin. It describes the remittance and transmittance of radiation through an absorbing and scattering medium.

It assumes that both the incident radiation is diffuse and that the material is not homogenous, with the particles being small in comparison to the thickness of the said material. This theory can be applied to the skin since the stratum corneum renders incident light diffuse and the collagen fibrils are tiny in comparison to the thickness of the dermis.

The theory divides a sample of radiation into two opposing fluxes, where I is the radiant flux in the direction of increasing sample depth, d, and J is the returning flux as a result of scattering up to the depth d. The remittance, R, and the transmittance, T, can be expressed as:

$$R = \frac{J_0(d)}{I_0} \qquad and \qquad T = \frac{I(d)}{I_0}$$

To calculate R and T for a given material, the depth d, the fraction of radiation absorbed, α, and the fraction of radiation scattered per unit length of tissue, ζ, must be known. The constants α and ζ were calculated experimentally by Anderson and Parrish, but are wavelength dependent, so R and T are therefore described as

$$R(\lambda,d,\alpha,\zeta) \quad \text{and} \quad T(\lambda,d,\alpha,\zeta).$$

As incident light is spectral, the spectral composition of R and T are:

$$S_R(\lambda) = R(\lambda,d,\alpha,\zeta)I_0(\lambda) \qquad and \qquad S_T(\lambda) = T(\lambda,d,\alpha,\zeta)I_0(\lambda)$$

These describe a two layer system that can be extended for a system of n layers and provided the thickness and composition of the layers are specified, the total remitted, $S_R(\lambda)$, and transmitted, $S_T(\lambda)$, light can be computed.

This model can be used to predict values of chosen primaries, such as red, green and blue (RGB):

$$r = \int_0^\infty R(\lambda,d,\alpha,\zeta)I_0(\lambda)S_r(\lambda)d(\lambda)$$

$$g = \int_0^\infty R(\lambda,d,\alpha,\zeta)I_0(\lambda)S_g(\lambda)d(\lambda)$$

$$b = \int_0^\infty R(\lambda,d,\alpha,\zeta)I_0(\lambda)S_b(\lambda)d(\lambda)$$

Other variables, such as bilirubin, oxy- and deoxyhaemoglobin can be factored into the equation so that a comprehensive model of light interaction with skin can be created.

The overall model of the interaction of light with the skin is a prediction of the transmittance of light through the epidermis, with some wavelength specific absorption by chromophores, the wavelength specific remittance by collagen in the papillary dermis and the absorption of this remitted light back through the epidermis. As light scattering in the epidermis is negligible, the Kubelka-Munk theory gives way to Bouger's law, meaning all calculations are relative to the dermal-epidermal junction. This is important when considering images with relevance to the dermal components of the skin.

Generating the SIAscans

It is now possible to plot all the possible values of the three colour primaries and in so doing, simulate changes in blood and melanin. This way a curved surface graph can be produced which demonstrates all the possible colours of normal human skin on a melanin and blood axis.

Each point on the surface of this plane will identify the unique combination of blood and melanin making up the colour of the skin at that point. A 3-dimensional colour space (with all the possible combinations of Red, Green and Blue) can now be represented as a 2-dimensional feature space (as all the possible combinations of blood and melanin).

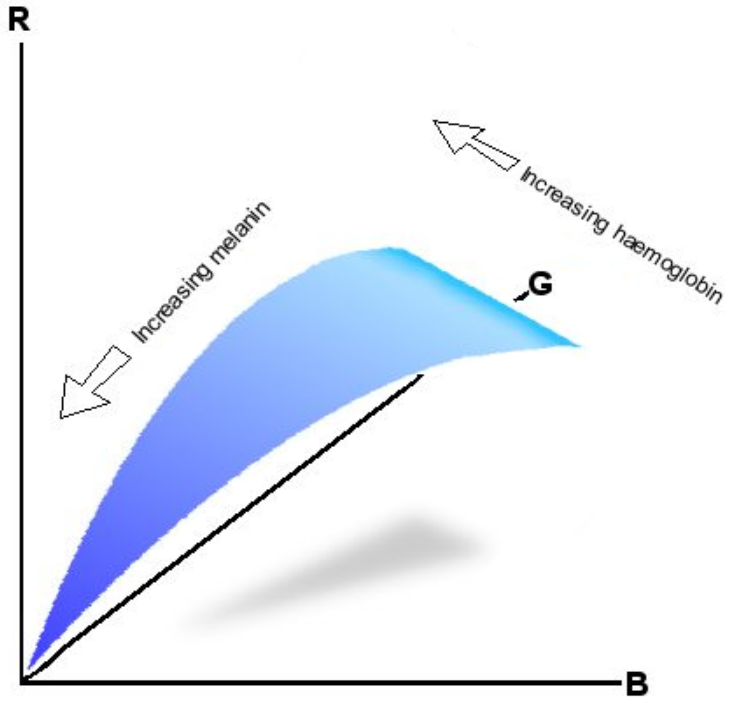

Fig E1 Graph showing all possible colours of skin in RGB colour space

This means the initial image of the skin can be displayed as two separate images, each showing the value of either blood or melanin.

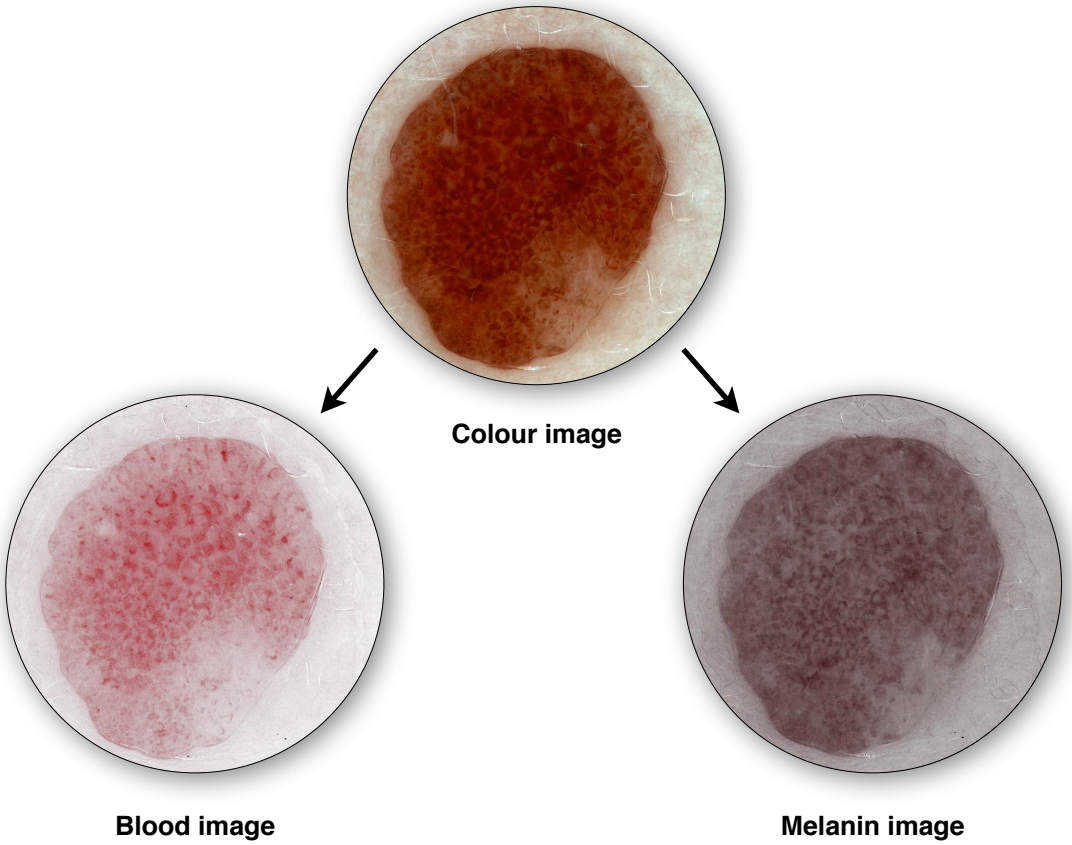

Fig E2 Colour image separated into blood and melanin components

The presence of melanin in the dermis (as with melanomas, blue naevi or melanophages) produces an abnormal skin colour plane towards the blue and green primaries. As it does not have any intersection with the plane of normal skin, it becomes impossible to quantify how much each component contributes to the overall colour of the skin, though it can be concluded that 'an amount' of dermal melanin is present.

Therefore, areas of dermal melanin can be identified as not existing in the planar surface of normal skin, allowing separation of the image into areas with epidermal and dermal melanin (Fig E3).

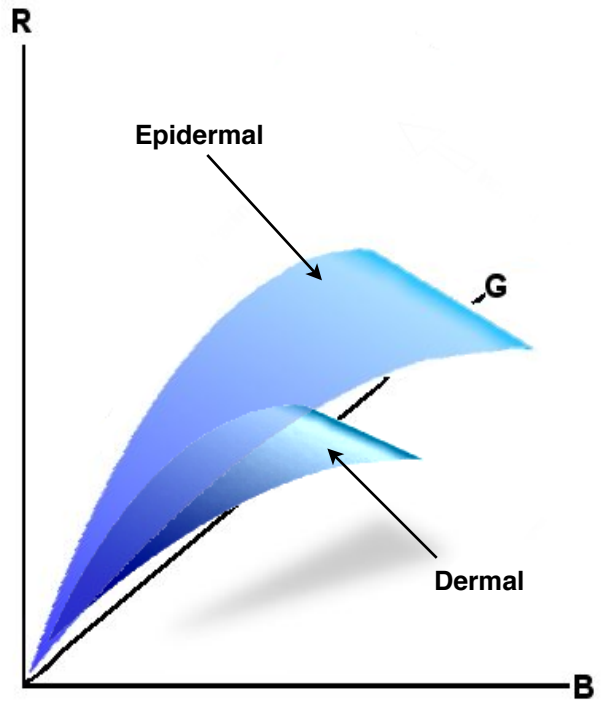

Fig E3 Graph showing the separate epidermal and dermal skin planes

Experimental attempts to use colour analysis alone to identify dermal melanin were unsuccessful and this was due to the fact that the skin model generated assumed that the thickness of the papillary dermis was a constant 200μm, whereas in real life it varies with different lesions and different areas of the body.[187]

As mentioned earlier, collagen remits light depending on the wavelength of light and the thickness of the dermis. Blue light is remitted at all thicknesses of collagen, whereas more red light is transmitted than remitted as the collagen layer becomes thinner. This would mean that skin with a thin papillary dermis is darker and more blue than skin with a thicker papillary dermis, which would appear brighter and more red.

To accommodate the variation in thickness of the papillary dermis in real skin, the model must be extended into the infra-red spectrum to measure the thickness of the papillary dermis. Between 600-800nm the absorption of melanin is approximately one tenth to one hundredth of its maximum compared

with the visible spectrum, with the remittance of light becoming more sensitive to papillary thickness. From 800-1000nm, melanin absorption is considerably less, such that papillary dermal thickness is the most significant element in skin colour.

This means a graph can be plotted for these primary wavelengths against varying papillary dermal thickness, allowing a non-invasive measurement of papillary dermal thickness related to its collagen content. The result of this is that the model of skin colour can now be standardised for a specific lesion or area of skin and an image of the underlying collagen architecture can also be produced.

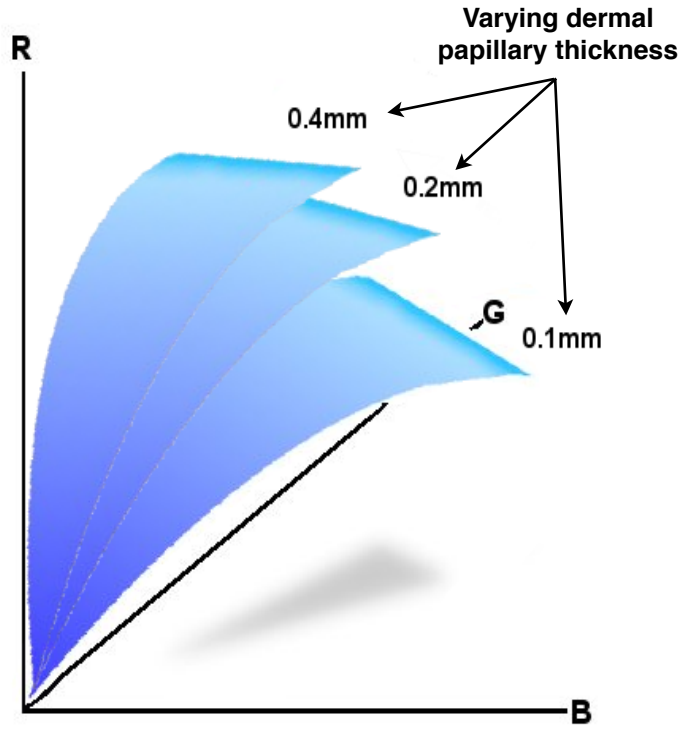

Fig E4 Graph showing the effect of altering papillary dermal thickness on the skin plane

References

1. Jinbow K, Fitzpatrick TB, Wick MM. Biology and physiology of melanin pigmentation. In: Goldsmith LA. (ed.) Physiology, biochemistry and molecular biology of the skin, 2nd edition New York : Oxford University Press. 1991, pp 873-909

2. Fitzpatrick TB. Ultra-violet induced pigmentary changes: benefits and hazards. *Curr Probl Dermatol.* 1986; 15: 25-38

3. Obata M, Tagami HJ. Alteration in murine epidermal Langerhans' cell populations by various UV irradiations, quantative and morpheologic studies on the effects of various wavelengths of monochromatic radiation on Ia-bearing cells. *J Invest Dermatol.* 1985; 84: 139-145

4. Tachibana T. The Merkel cell: recent findings and unresolved problems. *Arch Histol Cytol.* 1995; 58: 379-396

5. Lacour JP, Dubois D, Pisani A, et al. Anatomical mapping of Merkel cells in normal human adult epidermis. *Br J Dermatol.* 1991; 125: 535-542

6. Moll I, Bladt U, Jung EG. Presence of Merkel cells in sun-exposed and not sun-exposed skin: a quantitative study. *Arch Dermatol Res. 1990;* 282: 213-216

7. Moll R, Moll I, Franke WW. Identification of Merkel cells in human skin by specific cytokeratin antibodies: changes of cell density and distribution in fetal and adult plantar epidermis. *Differentiation*. 1984; 28: 136-154

8. Fitzpatrick TB. The validity and practicality of sun-reactive types I through VI. *Arch Dermatol.* 1988 Jun; 124(6): 869-871

9. Valverde P, Healy E, Jackson I, et al. Variants of the melanocytic stimulating hormone receptor gene are associated with red hair and fair skin in humans. *Nat Genet.* 1995; 11: 328-330

10. Pathak MA, Sinesi SJ, Szabo G. The effect of a single dose of ultraviolet radiation on epidermal melanocytes. *J Invest Dermatol.* 1965 Dec; 45(6): 520-528

11. Potten CS, Morris RJ. Epidermal stem cells in vitro. *J Cell Sci (Suppl).* 1988; 10: 45-62

12. Lavker RM, Sun T-T. Epidermal stem cells: Properties, markers and location. *Proc Natl Acad Sci USA.* 2000; 97: 13473-13475

13. Prockop DJ, Kivirikko KL, Tuderman L, et al. The biosynthesis of collagen and its disorders. Part 1. *New Eng J Med.* 1979; 301: 13-23

14. Holbrook KA. Melanocytes in human embryonic skin and fetal skin: Review and new findings. *Pigment Cell Red.* 1998; 1(suppl.): 6-17

15. Ortonne J-P. Photoprotective properties of skin melanin. *Br J Dermatol.* 2002; 146: 7-10

16. Toews GB, Bergstresser PR, Streilein JW, et al. Epidermal Langerhan's cell density determines whether contact hypersensitivity or unresponsiveness follows skin painting with DNFB. *J Immunol.* 1979; 124: 445-453

17. Botek AA, Lookingbill DP. The structure and function of sebaceous glands. In: Freinkel RK, Woodley DT (eds) The Biology of the Skin. New York : Parthenon publishing. 2002, pp 87-100

18. Hurley HJ. The eccrine sweat glands: Structure and function. In: Freinkel RK,Woodley DT (eds) The Biology of the Skin. New York : Parthenon publishing. 2002 pp 47-76

19. Robertshaw D. Apocrine sweat glands. In: Goldsmith LA. (ed) Physiology, biochemistry and molecular biology of the skin. 2nd edition. New York : Oxford University Press. 1991, pp 763-775

20. Wenstrup RJ, Murad S, Pinnell SR. Collagen. In: Goldsmith LA. (ed) Physiology, biochemistry and molecular biology of the skin. 2nd edition. New York : Oxford University Press. 1991, pp 481-508

21. Uitto J, Fazio M, Bashir M, et al. Elastic fibres of the connective tissue. In: Goldsmith LA. (ed) Physiology, biochemistry and molecular biology of the skin. 2nd edition. New York : Oxford University Press. 1991, pp 530-557

22. McKee PH, Calonje E, Granter SR. The structure and function of skin. In: McKee PH, Calonje E, Granter SR (eds) Pathology of the skin Vol 1. Third edition. Elsevier Mosby USA. 2005, p 32

23. Restrepo R, McKee PH, Calonje E. Diseases of the hair. In: McKee PH, Calonje E, Granter SR (eds) Pathology of the skin Vol 2. Third edition. Elsevier Mosby USA. 2005, p 1063-1066

24. Longley BJ, Scher RK. Diseases of the nails. In: McKee PH, Calonje E, Granter SR (eds) Pathology of the skin Vol 2. Third edition. Elsevier Mosby USA. 2005, p1127-1129

25. Braverman LM. Ultrastructure and organisation of the cutaneous microvasculature in normal and pathologic states. *J Invest Dermatol*. 1989; 93: 25-95

26. Kranning KK. Temperature regulation and the skin. In: Goldsmith LA. (ed) Physiology, biochemistry and molecular biology of the skin. 2nd edition. New York : Oxford University Press. 1991, pp 1085-1098

27. Ryan TJ. Structure and function of lymphatics. *J Invest Dermatol.* 1989; 93: 18s-24s

28. McKee PH, Calonje E, Granter SR. The structure and function of skin. In: McKee PH, Calonje E, Granter SR (eds) Pathology of the skin Vol 1. Third edition. Elsevier Mosby USA. 2005, p 35-36

29. McKee PH, Calonje E, Granter SR (eds) Pathology of the skin Vol 1 & 2. Third edition. Elsevier Mosby USA. 2005

30. Rhodes AR, Albert LS, Barnhill RL, et al. Sun-induced freckles in children and young adults. A correlation of clinical and histopathologic features. *Cancer.* 1992; 67: 1990-2001

31. Bhawan J. Lentigo. *Int J Dermatol.* 1996; 35: 229-239

32. Holly EA, Kelly JW, Shpall SN, et al. Number of melanocytic naevi as a major risk factor for melanoma. *BMJ .*1986; 292: 1555-1539

33. Nichols EM. Development and elimination of pigmented moles and the anatomical distribution of melanoma. *Cancer.* 1973; 32: 191-195

34. McKee PH, Calonje E, Granter SR. Melanocytic nevi. In: McKee PH, Calonje E, Granter SR (eds) Pathology of the skin Vol 2. Third edition. Elsevier Mosby USA. 2005, pp 1250-1259

35. Fallowfield ME, Collins G, Cook MG. Melanocytic lesions of the palm and sole. *Histopathology.* 1994; 24: 463-467

36. Copeman PWM, Lewis MG, Philips TM, et al. Immunological associations of the halo nevus with cutaneous melanoma. *Br J Dermatol.* 1973; 88: 127-137

37. Gonzales-Campora R, Galera-Davidson H, Vasquez-Ramirez FJ, et al. Blue naevus: Classical types and new related entities. *Pathol Res Pract.* 1994; 190: 627-634

38. Casso EM, Grin-jorgensen CM, Grant-Kels JM. Spitz Nevus. *J Am Acad Dermatol.* 1992; 27: 901-913

39. Barnhill RL, Flotte TJ, Fleischli M, et al. Cutaneous melanoma and atypical spitz tumours in childhood. *Cancer.* 1995; 76: 1833-1845

40. Roth ME, Grant-kels JM, Ackerman AB, et al. The histopathology of dyplastic naevi: Continued controversy. *Am J Dermatopathol.* 1991; 13: 38-51

41. Salopek TG, Friedman RJ. Dysplatic nevi. In: Rigel, DS, Freidman, RJ, Dzubow, LM, Reintgen, DS, Bystryn, JC, Marks, R (eds) Cancer of the Skin. Elsevier Saunders. 2005, p 203-219

42. Hoss DM, Grant-kels JM.Significant melanocytic lesions in infancy, childhood and adolescence. *Dermatol Clin.* 1986; 4: 29-44

43. Marghoob AA. Congenital melanocytic nevi. In: Rigel, DS, Freidman, RJ, Dzubow, LM, Reintgen, DS, Bystryn, JC, Marks, R (eds) Cancer of the Skin. Elsevier Saunders. 2005, p 221-241

44. Mehregan AH, Rahbari H. Benign epithelial tumours of the skin. Part 1: Epidermal tumours. *Cutis.* 1977; 19: 43-48

45. McKee PH, Calonje E, Granter SR. Connective tissue tumours. In: McKee PH, Calonje E, Granter SR (eds) Pathology of the skin Vol 2. Third edition. Elsevier Mosby USA. 2005, pp 1742-1752

46. Jimbow K. Current update and trends in melanin pigmentation and melanin biology. *Keio J Med*. 1995 Mar; 44(1): 9-18

47. Shore RE, Moseson M, Xue X, et al . Skin cancer after x-ray treatment for scalp ringworm. *Radiat Res.* 2002; 157(4): 410-418

48. Shore RE. Radiation induced skin cancers in humans. *Med Pediatr Oncol.* 2001; 36(5): 549-554

49. Stevens A, Spooner D. Malignant melanoma occurring within a previously irradiated area. *Clin Oncol (R Coll Radiol).* 1999; 11(6): 426-428

50. Hensley K, Floyd R.A. Reactive oxygen species and protein oxidation in aging: A look back, a look ahead. *Archives of Biochemistry and Biophysics*. 2002; 397(2): 377-383

51. Marks R, Measurement of biological aging in human epidermis. *Br J Dermatol*. 1981; 104: 627-633

52. Tan CY, Stratham B, Marks R, et al. Skin thickness measurement by pulsed ultrasound: Its reproducibility, validatron and variability. *Br J Dermatol.* 1982; 106: 657-667

53. Quevedo WC, Szabo G, Virks F. Influence of age and IJV on the population of dopa-positive melanocytes in human skin. *J Invest Dermatol.* 1969; 52: 287-290

54. Yaar M, Gilchrest BA. Aging of skin. In: Freedberg IM, Eisen AZ, Wolff K, Austen KF, Goldsmith LA, Katz SI. (eds). Fitzpatrick's dermatology in general medicine, vol 2. McGraw-Hill, New York. 2003, pp 1386-1398

55. Allsop RC, Harley CB, Evidence for a critical telomere length in senescent human fibroblasts. *Exp Cell Res.* 1995; 219: 130-136

56. Arlt W, Hewison M. Hormones and immune function: implications of aging. *Aging Cell.* 2004; 3: 209- 276

57. Swift ME, Burns AL, Gray KL, DiPietro LA. Age-related alterations in the inflammatory response to dermal lnjury. *J Invest Dermatol.* 2001; 117: 1027-1035

58. Schutzer WE, Mader SL. Age-related changes in vascular adrenergic signaling: clinical and mechanistic implications. *Ageing Res Rev.* 2003; 2: 169-190

59. Schneider EL. Aging and cultured human skin fibroblasts. *J Invest Dermatol.* 1979; 73: 15-18

60. Tsiyi T, Hamada T. Age related changes in human dermal elastic fibres. *Br J Dermatol .* 1981; 105: 57-63

61. Lavker RM, Zheng PS, Dong G. Aged skin: a study by light, transmission electron, and scanning electron microscopy. *J Invest Dermatol.* 1987; 88: 44s-51s

62. Kang S, Chung JH, Lee JH, Fisher GJ, Wan YS, Duell EA, et al. Topical N-acetyl cysteine and genistein prevent ultraviolet-light-induced signaling that leads to photoaging in human skin in vivo. *J Invest Dermatol*. 2003; 120(5): 835-841

63. Fisher, G.J., Wang, Z.Q., Datta, S.C., Varani, J., Kang, S., & Voorhees, J.J. Pathophysiology of premature skin aging induced by ultraviolet light. *New Eng J of Med*. 1997; 337(20): 1419-1428

64. Peak, MJ, Peak JG, Carnes, BA. Induction of direct and indirect single strand breaks in human cell DNA by far- and near-ultraviolet radiation: action spectrum and mechanisms. *Photochem Photobiol.* 1987; 45(3): 381-387

65. Scheinfeld. N, DeLeo, VA. Etiological factors in skin cancers: Environmental and biological. In: Rigel, DS, Freidman, RJ, Dzubow, LM, Reintgen, DS, Bystryn, JC, Marks, R (eds) Cancer of the Skin. Elsevier Saunders. 2005, pp 62-65

66. Lei U, Masmas TN, Frentz G. Occupational non-melanoma skin cancer. *Acta Derm Venereol.* 2001; 81(6): 415-417

67. Qu M, Muller HK, Woods GM. Chemical carcinogens and antigens contribute to cutaneous tumour promotion by depleting epidermal Langerhan's cells. *Carcinogenesis*. 1997; 18(6): 1277-1279

68. Simeonova PP, Luster MI. Mechanisms of arsenic carcinogenicity: Genetic or epigenetic mechanisms? *J Environ Pathol Toxicol Oncol.* 2000; 19(3): 281-286

69. Scheinfeld. N, DeLeo, VA. Etiological factors in skin cancers: Environmental and biological. In: Rigel, DS, Freidman, RJ, Dzubow, LM, Reintgen, DS, Bystryn, JC, Marks, R (eds) Cancer of the Skin. Elsevier Saunders. 2005, pp 61-70

70. Kurdina MI, Denisov LE, Vinogradova NN. Groups at high risk for skin cancer. *Vopr Onkol.* 1994; 40: 216-220

71. Dans M, Fakharzadeh SS. Genetic basis of skin cancer. In: Rigel, DS, Freidman, RJ, Dzubow, LM, Reintgen, DS, Bystryn, JC, Marks, R (eds) Cancer of the Skin. Elsevier Saunders. 2005, pp 20-23

72. Edwards MJ, Hirsch RM, Broadwater JR, Netscher DT, Ames FC. Squamous cell carcinoma arising in previously burned or irradiated skin. *Arch Surg.* 1989; 124(1): 115-117

73. Akguner M, Barutcu A, Yilmaz M, Karatas O, Vayvada H. Marjolin's ulcer and chronic burns scarring. *J Wound Care.* 1998; 7(3): 121-122

74. Pierard GE, Kort R, Letawe C. Biomechanical assessment of photodamage. Derivation of a cutaneous extrinsic aging score. *Skin Res & Tech.* 1995; 1: 17-20

75. Serup J. High frequency ultrasound examination of aged skin : Intrinsic, actinic and gravitational aging, including new concepts of stasis dermatitis and by ulcer. In: J Leveque (ed) Aging Skin. Properties and Functional Changes. Marcel Dekker : New York. 1993, pp 69

76. Marcen R, Pascual J, Tato AM, Teruel JL, Villafruela JJ, Fernandez M, Tenorio M, Burgos FJ, Ortuno J. Influence of immunosuppression on the prevalence of cancer after kidney transplantation. *Transplant Proc*. 2003 Aug; 35(5): 1714-1716

77. Wei Q, Matanoski GM, Farmer ER, Hedayati MA, Grossman L. DNA repair and aging in basal cell carcinoma: A molecular epidemiology study. *Proc Natl Acad Sci USA.* 1993; 90: 1614-1618

78. Katara G, Hemvani N, Chitnis S, Chitnis V, Chitnis DS. Surface disinfection by exposure to germicidal UV light. *Indian J Med Microbiol.* 2008 Jul-Sep; 26(3): 241-242

79. Kligman LH. Intensification of ultraviolet induced dermal damage by infrared radiation. *Arch Dermatol Res*. 1982; 272: 229

80. Yin L, Morita A, Tsuji T. Skin premature aging induced by tobacco smoking: The objective evidence of skin replica analysis. *J Dermatol Sci*. 2001; 27 (supp 1): s26-s31

81. Yin L, Morita A, Tsuji T. Tobacco smoking: A role in premature skin aging. *Nagoya Med J*. 2000; 43: 165-171

82. Lahmann C, Bergemann J, Harrision G, Young AR. Matrix metalloprotease-1 and skin aging in smokers. *Lancet*. 2001; 357: 935-936

83. Boyd AS, Stasko T, King LE Jr, Cameron GS, Pearse AD, Gaskell SA. Cigarette smoking associated elastotic changes in the skin. *J Am Acad Dermatol*. 1999; 41: 23-26

84. Valacchi G, Pagnin E, Corbacho AM, Olano E, Davis PA, Packer L, Cross CE. In vivo ozone exposure induced antioxidant/stress-related responses in murine lung and skin. *Free Radic Biol Med*. 2004; 36: 673-681

85. Thiele JJ, Traber MG, Tsang K, Cross CE, Packer L. In vivo exposure to ozone depletes vitamins C and E and induces lipid peroxidation in epidermal layers of murine skin. *Free Radic Biol Med.* 1997; 23: 385-391

86. Lovell C, Plastow SR, Russell-Jones R, et al. Collagen and elastin in actinic elastosis. *J Invest Dermatol.* 1984; 82: 566

87. Chen V, Fleischmajer R, Schwartz E, et al. Immunohistochemistry of elastotic material in sun damaged skin. *J Invest Dermatol.* 1986; 87: 334-337

88. Albrecht S, From L, Kahn, HJ. Lysosyme in abnormal dermal elasetic fibres of cutaneous aging, solar elastosis and pseudoxanthoma elasticum. *J Cut Path.* 1991; 18: 75-81

89. Talwar HS, Griffiths CE, Fisher GJ, Hamilton TA, Voorhees JJ. Reduced type I and type III pre-collagens in photodamaged adult human skin. *J Invest Dermatol*. 1995; 105: 285-290

90. Oxholm A, Oxholm P, Staberg, et al. Immunohistological detection of interleukin 1-like molecules and tumour necrosis factor in human epidermis before and after UVB irradiation in vivo. *Br J Dermatol.* 1988; 118: 493-503

91. Braverman IM, Fonferko E. Studies in cutaneous aging: II. The microvaculature. *J Invest Dermatol.* 1982; 78: 444-448

92. Bielenberg DR, Bucana CD, Sanchez R, Donawho CK, Kripke ML, Fidler IJ. Molecular regulation of UVB-induced angiogenesis. *J Invest Dermatol.* 1998; 111: 864-872

93. Yaar M. Clinical and histological manifestations of photodamaged skin. In: Gilchrest BA, Krutmann J (eds) Skin Aging. Springer, Berlin. 2006, p15

94. Lavker RM, Kligman A. Chronic heliodermatitis: A morphologic evaluation of chronic actinic dermal damage with emphasis on the role of mast cells. *J Invest Dermatol.* 1988; 90: 325-330

95. Griffiths CEM, Wang TS, Hamilton TA, et al. A photonumeric scale of the assessment of cutaneous photodamage. *Arch Dermatol*. 1992; 128: 347-351

96. Farr PM, Diffey BL. Quantitative studies on cutaneous erythema induced by ultraviolet radiation. *Br J Dermatol.* 1984; 111: 673-682

97. Cox NH, Eedy DJ, Morton CA. Guidelines for management of Bowen's disease. *Br J Dermatol.* 1999; 141: 633-641

98. Peterka ES, Lynch FW, Goltz RW. An association between Bowen's disease and cancer. *Arch Dermatol*. 1961; 84: 623-629

99. Kao GF. Carcinoma arising in Bowen's disease. *Arch Dermatol*. 1986; 122: 1124-1126

100. Thissen MR, Nieman FH, Ideler AH, et al. Cosmetic results of cryotherapy versus surgical excision for primary uncomplicated basal cell carcinomas of the head and neck. *Dermatol Surg*. 2000; 26: 759-764

101. Mikhail GR, Mohs FE. Mohs micrographic surgery. Philadelphia: W.B. Saunders. 1991, p 13

102. Gray DT, Suman VJ, Su WP, Clay RP, Harmsen WS, Roenigk RK. Trends in the population-based incidence of squamous cell carcinoma of the skin first diagnosed between 1984 and 1992. *Arch Dermatol*. 1997 Jun; 133(6): 735-470

103. Ramsay HM, Fryer AA, Hawley CM, et al. Non-melanoma skin cancer risk in the Queensland renal transplant population. *Br J Dermatol.* 2002; 147(5): 950–956

104. Staples MP, Elwood M, Burton RC, et al. Non-melanoma skin cancer in Australia: The 2002 national survey and trends since 1985. *Med J Aust.* 2006; 184(1): 6–10

105. Moloney FJ, Comber H, O'Lorcain P, et al. A population-based study of skin cancer incidence and prevalence in renal transplant recipients. *Br J Dermatol.* 2006; 154(3): 498–504

106. Jermal A, Tiwari RC, Murray T, et al. Cancer statistics 2004. *CA Cancer J Clin.* 2004; 54: 8-29

107. Elwood JM, Jopson J. Melanoma and sun exposure: An overview of published studies. *International J of Cancer.* 1997; 73: 198-203

108. Gruber SB, Barnhill RL, Stenn KS, et al. Nevomelanocytic proliferation in association with cutaneous melanoma: A multivariate analysis. *J Am Acad Dermatol*. 1989; 21: 773-780

109. Marks R, Dorevitch AP, Mason G. Do all melanomas come from moles? A study of the histological association between melanocytic nevi and melanoma. *Australas J Dermatol.* 1990; 31: 77-80

110. DeDavid M, Orlow SJ, Provost N, et al. A study of large congenital nevi and associated malignant melanomas: A review of cases in New York University registry and the world literature. *J Am Acad Dermatol.* 1997; 36: 428-433

111. Marks R, Rennie G, Selwood TS. Malignant transformation of solar keratoses to squamous cell carcinoma. *Lancet*. 1988; i: 795-797

112. Glogau RG. The risk of progression to invasive disease. *J Am Acad Dermatol*. 2000; 42(1): 23-24

113. Callen JP. Possible precursors to keratinocytic epidermal malignancies. In: Rigel, DS, Freidman, RJ, Dzubow, LM, Reintgen, DS, Bystryn, JC, Marks, R (eds) Cancer of the Skin. Elsevier Saunders. 2005, p 96-97

114. Miller DL, Weinstock MA. Non-melanoma skin cancer in the United States: Incidence. *J Am Acad Dermatol.* 1994; 30: 774-780

115. Mikhail GR, Nims LP, Kelly AP Jnr, et al. Metastatic basal cell carcinoma. Review, pathogenesis and report of two cases. *Arch Derm.* 1977; 113: 1261-1269

116. Domarus H Von, Steven PJ. Metastatic basal cell carcinoma. Report of five cases and review of 170 cases in the literature. *J Am Acad Dermatol.* 1984; 10: 1043-1060

117. Brody I. Contributions to the histiogenesis of basal cell carcinoma. *J Ultrastruct Res*. 1970; 33: 60-79

118. Kumamkiri M, Hashimoto K. Ultrastructural resemblance of basal cell epithelioma to primary epithelial germ. *J Cutan Pathol.* 1978; 5: 53-67

119. Asada M, Schaart F-M, DeAlmeida HL Jnr, et al. Solid basal cell epithelioma possibly originates from the outer root sheath of the hair follicle. *Acta Derm Venereol (Stockh).* 1993; 73: 286-292

120. Zackheim HS. Origin of the human basal cell epithelioma. *J Invst Dermatol*. 1963; 40: 283

121. Smith OD, Swerdlow MA. Histiogenesis of basal cell epithelioma. *AMA Arch Dermatol*. 1956; 74: 286

122. Kricker A, Armstrong BK, Emglish DR. Does intermittent sun exposure cause basal cell carcinoma? A case control study in Western Australia. *Int J Cancer.* 1995; 60: 489-494

123. Franceschi S, Levi F, Randimbison L, et al. Site distribution of different types of skin cancer. New aetiological clues. *Int J Cancer.* 1996; 67: 24-28

124. Franchimont C, Pierard CE, Cauwenberge DV, et al. Episodic progression and regression of basal cell carcinoma. *Br J Dermatol*. 1982; 106: 305-310

125. Kerr JFR, Searle J. A suggested explanation for the paradoxically slow growth of basal cell carcinomas that contain numerous mitotic figures. *J Pathol*. 1972; 107: 41-44

126. Wolf JE, Hubler WR. Tumour angiogenic factor and human skin tunours. *Arch Dermatol.* 1975; 111: 321-327

127. Vanderveen EE, Grekin RC, et al. Arachidonic metabolites in cutaneous carcinoma. Evidence suggesting that elevated levels of prostaglandins in basal cell carcinomas are associated with a aggressive growth pattern. *Arch Dermatol.* 1986; 122: 407-412

128. Borel DM. Cutaneous basosquamous carcinoma. Review of the literature and report of 35 cases. *Arch Pathol.* 1973; 95: 293-297

129. Brenn T, McKee PH. Tumours of the surface epithelium: Basal cell carcinoma. In: McKee PH, Calonje E, Granter SR (eds) Pathology of the skin Vol 2. Third edition Elsevier Mosby USA. 2005, p1173

130. Lang PG, Maize JC Snr. Basal cell carcinoma. In: Rigel, DS, Freidman, RJ, Dzubow, LM, Reintgen, DS, Bystryn, JC, Marks, R (eds) Cancer of the Skin. Elsevier Saunders. 2005, pp 114-117

131. Marcil I, Stern RS. Risks of developing a subsequent non-melanoma skin cancer in patients with a history of non-melanoma skin cancer: A critical review of the literature and meta-analysis. *Arch Dermatol.* 2000; 136: 1524-1530

132. Nguyen TH, Yoon J. Squamous cell carcinoma. In: Rigel, DS, Freidman, RJ, Dzubow, LM, Reintgen, DS, Bystryn, JC, Marks, R (eds) Cancer of the Skin. Elsevier Saunders. 2005, p 136-145

133. Fu W, Cockerell CJ. The actinic (solar) keratosis: A 21st-century perspective. *Arch Dermatol.* 2003; 139: 66-70

134. Marks R, Foley P, Goodman G, Hage BH, Selwood TS. Spontaneous remission of solar keatoses: The case for conservative management. *Br J Dermatol.* 1986; 115: 649-655

135. Mora RG, Perniciaro C. Cancer of the skin in blacks 1. A review of 163 black patients with cutaneous squamous cell carcinoma. *J Am Acad Dermatol*. 1981; 5: 535-543

136. Dinehart SM, Pollack SV. Metastases from squamous cell carcinoma of the skin and lip. *J Am Acad Dermatol.* 1989; 21: 241-248

137. Rowe DE, Carroll RJ, Day CL. Prognostic factors for local recurrence, metastasis and survival rates in squamous cell carcinoma of the skin, ear and lip. *J Am Acad Dermatol.* 1992; 26: 976-990

138. Breuninger H, Black B, Rassner G. Microstaging of squamous cell carcinomas. *Am J Clin Path.* 1990; 94: 624-627

139. Brenn T, McKee PH. Tumours of the surface epithelium: Variants of squamous cell carcinoma. In: McKee PH, Calonje E, Granter SR (eds) Pathology of the skin Vol 2. Third edition. Elsevier Mosby USA. 2005, p1221-1225

140. Salopek TG, Friedman RJ. Dysplastic nevi. In: Rigel, DS, Freidman, RJ, Dzubow, LM, Reintgen, DS, Bystryn, JC, Marks, R (eds) Cancer of the Skin. Elsevier Saunders. 2005, p 204

141. Di Fronzo LA, Wanek LA, Morton DL. Earlier diagnosis of second primary melanoma confirms the benefits of patient education and routine post-operative follow-up. *Cancer*. 2001; 91: 1520-1524

142. Hayward NK. Genetics of melanoma predisposition. *Oncogene.* 2003; 22: 3053-3062

143. Kefford RF, Newton Bishop JA, Bergman W, Tucker MA. Counseling and DNA testing for individuals perceived to be genetically predisposed to melanoma: A consensus statement of the Melanoma Genetics Consortium. *J Clin Oncol.* 1999; 17: 3245-3251

144. Gallagher RP, Elwood JM, Threlfall WJ, et al. Socioeconomic status, sunlight exposure and risk of malignant melanoma: The Western Canada Melanoma Study. *J Natl Cancer Inst*. 1987; 79: 647-652

145. Elwood JM, Gallagher RP, Hill GB, et al. Cutaneous melanoma in relation to intermittent and constant sun exposure: The Western Canada Melanoma Study. *Int J Cancer.* 1985; 35: 427-433

146. Ackerman AB. Malignant melanoma: A unifying concept. *Hum Pathol*. 1980; 11(6): 591-595

147. Ackerman AB, David KM. A unifying concept of malignant melanoma: Biologic aspects. *Hum Pathol.* 1986; 17(5): 438-440

148. Elder DE, Guerry D 4th, Epstein MN, et al. Invasive malignant melanomas lacking competence for metastasis. *Am J Derm.* 1984; 6(suppl): 55-61

149. Herlyn M, Clark WH, Rodeck U, Mancianti ML, Jambrosic J, Koprowski H. Biology of tumour progression in human melanocytes. *Lab Invest.* 1987; 55(5): 461-474

150. Brenn T, McKee PH. Melanoma. In: McKee PH, Calonje E, Granter SR (eds) Pathology of the skin Vol 2. Third edition. Elsevier Mosby USA. 2005, p1310-1312

151. Cather J, Cather JC, Cockerell CJ. Pathology of melanoma: New concepts. In: Rigel, DS, Freidman, RJ, Dzubow, LM, Reintgen, DS, Bystryn, JC, Marks, R (eds) Cancer of the Skin. Elsevier Saunders. 2005, p 249

152. Heenan PJ. Nodular melanoma is not a distinct entity. *Arch Derm*. 2003; 139(3): 387-388

153. Clark WH Jr, From L, Bernardino EA, et al. The histiogenesis and biologic behaviour of primary human malignant melanomas of the skin. *Cancer Res.* 1969; 29(3): 705-727

154. Breslow A. Thickness, cross-sectional areas and depth of invasion in the prognosis of cutaneous melanoma. *Ann Surg.* 1970; 172(5): 902-908

155. Kelly JW, Sagebiel RW, Clyman S. et al. Thin level IV malignant melanoma. A subset in which level is the major prognostic indicator. *Ann Surg.* 1985; 202(1): 98-103

156. Johnson T M, Sondak VK, Bichakjian CK, Sabel MS. The role of sentinel lymph node biopsy for melanoma: Evidence assessment. *J Am Acad Dermatol.* 2006 Jan; 54(1): 19-27

157. Huang CL, Halpern AC. Management of the patient with melanoma. In: Rigel, DS, Freidman, RJ, Dzubow, LM, Reintgen, DS, Bystryn, JC, Marks, R (eds) Cancer of the Skin. Elsevier Saunders. 2005, p 265-273

158. Friedman RJ. The importance of early detection of melanoma, physician and self-examination. In: Rigel, DS, Freidman, RJ, Dzubow, LM, Reintgen, DS, Bystryn, JC, Marks, R (eds) Cancer of the Skin. Elsevier Saunders. 2005, p 175-176

159. Balch CM, Gershenwald JE, Soong SJ, Thompson JF, Atkins MB, Byrd DR, Buzaid AC, Cochran AJ, Coit DG, Ding S, Eggermont AM, Flaherty KT, Gimotty PA, Kirkwood JM, McMasters KM, Mihm MC Jr, Morton DL, Ross MI, Sober AJ, Sondak VK. Final version of 2009 AJCC melanoma staging and classification. *J Clin Oncol*. 2009 Dec 20; 27(36): 6199-206

160. Cleaver JE. Defective repair replication of DNA in xeroderma pigmentosum. *Nature.* 1986; 218: 652-656

161. Oetting WS, Brilliant MH, King RA. The clinical spectrum of albinism in humans. *Mol Med Today.* 1996; 2:330-335

162. Grayson W, Calonje E, McKee PH. Infectious diseases of the skin: Epidermodysplasia verruciformis. In: McKee PH, Calonje E, Granter SR (eds) Pathology of the skin Vol 1. Third edition. Elsevier Mosby USA. 2005, p847-850

163. Brenn T, McKee PH. Tumours of the surface epithelium: Nevoid basal cell carcinoma syndrome. In: McKee PH, Calonje E, Granter SR (eds) Pathology of the skin Vol 2. Third edition. Elsevier Mosby USA. 2005, p1184-1185

164. Lang PG, Maize JC Snr. Basal cell carcinoma. In: Rigel, DS, Freidman, RJ, Dzubow, LM, Reintgen, DS, Bystryn, JC, Marks, R (eds) Cancer of the Skin. Elsevier Saunders. 2005, pp 103-105

165. Rao B, Lintner R. Adnexal cancers of the skin. In: Rigel, DS, Freidman, RJ, Dzubow, LM, Reintgen, DS, Bystryn, JC, Marks, R (eds) Cancer of the Skin. Elsevier Saunders. 2005, pp 291-302

166. Guillen DR, Cockerell CJ. Sarcomas of the skin. In: Rigel, DS, Freidman, RJ, Dzubow, LM, Reintgen, DS, Bystryn, JC, Marks, R (eds) Cancer of the Skin. Elsevier Saunders. 2005, pp 311-322

167. Niedt G. Paget's disease. In: Rigel, DS, Freidman, RJ, Dzubow, LM, Reintgen, DS, Bystryn, JC, Marks, R (eds) Cancer of the Skin. Elsevier Saunders. 2005, pp 303-309

168. Friedman-Kien AE, Cockerell CJ. Neoplastic disorders in HIV infected patients. In: Rigel, DS, Freidman, RJ, Dzubow, LM, Reintgen, DS, Bystryn, JC, Marks, R (eds) Cancer of the Skin. Elsevier Saunders. 2005, pp 339-347

169. Yiengpruksawan A, Coit DG, Thaler HT, et al. Merkel cell carcinoma. Prognosis and management. Arch Surg. 1991; 126(12): 1514-1519

170. Taylor G, Mollick DK, Heilman ER. Merkel cell carcinoma. In: Rigel, DS, Freidman, RJ, Dzubow, LM, Reintgen, DS, Bystryn, JC, Marks, R (eds) Cancer of the Skin. Elsevier Saunders. 2005, pp 323-327

171. Mackie RM. Clinical recognition of early invasive malignant melanoma. *BMJ*. 1990 Nov 3; 301(6759): 1005-1006

172. Mackie RM, Doherty VR. Seven point checklist for melanoma. *Clin and Exp Dermatol.* 1991 Mar; 16(2): 151-153

173. Friedman RJ, Rigel DS, Kapf AW. Early detection of malignant melanoma: the role of physician examination and self-examination of the skin. *CA Cancer J Clin.* 1085; 35(3): 130-151

174. Morton CA, Mackie RM. Clinical accuracy of the diagnosis of malignant melanoma. *Br J Dermatol*. 1998 Feb; 138(2): 283-287

175. Perednia DA, Gaines JA, Rossum AC. Variability in physician assessment of lesions in cutaneous images and its implications for skin screening and computer assisted diagnosis. *Arch Dermatol*. 1992; 128(3): 357-364

176. Claridge E, Hall PN, Keefe M, Allen JP. Shape analysis for classification of malignant melanoma. *J Biomed Eng*. 1992; 14(3): 229-234

177. Steiner A, Pehamberger H, Wolff K. In vivo epiluminescence microscopy of pigmented skin lesions - diagnosis of small pigmented skin lesions and early detection of malignant melanoma. *J Am Acad Dermatol*. 1987; 17(4): 584-591

178. Binder M, Schwarz M, Winkler A, Steiner A, Kaider A, Wolff K, Pehamberger H. Epiluminescence microscopy. A useful tool for the diagnosis of pigmented skin lesions for formally trained dermatologists. *Arch Dermatol*. 1995; 131(3): 286-291

179. Kittler H, Pehamberger H, Wolff K, Binder M. Diagnostic accuracy of dermatoscopy. *Lancet oncol*. 2002 Mar; 3(3): 159-165

180. Welzel J. Optical coherence tomography in dermatology: a review. *Skin Res Technol*. 2001 Feb; 7(1): 1-9

181. Piérard GE, et al. Cyanoacrylate skin surface stripping: an improved approach for distinguishing dysplastic naevi from malignant melanomas. *J of Cut Pathol*. 1988; 16(4): 180-182

182. El Gammal S, Hartwig R, Aygen S, Bauermann T, El Gammal C, Altmeter P. Improved resolution of magnetic resonance microscopy in the examination of skin tumours. *J Invest Dermatol*. 1996; 106(6): 1287-1292

183. Murali R, Thompson JF, Uren RF, Scolyer RA. Fine-needle biopsy of metastatic melanoma: clinical use and new applications. *Lancet Oncol.* 2010 Apr; 11(4): 391-400

184. Shinya O. Realtime image observations with confocal laser-scanning microscopy system. *Igaku No Ayumi*. 1998; 186(5): 345-348 (Japanese)

185. Hughes BR, Black D, Srivastava A, Dalziel K, Marks R. Comparison of techniques for the non-invasive assessment of skin tumours. *Clin and Exp Dermatol.* 2006; 12(2): 108-111

186. Anderson R, Parrish B. The optics of human skin. *J Inv Dermatol.* 1981; 77: 13-19

187. Cotton S. A non-invasive imaging system for assisting in the diagnosis of malignant melanoma. PhD Thesis, Faculty of Science, University of Birmingham. 1998

188. Wolff T, Tai E, Miller T. Screening for skin cancer: An update of the evidence for the U.S. Preventative Services Task Force. *Ann Intern Med.* 2009 Feb 3; 150(3): 194-198

189. ISO/IEC 10918-1:1994. Digital compression and coding of continuous-tone still images: Requirements and guidelines.

190. Ortonne J-P, Marks R. Solar elastotic degenerative change. In: Ortonne J-P, Marks R. (eds). Photodamaged skin: Clinical signs, causes and management. Martin Dunitz Ltd, London. 1999, pp 11-28

191. Rosso S, MacKie R, Zanetti R. Sun exposure, UV lamps and the risk of skin cancer: Epidemiological studies. *Eur J Cancer.* 1994; 30A: 584-560

192. Ortonne J-P, Marks R. Dyspigmentation and melanoma. In: Ortonne J-P, Marks R. (eds). Photodamaged skin: Clinical signs, causes and management. Martin Dunitz Ltd, London. 1999, pp 42

193. Field A. Discovering statistics using SPSS for windows. Second edition. Sage publications, London. 2005

194. StatSoft, Inc. Electronic Statistics Textbook. Tulsa, OK. 2010: Online at http://www.statsoft.com/textbook/

195. Richard MA et al Delays in diagnosis and melanoma prognosis (I): the role of patients. *Int J Cancer*. 2000; 89: 271-279

196. Walter FM, Humphrys E, Tso S, Johnson M, Cohn S. Patient understanding of moles and skin cancer, and factors influencing presentation in primary care: a qualitative study. *BMC Family Practice.* 2010; 11: 62

197. Allgar VL, Neal RD. Delays in the diagnosis of skin cancers: analysis of data from the National Survey of NHS Patients: Cancer. *Br J Cancer* 2005; 92: 1959-1970

198. Smith LK, Pope C, Botha JL. Patients' help-seeking experiences and delay in cancer presentation: a qualitative synthesis. *Lancet.* 2005; 366: 825-831

199. Bish A, Ramirez A, Burgess C, Hunter M. Understanding why women delay in seeking help for breast cancer symptoms. *J Psychosom Res.* 2005; 58: 321-326

200. Berry WD, Feldman S. Multiple Regression in Practice. Sage Publications, Beverly Hills, CA.1985

201. Baillie L, Askew D, Douglas N, Soyer HP. Strategies for assessing the degree of photodamage to skin: a systematic review of the literature. *Br J Dermatol*. 2011; 165: 735-742

202. Seddon JM, Egan KM, Zhang Y et al. Evaluation of skin microtopography as a measure of ultraviolet exposure. *Invest Ophthalmol Vis Sci.* 1992; 33: 1903–8

203. de Rigal J, Escoffier C, Querleux B et al. Assessment of aging of the human skin by in vivo ultrasound imaging. *J Invest Dermatol*. 1989; 93: 621–5

204. Gniadecka M. Effects of ageing on dermal echogenicity. *Skin Res Technol*. 2001; 7: 204–7

205. Hoffmann K, Dirschka TP, Stücker M et al. Assessment of actinic skin damage by 20 MHz sonography. *Photodermatol Photoimmunol Photomed*. 1994; 10: 97–101

206. Ulrich M, Rüter C, Astner S et al. Comparison of UV-induced skin changes in sun-exposed vs. sun-protected skin – preliminary evaluation by reflectance confocal microscopy. *Br J Dermatol.* 2009; 161 (Suppl. 3): 46–53

207. Horn M, Gerger A, Ahlgrimm-Siess V et al. Discrimination of actinic keratoses from normal skin with reflectance mode confocal microscopy. *Dermatol Surg.* 2008; 34: 620–5

208. Korde VR, Bonnema GT, Xu W et al. Using optical coherence tomography to evaluate skin sun damage and precancer. *Lasers Surg Med.* 2007; 39: 687–95

209. König K, Speicher M, Köhler MJ, Scharenberg R, Kaatz M. Clinical application of multiphoton tomography in combination with high-frequency ultrasound for evaluation of skin diseases. *J Biophotonics*. 2010; 3(12): 759-73

210. König K, Speicher M, Bückle R et al. Clinical optical coherence tomography combined with multiphoton tomography of patients with skin diseases. *J Biophotonics*. 2009; 2(6-7): 389-97

211. Köhler MJ, Hahn S, Preller A et al. Morphological skin ageing criteria by multiphoton laser scanning tomography: non-invasive in vivo scoring of the dermal fibre network. *Exp Dermatol.* 2008; 17(6): 519-23

212. Köhler MJ, König K, Elsner P et al. In vivo assessment of human skin aging by multiphoton laser scanning tomography. *Opt Lett.* 2006; 31(19): 2879-81

213. Lin SJ, Wu RJ, Tan HY et al. Evaluating cutaneous photoaging by use of multiphoton fluorescence and second-harmonic generation microscopy. *Opt Lett.* 2005; 30: 2275–7

214. Ramos-Vara, JA. Technical Aspects of Immunohistochemistry. *Vet Pathol.* 2005; 42 (4): 405–426

215. Chen VL, Fleischmajer R, Schwartz E et al. Immunochemistry of elastotic material in sun-damaged skin. *J Invest Dermatol.* 1986; 87: 334–7

216. Mera SL, Lovell CR, Jones RR, Davies JD. Elastic fibres in normal and sun-damaged skin: an immunohistochemical study. *Br J Dermatol.* 1987; 117: 21–7

217. Karagas MR, Zens MS, Nelson HH et al. Measures of cumulative exposure from a standardized sun exposure history questionnaire: a comparison with histologic assessment of solar skin damage. *Am J Epidemiol.* 2007; 165: 719–26

218. Marks R, Edwards C. The measurement of photodamage. *Br J Dermatol*. 1992; 127 Suppl 41: 7-13

219. Holman CDJ, Armstrong BK, Evans PR, et al. Relationship of solar keratosis and history of skin cancer to objective measures of actinic skin damage. *Br J Dermatol.* 1984; 110: 129

220. Holman CDJ, Evans PR, Lumsden GJ, Armstrong BK. The determinants of actinic skin damage: Problems of confounding among environmental and constitutional variables. *Am J Epidemiol.* 1984; 120: 414

221. Moon JS, Oh CH. Solar damage in skin tumors: quantification of elastotic material. *Dermatology.* 2001; 202: 289–92

222. Bhawan J, Andersen W, Lee J et al. Photoaging versus intrinsic aging: a morphologic assessment of facial skin. *J Cutan Pathol*. 1995; 22: 154–9

223. Matts PJ. New insights into skin appearance and measurement.*J Invest Derm Symp P*. 2008; 13: 6-9